Volume 118 Supplement 1 (2016) ISSN 0167-8140

ELSEVIER

Radiotherapy & Oncology

Journal of the European SocieTy for Radiotherapy and Oncology

ICTR-PHE 2016

INTERNATIONAL CONFERENCE ON TRANSLATIONAL RESEARCH IN RADIATION ONCOLOGY | PHYSICS FOR HEALTH IN EUROPE

February 15 – 19, 2016 CICG, Geneva, Switzerland

ESTRO European SocieTy for RADIOTHERAPY & ONCOLOGY

Radiotherapy &Oncology

Journal of the European SocieTy for Radiotherapy and Oncology

INFORMATION FOR AUTHORS

ARTICLES should deal with original research or reviews of topics defined in the aims of the journal. Radiotherapy and Oncology publishes original material only. It is therefore understood that the content of the paper has not previously been published in the same or a similar form and that it is not under consideration for publication elsewhere. The act of submitting a manuscript to the journal carries with it the right to publish that paper.

Radiotherapy and Oncology uses an online manuscript submission and peer review process.
Papers and correspondence should be submitted online at **http://www.ees.elsevier.com/ro** and the instructions on the site should be closely followed. Authors may submit manuscripts and track their progress to final decision. Reviewers can download manuscripts and submit their reports to the Editors electronically.

The full contact details for the Editorial Office are shown below:

Professor Jens Overgaard, M.D., Radiotherapy and Oncology Secretariat, Department of Experimental Clinical Oncology, Aarhus University Hospital, Nörrebrogade 44, Building 5, DK-8000 Aarhus C, Denmark (Tel.: +45 78 46 26 29; Fax: +45 86 19 71 09; E-mail: ro@oncology.dk)

TYPES OF PAPERS

1. *Full length original papers (max. 3000 words)*
Describe original scientific work in the field of radiation oncology or related areas. The content of the paper should be sufficient to reach valid conclusions. Full papers should include a structured abstract and be divided into sections (Introduction; Materials and Methods; Results; Discussion; References; Tables; Figures) and should not normally exceed 6 printed pages, including references and a maximum of 6 tables/figures. Additional material can be submitted as supplementary files.

2. *Short communications and Technical notes (max. 2000 words)*
Provide a brief but complete account of a particular piece of work, e.g. Phase I or II study, and should in total be no longer than 4 printed pages, normally including a maximum of 2 figures or tables. A summary of not more than 50 words should be included (not a structured abstract), but the manuscript can have fewer subheadings (e.g. short introduction; materials and methods; results and discussion). Authors are advised to see a recent issue of the journal for size and lay-out.

3. *Review articles*
Rigorous critical assessment of clinical and/or laboratory research in a field of interest to the journal and its subscribers. Reviews are normally solicited by the editors, and it is suggested that authors wishing to contribute a review article contact the editor-in-chief.

4. *Editorials and commentaries*
Editorials and commentaries relate to articles in the journal or to issues of relevance for the readership. This type of communication is normally solicited by the editors.

5. *Letters to the Editor*
On topics of current interest or comment upon material previously or simultaneously published in the journal. They should be limited to 500 words and may include 1 table or figure.

6. *Announcements*
The inclusion of announcements, etc. is at the discretion of the Editors and the Publisher and subject to space availability. Request for inclusion of meeting announcement should be send to the ESTRO secretariat (see address in journal).

Author inquiries
For inquiries relating to the submission of articles (including electronic submission where available) please visit this journal's homepage at http://www.elsevier.com/locate/radonc. For detailed instructions on the preparation of electronic artwork, please visit http://www.elsevier.com/artworkinstructions. Contact details for questions arising after acceptance of an article, especially those relating to proofs, will be provided by the publisher. You can track accepted articles at http://www.elsevier.com/trackarticle. You can also check our Author FAQs at http://www.elsevier.com/authorFAQ and/or contact Customer Support via http://support.elsevier.com

Language services. Authors who require information about language editing and copyediting services pre- and post-submission please visit http://webshop.elsevier.com/languageediting or our customer support site at http://support.elsevier.com.

A full and complete Guide for Authors is availabe online at http://www.thegreenjournal.com

Printed by Henry Ling Ltd., Dorchester, United Kingdom

♾ The paper used in this publication meets the requirements of ANSI/NISO Z39.48-1992 (Permanence of Paper)

Radiotherapy &Oncology

Journal of the European SocieTy for Radiotherapy and Oncology

Volume 118 Supplement 1 (2016)

Editor-in-Chief: J. Overgaard

ICTR-PHE 2016
International Conference on Translational Research in Radiation Oncology / Physics for Health in Europe

February 15-19, 2016 • Geneva, Switzerland

Recommended by

In collaboration with

Under the auspices of

In collaboration with

Radiotherapy & Oncology is available online:
For ESTRO members: http://www.thegreenjournal.com
For institutional libraries: http://www.sciencedirect.com

ELSEVIER

Amsterdam • Boston • London • New York • Oxford • Paris • Philadelphia • San Diego • St. Louis

International Standard Serial Number 0167-8140

Orders, claims, and journal inquiries: please contact the Elsevier Customer Service Department nearest you:

St. Louis: Elsevier Customer Service Department, 3251 Riverport Lane, Maryland Heights, MO 63043, USA; phone: (800) 6542452 [toll free within the USA]; (+1) (314) 4478871 [outside the USA]; fax: (+1) (314) 4478029; e-mail: JournalsCustomerService-usa@elsevier.com
Oxford: Elsevier Customer Service Department, The Boulevard, Langford Lane, Kidlington, Oxford OX5 1GB, UK; phone: (+44) (1865) 843434; fax: (+44) (1865) 843970; e-mail: JournalsCustomerServiceEMEA@elsevier.com
Tokyo: Elsevier Customer Service Department, 4F Higashi-Azabu, 1-Chome Bldg, 1-9-15 Higashi-Azabu, Minato-ku, Tokyo 106-0044, Japan; phone: (+81) (3) 5561 5037; fax: (+81) (3) 5561 5047; e-mail: JournalsCustomerServiceJapan@elsevier.com
Singapore: Elsevier Customer Service Department, 3 Killiney Road, #08-01 Winsland House I, Singapore 239519; phone: (+65) 63490222; fax: (+65) 67331510; e-mail: JournalsCustomerServiceAPAC@elsevier.com

Funding Body Agreements and Policies

Elsevier has established agreements and developed policies to allow authors whose articles appear in journals published by Elsevier, to comply with potential manuscript archiving requirements as specified as conditions of their grant awards. To learn more about existing agreements and policies please visit http://www.elsevier.com/fundingbodies

0167-8140(201602)118:S1;1-Q

Radiotherapy &Oncology

Journal of the European SocieTy for Radiotherapy and Oncology

AIMS AND SCOPE

Radiotherapy and Oncology publishes papers describing original research as well as review articles. It covers areas of interest relating to radiation oncology. This includes clinical radiotherapy, combined modality treatment, experimental work in radiobiology, chemobiology, hyperthermia and tumour biology, as well as physical aspects relevant to oncology, particularly in the field of imaging, dosimetry and radiation therapy planning. Papers on more general aspects of interest to the radiation oncologist including chemotherapy, surgery and immunology are also published.

Publication information: *Radiotherapy & Oncology* (ISSN 0167-8140). For 2016, volumes 118–121 (12 issues) are scheduled for publication. Subscription prices are available upon request from the Publisher or from the Elsevier Customer Service Department nearest you or from this journal's website (http://www.thegreenjournal.com). Further information is available on this journal and other Elsevier products through Elsevier's website (http://www.elsevier.com). Subscriptions are accepted on a prepaid basis only and are entered on a calendar year basis. Issues are sent by standard mail (surface within Europe, air delivery outside Europe). Priority rates are available upon request. Claims for missing issues should be made within six months of date of dispatch.

USA mailing notice: *Radiotherapy & Oncology* (ISSN 0167-8140) is published monthly by Elsevier Ireland Ltd. (Elsevier House, Brookvale Plaza, East Park, Shannon, Co. Clare, Ireland). Periodicals postage paid at Jamaica, NY 11431 and additional mailing offices (not valid for journal supplements).
USA POSTMASTER: Send change of address to *Radiotherapy & Oncology*, Elsevier Customer Service Department, 3251 Riverport Lane, Maryland Heights, MO 63043, USA.
AIRFREIGHT AND MAILING in USA by Air Business Ltd., c/o Worldnet Shipping Inc., 156-15, 146th Avenue, 2nd Floor, Jamaica, NY 11434, USA.

ICTR-PHE 2016

CONFERENCE CHAIRS

Jacques Bernier
Manjit Dosanjh

ADVISORY BOARD

Ugo Amaldi
Michael Baumann
Soeren M. Bentzen
Jacques Bernier
Thomas Beyer
Jean Bourhis
David Brizel
Jean-Francois Chatal
James Cox
Denis Dauvergne
Alberto Del Guerra
Manjit Dosanjh
Marco Durante
Wolfgang Enghardt
Zvi Fuks
Karin Haustermans
Robert Jeraj
Ulli Köster
Philippe Lambin
Paul Lecoq
Anthony Lomax
Radhe Mohan
Steve Myers
Dag Rune Olsen
Jens Overgaard
Katia Parodi
Philip Poortmans
Kevin Prise
Osman Ratib
Marcel Verheij
Brad Wouters

SESSION ORGANISERS

BIOLOGY

M. Durante, Darmstadt
K. Prise, Belfast
P. Lambin, Maastricht
B. Wouters, Toronto

PRE-CLINICAL and CLINICAL STRATEGIES

M. Baumann, Dresden
K. Haustermans, Leuven
Z. Fuks, New York
M. Verheij, Amsterdam

NUCLEAR MEDICINE

U. Köster, Grenoble
O. Ratib, Geneva
T. Beyer, Vienna
J-F. Chatal, Nantes

NEW TECHNOLOGIES

W. Enghardt, Dresden
A. Lomax, Villigen
R. Jeraj, Wisconsin
R. Mohan, Houston

DETECTORS and IMAGING

D. Dauvergne, Lyon
A. Del Guerra, Pisa
P. Lecoq, CERN
K. Parodi, Munich

RADIOTHERAPY

S.M. Bentzen, Maryland
J. Bourhis, Lausanne
D. Brizel, Durham
D.R. Olsen, Oslo

EXECUTIVE COMMITTEE

Ugo Amaldi, TERA
Jacques Bernier, Genolier and Geneva
Jean Bourhis, Lausanne
Alberto Costa, Milano
Manjit Dosanjh, CERN
Raymond Miralbell, Geneva
Steve Myers, CERN

ICTR-PHE 2016
International Conference on Translational Research in Radiation Oncology/Physics for Health in Europe
Uniting Physics, Biology and Medicine for better healthcare
Geneva International Conference Center, February 15 - 19, 2016

ICTR-PHE 2016
February 15-19, Geneva

1

CHIC – A Multi-scale Modelling Platform for in-silico Oncology

D. Abler[1], P. Büchler[1], G. S. Stamatakos[2]
[1] Institute for Surgical Technology & Biomechanics, University of Bern, Switzerland
[2] Institute of Communication and Computer Systems, University of Athens, Greece

Models of normal physiology and disease are necessary in cancer research and clinical practice to optimally exploit the available (pre)clinical multi-scale and multi-modality data. Relevant models often cover multiple spatio-temporal scales and require automated access to heterogeneous and confidential data, making their development, validation and deployment challenging.
The CHIC (Computational Horizons in Cancer) [1] project develops computational models for the cancer domain, as well as tools, services and a secure infrastructure for model and data access, and reuse. The architecture is designed to support the creation of complex disease models (hyper-models) by composition of reusable component models (hypo-models). It aims to provide individualized answers to concrete clinical questions by patient-specific parametrization of disease-specific hyper-models.
We introduce the CHIC project and illustrate its approach to multi-scale cancer modelling by coupled execution of two component models operating on distinct spatial scales:
- OncoSimulator (OS): a spatially discrete model of cancer cell proliferation and treatment effect in function of tumour, treatment and patient-specific parameters [2], implemented as cellular automaton model,
- Bio-mechanical Simulator (BMS): a macroscopic continuum model of mechanical effects caused by tumour expansion in patient-specific anatomy, implemented as finite element model, based on [3].
Both component models exchange information about the spatial distribution of cancer cells and mechanical pressure in order to simulate the evolution of tumour volume and shape. Latter is achieved by correcting simple spherical growth (OS) by mechanically induced growth anisotropy (BMS). Results are demonstrated on the clinical example of Glioblastoma Multiforme.
CHIC is working towards an extensible platform for in-silico oncology with a set of reusable component models at its core, covering sub-cellular, cellular and super-cellular scales. Viability of infrastructure and composite hyper-models is being evaluated against clinical questions in the treatment of Nephroblastoma, Glioblastoma and Non-small Cell Lung Cancer.

Keywords: in-silico oncology, multi-scale modelling

References:
[1] http://www.chic-vph.eu/
[2] Stamatakos, G., 2011. In silico oncology: PART I Clinically oriented cancer multilevel
modeling based on discrete event simulation. In: Deisboeck, T., Stamatakos, G. (Eds.), Multiscale Cancer Modeling. Chapman & Hall/CRC, Boca Raton, Florida, USA.
[3] C. P. May, E. Kolokotroni, G. S. Stamatakos, and P. Büchler, 'Coupling biomechanics to a cellular level model: An approach to patient-specific image driven multi-scale and multi-physics tumor simulation', *Progress in Biophysics and Molecular Biology*, vol. 107, no. 1, pp. 193–199, Oct. 2011.

2

The symbiosis of science of radiation biology with immunology: Impact on basic and translational research

M. M. Ahmed
Molecular Radiation Therapeutics Branch, Radiation Research Program, National Cancer Institute (NCI), NIH, Rockville, MD 20850

Recent evidence indicates that radiation is potent modulator of immune system. The field of radiation biology and immunology is at crossroads in cancer research. With this amalgamation, new clinical trials have emerged combining radiation therapy with immune modulating agents. Through this partnership, there is a promise to augment higher progression survival benefit than cancer immunotherapy as monotherapy. Merger of two fields can generate provocative themes that need the minds of basic immunologist to interact with radiation biologists to define radiation dose exposure, types of radiation, sequencing and dosing of vaccination and immune modulation biomarkers. Further, radiation biologist can learn from immunologist on what animal models can be utilized for primary and metastatic tumors. As the synergy is happening now between these two fields, there is greater focus in developing immune modulating agents for adjuvants to radiotherapy of solid tumors. This area is maturing for better understanding of the mechanistic actions of in-situ radiation vaccine. With this advent of advancement, there are vast opportunities to understand effects of radiation on tumor and normal tissue and how this damage cooperates with the host immune activation and injury. Such understanding can lead to identification of immune biomarkers that can be utilized in immune monitoring in tumor control and potentially synergize with other markers of normal tissue damage. This talk will focus on understanding the response of some key components of tumor immune microenvironment to radiation such as regulatory T-cells and myeloid cells in regulating immunogenic tumor cell death. The other focus will include how host immune machinery reacts to normal tissue injury and further any immune biomarkers can be validated for immune monitoring in clinical trials.

3

Toward brachytherapy with ytterbium sources

S. V. Akulinichev, S. A. Chaushansky and V. I. Derzhiev
Institute for nuclear research of RAS (INR), Moscow 117312, Russia

Heavy and quite expensive afterloaders with iridium sources are now widely used for the HDR brachytherapy of tumors. The cost of this kind of treatment, as well as the necessity of heavily shielded canyons and of special technology of source delivery and replacement, makes the brachytherapy with iridium sources less widespread. Moreover, the relatively hard radiation of iridium-192 often makes damage to healthy organs close to a tumor.
These problems of HDR brachytherapy can be resolved with ytterbium sources. Compared to other isotopes used for HDR brachytherapy, the isotope Yb-169, having the average photon emission energy of 93 KeV, requires a much lighter shielding. For example, the tungsten shield of only 2-3 cm makes the HDR therapeutic ytterbium source harmless for the personnel. Therefore a source loader with ytterbium sources may be a compact and cheap desktop device. Moreover, the treatment quality may be significantly improved due to ytterbium radiation collimation. In the figure we compare two ytterbium dose distributions in water: one behind the tungsten layer of 2 mm (lower line) and the other without it. It follows form this figure that only 2 mm of tungsten allow to effectively collimate the ytterbium source radiation – the suppressed dose is 30 times lower! This also means that a new cheep and accurate preloader, let's call it an "acculoader", with a hidden ytterbium source inside can be easily manufactured. In this case the target irradiation will begin just by the source pushing forward.

We created an AVLIS facility for the production of primary isotope Yb-168 with the enrichment above 20% and with a record capacity. In order to increase the activity and improve mechanical properties of ytterbium sources, we developed the technology of ytterbium ceramics production. The design of new compact source loader with ceramic ytterbium sources is now in progress.

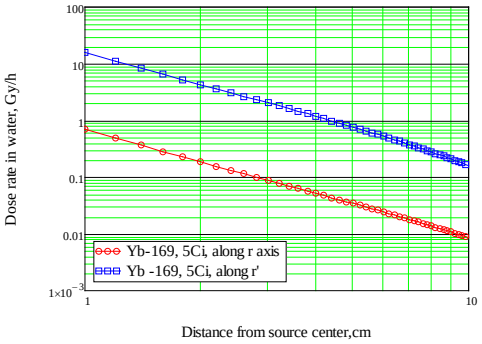

Keywords: brachytherapy, ytterbium source

4

Conformal proton therapy with passive scattering

S.V.Akulinichev[1], R. D. Ilic [2] and I.A. Yakovlev [1]
[1] Institute for nuclear research of RAS (INR), Moscow 117312, Russia
[2] Institute for Nuclear Sciences VINCA, 11001 Beograd, Serbia

In proton therapy, as well as in carbon ion therapy, two main methods of dose distribution formation can be used: the passive particle scattering and the particle scanning in several modifications. The pencil-beam scanning is now considered as a most advantageous method of dose distribution formation. Indeed, this method provides the conformance of dose delivery to a tumor of any size with no significant dose, delivered to healthy surrounding tissue. However, in some cases the beam scanning method may have problems. In particular, this is the case of small targets when the pencil beam width is comparable with the target size. The eye melanoma and small brain metastasis may be examples of such small tumors.
In these cases the application of the old method of passive beam scattering with a formation of individual dose distributions may be reasonable. However, this method in its classical version with a ridge filter, a bolus and a collimator is known to fail to provide the sufficiently conformal dose distribution with one field: either the maximal dose significantly exceeds the tumor volume on its proximate site or the dose value changes too much within the tumor volume.
We found a new construction of a two-component ridge filter which provides the dose distributions with no mentioned above shortcomings (the corresponding patent is pending). We have performed a series of calculations with the help of the original Monte-Carlo code SRNA in order to find the optimal construction of new ridge filters from the point of view of dose distribution accuracy and of the device manufacturability. In the figure the example of dose distribution calculated with the SRNA program is presented. As it follows from the figure, even with one field the 95% isodose line does not notably leave the tumor volume, represented by the black circle. The usual “wings” on proximate side of lower isodose lines are absent as well. The experimental tests of these new devices with proton beams of the INR linac are now in progress.

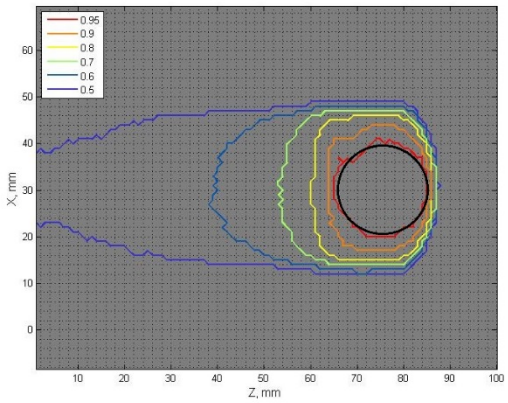

Keywords: proton therapy

5

Commissioning of a Compton camera for ion beam range verification via prompt γ detection using low-energy and clinical particle beams

S. Aldawood[1,2], J. Bortfeldt[1], M. Böhmer[3], I. Castelhano[1,4], G. Dedes[1], W. Enghardt[5], F. Fiedler[6], R. Gernhäuser[3], C. Golnik[5], S. Helmbrecht[6], F. Hueso-González[7], H. v. d. Kolff[1,8] , T. Kormoll[5], C. Lang[1], S. Liprandi[1], R. Lutter[1], L. Maier[3], T. Marinšek[1], G. Pausch[5] , J. Petzoldt[5] , M. Pocevicius[1], K. Römer[6], I. Valencia Lozano[1] , D. R. Schaart[8] , K. Parodi[1] and P. G. Thirolf[1]
[1] Faculty of Physics, Department of Medical Physics, Ludwig-Maximilians-University Munich, Germany
[2] Department of Physics and Astronomy, King Saud University, Riyadh, Saudi Arabia
[3] Physics Department E12, Technical University Munich, Garching, Germany
[4] Faculty of Science, University of Lisbon, Lisbon, Portugal
[5] National Center for Radiation Research in Oncology “OncoRay”, Dresden, Germany
[6] Radiation Physics Division, Helmholtz-Zentrum Dresden - Rossendorf, Dresden, Germany
[7] Institute of Radiooncology, Helmholtz-Zentrum Dresden - Rossendorf, Dresden, Germany
[8] Faculty of Applied Science, Radiation Science and Technology, Delft University of Technology, Delft, The Netherlands

Purpose: Recently, the interest of using hadron-therapy in cancer treatment, particularly for tumors in the vicinity of critical organs-at-risk, has grown due to the ability of providing high precision dose delivery. In order to fully exploit this feature, a precise monitoring of particle beam (proton, ions) is mandatory. Therefore, the purpose of our project is to develop an online imaging system based on a Compton camera to verify the particle beam (proton, ions) range by detecting prompt γ rays, induced as a result of nuclear reactions between the particle beam and biological tissue.
Material / Methods: The Compton camera consists of two main components: a scatterer (tracker), formed by a stack of six customized double-sided Si-strip detectors (DSSSD), and a monolithic $LaBr_3$ scintillation detector (50x50x30 mm^3) acting as an absorber detector. The DSSSD detector is processed by a compact ASIC based electronics, while the $LaBr_3$ detector is read out by a position-sensitive (16x16) multi-anode photomultiplier (PMT, Hamamatsu H9500), whose segments are processed individually using spectroscopy electronics. The energy and timing signals are digitized in a VME-based charge-to-digital converter and time-to-digital converter, respectively.
Results: The Compton camera components have been characterized in the laboratory using calibration sources. The time and energy resolution of the $LaBr_3$ detector were measured to be 273 ± 6 ps (FWHM) and 3.5%, using ^{60}Co and

^{137}Cs source, respectively. The spatial resolution of this detector so far has been determined to be about 5 mm, using the k-nearest-neighbour algorithm (k-NN) [1].
Moreover, the Compton camera has been commissioned at different particle beam facilities. The time-of-flight (TOF) capability of the system was evaluated at the Garching Tandem accelerator, using a 20 MeV pulsed (400 ns) deuteron beam hitting a water phantom, showing prompt γ rays well separated from the slower neutrons. The camera was further tested with different clinical proton beams from the research area of the University Proton Therapy Dresden (100, 160 and 225 MeV) stopping in either a water or a PMMA phantom, as indicated in Fig.1. For all three proton beam energies, the analysis of the prompt γ energy versus the TOF showed no significant neutron background. The Compton electron energy loss was extracted from each DSSSD layer, showing a gradual sequential increase of the energy loss from the first to the last layer.

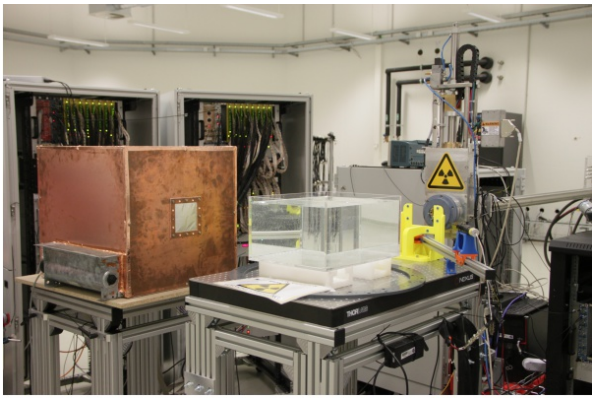

Figure 1: The Compton camera, enclosed in a Faraday light tight cage, is placed under 90º relative to the proton beam that hits a water phantom (here at the OncoRay facility, Universitäts Protonen Therapie Dresden).

Conclusion: A Compton camera is under development in Garching, designed for online ion beam range verification via prompt γ detection. The monolithic $LaBr_3$ detector was characterized in the laboratory exhibiting excellent energy and time resolution as well as a sufficient position resolution. The Compton camera was commissioned with a low-energy pulsed deuteron beam at the Garching Tandem accelerator and with high-energy clinical proton beams at the OncoRay facility, Dresden.

Keywords: Prompt γ imaging, Compton camera, Proton range verification

Acknowledgment: This work was supported by the DFG Cluster of Excellence MAP (Munich-Centre for Advanced Photonics).

References:
[1] H.T. van Dam et al., IEEE Trans. Nucl. Sci. 58 (2011) 2139.

6
RBE for Carbon ions In Vivo for Tumor Control and Normal Tissue Damage
B. S. Sørensen[1], M. R. Horsman[1], J. Alsner[1], J. Overgaard[1], M. Durante[2], M. Scholz[2], T. Friedrich[2], N. Bassler[3]
[1] Department of Experimental Clinical Oncology, Aarhus University Hospital, Aarhus, Denmark
[2] GSI Helmholtzzentrum für Schwerionenforschung (GSI), Department of Biophysics, Darmstadt, Germany
[3] Department of Physics, Aarhus University, Aarhus, Denmark

Purpose: Particle therapy provide a more favorable dose distribution compared to x-rays, but limited focus has been on the actual biological responses. Effects of carbon ion radiation in experimental tumor models has been investigated in a limited number of studies, the majority of these with tumor growth delay as biological endpoint. To elucidate the biological variation in radiation response in particle therapy, more in vivo studies are needed. The aim of the present study was to compare the biological effectiveness of carbon ions relative to x-rays between the clinical relevant endpoint tumor control and normal tissue damage, both acute and late effects.
Materials and Methods: CDF1 mice with C3H mouse mammary carcinoma placed subcutaneously on the foot of the right hind limb were irradiated with single fractions of either photons or ^{12}C ions, using a 30-mm spread-out Bragg peak. Endpoint of the study was local control (no tumor recurrence within 90 days). For the acute skin reaction, non-tumor bearing CDF1 mice were irradiated with a comparable radiation scheme, and monitored for acute skin damage. Late radiation induced fibrosis was measured up to 322 days following treatment.
Results: The TCD_{50} (dose producing tumor control in 50% of mice) values with 95% confidence interval were 29.7 (25.37-34.78) Gy for C ions and 43.94 (39.24- 49.2) Gy for photons. The corresponding RBE values were 1.48 (1.28-1.72). For acute skin damage the MDD_{50} (dose to produce moist desquamation in 50% of mice) values with 95% confidence interval were 26.34 (22.99-30.19) Gy for C ions and 35.84 (32.94-38.98) Gy for photons, resulting in a RBE of 1.36 (1.20-1.45). For late radiation-induced fibrosis the FD_{50} (dose to produce severe fibrosis in 50% of the mice) with 95% confidence interval were 26.5 (23.1 – 30.3) Gy for carbon ions and 39.8 (37.8 – 41.8) Gy for photons, with a RBE of 1.50 (1.33 – 1.69).
Conclusions: We have established TCD_{50}, MDD_{50} and FD_{50} values for local tumor control and normal tissue damage and the corresponding RBE values for carbon ions in a mouse model. The observed RBE values were very similar for tumor response, acute skin damage and late RIF when irradiated with large doses of high- linear energy transfer (LET) carbon ions. This study add information to the variation in biological effectiveness in different tumor and normal tissue models.
(Acta Oncologica, In Press)

7
PET scanning of ocular melanoma after proton irradiation
T. Amin[1], C. Lindsay[2], C. Hoehr[2], R. Barlow[1]
[1] University of Huddersfield, UK
[2] TRIUMF, Canada

The Proton Therapy Facility at TRIUMF is now in routine operation treating ocular tumours using 74 MeV protons extracted from the 500 MeV H^- cyclotron. In this work, the feasibility of using PET scanning for proton dose monitoring is investigated. Different lucite phantoms have been irradiated with a raw Bragg peak and a spread out Bragg peak of 74 MeV and scanned using two PET scanners at UBC hospital. Simulation programs GEANT4 and FLUKA are being used to validate against experimental measurements. GEANT4 has been coupled with EXFOR cross section data of proton induced reactions to calculate the axial activity of the phantoms. Despite the very simple setup, significant discrepancies between the codes have been observed for the activity profiles of ^{11}C and ^{15}O and ^{13}N, whereas the beam range in lucite has been found to have good agreement.

Keywords: PET, proton therapy

8
Radiation treatment monitoring using multifunctional imaging in prostate tumour xenografts
N. Arteaga-Marrero[1], C.B. Rygh[2,3], J.F. Mainou-Gomez[4], T.C.H. Adamsen[5,6], N. Lutay[7], R.K. Reed[2,8], D.R. Olsen[1]
[1] Department of Physics and Technology, University of Bergen, Bergen, Norway
[2] Department of Biomedicine, University of Bergen, Bergen, Norway
[3] Department of Health Sciences, Bergen University College, Bergen, Norway
[4] Department of Clinical Medicine, University of Bergen, Bergen, Norway

[5] Department of Radiology, Haukeland University Hospital, Bergen, Norway
[6] Department of Chemistry, University of Bergen, Bergen, Norway
[7] Division of Dermatology and Venereology, Department of Clinical Sciences, Lund University, Lund, Sweden
[8] Centre for Cancer Biomarkers (CCBIO), University of Bergen, Bergen, Norway

Functional multimodal imaging was used to assess early response to radiation treatment in the murine prostate tumour model CWR22.
Positron Emission Tomography (PET)/Computer Tomography (CT) and Dynamic Contrast-Enhanced Ultrasonography (DCE-US) were employed to determine the relationship between metabolic and microvascular parameters that reflect the tumour microenvironment, followed by immunohistochemical validation of microvessel density (MVD) and necrosis. Two experimental groups were tested according to the tracers used in PET/CT: ^{18}Fluorine-Fluoromisonidazole (^{18}F-FMISO) and ^{18}F-Fluorocholine (^{18}F-FCH) which are associated with hypoxia and choline metabolism, respectively [1,2]. PET/CT and DCE-US were acquired at day 0 and day 3. At day 1, radiation treatment was delivered as a single fraction of 10 Gy. PET/CT and DCE-US acquisition and quantification were performed as previously described [3,4]. Wilcoxon's matched-pairs test was used to determine intergroup differences at day 0 and day 3, and to assess intragroup differences from day 0 to day 3. Kendall's Tau-b test was employed to assess correlation between functional parameters derived from PET/CT and DCE-US. In addition, the relationship between functional and histological parameters was also tested. Bonferroni correction for multiple testing was employed and a significance level of 5% was considered in all tests.
In the ^{18}F-FMISO group, the maximum Standardized Uptake Values (SUVmax) and the mean SUV (SUVmean) were decreased for the treated mice, suggesting a decrease in hypoxia. Furthermore, the SUVmean of the tumour-to-muscle ratio was correlated to MVD at day 3. In addition, the eliminating rate constant of the contrast agent from the plasma k_{el} derived from DCE-US was correlated to the SUVmean of tumour-to-muscle ratio, necrosis, and MVD. In the ^{18}F-FCH group; heterogeneous and reduced tracer uptake was detected. The kurtosis of the amplitude of the contrast uptake *A* linked to DCE-US was significantly decreased for the control mice.
Our results demonstrated that the multimodal approach using ^{18}F-FMISO PET/CT and DCE-US has valuable diagnostic and prognostic potential for early non-invasive evaluation of radiotherapy.

Keywords: DCE-US, ^{18}F-Fluoromisonidazole (^{18}F-FMISO) PET, ^{18}F-Fluorocholine (^{18}F-FCH) PET

References:
[1] Heijmen L, ter Voert EGW, Punt CJA et al. Contrast Media Mol Imaging 2014; 9:237-245
[2] Fass L. Mol Oncol 2008; 2:115-152
[3] Arteaga-Marrero N, Brekke Rygh C, Mainou-Gomez JF, et al. Contrast Media Mol Imaging 2015; dOI:10.1002/cmmi.1645
[4] Arteaga-Marrero N, Brekke Rygh C, Mainou-Gomez JF, et al. J Transl Med 2015; *In press*

9
Ocular Melanoma cells in the presence of nanoparticles against cobalt 60 radiation therapy- Monte Carlo and In Vitro studies

S.Asadi[1], M. Vaez-zadeh[1], D.Kowsari[1], O.Pourdakan[1], M.Olfat[1], M. Rezaei Kanavi[2], S. Balagholi[2] and H. Ahmadieh[2]
[1] Department of Physics, K.N.Toosi University of Technology, Tehran, Iran
[2] Ophtalmic Research Center, Shahid Beheshti University of Medical Sciences, Tehran, Iran

The aim of this work is to study the effects of gold nanoparticles (GNPs) on cell viability in choroidal melanoma which is irradiated with cobalt source with Monte Carlo and In Vitro studies.
In the Monte Carlo phase of this study a cylinder with the radius of 1.7 cm and the length of 2.1 cm was simulated as tumor phantom through with MCNP5 code and was filled with the tumor composition which obtained from previous work. In a discrete simulation such a phantom was divided into three parts and the middle region was latticed and filled with different concentrations of 50, 100, 200, 400 and 600 µg GNPs with 50nm in diameter. In both simulations the array of 0.5*0.5*0.5 mm^3 voxels were utilized for scoring the average energy deposition to calculate the depth dose. The AECL Thetaron ^{60}Co external radiation therapy device with the distance of 80 cm from the center of the Phantom has been considered as radiation source. The dose value to these voxels was calculated utilizing F6 tally. The dose enhancement factor (DEF) which is defined as the ratio of the dose in a particular region of a tissue when GNPs are present to the same factor in the absence of such substances were calculated and compared for different concentrations. In the in-vitro study, GNPs were synthesized following the FERN method, by employing HAuCl4 gold halides that were then reduced by sodium citrate. Cancerous melanoma cells were extracted from a middle-aged human female and digested by the use of the Tripezyn enzyme. The noted cells were cultured under a DMEM environment within a T75 flask with an FBS of 20%, and were incubated in an atmosphere consisting of 5% CO2, under a steady temperature of 37 C. Melanoma cells were cultured in a 96-well plate, and received the required GNPs with specific concentrations of 600, 400, 200, 100 and 50µg through injection. The toxicity of the mentioned particles on the cells was then evaluated using a MTT Assay. The plate were then irradiated by the cobalt source in the presence and absence of GNPs. 48 hours and a week after irradiation, viability of the cells were assayed with MTT test again.
In both Monte-Carlo and in-vitro studies it was observed that the presence of GNPs could play an important role in dose enhancement and decrease the viability of cancerous cells. When the concentration of nanoparticles increases in the area of the tumor, a higher amount of radiation energy will be absorbed in the tumor area. As a result, the amount of the dose absorbed by the normal tissue will be decreased.

Keywords: In Vitro, GNPs, cobalt60, Choroidal Melanoma

References:
[1] S. Asadi, M. Vaez-zadeh, S. Farhad Masoudi, et al. "Gold nanoparticle-based brachytherapy enhancement in choroidal melanoma using a full Monte [2] Carlo model of the human eye". jornal of applied clinical medical physics.16(5):1-13, (2015).
[3] J.F. Heinfeld, D.N. Slatkin and H.M. Smilwitz, "The use of gold nanoparticles to enhance radiotherapy in mice". Phys. Med. Biol. 49:309-315, (2004).
[4] Frens, G. (1973) Controlled nucleation for the regulation of the particle size in monodisperse gold suspensions. Nat. Phys. Sci., 241: 20-22.

10
Laser therapy of human choroidal Melanoma in the presence of gold nanoparticles - Monte Carlo and In Vitro Study

S. Asadi[1], F. Rezaeai[1], M. Asgari[1], M. Vahidian[1], M. F. Samavat[1], M. Olfat[1]
[1] Department of Physics, K.N.Toosi University of Technology, Tehran, Iran

Purpose: The effects of gold nanoparticles (GNPs) on human choroidal melanoma which are irradiated with a diode laser beam of 810nm wavelength has been examined with both Monte Carlo and In Vitro studies.
Material and Method: In the Monte Carlo phase of this work, a human eye phantom has been simulated through with Geant4 code and a tumor with the apical height of 0.5mm was defined on the equator temporal to the eyeball. The tumor was latticed by identical cubes each with a volume of 0.1cm^3 and different concentrations of gold nanoparticles were

defined within that. The dose enhancement factor (DEF) has been calculated to compare the effects of GNPs in laser therapy of eye melanoma. In the In Vitro phase of this work the uveal Melanoma cells were cultivated in DMEM with 20% FBS. In the seventh passage the cells were grown on a 24-well plate in which the first five wells incubated with different concentrations of gold nanoparticles and the sixth well saved as control.
Results and Discussion: The MTT assay was done in order to evaluate the toxicity of these nanoparticles, so as to define the preferred concentrations of GNPs. After the cytotoxicity assay and determination of the concentration range of these nanoparticles, the sample has been injected by GNPs, then the dosimetry has been done after irradiation of target with laser beam. Within a time span of 48 hours, and also a week after the injection of the noted substances, viability of cells were evaluated with MTT assay. The results show that the higher concentration of GNPs show a higher decrease in cell viability. Making a comparison between Laser beam, cobalt source and low dose rate sources such as Iodine and Palladium in the study of the effects of GNPs in cancer therapy reports very interesting results and motivated us to do a full in vivo study in this regards. Regarding the numerous sources that are employed in the radiotherapy of the eye Melanoma, the possible effects of these sources, whilst accompanied by GNPs, is a matter of heated debate in altering the period of treatment and requires more comprehensive investigations. A full experimental investigation of the effects of GNPs on Choroidal Melanoma against different radiation sources could answer this question.

KeyWords: Diod Laser Beam, Choroidal Melanoma, GNPs

11

A systematic Monte Carlo study on the dosimetric and imaging properties of C-11 and O-15 beams.

F. Cerutti[1], M. Dosanjh[1], A. Ferrari[1], T. Mendonca[1], P.G. Ortega[1], K. Parodi[2], P.R. Sala[1,3], R. S. Augusto[1,2], T. Stora[1]
[1] CERN, Geneva, Switzerland
[2] LMU, Munich, Germany
[3] INFN, Sezione di Milano, Milan, Italy

Carbon ion therapy has been pioneered in USA since 1975[1], and in routine clinical use in Japan since 1994[2]. More recently, it has also been implemented in Europe (HIT, CNAO, MIT and soon MedAustron) and China, and more facilities are currently under planning worldwide[3]. The rationale behind hadrontherapy with carbon ions has to do with their better ballistic properties and higher LET (Linear Energy Transfer) when compared to the more widespread protons. The drawback being their greater complexity for production, planning and delivery[4].
Recent improvements in post-accelerated beam technology are expanding the range of beams available to include also radioactive nuclides, beyond the ^{12}C ion species, currently utilized for carbon ion therapy[5]. Furthermore, Monte Carlo particle transport codes such as FLUKA[6,7], which has been used in this work, are becoming even more refined and therefore suitable for use in treatment planning and in-vivo verification techniques aiming to improve the treatment dose assessment[8].
In this work, we systematically study the dosimetric performance and imaging properties of ^{11}C in a water phantom. These add up to the advantages of conventional ^{12}C ion therapy a stronger imaging signal, potentiating in-beam monitoring, and later dose intake assessment using PET instrumentation technologies. In addition to that, a similar study has been performed for ^{15}O.
FLUKA results confirmed the high potential of ^{11}C and ^{15}O in imaging, the former presenting no significant absorbed dose drawbacks compared to ^{12}C.

Keywords:
Carbon ion therapy, FLUKA, PET imaging

References:

[1] Castro JR, Saunders WM, Tobias CA, *et al*. Treatment of cancer with heavy charged particles. *Int J Radiat Oncol Biol Phys* 1982; 8: 2191-98.
[2] Kamada T, Tsujii H, Blakely EA, Debus J, De Neve W, Durante M, *et al.* Carbon ion radiotherapy in Japan: an assessment of 20 years of clinical experience. *Lancet Oncol* (2015) 16:e93-100. doi:10.1016/S1470-2045(14)70412-7.
[3] Jermann M. Particle Therapy Statistics in 2014. *Int J Particle Ther.* 2015;2(1):50-54
[4] Amaldi U, Kraft G, Radiotherapy with beams of carbon ions, *Rep. Prog. Phys.* 68, 1861 (2005)
[5] Mendonca T *et al*. Intense post-accelerated 11C beams for hadrontherapy: Treatment and at the same time 3D dose mapping by PET imaging. CERN-ACC-Note-2014-0028.
[6] Bohlen TT, Cerutti F, Chin MPW, Fassò A, Ferrari A, Ortega PG, Mairani A, Sala PR, Smirnov G, Vlachoudis V. The FLUKA Code: Developments and Challenges for High Energy and Medical Applications. *Nuclear Data Sheets* 120, 211-214 (2014).
[7] Ferrari A, Sala PR, Fassò A, Ranft J. FLUKA: A multi-particle transport code. CERN-2005-10 (2005), INFN/TC_05/11, SLAC-R-773.
[8] Bohlen TT *et al.* Benchmarking nuclear models of FLUKA and GEANT4 for carbon ion therapy. *Phys Med Biol* 2010; 55 5833

12

ODSH as a countermeasure for radiation-induced thrombocytopenia: Dosimetric studies

S. Avery[1], E. Tkaczynski[2], M. Lambert[2]
[1] Department of Radiation Oncology, University of Pennsylvania, Philadelphia, Pennsylvania, USA
[2] Department of Hematology, The Children's Hospital of Philadelphia, Philadelphia, Pennsylvania, USA

Purpose: The molecule ODSH has shown great promise in preliminary studies suggesting that it improves platelet count recovery and impacts survival when the sodium form is given as a subcutaneous injection[1]. A new formulation of the molecule will be studied and radiation physics support will be provided to assure accuracy of the results. Expansion of the program for these studies will include performing dose ranging and PK/PD studies in mice for the novel formulation as well as some biology studies examining the biology of the mechanism of action of the molecule. The dosimetric studies will characterize the radiation source in terms of dose rate and energy. Maintaining the accuracy and precision of the radiation exposure throughout the project is a key factor to understanding the biological effects[2]. Dose uniformity and reproducibility will be monitored throughout the project to minimize dose uncertainty.
Materials/Methods: Precision X-ray 320[3] was calibrated following TG-61 protocol. EBT2 film was exposed at 200, 400, 600 and 800 cGy to create calibration curve to be used in FilmProQA software developed by Ashland technologies. Mouse irradiations were taken 320kV, 12.5 mA to a total dose of 650 cGy. Gafchromic film was placed under the mice during irradiations and later analyzed with FilmProQA[4] to determine accuracy and uncertainties during the experiment. Film exposures were taken at 800 cGy before each measurement to adjust the calibrations curve for daily variations of the x-ray tube.
Results: Film analysis determined that dose uniformity in the irradiator can vary due to scatter and experimental setup and have an effect on the outcome of your experiment.
Conclusions: For experiments with small animal irradiators a quality assurance program should be an integral part of any radiation biology study.

Keywords: Radiation protection, quality assurance, small animal

References:

[1] Lambert MP, Xiao L, Nguyen Y, Kowalska MA, Poncz M. The role of platelet factor 4 in radiation-induced thrombocytopenia. Int J Radiation Oncology Biol Phys 80:1533-1540, 2011.

[2] Marc Desrosiers, Larry DeWerd, James Deye, Patricia Lindsay, Mark K. Murphy, Michael Mitch, Francesca Macchiarini, Strahinja Stojadinovic, Helen Stone. The Importance of Dosimetry Standardization in Radiobiology Journal of Research of the National Institute of Standards and Technology Volume 118 (2013).
[3] PXI Precision X-Ray. North Branford CT. http://pxinc.com/
[4] Ashland Advanced Materials Group. Bridgewater NJ. http://filmqapro.com/FilmQA_Pro.htm

13

X-Ray Phase contrast micro-imaging in neuroscience

G. Barbone[1], A. Bravin[2], B. Brun[2], A. Mittone[2], G. Le Duc[2], G. Battaglia[3], P. Romanelli[4], P. Coan[1,5]
[1]Department of Physics, Ludwig Maximilians University, 1 Am Coulombwall, Garching, 85748, Germany
[2] European Synchrotron Radiation Facility (ESRF), Grenoble 38043, France
[3] Department of Molecular Pathology, Neuropharmacology Section, I.R.C.C.S. Neuromed,
86077 Pozzilli, Italy
[4] AB Medica, 31 via Nerviano, 20020 Lainate, Milano, Italy
[5] Department of Clinical Radiology, Ludwig Maximilians University, 15 D Marchioninistr., Munich, 81377 Germany

Purpose: The advent of modern neuroimaging with computed tomography (CT) and magnetic resonance (MR) imaging has allowed for a better diagnosis and characterization of brain abnormalities and diseases. Despite the deep insights offered by these imaging methods, their sensitivity and/or spatial resolution are insufficient to study the structures of this very complex tissue at the cellular level. X-ray phase contrast imaging may provide the opportunity to overcome many of the limitations affecting current diagnostic methods [1-8].
Materials/methods: Pre-clinical imaging on the micro- and nano-scale with multidimensional resolution (spatial, temporal and chemical) is possible when high intensity, energy selective and collimated photon beam are used. Advanced X-ray phase contrast imaging techniques have been developed and used for investigating excised rat and human cerebella without the application of any stain or contrast agent.
Results: Images clearly depict the hippocampus and cerebellum regions (with white and gray matter) and the substantia nigra structure. Normal and tumor tissues are also effectively discriminated.
Conclusions: Proof of principle studies in phase contrast micro-CT were performed on irradiated rat brains, demonstrating the ability of the method in visualizing not only the fine architecture of the organ but also the effects of the treatment. Data are validated by comparison with histology. This presentation will give an overview of the recent results produced in pre-clinical neuroimaging research.

Keywords: Phase Contrast Imaging, Neuroscience, X-Ray

References:

[1] P. Coan et al. Investigative Radiology, 45(7), 2010.
[2] Pfeiffer et al. Physics in Medicine and Biology, 52(23), 2007.
[3] McDonald et al. J. Synchrotron Radiation, 16, 2009.
[4] Rutishauser et al. Optics Express, 19(25), 2011.
[5] Beltran et al. Physics in Medicine and Biology, 56(23), 2011.
[6] Schulz et al. J. Royal Society Interface, 7(53), 2010.
[7] Connor et al. Neuroimage, 46(4), 2009.
[8] Pinzer et al. Neuroimage, 61(4), 2012.

14

Alanine as a Dose Verification Tool for Carbon Ion In-Vivo Irradiation

N. Bassler[1], L. Grzanka[2,3], M. Scholz[4], T. Friedrich[4], M. Durante[4], P. Sharpe[5], H. Palmans[5], B. S. Sørensen[6]
[1] Dept. of Physics and Astronomy, Aarhus University, Denmark
[2] Institute of Nuclear Physics Polish Academy of Sciences, Cracow, Poland
[3] AGH University of Science and Technology, Krakow, Poland
[4] GSI Helmholtzzentrum für Schwerionenforschung, Darmstadt, Germany
[5] National Physical Laboratory, Acoustics and Ionising Radiation Division, United Kingdom
[6] Dept. of Experimental Clinical Oncology, Aarhus University Hospital, Denmark

Purpose: Alanine pellets provided by the National Physical Laboratory (UK) have been proposed as a dose verification tool in hadron beams. Multiple studies demonstrate a relatively weak and reproducible dependence on the mixed radiation environment found in Spread out Bragg peaks in ion therapy. Quenching effects can be modeled with little effort, in conjunction with Monte Carlo particle transport codes [1].
Methods: During the in-vivo irradiation with C-12 ions presented in the paper [2] several pellets of Alanine were positioned at the same SOBP depth where the tumor target was located. Alanine pellets were provided and read out by NPL in Teddington, UK. The resulting dose-to-water is translated to dose-to-alanine, and compared with the quenching corrected calculated dose-to-alanine calculated with Monte Carlo simulations.
The Monte Carlo particle transport code FLUKA was used to simulate the mixed particle spectrum along the beam. The Hansen & Olsen response model [1,3] is provided as a user function and linked into the FLUKA runtime.
Results: Most experimental dose-to-alanine valued agree within a few percent to the predicted and quenching corrected values. Quenching factors are found to be around 0.75 at the center of a 3 g/cm2 wide Carbon ion SOBP, 7.3 g/cm2 deep with a dose average LET of ~60 keV/µm.
Conclusions: We have successfully demonstrated the use of the Alanine dosimeter in an in-vivo dose verification setting. Alanine pellets appear to be a robust solid state dosimeter, provided information of the mixed radiation field can be retrieved by supplemental Monte Carlo calculations.

Keywords: Alanine, solid state dosimetry, carbon ions

References:

[1] N. Bassler, J.W. Hansen, H. Palmans, M. H. Holzscheiter, S. Kovacevic, NIM B, 266, 2008, p 929-936
[2] B.S. Sørensen, M.R. Horsman, J. Alsner, J. Overgaard, M. Durante, M. Scholz, T. Friedrich, N. Bassler, Acta Oncol.,54:9,2015 Epub ahead of print.
[3] J.W. Hansen, K.J. Olsen, Appl. Radiat. Isotopes 40, 935, 1989. p 10-12.

15

Variable RBE in proton therapy: comparison of model predictions and their impact on clinical-like cranial lesions

J. Bauer[1,2], G. Giovannini[2,3,4], T.T. Böhlen[3,6,*], G. Gabal[3,*], T. Tessonnier[2,3], K. Frey[3,*], J. Debus[1,2], A. Mairani[1,5], K. Parodi[1,2,3]
[1] Heidelberg Ion Beam Therapy Center, Heidelberg, Germany
[2] Department of Radiation Oncology, University Hospital Heidelberg, Germany
[3] Department of Medical Physics, Ludwig-Maximilians University Munich, Germany
[4] Department of Physics, University of Pavia, Italy
[5] Medical Physics Unit, CNAO Foundation Pavia, Italy
[6] European Organisation for Nuclear Research CERN, Geneva, Switzerland
* This author contributed to the work during her/his past employment at the indicated institution(s)

Purpose: Experimental evidence suggests a variable relative biological effectiveness (RBE) of clinical proton beams. As the spread in data is large a conservative choice of 1.1 is used in clinical practice world-wide. Due to an increasing interest several radio-biological models have been developed trying to represent the complex dependencies that determine RBE. We compare predictions obtained from such models for clinical-like cranial irradiations.
Material/methods: Three models proposed in the literature [1,2,3] were implemented to an in-house Monte-Carlo-based dose forward-calculation engine [4,5]. They were applied to

two scenarios defined by different tissue parameter values $(\alpha/\beta)_x$ representing high and low radio-sensitivity. We systematically compared RBE predictions as a function of $(\alpha/\beta)_x$ and proton linear energy transfer (LET) values in a spread-out Bragg peak (SOBP) in water and analysed results on patient-CT anatomy for cranial irradiation in terms of absorbed dose-to-water, dose-averaged LET (LET_D), RBE-weighted dose-to-water and biological range shift distributions.

Results: Different levels of agreement depending on $(\alpha/\beta)_x$ and LET values were found in the systematic comparison of RBE predictions. The SOBP study emphasizes a variation of LET_D and RBE not only as a function of depth but also of lateral distance from the central beam axis. Applying the different models to cranial treatment plans we observe consistent discrepancies from the values obtained for a constant RBE of 1.1 when using the variable RBE scheme in tissues with low $(\alpha/\beta)_x$, regardless of the model. An example is reported in figure 1. Biological range shifts of (0.6-2.4) mm (high $(\alpha/\beta)_x$) and (3.0-5.4) mm (low $(\alpha/\beta)_x$) were found in the fall-off analysis of individual profiles of RBE-weighted fraction dose along the beam penetration depth.

Conclusions: Although more experimental evidence is required to validate the accuracy of the investigated models, their consistent trend suggests that their main RBE dependencies should be included in treatment planning systems. Evaluation of the impact of a variable RBE scheme on the plan optimized using a constant RBE would thus be enabled, constituting a first step towards a more robust choice of biological dose delivery in proton therapy.

Keywords: Proton therapy, RBE-weighted dose, Monte Carlo

We acknowledge funding from BMBF (SPARTA), DFG (KFG Schwerionentherapie 214 and MAP Cluster of Excellence) and EU (ENVISION and Erasmus Exchange Program).

References:

[1] Carabe-Fernandez, A. et al., *Int. J. Rad. Biol. 83, 27-39* (2007)
[2] Wedenberg, M. et al., *Ancta Oncol. 52, 580-88* (2013)
[3] Elsaesser, T. et al., *Int. J. Rad. Oncol. 78(4), 1177-83* (2010)
[4] Bauer, J. et al., *Phys. Med. Biol. 59, 4635-59* (2014)
[5] Mairani, A. et al., *Phys. Med. Biol. 58, 2471-90* (2013)

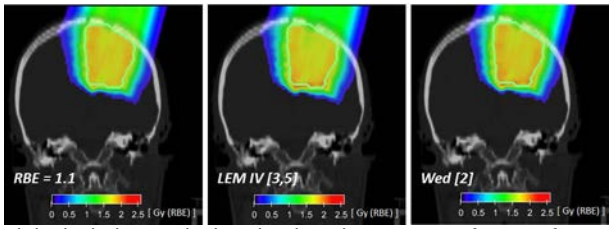

Biological dose calculated using the constant factor of 1.1 (left) or two different radio-biological models [2,3,5] for low $(\alpha/\beta)_x$, overlaid on the treatment planning CT image; Contour outlines the physical target volume.

16

Biological stratification in times of highly conformal radiotherapy - status and perspectives

M. Baumann[1,2,3,4]
[1] OncoRay – National Center for Radiation Research in Oncology, Faculty of Medicine and University Hospital Carl Gustav Carus, Technische Universität Dresden, Helmholtz-Zentrum Dresden – Rossendorf, Dresden, Germany
[2] Department of Radiation Oncology, Faculty of Medicine and University Hospital Carl Gustav Carus, Technische Universität Dresden, Dresden, Germany
[3] Helmholtz-Zentrum Dresden - Rossendorf, Institute of Radiooncology, Dresden, Germany
[4] German Cancer Consortium (DKTK), Dresden and German Cancer Research Center (DKFZ), Heidelberg, Germany

Radiotherapy has proven efficacy to inactivate cancer stem cells and is a highly personalized treatment modality, tailoring treatment plans for each individual patient based on precise anatomical information on tumor size and location as well as on normal tissues in the irradiated volume. Models based on clinical data, radiobiology and radiation physics are routinely used in radiotherapy for generating individualized space-resoluted radiation dose distributions, as well as for assessment of tumor control probability- vs. normal tissue complication-models. Tremendous improvement in high-precision radiation delivery and planning technology has been achieved during the past decades and rapidly been translated into clinical practice.

The new frontier in radiation oncology-related research is now to bring together advances in tumor and molecular biology with the full potential of high-precision radiation technology. Examples of these developments include the discovery and assessment of biomarkers specific for radiotherapy, the combination of radiotherapy with molecular targeted drugs, and the individualization of treatment planning by biological imaging. Individualized radiotherapy in the future will integrate biological information on the specific tumor and on surrounding normal tissues in the treatment strategy of patients. Novel predictive and prognostic markers demonstrate high potential for advancing personalized radiation oncology in preclinical and clinical-translational studies. So far this applies for stratified selection of total dose, however, in the future also personalized dose-distribution and fractionation parameters as well for the combined therapies of radiation with specific drugs might become predictable by biomarkers. A specific feature of personalized radiation oncology is that already broad biological stratification of patients has the potential to remarkable advance individualization of therapy as this information adds a power-function to the fully anatomically-personalized dose-distributions clinically achieved today.

This talk will review preclinical and clinical examples of potential strategies to increase cure rates by adding a biology dimension (e.g. predictive/ prognostic markers) to personalized radiation oncology.

Keywords: biological stratification, biomarkers, high precision radiotherapy, personalized radiation oncology

17

Accuracy of portal dosimetry in hybrid IMRT and VMAT treatment of the prostate

J. Bedford, I. Hanson, G. Smyth, A. Tree, D. Dearnaley and V. N. Hansen
The Institute of Cancer Research and The Royal Marsden NHS Foundation Trust, London, UK

Purpose: Several studies indicate the potential dosimetric benefit of combining IMRT and VMAT in a hybrid approach [1, 2]. This study evaluates the accuracy of in-vivo portal dosimetry for a variety of hybrid IMRT and VMAT plans for radiotherapy of the prostate.

Materials/methods: Hybrid IMRT and VMAT plans were retrospectively constructed for five prostate patients. Three PTVs were used, namely PTV74Gy, PTV71Gy and PTV60Gy. For each patient, seven 6MV plans were created: a conformal VMAT arc, a VMAT arc with limited modulation, and five hybrid IMRT / VMAT arcs, with 0%, 25%, 50%, 75% and 100% IMRT respectively, with 0% corresponding to normal VMAT and 100% corresponding to 11-beam IMRT. All plans consisted of a single anticlockwise arc with 111 segments ranging in gantry angle from 110° to 250°. The hybrid plans were created by grouping the control points into 20° groups, and then selecting the groups with the most complex intensity maps for sequencing as IMRT, with the remaining groups sequenced for VMAT.

Predicted integrated portal images were created for all plans as delivered to a water-equivalent phantom [3]. The plans were then delivered to the phantom as a single beam sequence using an Elekta Synergy accelerator with Agility head and integrated images were measured using an Elekta iViewGT portal imager. Predicted and measured images were compared in terms of mean gamma and percentage

gamma less than unity at the 3% / 3 mm level. The dose at the treatment isocentre was also measured using a Farmer ionisation chamber and treatment times were recorded.

Results: A typical treatment plan is shown in Figure 1, together with the predicted portal image, the measured portal image and the gamma comparison. Table 1 summarises the results for all plans and patients. Predicted images show particularly good agreement for conformal and limited-modulation VMAT plans due to the simplicity of the plans, but the agreement is also acceptable for the considerably more complex hybrid plans.

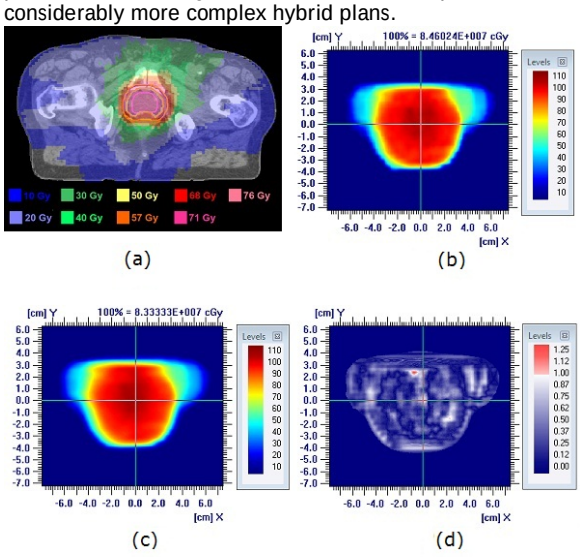

Figure 1. Typical results for a hybrid arc with 25% IMRT. (a) transaxial dose distribution, (b) predicted portal image, (c) measured portal image and (d) gamma distribution for 3% and 3 mm.

Table 1. Mean (±1 SD) gamma (G) and ionisation chamber results for conformal VMAT (C), limited-modulation VMAT (LM), and hybrid IMRT / VMAT (H).

	TECHNIQUE (with percentages of IMRT)						
	C VMAT	LM VMAT	H 0%	H 25%	H 50%	H 75%	H 100%
Mean G 3%/3mm	0.32±0.03	0.31±0.02	0.31±0.05	0.36±0.07	0.36±0.04	0.39±0.17	0.42±0.11
G<1 3%/3mm(%)	99.8±0.2	99.8±0.4	98.0±2.3	96.2±5.1	98.4±1.9	94.9±10.8	97.7±3.8
Total monitor units	319±13	352±14	345±15	378±14	391±16	404±13	410±12
Dose vs plan (%)	0.6±0.4	0.7±1.1	1.6±1.5	1.8±1.7	1.8±1.7	0.9±1.0	0.4±0.7
Delivery time (s)	44±2	56±2	76±4	201±9	276±16	380±28	439±36

Conclusions: Portal dosimetry can be carried out accurately and effectively for hybrid IMRT and VMAT treatments. The 25% IMRT hybrid plan is of most interest practically as it offers improved dosimetry without taking a long time to deliver, and this plan shows acceptable accuracy of verification with portal dosimetry.

Keywords: portal dosimetry, IMRT, VMAT

References:

[1] Matuszak MM, Steers JM, Long T, McShan DL, Fraass BA, Romeijn HE, Ten Haken RK. FusionArc optimization: a hybrid volumetric modulated arc therapy (VMAT) and intensity modulated radiation therapy (IMRT) planning strategy. Med Phys 2013;40:071713.

[2] Robar JL, Thomas C. HybridArc: A novel radiation therapy technique combining optimized dynamic arcs and intensity modulation. Med Dosim 2012;37:358-68.

[3] Bedford JL, Hanson IM, Hansen VN. Portal dosimetry for VMAT using integrated images obtained during treatment. Med Phys 2014;41:021725.

18

Implementation of an analytical solution to lateral dose prediction in a proton therapy treatment planning system.

E. V. Bellinzona[1,2,3], G. Landry[3], A. Fontana[2], A. Embriaco[1,2], A. Resch[3,6], M. Ciocca[4], A. Ferrari[5], F. Kamp[6,7], A. Mairani[4,8], P. Sala[9], T. Tessonnier[8], J. Wilkens[6], A. Rotondi[1,2], K. Parodi[3,8]

[1] Dipartimento di Fisica, Università degli Studi di Pavia, 27100 Pavia, Italy

[2] Istituto Nazionale di Fisica Nucleare (INFN), Sezione di Pavia, 27100 Pavia, Italy

[3] Department of Medical Physics, Ludwig Maximilians University, Munich, Germany

[4] Centro Nazionale di Adroterapia Oncologica (CNAO), 27100 Pavia, Italy

[5] European Organization for Nuclear Research CERN, CH-1211, Geneva 23, Switzerland

[6] Department of Radiation Oncology, Technische Universität München, Klinikum rechts der Isar, Munich D81675, Germany

[7] Department of Radiation Oncology, Ludwig-Maximilians-University, Marchioninistr. 15, 81377 München, Germany

[8] Heidelberg Ion Beam Therapy Center (HIT), Heidelberg, Germany

[9] Istituto Nazionale di Fisica Nucleare (INFN), Sezione di Milano, 20133 Milano, Italy

Purpose: This work aims to present a flexible computational model for the calculation of the lateral deflection of a pencil proton beam, and the preliminary results of its implementation in a Treatment Planning System (TPS) instead of the currently used Double Gaussian approximation (DGA) in water.

First evidences show that the model has better accuracy with fast computation time in water; it is reliable for any depth and for every kind of media and mixture, since energy loss effects by the primary process are fully taken into account.

Methods: Challenging issues in TPS for hadrontherapy are the accurate calculation of dose distribution, the reduction in memory space required to store the dose kernel of individual pencil beams and the shortening of computation time for dose optimization and calculation.

In this framework, prediction of lateral dose distributions is a topic of great interest because, currently, a DGA [1], [2] is typically used as approximation; although other parameterizations are also available [3], [4], [5]. The best accuracy in this kind of calculations can be obtained by Monte Carlo (MC) methods [6], but at the expense of a too long computing time.

As alternative, we propose a flexible model based on the full Molière theory for Coulomb multiple scattering [7]. The use of the original equations of the theory allows to remove any free parameter for the electromagnetic interaction with the advantage of full accuracy with a reasonable increase in the computing time. The contribution of the nuclear interactions are also fully taken into account with a two-parameters fit, on FLUKA simulation [8],[9]; this part is added to the electromagnetic core with a proper weight [10].

Model is currently under testing in a particle therapy extension of CERR - A Computational Environment for Radiotherapy Research [11], [12] TPS, in order to compare the results with the actual dose prediction in water.

Results and Conclusions: The model has been first compared to MC predictions for protons in water, for different depths and therapeutic energies, and also with some experimental data from Heidelberg Ion-Beam Therapy Center (HIT), generally showing very good agreement.

The comparison of the CERR dose distribution calculated using DGA with the one predicted by the computational model is shown in Figure 1 together with FLUKA MC prediction.

The DGA has a lateral cutoff distance from the central ray that is used to determine the points that do not require dose calculation that has been set at maximum possible value 4 (in multiples of the gaussian lateral extend at the end of the decay area).

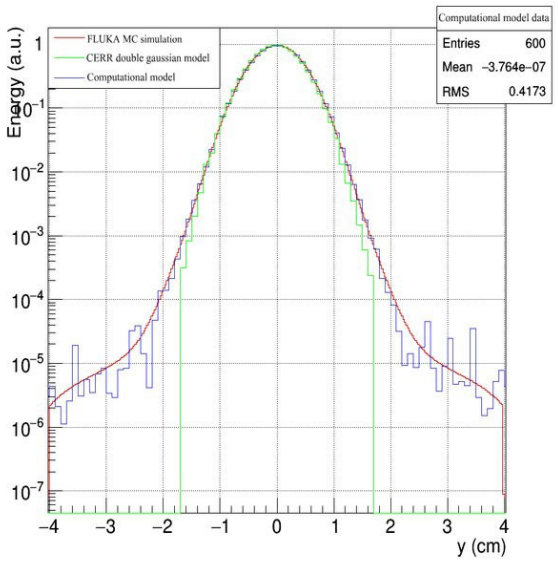

Fig.1 Comparison between Fluka MC simulation (red line), dose distribution evaluated with CERR using Double Gaussian model (green line) and dose predicted by standalone computational model (blue line) for a proton initial beam energy of 60MeV, initial σ of 0.4cm, at a normalized depth 0.9 (assuming Bragg peak position at 1)

The preliminary results show that the model is able to predict dose with better accuracy than DGA.
So, this model could be a step forward in lateral dose prediction for current TPS and as a future application, a useful tool for online dose-evaluation and adaptive planning; next step will be the implementation of different media and geometries.

Keywords:
Proton-therapy, Treatment Planning System, Molière lateral dose distribution.

References:
[1] Frühwirth R., Regler. M., Nuclear Instruments and Methods in Physics Research 369 (2000)
[2] Parodi K., Mairani A., Sommerer F., J. Radiat. Res. J Radiat Res 2013 Jul;54 Suppl 1:i91-6, (2013)
[3] Bellinzona V. E. et al., Physica Medica doi: 10.1016/j.ejmp.2015.05.004 (2015) [4] Soukup M. et al., Phys. Med. Biol. 50, 5089-5104 (2005)
[5] Pedroni E. et al.,Phys. Med and Biol. 50 541-61(2005) [6] Paganetti H., Phys Med Biol.; 57:R99-117 (2012)
[7] Bellinzona E. V., Ciocca M., Embriaco A., Ferrari A., Fontana A., Mairani A., Parodi K., Rotondi, A., Sala P., Tessonnier T., A model for the accurate computation of the lateral scattering of protons in water, (under review)
[8] Bohlen T.T. et al., Nuclear Data Sheets 120, 211-214, (2014)
[9] Ferrari A. et al., CERN-2005-10, INFN/TC05/11, SLAC-R-773, (2005)
[10] Ulmer W., Rad. Phys. and Chem. 76 1089-107 (2007)
[11] Deasy J.O . et al., Medical physics 30.5: 979-985(2003)
[12] Schell S. and Wilkens J. J., Medical Physics, 37(10):5330–40, 2010.

19

A clinical protocol for Simultaneous Integrated Boost for proton treatment of Head and Neck carcinoma

M. F. Belosi, R. Malyapa (MD), A. Bolsi, A. J. Lomax, D. C. Weber (MD) [1]
[1] Paul Scherrer Institut, Center for Proton Therapy (5232 Villigen)

Purpose: To define the clinical protocol for Head and Neck (H&N) patients treated with Proton Pencil Beam Scanning (PBS) at Paul Scherrer Institute (PSI, Villigen CH) with Simultaneous Integrated Boost (SIB). The focus was mainly to define the optimization parameters and the normalization procedure to obtain a steep gradient between the elective and the boost volume, in order to reduce over-dosage in the fall off area of the boost.
Material and Methods: 7 patients, treated at PSI for different H&N carcinomas, were selected for this study. They were all originally treated with two sequential series at 2GyRBE; the 1st one up to 54GyRBE to the elective Planning Target Volume (PTV1), followed by a second series up to 72GyRBE for the boost target volume (PTV2). In this study, all have been re-planned using a SIB regimen of 1.8GyRBE (up to 54GyRBE) to PTV1 and 2.36GyRBE (up to 70.8GyRBE) to PTV2 for a total of 30 fractions. Dose constraints to the OARs were kept as for the sequential approach [1]. All plans were designed on the PSIPlan Treatment Planning System using Intensity Modulated Proton Therapy (IMPT) with non-coplanar fields. The prescription dose of 100% corresponded to the average dose to PTV1, while the dose to PTV2 was optimized prescribing a boosting factor based on the ratio of the two different prescribed dose levels (i.e. 54GyRBE and 70.8 GyRBE). Depending on the ratio of the PTV1 and PTV2 volumes the boosting factor was prescribed to PTV2 or to a smaller structure (GTV or PTV2-3mm). To guarantee dose homogeneity in the dose gradient region between PTV1 and PTV2, the optimized SIB plans were normalized such that 54GyRBE corresponded to the average dose to [PTV1-(Boost volume+3mm)]. This avoided over-dosages close to PTV2 being compensated by under-dosages at the PTV1 margin.
Results: The choice of the boosted volume, the boosting factor, the quality and conformity of the SIB plans were observed to be dependent on the volume ratio PTV2/PTV1. For the analyzed patients, this ranged from 28.8% to 61.7%. For differences in the PTV1 to PTV2 volume larger than 40%, either a PTV2-3mm or the GTV itself were selected for the boosting. Else no gradient could be observed. When compared to the nominal sequential plan, the SIB approach resulted in both a lower mean dose to the ring area (average value for SIB: 55.2±1.0 GyRBE; average value for sequential: 64.1±3.6 GyRBE), and 0.6±0.4% as average ring volume receiving the 95% of the dose prescribed to the boost (the same dose parameter was >10% for all the original plans). A similar sparing of OARs was obtained with both treatment schedules.
Conclusion: Planning H&N patients with SIB optimization resulted in dose distributions which guaranteed the PTV2 and PTV1 coverage and conformity whilst keeping dose to OARs within tolerance. Therefore this approach can be transferred to the clinical operation and has already been applied to a first patient.

Keywords: over-boosting, gradient, boosting factor

References:
[1] Andrew Lauve, M. Morris, R. Schmidt-Ulrich et al. Simultaneous Integrated Boost intensity-modulated Radiotherapy for locally advanced Head-and-Neck squamous cell carcinomas: II-clinical results. Int J Rad Oncol Biol Phys 2004; 60 (2): 374-387.

20

Gamma Locator for Radionuclide Diagnostics Of Oncological Diseases

A. K. Berdnikova[1], V. N. Belyaev[1], A. I. Bolozdynya[1], V. A. Kantserov[1], V. V. Sosnovtsev[1], K. I. Zhukov[2]
[1] National Research Nuclear University MEPhI, Moscow, Russian Federation
[2] P.N. Lebedev Physical Institute of the Russian Academy of Sciences, Moscow, Russian Federation

Gamma locator is a handheld lightweight and compact gamma probe based on a scintillation crystal $LaBr_3$:Ce and silicone photomultiplier to be used for detection of gamma-radiation emitted by radionuclides such as ^{99m}Tc, ^{125}I, ^{111}In, ^{18}F [1].
There are two main applications of gamma locator: intraoperative detection of sentinel lymph nodes and non-invasive scanning the surface of the body. In the first case, a radiotracer is injected into the patient preoperatively and

surgeon checks the presence of metastasis in the lymph nodes after the removal of the tumor. In the second case, the gamma locator can detect tumors located superficially, and accurately determine their boundaries [2].
When selecting the scintillator the following requirements should be considered: high relative light yield compared to NaI(Tl), the high value of the effective atomic number. The lanthanum cerium bromine has demonstrated the best features: the light yield higher than that of NaI(Tl) (130%), high density, high atomic number provide high efficiency of photoelectric absorption of gamma rays, and the decay time of the order of tens of nanoseconds provides high temporal resolution of the detector. Silicon photomultiplier is a device for detection of low intensive and very fast (several hundred nanosecond duration) light flashes. SiPM is used due to its high detection efficiency, low bias voltage, compact dimensions and high gain of signals. Experimental studies have shown that a scintillator packaged together with the photodetector provides 4,1% FWHM energy resolution at 662 keV (Cs-137).
Gamma locator is constructed in cordless configuration and equipped with a lithium-ion battery. Indication is performed by an acoustic signal and LED. Adjusting of the bias voltage of the photodetector and the thresholds of the discriminator is carried out by changing the resistance of the trimmers.
The main technical characteristics of the prototype gamma locator were determined in the laboratory of NRNU MEPhI according to the NEMA NU3-2004 protocol [3]. Spatial resolution of gamma locator is the minimum distance between two point sources on which they can be resolved separately, or FWHM of the dependence of counting rate of the transverse distance between the detector and the source, and is measured to be 20 mm. Spatial selectivity is the polar angle, at which the count rate drops twice and it is measured to be 26 degrees. Sensitivity is 118 cps/MBq.
For the comparison performance of scintillation and semiconductor gamma locator the NEMA testing of the semiconductor CdTe-based commercial gamma probe was performed. The field of view of the CdTe gamma probe was formed with a lead collimator with 3 mm diameter aperture. Spatial resolution was measured to be 22 mm, and angular resolution is 30 degrees.

Keywords: gamma probe, miniature gamma detector, radioguided surgery

References:
[1] A. K. Yagnyukova, A. I. Bolozdynya, V. A. Kantserov, et al, "A γ Probe for Radionuclide Diagnostics of Cancer", Instruments and Experimental Techniques, 2015, Vol. 58, No. 1, pp. 153–157
[2] P. Fougeres, A. Kazandjian, V. Prat, H. Simon, M. Ricard, J. Bede, "Sentinel node in cancer diagnosis with surgical probes", Nucl. Instrum. and Methods in Physics Research. 2001. V. A 458. P. 34.
[3] Performance measurements and quality control guidelines for non-imaging intraoperative gamma probes, NEMA Standards Publication NU 3-2004.

21
Evaluation of the size of micrometric/nanometric dosimeters for use in radiotherapy and medical physics
M. Cunha[1], E. Testa[1], M. Beuve[1], J. Balosso[2,3], A. Chaikh[2,3]
[1] Université de Lyon, F-69622, Lyon, France; Université de Lyon 1, Villeurbanne; CNRS/IN2P3, Institut de Physique Nucléaire de Lyon
[2] Department of Radiation Oncology and Medical Physics, Grenoble University Hospital.
[3] Univ. Grenoble-Alpes, Grenoble, France.

When treating tumors with radiotherapy, it is of utmost importance to ensure that the prescribed dose is accurately delivered to the target volumes. In that sense, *in-vivo* dosimetry in real time was recently implemented in radiotherapy departments. Dosimeter performance depends necessarily on physical and geometrical parameters (e.g. beam energy and distance from source to skin), which implies the use of correction factors. Implantable dosimeters are therefore preferable in order to minimize the need for corrections. They should be as small as possible, but still they should provide reliable measurements to comply with the requirements of clinical practice in routine radiotherapy. The state-of-the-art of these kind of dosimeters was the subject of a review elsewhere (1), which reported that implantable detectors of submillimetric size are currently available. The purpose of this study is to assess by Monte-Carlo simulations how much the size of such dosimeters can be decreased without jeopardizing their performance in a clinical environment.
First, the interaction of photons from a ^{60}Co source with water was simulated with a Monte-Carlo tool (2). The calculations were performed for 0.3, 0.1, 1, 3 and 10 Gy. Then, the distributions of specific energy were obtained for volumes representing dosimeters at nanometric and micrometric scales. Cylinders with equal radii of 0.3, 0.1, 1, 3 and 10 µm were used for this purpose. The mean specific energy $<z_t>$ was calculated for each case. To evaluate how the dosimeter size would impact its performance in a clinical scenario, the probability *p* that a dosimeter measurement falls outside a given interval defined around $<z_t>$ was estimated. Intervals were defined as $[<z_t>-\gamma<z_t> ; <z_t>+\gamma<z_t>]$ with γ equal to 3%, 5% and 10%.
The pattern of the distributions of specific energy evolves with dosimeter size and irradiation dose. Fixing the irradiation dose and decreasing the dosimeter radius or fixing the radius and decreasing the irradiation dose strongly widened the range in measured values of specific energy, but also increased the probability of yielding a non-null measurement. In turn, for higher doses and radii, distributions tend to Gaussian curves.

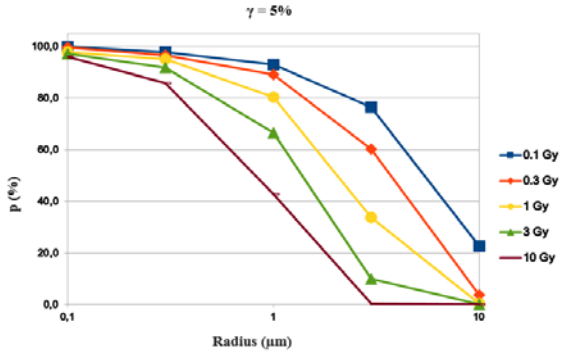

Concerning the probability of obtaining a measurement outside the defined interval, the larger the interval, the irradiation dose, and the dosimeter radius, the smaller this probability became (see figure above).
The simulation results showed that dosimeters at a nanometric scale are not able to yield statistically-reproducible measurements and are therefore unfit for use in clinical practice. Increasing the size to micrometric scale led to a decrease in the statistical fluctuations. Nevertheless, to have enough accuracy at routine clinical doses (approximately 2 Gy in the tumor volume), a dosimeter radius of at least 10 µm is required.

Keywords: radiotherapy; nano/microdosimeter; Monte-Carlo simulations

References
[1] Chaikh A, Beuve M, Balosso J. Nanotechnology in radiation oncology: The need for implantable nano dosimeters for in-vivo real time measurements. Int J Cancer Ther Oncol [Internet]. 2015 [cited 2015 Oct 30];3(2). Available from: http://www.ijcto.org/index.php/IJCTO/article/view/ijcto.32.17
[2] Gervais B, Beuve M, Olivera GH, Galassi ME. Numerical simulation of multiple ionization and high LET effects in liquid water radiolysis. Radiat Phys Chem. 2006 Apr;75(4):493–513.

22
From 2D to 3D: Proton radiography and proton CT in proton therapy: A simulation study

J. Takatsu[1], E. R. van der Graaf[2], M-J. van Goethem[3], S. Brandenburg[2],
A. K. Biegun[2]
[1] Department of Radiation Oncology, Graduate School of Medicine, Osaka University, Japan
[2] KVI-Center for Advanced Radiation Technology, University of Groningen, The Netherlands
[3] Department of Radiation Oncology, University Medical Center Groningen, University of Groningen, The Netherlands

Purpose: In order to reduce the uncertainty in translation of the X-ray Computed Tomography (CT) image into a map of proton stopping powers (3-4% and even up to 10% in regions containing bones [1-8]), proton radiography is being studied as an alternative imaging technique in proton therapy. We performed Geant4 Monte Carlo simulations for a 2-dimentional (2D) proton radiography system to obtain directly proton stopping powers of the imaged object. In the next step, the object was rotated every 10 degrees to obtain the 3D proton CT, and the iterative reconstruction method was used to reproduce the image.
Materials/methods: In our proton radiography simulation setup (figure) we used two ideal (100% efficiency) position sensitive detectors (red squares), with the size of 10x10 cm^2 each, to track a single proton entering and exiting a phantom under study. The residual energy of a proton was detected by a BaF_2 crystal (yellow cylinder), with a diameter of 15 cm, placed after the second position sensitive detector. A cylindrical phantom with a 2.5 cm diameter and 2.5 cm height was made of CT solid water (Gammex 357, ρ=1.015 g/cm^2) and filled with different materials: PMMA (ρ=1.18 g/cm^2, red insert), air ($\rho=1.21\bullet10^{-3}$ g/cm^2, below and/or above each inserts), and tissue-like materials: adipose (Gammex 453, ρ=0.92 g/cm^2, yellow insert) and cortical bone (Gammex 450, ρ=1.82 g/cm^2, blue insert) [9]. The phantom was irradiated with 3x3 cm^2 scattered proton beam with an energy of 150 MeV. It was irradiated with $2\bullet10^5$ protons at each of the 36 rotation angles. The phantom was placed perpendicularly to the beam direction allowing a proton to pass through a number of materials with different densities.

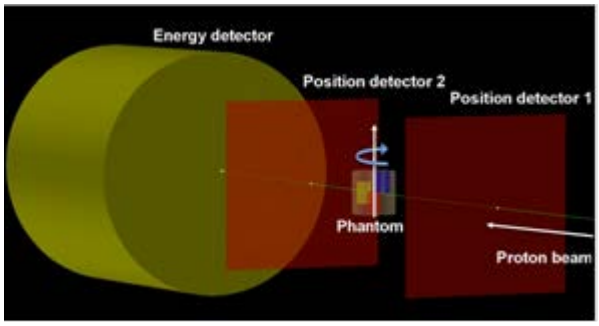

Results: First, the energy loss radiographs (a difference between proton beam energy and residual energy deposited in the energy detector) at each of the 36 phantom rotation angles were created. For the iterative reconstruction algorithm, a reference image of the phantom was created in two ways: (1) based on the energy loss in different phantom materials simulated with Geant4, and (2) using a simple back projection algorithm. The reconstruction agrees well with the actual phantom. A maximum of 50 iterations were used showing the smallest mean squared error already after 5 iterations.
Conclusion: First attempt to iteratively reconstruct the cylindrical phantom with more materials on the proton beam shows a satisfactory result. To improve the reconstruction at the material boundaries, additional local iterations will be applied.

Keywords: Proton radiography, proton CT, treatment planning

References:
[1] U. Schneider and E. Pedroni, *Proton radiography as a tool for quality control in proton therapy*, Med Phys 22(4) (1995) 353-363
[2] U. Schneider, E. Pedroni and A. Lomax, *The calibration of CT Hounsfield units for radiotherapy treatment planning*, Phys Med Biol 41 (1996) 111-124
[3] W. Schneider, T. Bortfeld and W. Schlegel, *Correlation between CT numbers and tissue parameters needed for Monte Carlo simulations of clinical dose distributions*, Phys Med Biol 45 (2000) 459-478
[4] G. Cirrone et al., *The Italian project for a proton imaging device*, Nucl Instr Meth in Phys Res A576 (2007) 194-197
[5] H. Paganetti, *Range uncertainties in proton therapy and the role of Monte Carlo simulations*, Phys Med Biol 57 (2012) R99-R117
[6] T. Plautz et al., *200 MeV Proton Radiography Studies with a Hand Phantom Using a Prototype Proton CT Scanner*, IEEE Trans on Med Imag 33 (4) (2014) 875-881
[7] G. Landry et al., *Deriving concentrations of oxygen and carbon in human tissues using single- and dual-energy CT for ion therapy applications*, Phys Med Biol 58 (2013) 5029–5048
[8] J. Schuemann et al., *Site-specific range uncertainties caused by dose calculation algorithms for proton therapy*, Phys Med Biol 59 (2014) 4007-4031
[9] www.gammex.com

23
GPU based iterative CBCT for prospective motion compensated algorithm for radiation therapy

Author names – Initial. Surname (order the authors as you would like them to appear; underline the speaker's name)
A. Biguri[1], M. Dosanjh[2], S. Hancock[2], M. Soleimani[1]
[1] Engineering Tomography Lab (ETL), Electronic and Electrical Engineering, University of Bath, UK
[2] CERN, Geneva, Switzerland

Purpose: One of the common imaging techniques in image guided radiation therapy (IGRT) is cone beam computed tomography (CBCT). CBCT is used for tumor localization in pre-treatment planning. In lung radiation therapy, the motion artefacts severely affect the quality of reconstructed images. As the data acquisition can take over a minute, the motion generated by the patient breathing can distort the tomograms, this distortion being propagated in the image reconstruction step. We propose an electrical impedance tomography (EIT)-CBCT dual modality for motion corrected image reconstruction [2]. Iterative algebraic reconstruction method can potentially provide a suitable image reconstruction tool for such dual modality. This paper present an improved GPU based CBCT image reconstruction. Efficient computation of forward and backward projections is implemented in GPU, which is the main building block of various iterative reconstruction methods.
Materials/methods: The projection and backprojection steps have been accelerated in our GPU code, using the Compute Unified Device Architecture (CUDA) [1]. The ray-driven projection uses the texture memory that has a hardware implemented trilinear interpolation. Using a per-ray separation for the multithreading step, the integral of the x-rays is computed, with a user specified length that defines the tradeoff between for accuracy and speed. In the backprojection step, a voxel-based weighted backprojection is performed, similar to the Feldkamp Davis Kress (FDK) algorithm, to avoid the aliasing effect common in algebraic methods with diverging rays [4]. To simulate reality a human thorax-like digital phantom has been used. Limited (45) projections have been simulated and Poisson noise added. The commonly use FDK and simultaneous iterative reconstruction technique (SART) have been simulated.
Results: Figure 1 shows the reconstructed images. For a 512^3 voxels with 512^2 detector pixels the GPU based code takes 5s for FDK and a single SART iteration on the high precision setting (integral length= voxel size/10), and 0.5s for a similar precision as a matrix based method (integral length= voxel size). The image reconstructed with SART had 300 iterations, 2.5 minutes in the lower precision setting.

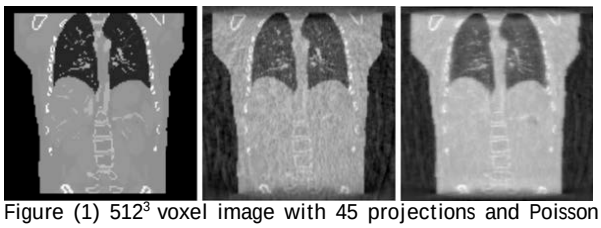

Figure (1) 512^3 voxel image with 45 projections and Poisson noise, (a) original (b) reconstruction using FDK, (c) reconstruction using SART.

In terms of speedup, a CPU projection takes 24s on average in an Intel Core i7-4930K with 32Gb of RAM while a GPU projection takes 137ms in high accuracy settings and 17ms with the same accuracy in a NVIDIA Tesla k40c, resulting on a speedup of 175% and 1400% respectively.
Figure 2 shows speed results for a single forward projection of a single angle in both low and high accuracy settings for different detector and image sizes, in logarithmic scale. It is easy to see in the figure that the algorithm is $O(n^3)$ for the image size and $O(n^2)$ for the detector size. Note that in the biggest image sizes memory bandwidth is a relevant factor in the time, as the image size in memory gets over 8Gb. Times for backprojection are always around 10% of the times for forward projection.

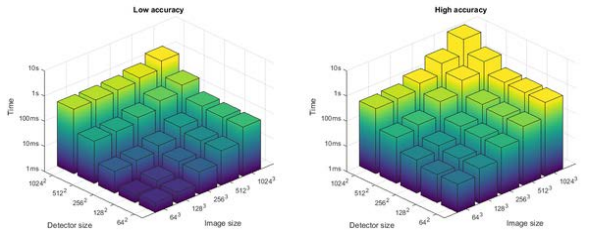

Figure (2) Time for a single projection in the GPU, compared against the number of voxels and the number of detector pixels, for different accuracy levels, (a) 1 sample per voxel (as in matrix based methods), (b) 10 samples per voxel.
Conclusions: The GPU based code speeds up the image reconstruction to over 3 orders of magnitude than CPU based algorithms, allowing the use of iterative reconstruction methods in clinically reasonable time scales. The future work involves modifying the algorithm for motion correction using the concepts from phase space tomography at CERN[3]. Additionally, an EIT based real-time motion detection will be used to better estimate patient motion, which can then be fed into CBCT reconstruction algorithm allowing for a dual modality based 4D CBCT.

Keywords: Cone Beam Computed Tomography, motion corrected imaging, electrical impedance tomography, lung radiation therapy, GPU

References:
[1] GPU-based cone beam computed tomography. Noël PB, Walczak AM, Xu J, Corso JJ, Hoffmann KR, Schafer S. Comput Methods Programs Biomed. 2010 Jun;98(3):271-7. doi: 10.1016/j.cmpb.2009.08.006. Epub 2009 Sep 25.
[2] Motion-compensated cone beam computed tomography using a conjugate gradient least-squares algorithm and electrical impedance tomography imaging motion data. Pengpen T, Soleimani M. Philos Trans A Math Phys Eng Sci. 2015 Jun 13;373(2043). pii: 20140390. doi: 10.1098/rsta.2014.0390.
[3] Longitudinal phase space tomography with space charge, S. Hancock, S. Koscielniak, M. Lindroos, International Computational Accelerator Physics Conference, Darmstadt, Germany, 10 - 14 Sep 2000. Publ. in: Physical Review Special Topics - Accelerators and Beams, vol. 3, 124202 (2000), (CERN-PS-2000-068-OP).
[4] Artefacts in CBCT: a review. Schulze R1, Heil U, Gross D, Bruellmann DD, Dranischnikow E, Schwanecke U, Schoemer E. Dentomaxillofac Radiol. 2011 Jul;40(5):265-73. doi: 10.1259/dmfr/30642039.

24

Current and future strategies developed at Paul Scherrer Institute

Bolsi A. [1], D.C. Weber[1], T. Lomax[1] and the CPT team.
[1] Center for Proton Therapy, Paul Scherrer Institute, Villigen CH

The Center for Proton Therapy at PSI has been the worldwide pioneer of pencil beam scanned (PBS) proton therapy. Clinical operation started in 1996 on Gantry1, with Intensity Modulated Proton Therapy already being delivered clinically in 1999. Currently the facility is composed of two gantries and one horizontal beam line for ocular therapy. Gantry2, clinically operational since 2013, is a new generation proton PBS gantry, developed in-house at PSI, whilst Gantry3, currently in the technical commissioning phase, will be a ProBeam Gantry from Varian Medical System. First patient treatments on this facility will be at the end of 2016.
Our future strategies are in a number of directions. First, we are working on significantly increasing the delivery speed of PBS treatments using continuous line scanning rather than discrete spots. This has already been demonstrated as a proof-of-principle on Gantry2, and the major work currently is on the development of fast beam monitoring, together with strategies for analyzing the resulting measured profiles.
Second, the treatment of moving targets (4D) will be clinically implemented based on different motion mitigation techniques, including advanced rescanning, gating and continuous scanning. For the optimization of the 4D treatment delivery, different scanning techniques (i.e. volumetric and layered rescanning) have been evaluated and both will be implemented clinically. In order to calculate the dosimetric effect of the interplay between motion and scanning, our in house developed TPS system has been upgraded to include a fast and comprehensive 4D dose calculation option based on a deformable dose calculation grid, where the timing of the delivery parameters and the patient breathing (including variable breathing patterns) can be accurately taken into account.
Our third aim is the clinical implementation of daily adaptive proton therapy, in order to more accurately take into account daily anatomical and positioning variations. As a CT-on-rails scanner is installed in the Gantry2 bunker, 3D planning images can be acquired on a daily basis and used for a daily optimization of the plan before the daily delivery. In addition, on the ProBeam system, Cone-Beam CT acquisitions will be possible, allowing us to also investigate the usefulness of CBCT for daily adaptive approaches. In the daily optimization process, the cumulative dose delivered to the patient will be estimated using log-file based dose calculations as a type of 'entrance-dosimetry' which can reconstruct the actual delivered dose in the patient geometry of the day. This is based on machine log files, which are saved for each delivery, and which include all the machine parameters for the specific delivery (i.e. exact spot position, spot weight, MU per spot[1]). Finally, we are also investigating advanced uses of MRI imaging in proton therapy, for instance to monitor anatomical changes, organ motion and in-vivo range verification.

Keywords: spot scanning, 4D treatment, adaptive proton therapy

References:
[1] Scandurra D., Albertini F., van der Meer R., Meier G., Weber D.C., Bolsi A., Lomax T. Assessing the quality of proton PBS treatment delivery using machine log files: comprehensive analysis of clinical treatments delivered at PSI Gantry 2. Accepted for publication, PMB.

25

Imaging for online control of particle therapy

T. Bortfeld[1] and J. Verburg[1]
[1] Department of Radiation Oncology, Massachusetts General Hospital and Harvard Medical School

The finite range of a proton beam or heavier charged particle beam can be a double-edged sword. While it is the biggest physical/dosimetric advantage of particle beam therapy, the range over- or undershoot typically requires extra margins that can compromise the conformality of the dose distributions substantially. Recent developments aim at imaging the range of the particle beam in the patient, to (1) verify the range, and (2) potentially correct for any range discrepancies. We will review the state of the art of imaging for range assessment, focusing in particular on prompt gamma imaging.
Significant progress has recently been made in the field of prompt gamma imaging. Range errors of 1 mm are detectable in phantoms. Spectroscopic methods potentially allow one to obtain information about the elemental composition of the tissue. Commercial systems are under development and have recently been tested in the clinic. In addition to systems consisting of a detector-collimator combination, Compton cameras are under development for the 3D reconstruction of the prompt gamma sources. Prompt gamma imaging competes with other range imaging techniques such as PET imaging of oxygen-15 and carbon-11, and MRI imaging of the biological changes resulting from irradiating tissues. Another recent development is thermo-acoustic imaging, utilizing the ultrasound signal that a high intensity particle beam produces in tissue due to quick thermal expansion.
Once the particle range in the patient can be measured (a) in the patient, (b) in realtime, (c) with millimeter accuracy, the range margins can be reduced, resulting in significant improvements of treatment quality for many disease sites. Unfortunately, none of the techniques developed so far fulfill all criteria (a,b,c) above. Millimeter accuracy is sometimes achievable but not in patients or not in all patients. Realtime measurement and control is only feasible with prompt gamma and thermo-acoustic imaging. Of the techniques currently under development, it appears that prompt gamma imaging has the best chance of fulfilling all the criteria above and becoming a valuable tool for particle range control in the clinic in the near future.

Keywords: particle therapy, range uncertainties, prompt gamma, imaging

References:
[1] Knopf AC, Lomax A. In vivo proton range verification: a review. Phys Med Biol. 58(15):R131-60, 2013.
[2] Verburg JM, Seco J. Proton range verification through prompt gamma-ray spectroscopy. Phys Med Biol. 59(23):7089-106, 2014.
[3] Yuan Y, Andronesi OC, Bortfeld TR, Richter C, Wolf R, Guimaraes AR, Hong TS, Seco J. Feasibility study of in vivo MRI based dosimetric verification of proton end-of-range for liver cancer patients. Radiother Oncol. 106(3):378-82, 2013.
[4] Assmann W, Kellnberger S, Reinhardt S, Lehrack S, Edlich A, Thirolf PG, Moser M, Dollinger G, Omar M, Ntziachristos V, Parodi K. Ionoacoustic characterization of the proton Bragg peak with submillimeter accuracy. Med Phys. 42(2):567-74, 2015.

26
Investigation on novel solution for a positioning system in protontherapy
F. Bourhaleb[1,3,4], R. Prisco[2], V. Dimiccoli[2] , F. Dalmasso[1,4],A. Attili[4],E. Menghi[5], G. Russo[1]
[1] I-See L.td, via Pietro Giuria 1, 10125, Turin, Italy
[2] ITEL L.td, via Labriola 39, 70037 Ruvo di Puglia BA
[3] University of Turin, Physics faculty, via Pietro Giuria 1, 10125, Turin, Italy
[4] National Institute of Nuclear Physics, via Pietro Giuria 1, 10125, Turin, Italy
[5] IRST, Fisica Sanitaria, via Piero Maroncelli, 40 47014 Meldola (FC), Italy

Aim: Protontherapy provided many evidences on the quality and accuracy in planning a treatment. Pencil-beam scanning technology with protons enables clinicians to precisely manipulate and direct the beam so that its energy conforms exactly to the unique size and shape of the tumor. This technique shows remarkable advantages in conforming the dose to the target.
However, the main issue for many years has been the non-accessible technology behind it. The huge expenses compared with conventional radiation therapy remain costs issues.
Lowering costs providing a new solution for proton therapy facilities with active scanning technique is opening a new perspective in this field, allowing a larger use of proton beams.
One of constraints that can drastically lower the costs is the use of a fixed source and not a grantry.
Methods: The scope of this study is providing a full investigation from the positioning to the dose delivery to the patient, using an alternative position in system that reproduce configurations gantry-couch like, and propose additional not-standard configurations that help a better planning.
A robot arm handling a couch offers an automated movement of the patient around the nozzle, providing more freedom and compensating the lack of gantry. The positioning system is controlled and interfaced with a dedicated software translating and converting complex motions to equivalent once in more standard positioning.
Results: Full Monte Carlo investigations for plan with different setting are realized to check configurations of Nozzle-Robotic system and their impact on the treatment planning. It is possible then to see when we get advantages in combining such solutions. This is reached once we have a system well integrated within the the full workflow and the planning system.

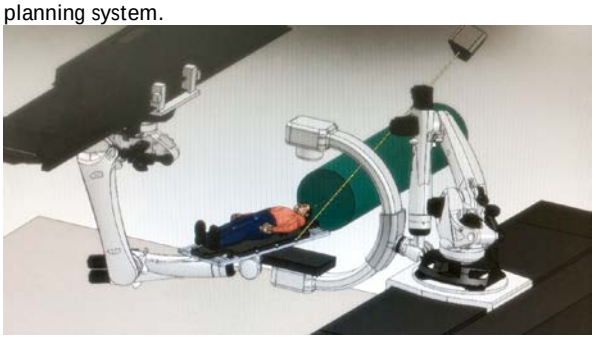

Keywords:
Positioning, Monte Carlo, treatment planning, protontherapy

References:
[1] J Pardo, M Donetti, F Bourhaleb, A Ansarinejad , A Attili. Heuristic optimization of the scanning path of particle therapy beams. Medical Physics. 07/2009; 36(6):2043-51
[2] F. Bourhaleb, A. Attili, G. Russo. Monte Carlo Simulations for Beam Delivery Line Design in Radiation Therapy with Heavy Ion Beams.
Chap7, ISBN 978-953-307-427-6, Published: February 28, 2011

27
An online beam monitor detector for medical applications of ion beams
M. Auger[1], S. Braccini[1], T. Carzaniga[1], A. Ereditato[1], K. P. Nesteruk[1], P. Scampoli[1,2]
[1] Albert Einstein Center for Fundamental Physics (AEC) - Laboratory for High Energy Physics (LHEP), University of Bern
[2] Department of Physics, University of Naples Federico II

Purpose: In medical applications, about 20 MeV and 100 μA proton beams are used for the production of PET radioisotopes. In hadrontherapy, energies of hundreds MeV per nucleon and intensities below 1 nA are employed. To monitor beams in this wide range of intensities with a single detector, the Universal BEam Monitoring detector (UniBEaM) based on doped silica and optical fibres was designed, built and tested.
Materials and methods: The UniBEaM detector is based on a single doped silica fibre moved through the beam. The

collected light signal provides information on the beam profile. A first prototype was developed and tested with 2 MeV protons [1]. On this basis, a fully motorized device was designed and built for the Bern medical cyclotron [2], which is used for the production of PET radioisotopes and multi-disciplinary research activities. The 10 cm long and 400 μm diameter sensing fiber is connected with a commercial optical fiber transporting the signal outside of the bunker. Cerium, antimony doped and non-doped sensing silica fibres were used, according to the intensity range. The fibres operate in vacuum and the signal is read out by a photo diode or by a PMT. The read out device, the control of the motor and the DAQ are integrated into a single compact apparatus.
Results: The UniBEaM detector was tested at the Bern medical cyclotron delivering beams from a few pA to 150 μA [3]. Two beam profiles are reported in Figure 1, taken at 50 pA and 1 μA, respectively. Due to their higher light yield, Ce doped fibres were used for intensities in the pico- and nanoampere range. Here the signal is recorded at successive steady positions of the fibre by single photon counting. For intensities from 100 nA to 1 μA, Sb doped fibres read out by a photodiode were used. The fiber is now moved continuously and the amplitude of the signal recorded. From 1 nA to 1 μA, the output signal was found to be linear with respect to the beam intensity. In this range, the position of the beam can be measured with a precision of about 0.1 mm, allowing the use of the UniBEaM detector for beam dynamics studies [4]. At intensities above 1 μA, a non-doped sensing fibre was used. Due to the dependence of the light transmission on temperature, the beam profile was found to be distorted, with a consequent non-linearity of the signal with respect to intensity. Nevertheless, the position of the beam can be monitored. This is a key feature for radioisotope production, especially if a solid target is used.
Conclusions: The UniBEaM detector is based on the collection of the optical signal produced by an ion beam traversing a silica fiber. This device was successfully tested at the Bern medical cyclotron at intensities ranging from a few pA to about 20 μA, opening the way for its use in the production of medical radioisotopes and cancer hadrontherapy. Its commercialization is underway.

Keywords: Beam monitoring detectors, radioisotope production, hadrontherapy

References:
[1] S. Braccini et al., A beam monitor detector based on doped silica and optical fibres, Journal of Instrumentation 2012 JINST 7 T02001
[2] S. Braccini et al., The new Bern cyclotron laboratory for radioisotope production and research, Proceedings of the second International Particle Accelerator Conference (IPAC2011), San Sebastián, Spain (2011) 3618, THPS080
[3] M. Auger et al., Low current performance of the Bern medical cyclotron down to the pA range, Meas. Sci. Technol. 26 (2015) 094006
[4] K. P. Nesteruk et al., Study of the transverse beam emittance of the Bern medical cyclotron, Proceedings of IBIC2015, Melbourne, Australia (2015), MOPB041

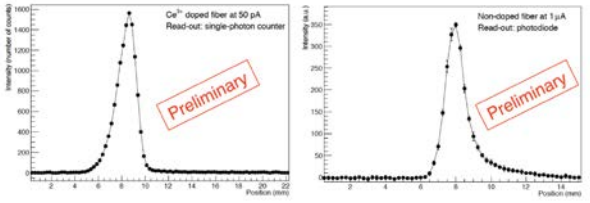

Figure 1 – Beam profiles measured at 50 pA (left) and 1 □A (right).

28
MRT (Microbeam Radiation Therapy (MRT): achievements and future perspectives
E. Bräuer-Krisch[1]
on behalf of the MRT scientific MRT collaborations
[1] ESRF, European Synchrotron Radiation Facility, Grenoble, France.

Microbeam Radiation Therapy (MRT) is a novel technique[1] using spatially fractionated, intense, highly collimated, parallel arrays of X-ray beams generated at 3rd generation synchrotron facilities like the ESRF in Grenoble, France. The insertion of an adequate multislit collimator[2] produces microbeams with a FWHM between 20 and 100 μm with separations between 100 and 400 μm to be delivered at an extremely high dose rate (up to 20kGy/sec) to best exploit the dose volume effect with peak entrance dose values well above several hundreds of Gy, demonstrating a very high normal tissue tolerance even for the immature tissue [3]. The differential effects[4] between normal tissue vasculature and tumor vascular networks promote this novel approach and questions one of the dogmas in radiation therapy: namely, that radiation therapy is aiming at a dose distributions with the primary goal to maximize the dose at the target, while minimizing the dose to the normal tissue in order to generally optimize the treatment in cancer therapy. An overview of the most important findings in radiation biology as well as achievements in Medical Physics will be summarized reflecting the current status of the project.

Keywords: Micro-beams, Synchrotron, MRT, Radiation Therapy.

References:
[1] Elke Bräuer-Krisch et al."Effects of pulsed spatial fractionated microscopic beams on normal and tumoral brain tissue" Review article in Press: Special Issue of Mutation Research - Spatio-Temporal Radiation Biology MUTREV-7944
[2] E. Bräuer-Krisch et al. "New Technology enables high precision Multi Slit Collimators for MRT " RSI 80, 074301 (2009)
[3] Laissue JA. et al. The weanling piglet cerebellum: a surrogate for tolerance to MRT (microbeam radiation therapy) in pediatric neuro-oncology. Proceedings of SPIE 2001, 4508: 65-73.
[4] A. Bouchet et al. 'Preferential effect of synchrotron microbeam radiation therapy on intracerebral 9L gliosarcoma vascular networks" Int. J. Radiation Oncology Biol. Phys., Vol. 78, No. 5, pp. 1503–1512, 2010

29
Evaluation of long-term effects of synchrotron-generated microbeams on rat hippocampal neurogenesis
P. Di Pietro[1], D. Bucci[1], A. De Fusco[1], G. Le Duc[2], E. Bräuer-Krisch[2], G. Battaglia[1], P. Romanelli[3,4], A. Bravin[2]
Author Name[1], Author Name[2]
[1]I.R.C.C.S. Neuromed, Pozzilli, Italy;
[2]European Synchrotron Radiation Facility, Grenoble, France;
[3]Centro Diagnostico Italiano, Brain Radiosurgery, Cyberknife Center, Milano, Italy;
[4]AB Medica, Lainate, Italy

Purpose: Therapeutic irradiation of brain cancers is associated with severe cognitive deficits in patients who survive long enough after irradiation. Radiotherapy-induced brain damage and dementia are associated to deficits in hippocampal-dependent mechanisms of learning and memory [1]. In preclinical rodent models, synchrotron-generated arrays of microbeams have shown unprecedented therapeutic effect on aggressive tumors of the central nervous system; furthermore microbeams are very well tolerated by normal tissues [2,3]. This latter effect is due to a minimal dose spreading outside the microbeam path. Recently, we showed that irradiation of the sensorimotor cortex of epileptic rats with synchrotron-generated microbeams reduces seizures without disrupting neurological functions [4]. Here we explored the long-term effects of microbeam versus broadbeam irradiation on hippocampal neurogenesis.
Materials/Methods: Two groups of male Wistar rats (175-200 g, two months of age) were irradiated with 5 or 10 Gy broadbeams, 3 groups were irradiated with 9 parallel microbeam arrays (75 μm wide, spaced 200 μm center-to-center; peak entrance dose: 150, 300 or 600 Gy). The control group was not irradiated. Eight months later, we assessed cognitive functions by the Morris water maze, depressive-like

behaviors by the Porsolt forced swim test, and locomotor activity and anxiety by the open field test. We also studied adult neurogenesis within the hippocampal dentate gyrus by using the thymidine analogue BrdU to label replicating stem cells. Ten months after irradiation animals were killed and brain tissue used for histology and immunohistochemistry.
Results: Microbeam irradiation did not alter cognitive performance. Interestingly, microbeam irradiation (300 Gy) significantly reduced the immobility time in the forced swim test without affecting locomotor activity as compared to control rats and 5-10 Gy irradiated rats. Histological analysis showed that microbeam irradiation did not alter the cytoarchitecture of the hippocampus with cell death observed only along the irradiation pathway. We did not observe a reduction of hippocampal neurogenesis, assessed by stereological counts of BrdU-positive cells in the dentate gyrus of the hippocampus at 10 months after microbeam irradiation.
Conclusions: These data shed light on the biological effects of microbeam irradiation on the CNS and may open new potential therapeutic strategies in cancer treatment and other CNS disorders.
Keywords: Microbeam radiation therapy, Hippocampus, Neurogenesis

References:
[1] Sienkiewicz et al, Int J Radiat Biol, 65:611, 1994
[2] Anschel et al, Neurosurg Rev, 34:133-142, 2011
[3] Bräuer-Krisch et al, Mutat Res, 704, 160-166, 2010
[4] Romanelli et al, PLoS One, 8:e53549, 2013

30
What are the Dominant Radiobiological Mechanisms at Play in Stereotactic Radiotherapy?
D. J. Brenner and I. Shuryak
Center for Radiological Research, Columbia University Medical Center, New York, NY, USA

Recent clinical results using Stereotactic Radiation Therapy (SRT) are very encouraging. Our goal is to investigate whether the excellent SRT tumor control data imply that there are new tumoricidal mechanisms that determine tumor control at high SRT doses – new mechanisms which are not present or have little effect at conventional radiotherapeutic doses.
To accomplish this, we investigate whether the standard LQ model with heterogeneity can provide as good a description of the SRT data as can models with extra terms describing unique high-dose tumor control mechanisms.
We analyzed published TCP data for lung tumors or brain metastases from 3000 SRT patients, covering a wide range of doses and fraction numbers. We used: (a) a linear-quadratic model (including heterogeneity), which assumes the same mechanisms at all doses, and (b) alternative models with terms describing distinct tumoricidal mechanisms at high doses.
Both for lung and brain data, the LQ model provided a significantly better fit over the entire range of treatment doses than did any of the models requiring extra terms at high doses. Analyzing the data as a function of fractionation (1 fraction *vs*. >1 fraction), there was no significant effect on TCP in the lung data, whereas for brain data multi-fraction SRT was associated with higher TCP than single-fraction treatment.
This analysis suggests that distinct tumoricidal mechanisms do not determine tumor control at high doses/fraction. Rather the excellent clinical outcomes seen with SRT are the result of the excellent dose distributions which SRT provides, which allow delivery of larger doses to the tumor than is possible with conventional radiotherapy. Finally, there is plausible evidence suggesting that multi-fraction SRT is superior to single-dose SRT.

Keywords: Stereotactic Radiotherapy Mechanisms

31
GEANT4 simulation of dose deposition in patients from TomoTherapy Hi-Art Megavoltage computed tomography (MVCT) imaging.
F. Brochu[1], N. Burnet[2], R. Jena[3], S. Thomas[4].
[1] HEP Group, Department of Physics, University of Cambridge,JJ Thomson Avenue, CAMBRIDGE CB3 0HE, United Kingdom
[2] Department of Oncology, University of Cambridge, Cambridge Biomedical Campus, Addenbrooke's Hospital, Cambridge, UK
[3] Oncology Centre, Addenbrooke's Hospital, Cambridge, UK
[4] Department of Medical Physics, University of Cambridge, Addenbrooke's Hospital, Cambridge, UK

Purpose: Image-guided radiotherapy (IGRT) is a technique used to optimise RT beam delivery to the tumour by following its evolution over time through regular MVCT imaging of the treatment area.
However, its application is limited by clinical concerns over the additional dose coming from MVCT imaging, which we evaluate in this study.
Methods: We use the particle transport framework GEANT4[1] to model the X-ray beam line from the Tomotherapy Hi-Art RT treatment machine at the Addenbrooke's hospital and evaluate the imaging dose delivered to the vicinity of the tumour. Dose maps are obtained by combining simulations of the CT scan using a static beam line with 51 different exposition angles.
All GEANT4 simulations were performed on UK grid resources[2] to maximize parallel throughput, using anonymised data.
Results: Simulated beam profiles (PDD, longitudinal and lateral) with different MLC beam patterns were compared to actual calibration data taken in water tank at Addenbrooke's hospital. The agreement between the model and the calibration is quantified by the Gamma index[3]. Less than 2% of the simulated points exceed Gamma(1%,1mm)
We also simulated the imaging dose distribution in a prostate patient treated in 34 fractions, each fraction starting with one MV CT used for image guidance. We used a fan beam width of 4 mm with a pitch of 2 mm. The results are shown in Figure 1.

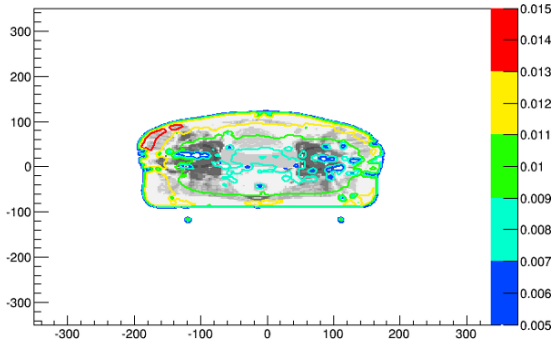

Figure 1: Normalised imaging dose distributions in Gy for a prostate cancer patient, in a transverse plane in the treatment region.

The maximum simulated dose is about 1.5 cGy on a single MVCT, in agreement with results found in [4] using proprietary software. For comparison, the treatment dose in the same area goes up to 2 Gy per fraction.
Conclusions: We have successfully modeled the Megavoltage imaging beam line of the Tomotherapy Hi-Art machine used for radiotherapy at the Addenbrooke's hospital using Geant 4 and used it to derive dose maps in the patient.
Doses were found to be in agreement with other published results and negligible with respect to the treatment dose.

Keywords: MVCT, dose, Monte-Carlo, Geant4

References:

[1] S. Agostinelli et al, "GEANT4—a simulation toolkit",NIM A506 Vol 3. (2003) 250-303.
J. Allison et al,"Geant4 developments and applications", IEEE Trans. Nucl. Sci. 53 Vol 1 (2006) 270-278.
[2] http://www.gridpp.ac.uk
[3] D.A. Low, W.B. Harms,S. Mutic and J.A. Purdy, "A technique for the quantitative evaluation of dose distributions", Medical Physics 25(5), 656-661 (1998).
[4] A. P. Shah et al. "Patient dose from megavoltage computed tomography imaging", Int. J. Rad. Oncol. Biol. Phys. 70(5), 1579-1587 (2008).

32

Recurrent glioblastoma multiforme – targeted alpha therapy with ^{213}Bi-DOTA-Substance P

L. Krolicki[1], B. Królicki[3], A. Morgenstern[2]; J. Kunikowska[1], H. Koziara[3], M. Jakuciński[4], C. Apostolidis[2], F. Bruchertseifer[2]
[1] Department of Nuclear Medicine, Medical University of Warsaw, Warsaw, Poland
[2] European Commission, Joint Research Centre, Institute for Transuranium Elements, Karlsruhe, Germany
[3] Department of Neurosurgery, Institute of Psychiatry and Neurology, Warsaw, Poland
[4] Department of Nuclear Medicine, Brodnowski Hospital, Warsaw, Poland

Glioblastoma multiforme (GBM) is the most common and malignant primary brain tumor. The median survival time is 14.6 months from time of diagnosis, in spite of aggressive surgery, radiation therapy and chemotherapy. Only 3 to 5% of patients survive more than three years. Recurrence of GBM is nearly universal, confers a dismal prognosis with a 6-months progression free survival (6M-PFS) rate of 15% to 21% and a median survival of 6.2 months. Advancements in the past decades have not significantly increased the overall survival of patients with this disease. GBM has been demonstrated NK-1 receptor system and Substance P can be used as a ligand for targeted therapy. Alpha emitter, like ^{213}Bi offers the new potential for selective irradiation of tumors, with minimizing damage to adjacent tissue.
Material and methods: 21 patients with primary recurrent glia tumor IV after standard therapy were included in the study during two years. Following intracavitary or intratumoral insertion of 1-2 catheter systems, patients were treated with 1–8 doses of 2 GBq ^{213}Bi-DOTA-Substance P (^{213}Bi-SP) in intervals of 2 months. ^{68}Ga-DOTA-Substance P (^{68}Ga-SP) was co-injected with the therapeutic doses to assess biodistribution using PET/CT. Therapeutic response was monitored with MRI. Study was approved by the ethical committee of the Medical University of Warsaw.
Results: Treatment with activity up to 13 GBq ^{213}Bi-SP was tolerated well with only mild transient adverse reactions: in 1 patient transient increase of focal neurological symptoms and in 3 patients episodes of epileptic seizures several days after treatment. PET/CT imaging showed high retention of the radiolabeled peptide at the tumor site.
Out of 21 evaluable patients, 17 progressed within the follow-up period, 5 of them are alive at the end of follow-up. Four patients were excluded from evaluation due to lack of data. Median progression free survival was 3.7 months, with a 6 months progression free survival rate of 19% . The median overall survival from the first diagnosis was 25.2 months, and from the start of ^{213}Bi-SP was 6.5 months. Follow up of therapeutic responses and toxicity is continued and patient recruitment is ongoing. Busk

Conclusions: Treatment of recurrent GBM with ^{213}Bi-SP is safe and well tolerated. Targeted alpha therapy with ^{213}Bi-SP may evolve as a promising novel option for treatment of recurrent GBM.

Keywords:targeted alpha therapy; ^{213}Bi-DOTA-Substance P; glioblastoma multiforme

33

Increasing PET scanner resolution using a Silicon detector probe

K. Brzezinski[1,2], J. F. Oliver[1], J. Gillam[1,3] and M. Rafecas[1,4]
[1] Instituto de Física Corpuscular (CSIC/Universitat de València), c/ Catedrático José Beltrán, 2. E-46980 Paterna, Valencia, Spain
[2] Now with KVI-Center for Advanced Radiation Technology, University of Groningen, Zernikelaan 25, 9747AA Groningen, The Netherlands
[3] Now with Brain and Mind Research Institute (Faculty of Health Sciences), University of Sydney, 94 Mallett St., Camperdown, NSW 2050, Australia.
[4] Now with the University of Lubeck, Institute of Medical Engineering, Ratzeburger Allee 160, 23538 Lübeck, Germany

A high-resolution silicon detector probe, in coincidence with a conventional
PET scanner, is expected to provide images of higher spatial resolution than those achievable using the scanner alone, due to the finer pixelization of the probe detector[1]. A PET-probe prototype is being developed utilizing this principle [2]. The system includes a probe consisting of ten layers of silicon detectors, each a 80×52 array of 1×1×1 mm^3 pixels, to be operated in coincidence with a modern clinical PET scanner. Detailed simulation studies of this system have been performed to assess the effect of the additional probe information on the quality of the reconstructed images.
Using the Monte-Carlo simulation package GATE, a grid of point sources was simulated to study the contribution of the probe to the system resolution at different locations over the field of view (FOV). A resolution phantom was used to demonstrate the effect on image resolution for two probe positions. A homogeneous source distribution with hot and cold regions was used to demonstrate that the localized improvement in resolution does not come at the expense of the overall quality of the image. An imaging study using experimental probe data was also performed. The list-mode maximum likelihood–expectation maximization (ML–EM) algorithm[3] was used for image reconstruction in all cases.
As expected, the point spread function of the PET-probe system was found to be non-isotropic and vary with position, offering improvement in specific regions. An increase in resolution, of factors of up to 2, was observed in the region close to the probe. Images of the resolution phantom showed visible enhancement in resolution when including the probe in the simulations, as can be seen in figure 1. The image quality study demonstrated that contrast and spill-over ratio in other areas of the FOV were not sacrificed for this enhancement. The improvement in resolution when using the Si detector probe was also observed using the experimental prototype. In this context, previously unrecoverable features in a resolution phantom could be resolved when probe data was included during image reconstruction. Remaining challenges in developing the PET-probe system include overcoming the limitations imposed by the timing performance of the Si detectors and more detailed system modeling in image reconstruction.

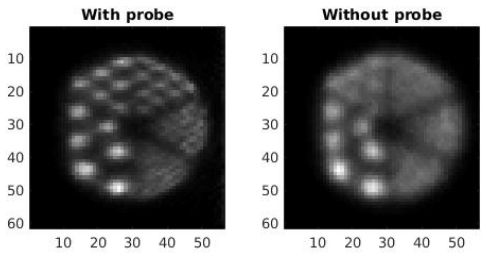

Figure 1: Images of the resolution phantom reconstructed using data from the probe and from the scanner alone. The probe is located to the right of the image, in close proximity to the phantom. The phantom features are 4.8, 4.0, 3.2, 2.4, 1.6 and 1.2 mm in diameter. Pixels are 1 × 1 × 1 mm3

Keywords: PET, Si detectors, PET insert

References:
[1] Tai Y C, Wu H, Pal D and O'Sullivan J A, Virtual-pinhole PET, J. Nucl. Med. 49 471–9 (2008)

[2] Brzeziński K, Oliver J F, Gillam J, Rafecas M, Study of a high-resolution PET system using a Silicon detector probe, Phys Med Biol, **59** (2014) 6117-40
[3] Shepp L A and Vardi Y, Maximum likelihood reconstruction for emission tomography, IEEE Trans. Med. Imaging **1** 113–22 (1982)

34
Short-lived Positron Emitters in Beam-on PET Imaging During Proton Therapy
P. Dendooven[1,5], H. J. T. Buitenhuis[1], F. Diblen[1,3], A. K. Biegun[1], F. Fiedler[4], M-J. van Goethem[2], E. R. van der Graaf[1], S. Brandenburg[1]
[1] KVI-Center for Advanced Radiation Technology, University of Groningen, Groningen, The Netherlands
[2] University of Groningen, University Medical Center Groningen, Department of Radiation Oncology, Groningen, The Netherlands
[3] MEDISIP, Department of Electronics and Information Systems, Ghent University-iMinds Medical IT-IBiTech, Ghent, Belgium
[4] Helmholtz-Zentrum Dresden - Rossendorf, Institute of Radiation Physics, Dresden, Germany
[5] Helsinki Institute of Physics, Helsinki, Finland

Positron emission tomography is so far the only method for in-vivo dose delivery verification in hadron therapy that is in clinical use. PET imaging during irradiation maximizes the number of detected counts and minimizes washout. In such a scenario, also short-lived positron emitters will be observed. As very little is known on the production of these nuclides, we determined which ones are relevant for proton therapy treatment verification.
In order to be relevant, nuclides have to be produced close to the distal edge and thus at rather low proton energy. Therefore we measured the integral production of short-lived positron emitters in the stopping of 55 MeV protons in carbon, oxygen, phosphorus and calcium. The experiments were performed at the irradiation facility of the AGOR cyclotron at KVI-Center for Advanced Radiation Technology, University of Groningen. The positron emitters were identified based on their half-life. In order to do this, the proton beam was pulsed, i.e. delivered as a succession of beam-on and beam-off periods, and the time evolution of the 511 keV positron annihilation photons was recorded. A half-life analysis of the beam-off period allowed to determine the production rates of separate nuclides. The 511 keV photons were detected by a germanium clover detector [1]. A correction for the escape of positrons from the target, determined via Monte Carlo simulations, was applied.
In the stopping of 55 MeV protons, the most copiously produced short-lived nuclides and their production rates relative to the relevant long-lived nuclides are: 12N (T1/2 = 11 ms) on carbon (9% of the 11C production), 29P (T1/2 = 4.1 s) on phosphorus (20% of the 30P production) and 38mK (T1/2 = 0.92 s) on calcium (113% of the 38gK production). No short-lived nuclides are produced on water (i.e. oxygen). The experimental production rates are used to calculate the production on PMMA and a representative set of 4 tissue materials. [fig. 1] The number of decays per 55 MeV proton stopped in these materials, integrated over an irradiation, is calculated as function of the duration of the irradiation. The most noticeable result is that for an irradiation in (carbon-rich) adipose tissue, 12N will dominate the PET image up to an irradiation duration of 70 s. On bone tissue, 15O dominates over 12N after 8-15 s (depending on the carbon-to-oxygen ratio). Considering nuclides created on phosphorus and calcium, the short-lived ones provide 2.5 times more decays than the long-lived ones during a 70 s irradiation. Bone tissue will thus be better visible in beam-on PET compared to PET imaging after an irradiation.
The results warrant detailed investigations into the energy-dependent production of 12N, 29P and 38mK and their effect on PET imaging during proton irradiations.

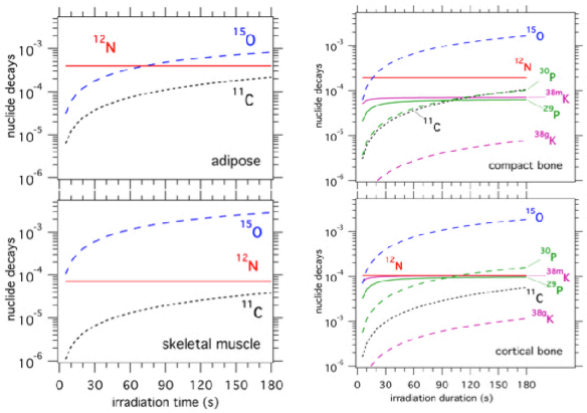

Figure 1: Number of decays of PET nuclides per 55 MeV proton stopped and integrated over an irradiation, as function of the duration of the irradiation for adipose, skeletal muscle, compact bone and cortical bone tissue. Short-lived nuclides are shown with solid lines, long-lived ones with dashed lines

Keywords: Proton therapy dose delivery verification, short-lived positron emitters, Positron Emission Tomography

References:
[1] G. Duchêne *et al*, "The Clover: a new generation of composite Ge detectors," *Nucl. Instrum. Meth. Phys. Res. A* vol. 432, pp. 90-110, 1999

35
PET Scanning Protocols for In-Situ Dose Delivery Verification of Proton Therapy
H. J. T. Buitenhuis[1], P. Dendooven[1,4], A. K. Biegun[1], A. J. van der Borden[2],
F. Diblen[1,3], M-J. van Goethem[2], A. van der Schaaf[2], A. A. van 't Veld[2],
S. Brandenburg[1]
[1] KVI-Center for Advanced Radiation Technology, University of Groningen, Groningen, The Netherlands
[2] University of Groningen, University Medical Center Groningen, Department of Radiation Oncology, Groningen, The Netherlands
[3] MEDISIP, Department of Electronics and Information Systems, Ghent University-iMinds Medical IT-IBiTech, Ghent, Belgium
[4] Helsinki Institute of Physics, Helsinki, Finland

Positron emission tomography is so far the only method for in-vivo dose delivery verification in hadron therapy that is in clinical use. A PET scanner placed in the treatment position (in-situ) will be able to obtain the highest number of counts, as it minimizes the decay of the positron emitting nuclei before the scan is started as well as reduces the effect of biological washout. We investigated the influence of the scan protocol, i.e. the moment when a scan in done in relation to the treatment delivery, on the ability to measure unacceptable deviations from the treatment plan.
We developed a Geant4-based Monte-Carlo framework for proton therapy simulations. Four patient cases are studied: two head-and-neck, one sarcoma near the spine, and one breast cancer case. For each irradiation field, the production of the following PET isotopes is calculated: 15O, 11C, 10C, 14O, 30P, 38K, and 13N. The time sequence of the pencil beam scanning irradiation, the decay of the PET isotopes during the irradiation, and biological washout are included in the simulation. The production of these nuclei is then used to calculate a PET image for two scan protocols: a scan of 120 seconds after the first field, or a scan of 120 seconds after the last field. To mimic a typical scanner spatial resolution, the images are blurred using a Gaussian blurring function with 4 mm FWHM.
Deviations from the treatment plan are simulated by shifting the patient 4 mm perpendicular to the field angle, or by increasing the patient density by 3%. The PET image is then simulated again for each scanning protocol. The ability of

each protocol to detect these deviations from the treatment plan is investigated by comparing the planned and the modified PET image. Several analysis methods are used: line profiles coupled to the field-directions, structural similarity index analysis [1], and gamma index analysis. [2]
Preliminary data shows that a difference in density is best detected by starting the scan directly after the first field. However, shifts perpendicular to the field directions are better detected when the scan is done after the last field, due to the increased activity and counting-rate.

Keywords: Positron Emission Tomography, proton therapy dose delivery verification, scanning protocols

References:
[1] Zhou Wang *et al*. "Image Quality Assessment: From Error Visibility to Structural Similarity" *IEEE Transactions on Image Processing*, vol. 13, no. 4, April 2004
[2] D A Low *et al*. "A technique for the quantitative evaluation of dose distributions" *Medical Physics*, vol 25, no. 5, pp. 656-61, May 1998

36
CTV-PTV margin reduction using prediction of respiration-induced tumour motion
W. Bukhari, S-M. Hong
Kyungpook National University

Purpose: Adaptive radiotherapy aims to synchronize the treatment beam with the tumour motion. It requires the prediction of respiratory motion which has received much attention for over a decade. The performance of prediction algorithms to the dose delivery to the tumour is evaluated for the first time in terms of CTV-PTV margin.
Methods and Materials: Clinical tumour volume (CTV) is outlined in treatment planning and is aimed to be irradiated with sufficient dose. Owing to uncertainties including respiration-induced motion, a sufficient margin around CTV is defined to form planning target volume (PTV). PTV is irradiated to ensure sufficient dose delivery to CTV, whereas CTV-PTV margin should be minimal to avoid irradiating normal tissues outside CTV. In this work, we adopt tumour control probability (TCP) to quantify sufficient dose delivery using TCP model based on Poisson statistics. The CTV-PTV margin required to yield 90% TCP is evaluated for no prediction (a baseline algorithm that refers to using the current measurement as a lookahead prediction.) and recently proposed EKF-GPRN prediction algorithm [1] at lookahead lengths of 192 ms, 384 ms and 576 ms.
A large database of 304 three dimensional respiratory motion traces from a group of 31 patients is employed to evaluate algorithms. We assume that a spherical-shaped CTV with a radius of 2.5 mm undergoes 3-D motion along these traces. Algorithms are used to predict the center of CTV and the prediction error is considered as the deviation of treatment beam from the CTV.
Results: Patient-wise statistics for CTV-PTV margin required to achieve 90% TCP are given for each algorithm in the following table. The values in the parenthesis are percent ratios relative to no prediction. The results show that EKF-GPRN reduces the required CTV-PTV margin to around 20% on average, compared to no prediction across all the lookahead lengths. It indicates that EKF-GPRN can significantly improve dose conformality and effectively reduce normal tissue exposure.

Lookahead Length		No Prediction (mm)	EKF-GPRN (mm)
192 ms	mean	0.54	0.09 (17)
	std dev	0.26	0.05 (19)
	90th percentile	0.79	0.19 (24)
	max	1.43	0.22 (15)
384 ms	mean	1.30	0.27 (21)
	std dev	0.61	0.19 (31)
	90th percentile	1.94	0.34 (18)
	max	3.29	0.97 (29)
576 ms	mean	2.06	0.49 (24)
	std dev	0.91	0.36 (40)
	90th percentile	2.93	0.72 (25)
	max	4.95	1.88 (38)

Keywords: Radiotherapy, respiratory motion, prediction

Acknowledgements:
This work was supported by the Institute for Information and Communications Technology Promotion (IITP) grant funded by the Korean Government (MSIP) (10041145, Self-Organizing Software Platform for Welfare Devices)

References:
[1] W. Bukhari and S-M. Hong, "Respiratory Motion Prediction in 3-D using an Extended Kalman Filter and Gaussian Process Regression Network", 37th Ann. Intl. Conf. IEEE Engineering in Medicine and Biology (EMBC 2015).

37
Robustness and reliability of PET-based identification and quantification of tumor hypoxia, using simple static or more complex scan acquisitions
M. Busk[1], A. B. Iversen[1], J. B. Petersen[1], O. L. Munk[2], S. Jakobsen[2], J. Frøkiær [2], J. Overgaard[1] and M. R. Horsman[1].
[1] Department of Experimental Clinical Oncology, Aarhus University Hospital, Aarhus, Denmark (AUH)
[2] PET centre, AUH, Aarhus, Denmark

Purpose: Tumor hypoxia is linked to poor prognosis, but personalized hypoxic intervention with radiosensitizers (e.g., nimorazole), bioreductive drugs or dose escalation to hypoxic tumor volumes may improve outcome. Hypoxia-selective PET tracers like FMISO and FAZA are available, but inherent weaknesses of PET in general (low resolution) and hypoxia PET in particular (low image contrast due to slow tracer retention and clearance) may compromise the quantitative accuracy and reproducibility of hypoxia PET.
Methods: To assess the severity of this problem, and refine and optimize scan protocols to overcome them, various human and rodent tumors were established in mice. Subsequently, mice were scanned using different scan protocols on a high-resolution (~1 mm) Mediso nanoPET/MRI. Some mice were scanned dynamically for 3-hours to allow full pharmacokinetic analysis (PET imaging gold standard) followed by tumor dissection, cryosectioning and high-resolution analysis of tracer distribution (autoradiography) and hypoxia (pimonidazole), on multiple tissue sections covering the whole tumor volume. Other mice were scanned statically at two different post-injection (PI) time points, to mimic the image contrast obtainable clinically (1.5h PI) and a much better contrast (3h PI), which can only be obtained in rodents due to rapid clearance of unbound tracer in organisms with high metabolic rates. On the next day, the same mice were scanned again at 1.5h PI or at 1.5 and 3h PI followed by invasive tissue analysis as described above.
Results/Conclusions: An analysis of the distribution of FAZA (autoradiograms) and hypoxia (pimonidazole) on tissue sections revealed that 3h PI static scans, provide highly accurate spatial information on hypoxia, and thus serve as a gold standard. Despite a dramatic increase in inter-tissue and intra-tumoral image contrast at late scan times (3h PI), a voxel-by-voxel comparison revealed an excellent correlation between early (1.5h) and delayed (3h) scans. In addition, the day-to-day spatial reproducibility (overall tracer uptake and its spatial distribution) was good, even when scans were acquired at a clinical achievable contrast. Taken together, these results suggest that target definition is reasonable robust and reliable at a clinical achievable contrast. In contrast a simplified, and thus clinically feasible, dynamic model that both integrates information on blood flow/tracer wash-in (deduced from the FAZA signal during the first 15 min of the scan) and tracer retention (deduced at 1.5 h PI), was unexpectedly less reliable, in terms of hypoxia-specificity, than the uncorrected low-contrast static scan. This may relate to an uncoupling between blood flow and oxygen delivery capacity in the abnormal tumor vasculature. Whether, similar limitations apply to full dynamic scans are currently being investigated, using a variety of differing pharmacokinetic models.

38
Single particle detection for spectroscopic CT and tracking in hadron therapy using Medipix chips

M. Campbell[1], J. Alozy[1], R. Ballabriga[1], E. Frojdh[1,2*], E.H.M. Heijne[1,3], X. Llopart[1], T.Poikela[1], E. Santin[1], L.Tlustos[1,4], P. Valerio[1] and W.Wong[1,5]
[1] PH Department, CERN 1211 Geneva 23, Switzerland
[2] Mid Sweden University, Sundsvall, Mid Sweden
[3]Czech Technical University in Prague, Institute for Experimental and Applied Physics, Czech Republic
[4] University of Freiburg, Freiburg, Germany
[5]University of Houston, Houston, TX, USA
[*]now with PSI, Villigen, Switzerland

Tracking detectors at the LHC rely on hybrid pixel detectors which tag each particle with an extremely high signal to noise ratio and with a time precision of at most 25ns. The same technology has been adapted to numerous other applications by successive Medipix Collaborations. The most recent imaging chip, called Medipix3, permits spectroscopic X-ray imaging at high spatial resolution and relatively high fluxes by using inter-pixel hit-by-hit processing. The Timepix3 chip, on the other hand, takes the opposite approach detecting each hit with a time precision of 1.6ns and sending all data off chip for analysis. Both chips have opened new applications in the medical field: the first for spectroscopic X-ray imaging and CT and the second for beam and dose monitoring during hadron therapy. The presentation will describe the detection technology and focus on some examples of medical applications.

Keywords: Medipix, tracking detectors, CT, hadron therapy

39
Development of a PET Insert for Human Brain Imaging: Detection System

N. Campos Rivera[1], B. Seitz[1]
[1] University of Glasgow, Glasgow G12 8QQ, U.K.

In recent years, the combination of techniques such as PET (Positron Emission Tomography) and MRI (Magnetic Resonance Imaging) has shown a great potential to study the processes and progression of diseases (cancer, Alzheimer's) as well as to control and observe novel treatments response.
A brain-size PET detector ring insert for an MRI system is being developed that, if successful, can be inserted into any existing MRI system to enable simultaneous PET and MRI images of the brain to be acquired without mutual interference.
The PET insert consists of detector blocks arranged in a ring of 30 cm diameter. Each detector block is composed of a LYSO array coupled to the Philips Digital Photon Counting. We divided the study of the detection system in three stages. First, we characterized the coupling of the scintillator crystal with the SiPM (Silicon Photomultiplier). Next, we simulated the behaviour or the ring insert using Monte Carlo methods. Finally, we verified the simulation results with the collected data.
As a result of this methodology, we obtained the I-V curves and the energy and time resolution of our system. Results show that the coupling is appropriate and that the sensibility of our system is adequate to move to the next study phase: MRI compatibility.

Keywords: positron emission tomography, PET, PET/MRI, detectors, magnetic resonance imaging

40
A local and global liver function model

Y. Cao,[1] H. Wang,[1] A. Jackson,[2] R. K. Ten Haken,[1] T. S. Lawrence,[1] and M. Feng[1]
[1] Department of Radiation Oncology, University of Michigan, Ann Arbor, Michigan; [2]Department of Medical Physics, Memorial Sloan Kettering Cancer Center, New York

As the use of SBRT for liver tumors increases and repeated treatments for the same patient become more common, it is increasingly important to predict liver function reserve rather than only likelihood of radiation-induced liver disease after SBRT. This study aimed to develop a local and global function model in the liver based upon regional and organ function measurements to support individualized adaptive RT.
This local and global liver function model was constructed with the assumption of parallel architecture in the liver, so that the global function of the organ was composed of the sum of local function of subunits similar to a previous model [1]. A major advance in this model is the addition of incorporation of functional variability of the liver across the patients as well as the function probability variability over the subunits between 0 and 1, instead of being a binary number of 0 or 1. This model was fitted to 59 datasets of liver regional and global organ function measures from 23 patients obtained prior to, during and 1 month after RT. The local function probability of a subunit was modeled by a previously published sigmoid function related to MRI-derived regional portal venous perfusion values. The global function was fitted to an indocyanine green retention rate at 15 min. Cross-validation was performed by leave-m-out tests. Fitting was also performed separately for the patients with hepatocellular carcinoma (HCC) vs all others due to likely differences in the liver function as well as radiation sensitivity.
The fitted liver function model showed that 1) a portal venous perfusion value of 68.6 ml/(100g·min) yielded a local function probability of 0.5; 2) the local function probability reached 0.9 at a perfusion value of 98 ml/(100g·min); and 3) at an average function probability of 0.03 (corresponding perfusion of 38 ml/(100g·min)) or lower, the subunits did not contribute to the global function. Cross-validations showed that the model parameters were stable. Further, the same amount of portal venous perfusion was translated into less local function probability in patients with HCC than without HCC, reflecting the compromised local liver function by cirrhosis (Fig 1).
The utility of this liver function model was explored, including assessing for individual regional dose response functions that substantially differed from the population average dose response and for dose re-distribution planning by maximizing global liver function by sparing local highly functional regions. This model could be a valuable tool for individualized treatment planning of RT.

Keywords: liver function model, function reserve, individualized RT

References:
[1] Jackson A, Ten Haken RK, Robertson JM, Kessler ML, Kutcher GJ, Lawrence TS. Analysis of clinical complication data for radiation hepatitis using a parallel architecture model. *International journal of radiation oncology, biology, physics* 1995;31:883-891.

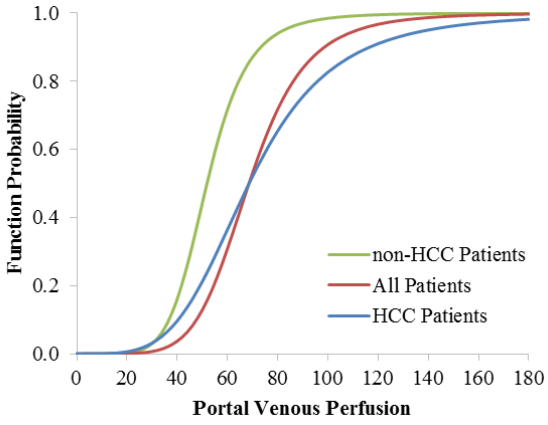

Fig. 1 The local and global liver function models fitted to the data divided based upon the patients who had HCC vs non-HCC tumors. Red curves represent the model fitted to all the data.

41

A Hypercellular Component of Glioblastoma Identified by High b-value Diffusion Weighted Imaging

Y. Cao,[1,2,3] D. Wahl,[1] P. Pramanik,[1,3] M. Kim,[1] T.S. Lawrence,[1] H. Parmar[2]
[1] Department of Radiation Oncology, University of Michigan, Ann Arbor, Michigan;
[2] Department of Radiology, University of Michigan, Ann Arbor, Michigan;
[3] Department of Biomedical Engineering, University of Michigan, Ann Arbor, Michigan

Glioblastomas (GBM) may receive inadequate radiation dose coverage, specially the nonenhanced hypercellular component, using post-Gd T1 weighted and T2 FLAIR images for radiation target definition. A mixture of edema, micro-necrosis, tumor cells and normal tissue in a single image voxel result in an unpredictable value on diffusion images using a conventional b-value of 1000 s/mm^2 or less. This study aimed to develop a technique to identify the hypercellular components of GBM by using high b-value diffusion weighted imaging (DWI) to suppress fluid, edema, micro-necrosis and even normal tissue to an extent. The hypercellular volume (HCV) of the tumor was evaluated for radiation dose coverage and prediction of progression-free survival (PFS).

Forty patients with newly diagnosed GBM underwent chemoradiotherapy post-resection/biopsy. The target definition was based upon conventional MRI and RT treatment planning followed standard guidelines. Pre-RT DWI was acquired with b-values of 0, 1000, and 3000 s/mm^2. A HCV was defined on the DWI with b=3000 s/mm^2 by a threshold obtained from normal tissue. The nonenhanced HCV was delineated by comparing to the Gd-enhanced gross tumor volume (GTV-Gd) on T1-weighted images. Radiation coverage of the HCV was evaluated by the 95% prescribed dose-volume (95%PDV) of the planned dose distribution. Association between HCV and PFS or other clinical covariates were assessed using univariate proportional hazards regression models.

For the first 21 patients with a minimum follow-up of 18 months, the HCVs varied 0.58-67 cc (median: 9.8cc), 7 times smaller than the FLAIR-defined CTV. The non-enhanced HCV was 0.15-60 cc (median: 2.5cc). However, incomplete dose coverage of the HCV was seen in 14 patients, in whom 6 had at least 1-cc HCV missed by the 95%PDV (range: 1.01-25.4cc). Of the 21 patients, 15 had progressed, 5 patients earlier within 6 months post-RT, and 10 patients >6 months post-RT. HCV and nonenhanced HCV were significant negative predictors for PFS ($p<0.002$ and $p<0.01$, respectively). The component of the HCV that was not covered by the 95%PDV was a significant negative predictor for PFS ($p<0.05$). The proportion of pre-RT HCVs that overlapped with recurrent Gd-enhanced tumor volume was 78% (range: 65-89%) for the 5 earlier progressors, and 53% (range: 0-85%) for the later progressors.

The HCV identified by high b-value DWI most likely represents an aggressive component of the tumor, and analysis of the data from the whole cohort is in progress. Pathological validation is on-going. Post-Gd T1 weighted images (a qualitative measure of vascular leakage) and T2 FLAIR images (influenced by edema) are not adequate for radiation target definition of GBM. Selectively boosting the HCV component of GBM will be tested in a prospective clinical trial.

Keywords: glioblastoma, high b-value diffusion weighted imaging, radiation

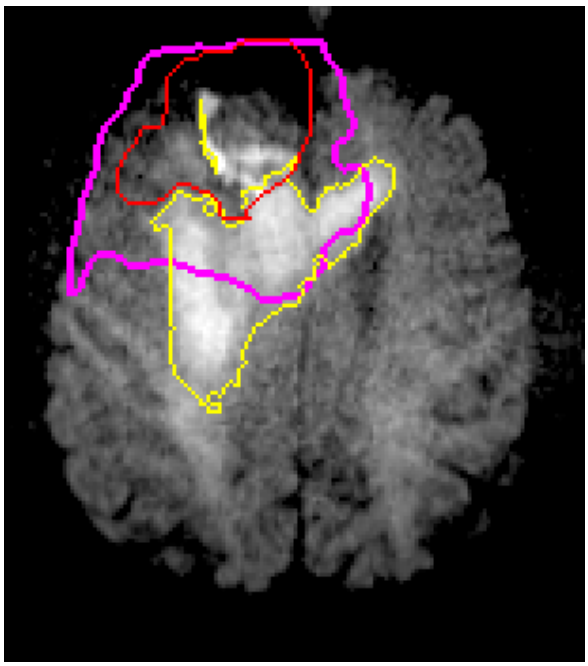

Fig 1. Diffusion weighted images with b=3000. Yellow: HCV; Red: post-Gd GTV; Pink: 95%PDV.

42

Early variation of FDG-PET radiomics features in NSCLC is related to overall survival - the "delta radiomics" concept

S. Carvalho[1], R. T. H. Leijenaar[1], E. G. C. Troost[1,2], W. van Elmpt[1], J-P. Muratet[3], F. Denis[3], D. De Ruysscher [1], H. J. W. L. Aerts[1,4], P. Lambin[1]
[1] Department of Radiation Oncology (MAASTRO), GROW – School for Oncology and Developmental Biology, Maastricht University Medical Centre (MUMC +), Maastricht, the Netherlands
[2] Institute of Radiooncology, Helmholtz-Zentrum Dresden-Rossendorf, Germany
[3] Centre Jean Bernard, Clinique Victor Hugo, Le Mans, France
[4] Department of Radiation Oncology and Radiology, Dana-Farber Cancer Institute, Brigham and Women's Hospital, Harvard Medical School, Boston, MA, USA

Early assessment of therapeutic response in NSCLC is of major importance to individualize treatment, ultimately improving outcome. Radiomics comprises the extraction of a large set of quantitative descriptors from medical images (*1*). We hypothesised that a Radiomics analysis of variation of metabolic uptake patterns of repeated FDG-PET (Figure 1) allows early response assessment and validated our findings in external datasets.

A prospective dataset of 54 stage IIIa-IV NSCLC patients referred for radical (chemo)radiotherapy was used for prediction model development. The validation datasets included 32 stage IIb-IIIb (details in (*2*)) and 26 stage IIa-IIIb (details in (*3*)) NSCLC patients. FDG-PET scans were acquired before and during second week of radiotherapy. Radiomics analysis included descriptors of shape and size, first order statistics, textural information [run-length grey level (RLGL), grey level co-occurrence (GLCM) and grey level size zone matrices (GLSZM)] and intensity volume histograms (IVH). For analysis, solely features with a high intraclass correlation (ICC) on both test-retest and inter-observer stability analysis were kept (*4*). Cox Proportional Hazard Regression was performed for overall survival assessment, with the relative percentage variation of each feature between subsequent scans as continuous covariates:

$$\frac{(During_{treatment} - Pre_{treatment})}{Pre_{treatment}} \times 100\%$$

A least absolute shrinkage and selection operator (LASSO) method was used for feature selection. Model performance was evaluated using Harrell's concordance-index (c-index).
Fitted model included sum entropy (GLCM), high intensity large area emphasis (GLSZM), volume with a minimum relative intensity of 60% of the maximum SUV – AVRI60% (IVH), grey level non-uniformity and long run emphasis (RLGL) and volume (shape) – Table 1. Internal performance of the model was 0.64 ($p<0.01$), while externally it achieved a performance of 0.61 ($p = 0.05$) and 0.58 (0.20), with no further calibration done. Maximum and mean SUV had a univariable performance in the training data of 0.51 and 0.55, respectively.
The reduced accuracy of the model validation can be associated with dissimilarities among data, particularly the different timing and delivered dose of the second scan. Nevertheless, we do see benefit on a timely assessment of response to radiotherapy using the described imaging analysis, particularly when compared with the limited capacity of humans to infer accurate predictions and risk groups identification (*5*). From the Radiomics analysis one can optimally benefit from early response metrics based on changes in metabolism measured with FDG-PET, even before anatomic changes become noticeable, while treatment can still be adapted.
We developed and validated a predictive model on the percentage variation of Radiomics features, the so-called "Delta Radiomics" concept, from repeated FDG-PET scans of NSCLC patients.

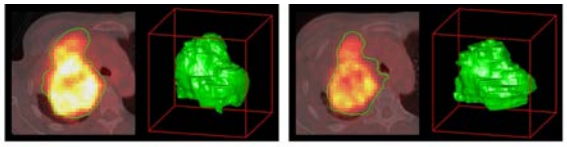

Figure 1 - Example of a pre-treatment (left) and during radiotherapy (right) PET-CT scan of a NSCLC patients from the development dataset.
Table 1 - Developed model after LASSO feature selection on the training dataset. Hazard ratios (HR) and corresponding p-value are presented for the final model. Performance is expressed as the concordance-index (c-index) both internally as for the two validation datasets.

Features	HR	p-value	Internal c-index	Validation c-index 1	Validation c-index 2
Shape – Volume	0.99	0.18			
RLGL – Grey level non-uniformity	1.01	0.02			
RLGL – Long run emphasis	0.98	0.06	0.64	0.61	0.58
GLCM – Sum entropy	0.98	0.20	(p<0.01)	(p=0.05)	(p=0.20)
GLSZM – High intensity large area emphasis	1.00	0.48			
IVH – $AVRI_{60\%}$	1.00	0.50			

Keywords: Early response assessment, non-small cell lung cancer, ^{18}F-FDG-PET imaging, metabolic metrics

References:
[1] Lambin P, Rios-Velazquez E, Leijenaar R, et al. Radiomics: extracting more information from medical images using advanced feature analysis. *Eur J Cancer.* 2012;48:441-446.
[2] van Elmpt W, Ollers M, Dingemans AM, Lambin P, De Ruysscher D. Response assessment using 18F-FDG PET early in the course of radiotherapy correlates with survival in advanced-stage non-small cell lung cancer. *J Nucl Med.* 2012;53:1514-1520.
[3] Yossi S, Krhili S, Muratet JP, Septans AL, Campion L, Denis F. Early assessment of metabolic response by 18F-FDG PET during concomitant radiochemotherapy of non-small cell lung carcinoma is associated with survival: a retrospective single-center study. *Clin Nucl Med.* 2015;40:e215-221.
[4] Leijenaar RT, Carvalho S, Velazquez ER, et al. Stability of FDG-PET Radiomics features: an integrated analysis of test-retest and inter-observer variability. *Acta Oncol.* 2013;52:1391-1397.
[5] Oberije C, Nalbantov G, Dekker A, et al. A prospective study comparing the predictions of doctors versus models for treatment outcome of lung cancer patients: a step toward individualized care and shared decision making. *Radiother Oncol.* 2014;112:37-43.

43
Proton scattering radiography using an emulsion detector: a feasibility study

A. Ariga[1], T. Ariga[1], M. Auger[1], S. Braccini[1], T. Carzaniga[1], A. Ereditato[1], K. P. Nesteruk[1], C. Pistillo[1], P. Scampoli[1,2]
[1] Albert Einstein Center for Fundamental Physics (AEC) - Laboratory for High Energy Physics (LHEP), University of Bern
[2] Department of Physics University of Naples Federico II

Purpose: Proton radiography is an imaging technique in proton therapy giving direct information on the density of the tissues, a useful tool to enhance the precision of proton therapy. It is usually performed as a proton range radiography by measuring the position and the residual range of the protons after the target. The properties of the traversed materials are directly related to multiple scattering so that it is possible to obtain an image through the assessment of the proton angular distribution. This work aims at studying the possibility of performing proton scattering radiography using only one nuclear emulsion film.
Materials and methods: Nuclear emulsion films allow for high-precision tracking of charged particles and, in particular, for reconstructing their angular distribution with a resolution of the order of 1 mrad. Specific detectors for medical applications can be built by interposing double-sided emulsion films with tissue equivalent materials, as it was done for proton range radiography [1] and to study the halo of a proton pencil beam [2]. In the present study, a detector composed by only one emulsion film was exposed to a 138 MeV proton pencil beam at the Gantry 1 at PSI. Two phantoms were placed in front of the detector: the "step" phantom consisted of two different thicknesses of PMMA (3 and 4 cm, respectively); the "rod" phantom had a total thickness of 4.5 cm and contained five aluminum rods (5 × 5 mm^2 section) positioned at different depths in a PMMA structure. Following the chemical development and the automatic microscopic scanning of the emulsion film, proton tracks were identified and their angular distribution reconstructed.
Results: The RMS of the scattering angle was measured for different segmentations of the emulsion film. Areas were chosen as strips parallel to the direction of the step or of the rods, for the first and the second phantom, respectively. To evaluate the resolution, strips of different sizes were considered. As shown in figure 1 (left), the step is clearly identified as a sharp drop of the RMS of the scattering angle. The signal due to the rods is visible as an enhancement of the RMS corresponding to their positions. The rod located nearest to the detector shows a sharper peak while the farthest one appears broader due to the larger distance travelled by the protons. While the contrast for the step phantom is found to be basically the same for range and scattering proton radiography, the signal due to the rods is more evident with respect to what was obtained with proton range radiography [1]. These preliminary results suggest that atomic number plays a fundamental role to increase the contrast of the image.
Conclusions: A feasibility study of proton scattering radiography with a new method based on a single emulsion detector has been performed. The first preliminary results are promising and further studies are under way encompassing in particular Monte Carlo simulations.

Keywords: Proton radiography, proton therapy, nuclear emulsion detectors

References:
[1] S. Braccini et al., First results on proton radiography with nuclear emulsion detectors, Journal of Instrumentation 2010 JINST 54 P09001.
[2] A. Ariga et al., Characterization of the dose distribution in the halo region of a clinical proton pencil beam using emulsion film detectors, Journal of Instrumentation 2015 JINST 10 P01007.

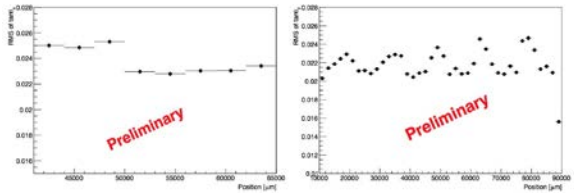

Figure 1 – Proton scattering radiography of a 1 cm PMMA step (left) and of 5x5 mm^2 rods embedded in PPMA (right)

44

Development of a track structure detector for biologically weighted treatment planning in particle therapy

M. Casiraghi[1], F. Vasi[1], V.A. Bashkirov[3] and R.W. Schulte[3]
[1] Center for Proton Therapy, Paul Scherrer Institut, Villigen, Switzerland
[3] Department of Basic Sciences, Loma Linda University, Loma Linda CA, USA

The biological effects of ionizing radiation are determined by the degree of ionization clustering in sensitive biological targets. In Monte Carlo (MC) simulations with geometric DNA models, correlation between the frequency of ionization cluster sizes and resulting clustered DNA damages has been observed [1]. Experimental characterization of radiation track structure on the nanometric scale can be used for assessing biological radiation quality. This approach has important applications in particle therapy, overcoming limitations of the current approach based on rescaling the absorbed dose by the RBE. Measurements of track structure are essential for the validation of MC simulations, which can be applied to patient geometries to produce biologically uniform dose distributions, as recently demonstrated for a simple beam geometry [2]. We are currently developing a compact single-ion gas detector for track structure measurements [3] with applications in clinical particle beams.
The concept of the detector is shown in fig. 1. Radiation-induced positive ions are drifted and focused into the millimetric holes of a THGEM-like structure made of a single-side-clad dielectric plate. Here, ions are accelerated in a strong electric field producing a limited discharge that is spatially restricted to the holes and is confined in time due to the high resistivity of the cathode in contact to the bottom side of the board. Registering the coordinates of the hole position and using the time difference between signals as information on the third dimension, the 3D spatial distribution of the initial ionization events can be reconstructed. Track structure simulations are then used for obtaining scaling factors to convert the spatial distribution of ionizations measured in low-pressure gas to nanoscopic distributions in water [4]. Simulations of track structure for applications to particle therapy were also performed with Geant4-DNA.
Detector characterization has been performed with a ^{241}Am source and low energy alpha and proton microbeams. Ionizations produced in propane and argon gas were detected with single-ion sensitivity. The ion detection efficiency was enhanced by increasing the GEM thickness up to 1 cm, consequently increasing the likelihood of ion impact ionization. Detector dead times of the order several tens of ms strongly affected the detector performance. This is ascribed to the long cathode recharge time. Materials with different resistivity have been tested; however, further work is necessary to find the optimal material. Geant4-DNA simulations showed the feasibility of track structure to produce biologically-weighted particle therapy plans. Assuming that the detector performance can be further improved, it could become an essential tool to validate track-structure-based treatment planning.

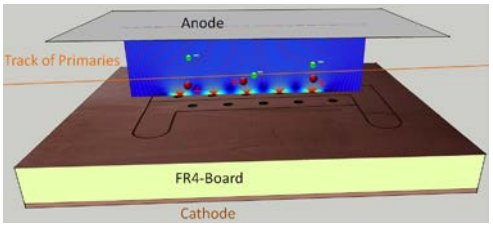

Figure 1: Sketch of one of the detector configurations used in the tests. From the top: anode providing drift field (10 V/cm); low pressure drift region (2-3 mBar of propane or Argon); THGEM (1 cm thickness) with 10 holes of 1.5 mm diameter and top readout electrodes; resistive cathode connected to high voltage (1-2 kV). Electric field lines calculated with COMSOL software are shown.

Keywords: track structure, radiation biological effect, THGEM

References:
[1] Nikjoo H. Radiation track and DNA damage. Int. J. Rad. Res. 1, 1 (2003).
[2] Casiraghi M. and Schulte R.W Nanodosimetry-Based Plan Optimization for Particle Therapy. Comput. Math. Meth. Med., vol. 2015 (2015).
[3] Bashkirov V. A., Hurley R. F. and Schulte R. W. A novel detector for 2D ion detection in low-pressure gas and its applications. In: NSS/MIC Conference Record, IEEE, 694-698, (2009).
[4] Grosswendt B. Nanodosimetry, from radiation physics to radiation biology. Radiat. Prot. Dosim. 115, 1-9 (2005).

45

Clinical validation of the M5L lung Computer-Assisted Detection system.

E. Lopez Torres[1,2], A. Traverso[3,1], S. Bagnasco[1], C. Bracco[4], D. Campanella[5], M.E. Fantacci[6,7], S. Lusso[1], D. Regge[5], M. Saletta[1], M. Stasi[4,1], S. Vallero[1], L. Vassallo[5], P. Cerello[1]
[1] INFN, Sezione di Torino, Torino, Italy
[2] CEADEN, Havana, Cuba.
[3] Physics Department, Polytechnic University of Torino, Torino, Italy.
[4] Medical Physics Unit, Candiolo Cancer Institute-FPO, Candiolo, Italy.
[5] Radiology Unit, Candiolo Cancer Institute-FPO, Candiolo, Italy.
[6] Physics Department, University of Pisa, Pisa, Italy.
[7] INFN, Sezione di Pisa, Pisa, Italy

Lung cancer is one of the leading causes of death in the world. Early diagnosis could be crucial in trying to reduce the mortality: several screening trials, conducted over the last decade in Europe and the US, showed a reduction in 5-year mortality for the branch undergoing chest CT instead of RX [1]. Alongside screening programmes, several Computer-Assisted Detection (CAD) systems were developed, in order to support radiologists in the diagnosis.
The M5L CAD, developed by the INFN in collaboration with CEADEN (Habana, Cuba), is based on a multi-thread approach: it combines the results of two independent algorithms, based on Voxel-Based Neural Analysis (VBNA) [2] and on Virtual Ant Colonies (lungCAM) [3], and provides a framework for further extension to others.
M5L was recently validated on the full LIDC database, the largest publicly available with its 1018 CTs, as well as other datasets (ANODE09, ITALUNG_CT): its sensitivity [4] is about 80% in the 4-6 false positive findings/scan range, which, considering the fact M5L was applied in a clinical-like approach, with no optimization and no data selection, is satisfactory.
Having demonstrated the algorithm generalization capabilities (the training classifier procedure only used 69 of the 1018 LIDC CTs), the development team tackled the issue of making it available to the largest possible user community. Therefore, a Web/Cloud prototype was designed and implemented: CTs are uploaded through a Web front-end interface and analysed by the cloud-backend

at the INFN-Torino Computer Centre.
The proposed approach implements data security by means of CT anonymisation and secure transfer protocol (*https*), and avoids all the issues related to the software deployment on a distributed environment. CT scans can be uploaded asynchronously by ICT staff in health facilities, while the M5L results are directly sent to the radiologist e-mail accounts in DICOM-compatible format (fig. 1).
Clinical validation on oncological patients undergoing staging or restaging has recently started at IRCCS Candiolo, Italy
The service is available to other institutions willing to join the M5L clinical validation protocol.

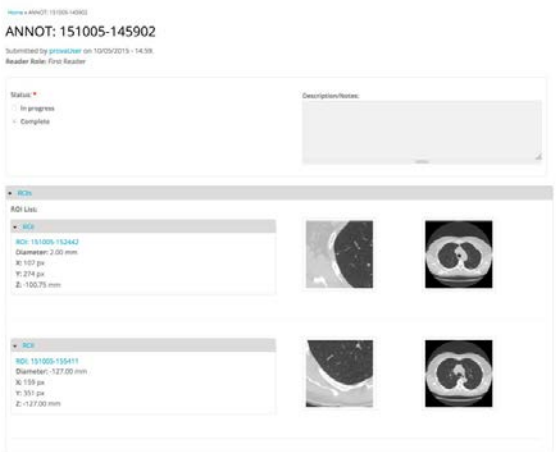

Figure 1: An example of the M5L CAD results as visualised by the radiologists on the M5L web interface.

Keywords: lung cancer, Computer-Assisted Detection, clinical validation

References:
[1] N.L.S.T.R. Team, et al., Reduced lung-cancer mortality with low-dose computed tomographic screening, The New England Journal of Medicine 365 (5) (2011) 395.
[2] A. Retico et al., Pleural nodule identification in low-dose and thin-slice lung computed tomography, Computers in Biology and Medicine 39 (12) (2009) 1137–1144.
[3] P. Cerello et al., 3-d object segmentation using ant colonies, Pattern Recognition 43 (4) (2010) 1476–1490.
[4] E. Lopez Torres et al., Large scale validation of the M5L lung cad on heterogeneous CT datasets, Medical Physics 42 (4) (2015) 1477–1489.

46
Measurements of Reactive Oxygen Species production induced by Gold Nanoparticles in Radiotherapy protocols.
L. Bocchini [1,2], A. Gobbato[1], A. Attili [1], C. Cutaia[3], V. Ferrero[1,2], C. Pontremoli[4], L. Radici[3], Stasi [3,1], S. Visentin [4,1], P. Cerello[1]
[1] INFN, Sezione di Torino, Torino, Italy
[2] Physics Department, University of Torino, Torino, Italy.
[3] Medical Physics Dep., A.O. Ordine Mauriziano, Torino, Italy.
[4] Molecular Biotechnology and Health Sciences Department, University of Torino, Torino, Italy

Metallic nanoparticles have shown radiosensitizing properties both in radio- and in hadron-therapy conditions. However, it is not demonstrated what the mechanisms that induce the extra damage are, although Reactive Oxygen Species (ROS) production, known to be crucial in radiotherapy, is a strong candidate.
Few direct measurements of ROS production are reporte in the literature [1,2] and no studies were found in typical radiotherapy treatment conditions.
A protocol for measuring the OH* radical production in Phosphate-buffered saline (PBS) solution, based on the fluorimetric properties of oxygen-quenched Terephthalic acid, was designed and validated. Correction factors associated to GNP-induced adsorption, absorption and diffusion at the fluorimetric excitation and emission wavelengths were carefully evaluated.
ROS production induced by photon beams at 6 and 15 MV was then measured in standard PBS solution as well as in the presence of Gold Nano Partticles (GNPs) with a 5 nm and 20 nm diameters, at 5 µmol and 10 µmol concentrations.
A relevant ROS extra production was observed for GNP with 5 nm diameter, up to about 45% at 10 µmol and 25% at 5 µmol, as shown in fig. 1 as a function of the delivered dose.
Measurements with 20 nm diameter GNPs are consistent with a ROS production increase of the order of 10%. However, in that condition the experimental error would not allow the conclusion that ROS production was actually enhanced.
The ROS enhancement, expected to be linearly depedent on the GNP surface to volume ratio, is indeed consistent with the hypothesis, within the experimental errors.
Further measurements with 10 nm and 2 nm GNPs are planned, in order to verify the linear dependence on the inverse radius with higher precision.

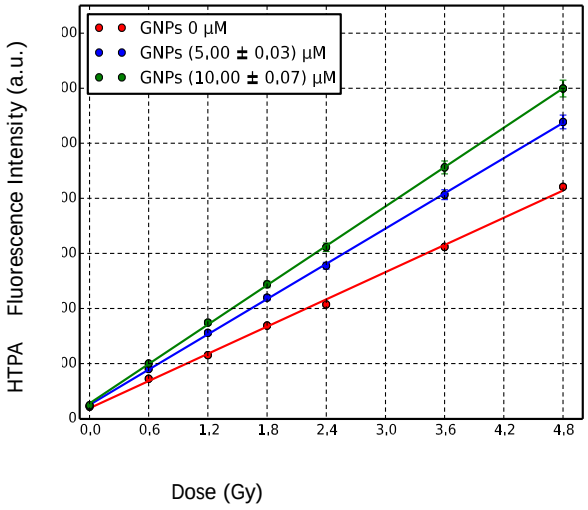

Fig. 1: Observed fluorescence intensity as a function of the delivered dose for the samples with 0 (red), 5 (blue) and 10 µmol (green) GNPs exposed to 15 MV photon beams.

Keywords: Radiotherapy, Gold Nanoparticles, Reactive Oxygen Species

References:
[1] Misawa, M., & Takahashi, J. (2011). Generation of reactive oxygen species induced by gold nanoparticles under x-ray and UV irradiations. *Nanomedicine: Nanotechnology, Biology and Medicine*, *7*(5), 604-614.
[2] Geng, F., Song, K., Xing, J. Z., Yuan, C., Yan, S., Yang, Q. & Kong, B. (2011). Thio-glucose bound gold nanoparticles enhance radio-cytotoxic targeting of ovarian cancer. *Nanotechnology*, *22*(28), 285101.

47

The use of radiobiological TCP and NTCP models to validate the dose calculation algorithm and readjust the prescribed dose

A. Chaikh[1,2], J. Balosso[1,2]
[1] Department of Radiation Oncology and Medical physics, University Hospital of Grenoble, France.
[2] Université Grenoble-Alpes, Grenoble, France.
Corresponding author: Abdulhamid Chaikh
Tel.:+33 6 25 73 78 99, fax:+33 476765629
E-mail: abdulhamedc@yahoo.com

Purpose: This study introduces an advanced method to evaluate and extent the adjustment of the prescribed dose to maintain the same clinical results, when changing the dose calculation algorithm type (a), i.e density correction method to more recently type (b) algorithm, i.e AAA.
Material and methods: 10 cases with lung cancer were studied. For each case, 3 treatment plans were generated. Plan 1 was generated using type (a) algorithm, and Plan 2 using type (b) algorithm. In plan 3 the dose was calculated with type (b) algorithm using monitor units from plan 1 as input. A global analysis based on 2D and 3D gamma (γ) was made to evaluate the under / overestimation of calculated dose. Clinical evaluation was carried out using Tumour Control Probability (TCP) and Normal Tissue Complication Probabilities (NTCP) based on Uniform Equivalent Dose model. Assuming a constant TCP, the ratio "R= TCP/NTCP" and Uncomplicated Tumor Control Probability (UTCP) were calculated to measure the clinical benefit – toxicity. Wilcoxon test was used to evaluate the significance of the differences and the correlation coefficient (r) was calculated using Spearman's rank test.
Results: The dose calculated with algorithm type (b) was significantly overestimated to organs at risks while the delivered dose in MU was underestimated, $p < 0.001$. Therefore, γ maps confirmed the dosimetric results. Moreover, there were a significant difference for NTCP for lung and heart. The ratio "R" from plan 1 and plan 2 were significantly different, indicating that to maintain the same effect benefit and toxicity the prescribed dose should be readjusted.
Conclusion: We assessed the prescribed dose using the radiobiological models. The ratio of benefit was significantly changed when moving from type (a) algorithm to type (b) algorithm. This indicate that the prescribed dose should be readjusted when type (b) algorithm will be integrated in radiation oncology. A discussion between oncologist and physicist is quite necessary in order to readjust the prescribed dose.

Key words: TCP, NTCP, EUD, gamma maps.

48

62 MeV Proton beams induced DNA damage in hypoxic conditions.

P. Chaudhary[1], T. Marshall[1], L. Manti[4], F. J. Currell[3], F. Romano[5], P. G. Cirrone[5], G. Schettino[1,2,] K. M. Prise[1]
[1] Centre for Cancer Research and Cell Biology, Queen's University Belfast, UK
[2] National Physical Laboratory, Hampton Road, Teddington, Middlesex, England, UK
[3] School of Mathematics and Physics, Queen's University Belfast, UK
[4] Department of Physics, University of Naples Federico II, Italy.
[5] Istituto Nazionale di Fisica Nucleare, LNS, Catania, Italy

Purpose: Hypoxia represents one of the most important challenges of current radiotherapy that can potentially affect the treatment planning and outcome. For the optimization of proton therapy and its application in treating hypoxic tumors such as dose and LET painting it is important to study the DNA damage response of normal cells under hypoxic and radio resistant conditions. The present study is aimed at understanding the variations in DNA double strand breaks induction and repair along prisitine and Spread-Out-Bragg-Peak Proton beams under hypoxic.
Materials and methods: DNA DSB damage and repair response was studied in AG01522 cells irradiated at various positions along the 62 MeV therapeutic protons Bragg peak at the CATANA beam line of the Institute of Nuclear Physics (INFN) Catania, Italy. Hypoxia was mimicked by using Cobalt chloride (CoCl2) and Dimethyl Sulphoxide (DMSO) was used as a Reactive Oxygen Species (ROS) scavenger. Hypoxia induction was confirmed by immunofluorescent staining of Hypoxia inducible factor-1 alpha (HIF-1α) and DNA DSB induction was quantified using p53 Binding protein-1 (53BP1) foci.
Results: The presence of DMSO and CoCl2 reduced the 53BP1 foci by 40% as compared to foci induction under normoxic conditions (30 minutes) in the cells irradiated at the entrance position of pristine beam. Cells irradiated at the Bragg peak revealed a significant induction of residual DSB damage even in presence of DMSO and CoCl2 at 24 hrs. Cells irradiated at distal end positions of the SOBP also revealed a significant induction of the 53BP1 foci irrespective of the oxygenation conditions of the medium.
Conclusions: Our results indicate the variations in the induction and repair of DNA DSBs in presence of ROS scavenger and Hypoxia along the Bragg peak. These findings can be of potential application in the tumor treatment planning of hypoxic tumors especially near the critical organs and combining DNA repair inhibitors approach.

Key words: Hypoxia, 53BP1, SOBP

49

Laser accelerated ultra high dose rate protons induced DNA damage under hypoxic conditions

P. Chaudhary[1], D. Gwynne[2] , D. Doria[2] ,L. Romagnani[4], C. Maiorino[1], H. Padda[5], A. Alejo[2], N. Booth[3], D. Carroll[3], S. Kar[2], P.McKenna[5], M. Borghesi[2] and K. M. Prise[1]
[1] Centre for Cancer Research and Cell Biology, Queen's University Belfast, UK
[2] Centre of Plasma Physics, Queen's University Belfast, UK
[3] Experimental Science Group, Central Laser Facility, Rutherford Appleton Laboratory, Didcot, Oxford, UK
[4] Laboratoire LULI Ecole Polytechnique, Cedex, France
[5] SUPA Department of Physics, University of Strathclyde, Glasgow G4 0NG, UK

Purpose: Hypoxic tumors still pose a challenge for modern radiotherapy. Hadrontherapy has gained momentum world wide as an effective modality for tumor therapy including success in inducing cell death in cancer cells under hypoxia as reported by several investigators. Significant advances in laser technologies have led to the prospect of using laser-accelerated ions, emitted in ultrashort bursts, as a future, cost-saving alternative to conventional accelerators. An understanding of the radiobiological effects at the ultrahigh dose rate delivered by these short ions pulses on human cells under hypoxic conditions is important for the development and further advancement of this technology towards clinical applications.
Materials and methods: Laser accelerated 15-18 MeV protons generated using the Nd:glass VULCAN laser system at the Rutherford Appleton Laboratory, Oxford, UK, were delivered, by a compact magnetic transport system, to cell samples at dose rates exceeding 10^9 Gy/s. Dosimetry was validated using EBT2 gafchromic films and CR-39 tracks detector. Normal human skin fibroblasts (AG01522 cells) monolayers grown in custom made stainless steel, on 3 μm thin Mylar dishes were pre-gassed with hypoxic gas mixture (95% nitrogen and 5% Carbon-di-oxide) for 4 hours and irradiated inside portable beam-line hypoxia chambers. Hypoxia induction was confirmed using HIF-1 alpha immuostaining. DNA damage and repair kinetics was studied using 53BP1 foci formation assay up to 24 hours after irradiation under both normoxic and hypoxic conditions.
Results: Our preliminary data suggests the effectiveness of Laser accelerated protons in DNA damage induction under both normoxic and hypoxic conditions. We observed a small reduction in average foci induction at initial time points in hypoxic cells, which was not seen after 2 hrs.

Conclusions: We report here for the first time measurements of DNA damage with pulsed protons at ultrahigh dose rate (10^9-10^{10} Gy/s) under hypoxic conditions.

Key words: 53BP1, HIF-1 alpha,

50

Faster QA through improved proton calorimetry. Another spin-off from particle physics

C. Chirvase[1], R. Barlow[1], A. Basharina-Freshville[2], S. Jolly2, R. Saakyan[2]
[1] University of Huddersfield, UK
[2] University College London, UK

We have used the calorimeter module originally designed for the SuperNEMO experiment to measure the energies of protons at the Clatterbridge proton therapy cyclotron.
Such measurements are necessary for time consuming QA checks, and by improving the rates and energy resolution this time can be considerably reduced.
Preliminary results show that an energy resolution of sigma 0.7% can be achieved for low rates which will later be compared to the high rate data. We hope to extend this technique to proton radiography as well.

Keywords: proton therapy, radiography, scintillator

51

Study of Dosimetric Characteristics of a commercial OSLD system

A. Chougule
Professor Radiological Physics, SMS Medical College, Jaipur, INDIA

Introduction: Cancer treatment by radiotherapy is a complex process and needs accurate radiation treatment delivery and can be verified using in vivo measurements. Optically stimulated luminescence dosimeter [OSLD] has been used extensively for beam dosimetry, radiation protection including in vivo measurements due to their simple readout process and multiple times readout facility.
Aim and Objective: The aim of the present work is to study the dosimetric characteristics of commercial OSL system by Landauer Inc. before using it for clinical practice in radiotherapy.
Material and Methods: The OSLD system used is a commercial InLight™ microstar reader system, manufactured by Landauer Inc. The detector consist of Al_2O_3:C nanodot as OSL material, enveloped in special light protective plastic holders. In the present study the irradiations are carried out in 30*30 cm^2 solid water slab phantoms. Bhabhatron – II cobalt 60 telecobalt radiation is used for most of the measurements carried out. Clinac – iX is also used for 6 MV and 10MV energy photon beams to study dose rate and energy dependence. Absolute dose is measured using a 30013 PTW ionization chamber in solid water and compared with OSL dosimeter measurements.
Unless otherwise mentioned, all irradiations carried out using an SSD setup (80cm for co-60 and 100cm for linac) with 10*10cm^2 field size.OSL response with given dose is investigated for doses ranging from 0.5 to 4Gy. Energy dependence of OSL is investigated for Co-60, 6MV, 10MV beams, delivering a dose of 50 cGy each. Further the dose rate dependence of OSL detector is evaluated for dose rates of 200, 400, 600 cGy/min in accelerator with 6MV energy beam. We also studied the field size dependence by irradiating OSLD chips to 50 cGy dose for various field sizes ranging from 4*4 to 35*35 cm^2 for cobalt -60 beam. The dosimeter angular response is studied at various gantry angles from 90º to 270º, at an interval of 30º, with and without build up respectively.
Results: In present study it was observed that the OSL dose deviation is about - 4.5% as compared with ionization chamber. Further the reproducibility of detector is found to be within 3.44% standard deviation, with COV 0.035. There is no significant energy dependence of Al_2O_3:C detector for the energy range Co-60 to 10MV. The detector response was found to be linear in the dose range of 0.5 to 4Gy. The detector response is almost independent in clinical dose rate range, nearly independent of field size and is independent to angle of incidence of beam.
Discussion: The dosimetric characteristics of OSL system were studied and found that OSL response is energy and dose rate independent. The stability of system and linear dose response relationship makes it a good dosimeter for in vivo dosimetry in clinical radiotherapy.

Keywords: OSLD, invivo dosimetry, radiotherapy

52

Simulation of recombination in an air filled ionization chamber

J. B. Christensen[1], H. Tölli[2], B. Thomsen[1], N. Bassler[1],
[1] Department of Physics and Astronomy, Aarhus University, Denmark
[2] Department of Radiation Sciences, Umeå University, Sweden

Background: Air filled ionization chambers are the dosimeters of choice for photon therapy as well as particle therapy. Dosimetry protocols for ion beams take recombination effects into account, where the generated charge in the ionization chamber may recombine before it is picked up by the electrode. It is well established that intra-track recombination (initial recombination) is negligible in medical photon and electron beams, but must be accounted for in beams with heavy ions. However, the underlying assumptions for establishing the recommended method for correction for inter-track recombination (general recombination) still remains unclear today [1]. The current two-voltage method only is applicable for low LET-beams, with no initial recombination present [2,3], and this progress report focuses on a detailed recombination study of ion beams.
Here, we calculate the columnar recombination when the ion track is

- parallel to the electric field
- rotated with an angle between 0 and $\pi/2$ relative to the external field which was estimated analytically by Jaffé [4] and later confirmed experimentally by Kanai et al [5].

The general recombination is investigated by

- sampling two parallel ion tracks at different separation and initialized at different times
- comparing the simulation of a continuous beam with Greening's formula [6] for collection efficiency.

Simulations are confirmed by comparison with experimental data.
Methods: We have investigated positive and negative charge carrier distributions (CCDs) by solving the differential equation using a finite difference approach,

$$\frac{\partial n_{\pm}}{\partial t} = -D_{\pm}\nabla^2 n_{\pm} \mp \vec{\nabla}\cdot\left(\mu_{\pm}\vec{E}n_{\pm}\right) - \alpha n_{+}n_{-}$$

with derived from the initial CCDs, the diffusion constant, the mobility, for positive and negative CCDs, $\vec{E}$ the electric field vector, and the recombination constant.
Results: Our simulations reproduced the analytical solution from Jaffé and the experimental results by Kanai et al. On this platform we could also verify the Greening analytical solution.
Conclusion: The simulations of pulsed and continuous beams are seen to agree well with the known theories and experimental data, and the program is thus capable of reproducing the initial and general recombination processes taking place in high LET-beams. This allows a deeper study of the actual recombination processes taking place when several ion tracks are present and ultimately account for the overall recombination in air filled ionization chambers irradiated with high LET-beams.

Keywords: ionization chambers, recombination, high LET

References:
[1] International Atomic Energy Agency (IAEA), Technical Reports Series 398, IAEA 2000.
[2] Tölli, H. et al, Phys. Med. Biol. 55 (2010) 4247.
[3] Andersson, J. et al., Phys. Med. Biol. 56 (2011) 299.
[4] Jaffé, G., Ann. Physik (4) 42 (1913) 303.
[5] Kanai,T., et al, Phys. Med. Biol. 43 (1998) 3549.
[6] Greening, J. R, Phys. Med. Biol. 2 (1964) 143.

53

Local Tumor Flare Following Radiosurgery and Ipilimumab (Ipi) for Melanoma Brain Metastases: Increased Immune Response?

C. Chung[1,3], L. Khoja[1,3], G. Kurtz[1,3], M. Bernstein[2,3], A. Joshua[1,3], D. Hogg[1,3], G. Zadeh[2,3], N. Laperriere[1,3], C. Menard[1,3], B.A. Millar[1,3], P. Kongkham[2,3], M. Butler[1,3]
[1] University Health Network-Princess Margaret Cancer Centre
[2] University Health Network-Toronto Western Hospital
[3] University of Toronto

Background: The anti-CTLA4 antibody, ipilumumab (ipi), improves survival in metastatic melanoma. With increased survival and improved extracranial control, a greater proportion of melanoma patients develop brain metastases. The effects of combining radiotherapy (RT), whole brain RT (WBRT) or stereotactic radiosurgery (SRS) with Ipi are unclear. This study reports the incidence and factors associated with acute radiation effect (ARE), in patients with melanoma brain metastases treated with ipi and brain RT.
Methods: All patients with melanoma brain metastases who received WBRT or SRS and ipi at our institution from 2008-2014 were included. Outcome measures included incidence of ARE, treatment response, progression free survival (PFS) and overall survival (OS). Variables included baseline patient characteristics, type of RT (WBRT or SRS), dosimetric parameters (including V12 Gy for SRS), time between RT and ipi treatment. Using our prospective brain metastases database, incidence of ARE was compared against patients treated with SRS alone at our institution.
Results: A total of 688 patients in our database received SRS upfront and 54 pts met eligibility for evaluation of RT and ipi of which 34 were evaluable (20 were excluded due to lack of follow up imaging). With a median follow up of 7.4 months, OS was 6.4 months and PFS was 2.7 months. In patients treated with WBRT alone, no ARE was seen. In those who received SRS with ipi, 11/27 (41%) patients developed ARE. Of these, 7 patients had received RT within 4 months of ipi (SRS = 4, SRS+WBRT = 3) and 4 received RT outside of this window (SRS = 2, SRS+WBRT= 2). Out of the 688 patients treated with upfront SRS, 11% developed ARE. Larger tumor volume and higher V12Gy were associated with a higher rate of ARE. A total of 6 patients received steroids for symptomatic ARE of which only 1 patient did not respond and required surgical intervention. The pathology showed treated melanoma along with necrosis, and predominantly inflammatory T cells and macrophages.
Conclusions: The incidence of ARE was greater in patients treated with SRS and ipi (41%) compared to SRS alone (10%). In contrast, no ARE was seen after WBRT and ipi. In the majority of cases, symptomatic ARE responded to steroids. In 1 case requiring surgery, pathology demonstrated an increased immunological effect.

Keywords: immunotherapy, brain metastases, radiotherapy, radiosurgery, whole brain radiation, acute radiation effect, radionecrosis

54

The GEMpix detector as a real-time 2D dosimeter in external photon beam radiotherapy

G. Claps[1,3] , F. Murtas[3], E. Soldani[3], M. D. Falco[4], L. Quintieri[2]
[1] Unità Tecnica Fusione, ENEA, C.R. Frascati, Via E. Fermi, 45 - 00044 Frascati, Rome, Italy
[2] Istituto Nazionale di Metrologia delle Radiazioni Ionizzanti, ENEA, C.R. Casaccia, Via Anguillarese 301, 00123 Santa Maria di Galeria, Rome, Italy
[3] Istituto Nazionale di Fisica Nucleare, Via E. Fermi, 40, 00044 Frascati, Rome Italy
[4] Policlinico SS. Annunziata, Via dei Vestini, 66100 Chieti, Italy

Radiotherapy with external photon or electron beams represents one of the most widespread methods in the treatment of cancer disease. Recently the irradiation techniques have reached an accuracy of few mm. Intensity-Modulated-Radiation-Therapy (IMRT) is one of the most advanced irradiation techniques with external X-ray beams. It allows to conform in more detail the beam to the tumor volume adjusting a set of programmable multi-leaf collimator which can assume very different shapes. Then a very accurate instrument is required to verify the real released doses. Pre-treatment quality assurance play a central role in a typically radiotherapy treatment session because guarantees the success the treatment.
Devices devoted to quality assurance are dosimeter with different forms and dimensions. An important category is represented by 2D devices which are able to provide a measure of the dose distribution on a given area. The most common are ionization chamber arrays, films and Electronic Portal Imaging Devices (EPID). All these devices presents some drawbacks which limit their performance like 2D dosimeters, especially for IMRT. Ionization chamber arrays have a spatial resolution limited to few mm. Film dosimeters, on the contrary, can provide an higher spatial resolution with the drawback that it must be processed after taking into account other parameters which can influence the correct dose measure like fading, UV sensitivity, temperature and so on. EPID is applied as a 2D dosimeter, but an algorithm software is needed to convert the registered signal by an EPID into dose values and it is difficult to realize a unique software devoted to this aim.
The present work will demonstrate that detectors based on the Gas Electron Multiplier (GEM) technology [1] with a medipix C-MOS read-out can be a valid alternative for 2D dosimetry respect to the traditional devices. This type of detector, called “GEMpix” [2], shows some interesting characteristics which can overcome the typical drawbacks observed in the traditional 2D dosimeters [3]. In particular the GEMpix, working in a bi-GEM configuration, can perform 2D real time dose distribution measurements with a spatial resolution comparable the gafchromic films. A comparison between GEMpix and gafchromics has been performed in order to test its ability to work as 2D dosimeter. Dose matching between the two dosimeters has been evaluated applying a the gamma-index test analysis with the commonly accepted criteria of distance to agreement < 3 mm and dose difference < 3%.

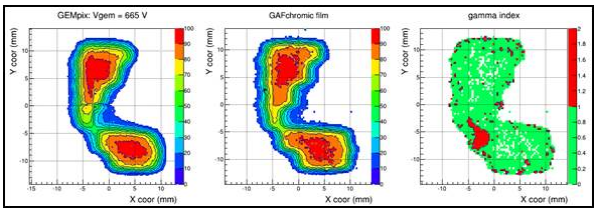

The figure shows a particular dose distribution as measured by GEMpix and by a gafchromic film. In the third panel a gamma index test map shows the areas where gamma index is less 1. This is verified in the 90,5 % of points.

Keywords: dosimetry, IMRT, GEM

References:
[1] F. Sauli, *“Nucl. Instr. and Meth.”* A 386 (1987) 531.
[2] F.Murtas, Applications of triple GEM detectors beyond particle and nuclear physics, 2014 JINST 9 C01058
[3] G. Claps, *A study of a triple GEM detector as real time dosimeter in external photon beam radiotherapy, PhD Thesis, University of Tor Vergata, 3 June 2015, Rome*

55

The International Cancer Expert Corps (ICEC): Implementing a global force to address the catastrophic rise in cancer in the developing world.

C. N. Coleman [1], S. C. Formenti[2],N. Chao[3], S. Grover[4]; D. Rodin[5]; D. G. Petereit[6]; B. Vikram[7]; D. A. Pistenmaa[1]; M. Mohiuddin[8]; T. R. Williams[9].
[1] International Cancer Expert Corps, New York, NY
[2] Cornell University Medical School, New York, NY
[3] Duke Cancer Institute, Durham, NC
[4] University of Pennsylvania, Philadelphia, PA
[5] University of Toronto, Toronto, Canada
[6] American Indian "Walking Forward" Program, Rapid City, SD
[7] National Cancer Institute, Bethesda, MD
[8] Radiation Oncology Consultants, Ltd., Park Ridge, IL, USA.
[9] Lynn Cancer Institute at Boca Raton Regional Hospital, Boca Raton, FL , USA.

Purpose: The growing burden of cancer and non-communicable diseases in the developing world is well recognized by the WHO and IAEA culminating in a declaration of the need to address them by the UN General Assembly in 2011. It is projected that ~75% of cancer cases will be in Low & Lower-Middle Income Countries (LMIC) by 2025. Effective solutions require technological and logistical approaches and sufficient expertise to establish sustainable capacity and capability in country.
Materials/methods: Recognizing that the essential component for any solution requires expertise, the ICEC (1,2) was established in 2013 as a not-for-profit non-government organization to address the human resources shortage. An extensive analysis by the Global Task Force for Radiation for Cancer Control under the auspices of the Union for International Cancer Control indicates that a solution is both possible and economically feasible (3).
Results: There is a confluence of forces and opportunities that makes the solution to what appears to be an overwhelming problem one that can and must be addressed. This includes:
a) the necessity for collaboration among existing programs, allowing for individual recognition and approaches while minimizing competition that can dissuade investment
b) a cohort of early stage career cancer experts committed to global health
c) participation of the private sector in global cancer education and training
d) success in addressing health disparities in indigenous populations in resource-rich countries that is part of global cancer care
e) an influx of retirees seeking opportunities to use their skills
f) interest in eliminating dangerous nuclear material especially in unstable countries
The ICEC mentorship model is in active organizational and funding development. Essential features and challenges are:
a) establishing a career path with metrics for academic advancement so that time, effort and contributions become an integral component of a medical career and not an extracurricular activity
b) supporting time and effort in both resource-rich and –poor countries
c) conducting guideline/protocol-based multi-modality cancer care at international standards so that LMICs can participate fully in research and training
d) being multi-national from the outset, capitalizing on existing twinning programs
e) creating an essential role for radiation therapy.
f) incorporating innovations in physics, information technology and telecommunications
Conclusions: The need, opportunity and a path forward for reducing the global burden of cancer are in hand. A concerted effort and sustainable investment by a broad range of partners are essential. The ICEC addresses the sustainable human resources problem with catalytic and disruptive innovation in cancer care delivery including a career path, economics, technology, public-private partnerships as well as visionary leaders and investors.

Key words: Global health, health disparities, disruptive innovation

References:
[1] Coleman CN et al Sci Transl Med. 2014 Oct 22;6(259):259
[2] Coleman CN et al, Front Oncol. 2014 Nov 19;4:33
[3] Atun R, et al. Lancet Oncol. 2015 Sep;16(10):1153-86
[4] Olson AC et al. Int J Radiat Oncol Biol Phys. 2015 Nov 1;93(3):493-6.

56

Comparison of Arterial Input Functions by Magnitude and Phase Signal Measurement in DCE MRI of brain cancer patients

C. Coolens[1,2,3], W. Foltz[1,2], B. Driscoll[1], C. Pellow[1], C. Chung[1,2]
[1] Radiation Medicine Program, Princess Margaret Cancer Centre, Toronto, Canada
[2] Department of Radiation Oncology, University of Toronto, Toronto, Canada.
[3] Institute of Biomaterials and Biomedical Engineering, Toronto, Canada

Purpose: The aim of this work is to (1) investigate the accuracy and robustness of magnitude and phase-derived arterial input functions (AIF) as compared to “gold standard” volumetric DCE-CT; and (2) evaluate the impact of individualized magnitude and phase signal AIF measurements on resulting perfusion parameter maps using a common 4D temporal dynamic analysis (TDA) method in metastatic brain cancer patients treated with stereotactic radiosurgery.
Methods: We evaluated 14 brain metastases imaged with volumetric DCE-CT (Toshiba, Aquilion ONE) and DCE-MRI (IMRIS 3T Verio) at baseline then 7 and 21 days post-radiosurgery. Both variable-flip-angle (VFA) T1 measurements and dynamic imaging used 3D-FLASH with matched TE/TR of 1.8/4.8ms, with 1x1x5 mm voxels. Voxel-based whole brain TDA was performed on all data using in-house software to: (1) compare the AIF curve from DCE-CT using the internal carotid artery (AIF) and sagittal sinus (VIF) curve from the DCE-CT against DCE-MRI [magnitude (VIFmag) and phase-based (VIFph)] (2) compare kinetic parameters area under the curve (AUC) and K_{trans}, assuming the Modified Tofts model when using individual CT AIF, MRI Magnitude and Phase-based VIF (Sagittal Sinus) and population-based AIF as well as individual voxel-based T_{10} maps versus assumed T_{10}= 2400 msec.
Results: The AUC of individual AIF and VIF on DCE-CT were similar and resulting median K_{trans} (0.048 +/- 0.03 s^{-1}) was also similar. For DCE-MRI, using measured voxel-based T_{10} maps, the resulting K_{trans} was higher than for CT using individual VIFmag (0.181 +/- 0.11 s^{-1}) or VIFph (0.121 +/- 0.099 s^{-1}). This is likely resulting from the smaller AIF peak since the population AIF (which more closely resembles CT) correlates better to DCE-CT metrics. The measured median T_{10} value was 1572 +/- 594 (n=41) and using the assuming T_{10}=2400 ms resulted in significantly higher K_{trans} (0.3 +/- 0.14 s^{-1}) and AUC ($p<0.0006$). Voxel-wise correlation between K_{trans} values than from CT and $MRI_{popAIF,T10}$ resulted in high R^2 values (~0.5, $p<0.05$) for all imaging days and showed good interchangeability (see Bland-Altman plot in Figure 1).
Conclusion: This preliminary data highlights the stability of DCE-CT calculations as well as susceptibility of DCE-MRI K_{trans} measurements to various imaging factors, including AIF selection and T_{10} values used in the model. Using the same voxel-based analysis platform for both DCE-CT and MR significantly improved correlation values confirming the need to take into account tumor heterogeneity when assessing functional data.

Keywords: Brain metastases, biomarker, perfusion imaging

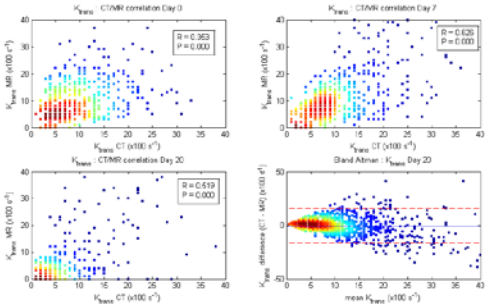

57
Focal adhesion signaling and therapy resistance in cancer
N. Cordes[1-5]
[1] OncoRay – National Center for Radiation Research in Oncology, Faculty of Medicine and University Hospital Carl Gustav Carus, Technische Universität Dresden, Germany and Helmholtz-Zentrum Dresden - Rossendorf, Dresden, Germany
[2] Department of Radiation Oncology, University Hospital Carl Gustav Carus, Technische Universität Dresden, Germany
[3] Helmholtz-Zentrum Dresden - Rossendorf, Institute of Radiooncology, Dresden, Germany
[4] German Cancer Consortium (DKTK), Dresden, Germany
[5] German Cancer Research Center (DKFZ), Heidelberg, Germany

Purpose: Intrinsic and acquired resistance of tumor cells to therapy originates from multiple avenues. One avenue includes extracellular matrix (ECM) and proteins that facilitate cell interaction with ECM. These focal adhesion (FA) proteins coalesce at specific membrane sites as large multiprotein complexes functioning as signaling hubs and structural nexus. Molecular targeting of various FA proteins has shown promising preclinical data. Even more interesting are rather recent findings about activation of prosurvival bypass signaling under specific inhibition of integrins and their dependence on ECM stiffness.
Materials/methods: Different tumor models were investigated such as head and neck, pancreatic ductal carcinoma, glioblastoma. We performed a systematic targeting of FA proteins using siRNA or antibodies where applicable. In-vitro and in-vivo survival assays and a variety of mechanistic studies were conducted.
Results: To date, integrins turned out as most promising druggable candidates. Most interesting, molecular targeting generally showed to prominently induce unfavorable prosurvival signaling. Multitargeting strategies were successful to abrogate this bypass signaling and optimize radiochemosensitization.
Conclusions: Integrins and other FA proteins are promising cancer targets. Identification of underlying mechanisms is still the needle eye. From our data, multitargeting approaches on top of conventional radiochemotherapy look beneficial as specific tumor cell functions can be inhibited.

Keywords:
Focal adhesions, resistance, bypass signaling

References:
[1] Eke I, Deuse Y, Hehlgans S, Gurtner K, Krause M, Baumann M, Shevchenko A, Sandfort V, Cordes N. ß1 integrin/FAK/Cortactin signaling is essential for human head and neck cancer resistance to radiotherapy. J Clin Invest, 2012, 122(4):1529-40
[2] Eke I, Schneider L, Förster C, Zips D, Kunz-Schughart LA, Cordes N. EGFR/JIP-4/JNK2 signaling attenuates Cetuximab-mediated radiosensitization of squamous cell carcinoma cells. Cancer Res, 2013, Jan 1;73(1):297-306.
[3] Vehlow A, Cordes N. Invasion as target for therapy of glioblastoma multiforme. Biochim Biophys Acta, 2013 Jul 24. doi:pii: S0304-419X(13)00038-3. 10.1016/j.bbcan.2013.07.001. [Epub ahead of print]
[4] Eke I, Zscheppang K, Dickreuter E, Hickmann L, Mazzeo E, Unger K, Krause M, Cordes N. Simultaneous ß1 integrin-EGFR targeting and radiosensitization of human head and neck cancer. J Natl Cancer Inst, 2015 Feb 5;107(2)
[5] Steglich A, Vehlow A, Eke I, Cordes N. α integrin targeting for radiosensitization of three-dimensionally grown human head and neck squamous cell carcinoma cells. Cancer Lett, 2015 Feb 28;357(2):542-8
[6] Dickreuter E, Eke I, Krause M, Borgmann K, van Vugt MA, Cordes N. Targeting of beta1 integrins impairs DNA repair for radiosensitization of head and neck cancer cells. Oncogene, 2015 Jun 15. doi: 10.1038/onc.2015.212. [Epub ahead of print]

58
Evaluation study of in-beam PET performances with a Carbon ion linac (CABOTO)
C. Cuccagna[1,2], R. S. Augusto[3,4], W. Kozlowska[3,5], P. G. Ortega[3], V. Vlachoudis[3], A. Ferrari[3], U. Amaldi[1]
[1] Tera Foundation
[2] University of Geneva
[3] CERN
[4] LMU Munich
[5] Medical University of Vienna

Purpose: In-Beam PET is a *well-established* method for dose monitoring in hadrontherapy, but its effectiveness is still limited by the accelerator duty cycle [1]. CABOTO [2, 3], CArbon BOoster for Therapy in Oncology, is an innovative development project of an efficient high-frequency linac for hadrontherapy that can accelerate ^{12}C ions and H_2 molecules up to 430 MeV/u, bunched in pulses of the order of 2-5 µs with a repetition rate of 360 Hz.
Thanks to its low duty cycle (less than 0.1%), CABOTO allows the γ-pair acquisition with PET during 99.9% of the treatment time. The main goal of this research is to describe how the CABOTO time-structure influences the in-beam PET images, reconstructed by acquiring the γ-coincidences during the irradiation time as well as in a period following it.
Methods and Materials: The study has been carried out performing several simulations with the FLUKA Monte Carlo code [4, 5] together with MATLAB routines written to take into account analytically the CABOTO time structure.
In a first set of simulations, the $ß^+$ emitter isotopes, produced by the interaction of a pencil beam (protons and ^{12}C-ions) with a water phantom, are identified. Due to the special time structure, the PET detector is sensitive also to γ-pair produced in the $ß^+$-decays of isotopes having half-lives ($T_{1/2}$) in the ms range; the most relevant ones are ^{13}O ($T_{1/2}$=8.6 ms), ^{12}N ($T_{1/2}$=11 ms), ^{9}C ($T_{1/2}$=126.5 ms), ^{8}B ($T_{1/2}$=770 ms). Considering the CABOTO time structure and the acquisition time window as defined before, the $ß^+$ activity versus time has been extrapolated for all $ß^+$ emitters.
A second set of simulations including a PET detector has been carried out, using a modified version of the routines originally developed in Fluka for conventional PET [6]. Arrival times of gamma pair coincidences on the PET detector have been scored and analysed in order to verify their correspondence to the beam irradiation profile. The history of each coincidence has been traced in order to identify the parent isotope, which helps to discriminate and evaluate the true signal versus the background noise. Based on this information, the PET images could be reconstructed from the true coincidences from both the online and offline signal, and quantify the differences.
Results & Conclusions: This work describes the results obtained in the study of the influence of CABOTO time structure on the PET scanner reconstruction. The $ß^+$ activity collected during the irradiation with a single pencil beam has been computed together with the estimated background during the irradiation. The effect of the very short half-life $ß^+$ emitters, which produce positrons of longer ranges, has been studied. Preliminary results obtained in a simulation on a real patient case, with all the beam spots delivered with the correct time structure, are also presented.

Keywords: in-beam PET, hadrontherapy, Monte Carlo

References:

[1] G. Sportelli et al., *First full-beam PET acquisitions in proton therapy with a modular dual-head dedicated system*, Phys. Med. Biol. 59 (2014) 43-60
[2] U. Amaldi, S. Braccini, P. Puggioni, *High Frequency Linacs for Hadrontherapy*, RAST 2 (2000) 111
[3] S. Verdú-Andrés, U. Amaldi ,Á. Faus-Golfe, *CABOTO, a high-gradient linac for hadrontherapy, J. of Radiation Research, 2013, 54, i155–i161*
[4] T.T. Bohlen, F. Cerutti, M.P.W. Chin, A. Fasso`, A. Ferrari, P.G. Ortega,
A. Mairani, P.R. Sala, G. Smirnov, and V. Vlachoudis, *The FLUKA Code: Developments and Challenges for High Energy and Medical Applications*
Nuclear Data Sheets 120, 211-214 (2014)
[5] A. Ferrari, P.R. Sala, A. Fasso`, and J. Ranft *FLUKA: a multi-particle transport code*, CERN-2005-10 (2005), INFN/TC_05/11, SLAC-R-773
[6] P. G. Ortega, T. T. Boehlen, F. Cerutti, M. P. W. Chin, A. Ferrari, A. Mairani, C. Mancini, P. R. Sala & V. Vlachoudis, *A dedicated tool for PET scanner simulations using FLUKA*, 3rd International Conference on Advancements in Nuclear Instrumentation Measurement, Methods and their Applications (ANIMMA), 2013.

59

Nanox™: A new multiscale theoretical framework to predict cell survival in the context of particle therapy

M. Cunha[1], C. Monini[1], E. Testa[1], M. Beuve[1]
[1] Université de Lyon, F-69622, Lyon, France; Université de Lyon 1, Villeurbanne; CNRS/IN2P3, Institut de Physique Nucléaire de Lyon

The number of facilities that offer tumor treatment with particle therapy has been increasing substantially over the past decades. The dose distribution deposited by ions, and for the heaviest, their higher biological effectiveness, make them more interesting to destroy localized tumors while sparing healthy tissues. Such an effectiveness is quantified through the RBE (relative biological effectiveness), which is a complex function of multiple parameters like cell line, cell cycle stage, radiation quality and irradiation conditions. Therefore, determining the value of RBE for every scenario is a challenging task that requires modeling to comply with the demands of a clinical environment.
Several solutions have already been developed and a few are currently used in treatment planning [1-4]. Nevertheless, despite the progress these models have allowed, they present some shortcomings [5-7] that may limit their improvement. We present thereby a new approach that gathers some principles of the existing ones and addresses some of their weaknesses. The innovative features of Nanox™ are that it is fully based on statistical physics, taking in particular into account the fluctuations in energy deposition at multiple scales, and that it introduces the concept of a chemical dose. The latter is chosen as a parameter defined at the cell scale to represent the induction of cell death by "non-local" events as the accumulation of cellular oxidative stress or sub-lethal lesions induced by the produced radical species. Such "non-local" events are complementary to the so-called "local" events, which take place at a very localized (nanometric) scale. The "local" events are considered as lethal since a single event can cause cell death.
The cell survival predicted by Nanox™ for V79 cell line was compared with experimental results for photons, protons and carbon ions, and even others like neon and argon ions. A good agreement was found in all cases. In particular, the model is able to describe the effectiveness of ions, including the overkill effect at higher LET values. Moreover, Nanox™ can reproduce the typical shoulder in cell survival curves. This was possible due to the introduction of the "non-local" events, through the chemical dose, which varies with LET. It is worthwhile to note that such results were obtained through the adjustment of a reduced number of free parameters.
The first results of Nanox™, obtained for V79 cell line, give us confidence that this model has potential for application in a clinical scenario in the context of particle therapy. Although it requires the tuning of only a few free parameters, Nanox™ is based on solid principles and a thorough mathematical implementation, which renders this approach simple but reliable for application in clinical practice.

Keywords: RBE; multiscale dosimetry; oxidative stress

References:
[1] Krämer M, Scholz M. Treatment planning for heavy-ion radiotherapy: calculation and optimization of biologically effective dose. Phys Med Biol 2000;45(11):3319–30. doi:10.1088/0031-9155/45/11/314.
[2] Krämer M, Scifoni E, Waelzlein C, et al. Ion beams in radiotherapy – from tracks to treatment planning. J Phys Conf Ser 2012;373:012017.
doi:10.1088/1742-6596/373/1/012017.
[3] Endo M, Koyama-Ito H, Minohara Si, et al. HIPLAN – a heavy ion treatment planning system at HIMAC. J JASTRO 1996;8(3):231–8. doi:10.11182/jastro1989.8.231.
[4] Mizota M, Kanai T, Yusa K, et al. Reconstruction of biologically equivalent dose distribution on CT-image from measured physical dose distribution of therapeutic beam in water phantom. Phys Med Biol 2002;47(6):935–45. doi:10.1088/0031-9155/47/6/306.
[5] Schardt D, Elsässer T, Schulz-Ertner D. Heavy-ion tumor therapy: Physical and radiobiological benefits. Rev Mod Phys 2010;82(1):383–425. doi:10.1103/RevModPhys.82.383.
[6] Beuve M. Formalization and theoretical analysis of the local effect model. Radiat Res 2009;172(3):394–402. doi:10.1667/RR1544.1.
[7] Russo G, Attili A, Bourhaleb F, et al. Analysis of the reliability of the local effect model for the use in carbon ion treatment planning systems. Radiat Prot Dosim 2011;143(2-):497–502. doi:10.1093/rpd/ncq407.

60

Expert knowledge and data-driven Bayesian Networks to predict post-RT dyspnea and 2-year survival

T.M. Deist[1], A. Jochems[1], C.Oberije[1], B. Reymen[1], K. Vandecasteele[2], Y. Lievens[2], R. Wanders[1], K. Lindberg[3], D. De Ruysscher[4], W. van Elmpt[1], S. Vinod[5], C. Faivre-Finn[6], A. Dekker[1], P. Lambin[1]
[1] Department of Radiation Oncology (Maastro Clinic), GROW – School for Oncology and Developmental Biology, Maastricht University Medical Centre.
[2] Department of Radiation Oncology, Ghent University Hospital, Ghent, Belgium.
[3] Karolinska Institutet, Karolinska University Hospital, Stockholm, Sweden
[4] Universitaire Ziekenhuizen Leuven, KU Leuven, Belgium
[5] South Western Sydney Clinical School, University of New South Wales, Liverpool, Australia
[6] Institute of Cancer Sciences, The University of Manchester, Manchester Academic Health Science Centre, The Christie NHS Foundation Trust, Manchester, UK

Purpose: The advent of personalized medicine in radiotherapy (RT) is accompanied by the need for accurate outcome prediction. The current state of predictions made by physicians for patient survival and toxicity after lung radiotherapy is comparable to flipping a coin (Oberije et al.,Radiother. Oncol. 2014). In order to assess the value of expert knowledge in prediction modelling (rather than directly predicting outcomes), expert-based and data-driven prediction models were built and compared. Models for two endpoints were created: 2-year survival in NSCLC non-surgery patients and severe dyspnea (CTCAE dyspnea scores ≥ 2) after RT.
Materials/methods: Data from lung cancer patients (994 for dyspnea, 452 for 2-year survival) treated in clinical routine were collected. 10 experts (4 experts participated for both endpoints) selected causal links between patient, disease, treatment, and dose-related variables (19 for dyspnea, 17 for 2-year survival) and the two outcomes. The selected links were used to construct Bayesian Networks (BN) for a comparison with BNs based on a data-driven algorithm. These models were then learned on 80% and validated on 20% of the patient data. Discrimination in the validation data sets is assessed by the Area under the Curve (AUC).

Results: Expert networks were more complex with up to 30 arcs while the data-driven algorithm selected no more than 6 arcs. Expert and data-driven models were not significantly different in discriminative ability (see 95% confidence intervals in table). Further, AUCs of all models except expert 6 were not significantly different from 0.5. Patients with 2-year survival could be discriminated better as it was significantly different from chance in 4 expert models and the data-driven model. The data-driven model was significantly better than two expert models.
Conclusions: Discrimination of patients with 2-year survival after lung RT is achievable with both methodologies – expert-based and data-driven models. Reliable discrimination of patients with severe dyspnea after RT is not achievable with the presented models learned on data of 792 patients. Neither expert-based or data-driven models outperform each other. Thus, there is dire need for biomarkers predictive of radiation-induced dyspnea. For both endpoints, the algorithmically derived models are more parsimonious and perform as well as the expert-based models or better.

		Predicting Severe Dyspnea (CTCAE dyspnea scores ≥2)				2-Year Survival			
		AUC	AUC 95%CI	(AUC - $AUC_{Alg.}$) 95% CI	# Arcs	AUC	AUC 95%CI	(AUC - $AUC_{Alg.}$) 95% CI	# Arcs
Expert	1	0.58	[0.42,0.73]	[-0.07,0.22]	30	0.59	[0.48,0.7]	[-0.27,0.01]	19
	2	0.61	[0.43,0.77]	[-0.14,0.32]	9	0.65	[0.54,0.76]	[-0.21,0.07]	15
	3	0.49	[0.32,0.65]	[-0.19,0.15]	23	0.69	[0.58,0.8]	[-0.13,0.1]	17
	4	0.59	[0.45,0.73]	[-0.06,0.22]	22	0.56	[0.44,0.68]	[-0.32,-0.01]	23
	5	0.65	[0.5,0.8]	[-0.05,0.32]	20	0.53	[0.4,0.65]	[-0.36,-0.01]	13
	6	0.69	[0.56,0.83]	[-0.03,0.39]	14	0.64	[0.53,0.75]	[-0.21,0.05]	16
	7	0.57	[0.43,0.7]	[-0.08,0.2]	7	0.68	[0.57,0.79]	[-0.19,0.12]	20
Alg.		0.52	[0.38,0.66]	[0,0]	6	0.72	[0.6,0.82]	[0,0]	4

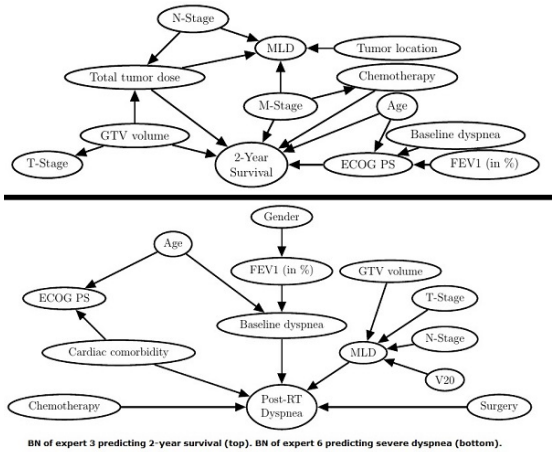

BN of expert 3 predicting 2-year survival (top). BN of expert 6 predicting severe dyspnea (bottom).

Keywords: personalized radiotherapy, Bayesian prediction modelling

References:
[1] Oberije C, Nalbantov G, Dekker A, Boersma L, Borger J, Reymen B, et al. A prospective study comparing the predictions of doctors versus models for treatment outcome of lung cancer patients: A step toward individualized care and shared decision making. Radiother Oncol. 2014 Jul;112(1):37–43.

61
Proton Radiation Therapy: Current Status at Massachusetts General Hospital
T. DeLaney
Massachusetts General Hospital, Harvard Medical School, Boston, MA

Purpose: Because of the absence of exit dose beyond the Bragg peak, protons can improve the radiotherapy physical dose distribution. This offers the potential for dose escalation to improve local control in anatomic sites and histologies where local control of tumor is suboptimal with photons. At the same time, the reduction in the normal tissue dose/volume profile is anticipated to reduce acute and late normal tissue toxicity. The competing technologies include intensity modulated photon radiation therapy (IMRT) as well as heavier charged particles. Massachusetts General Hospital (MGH) has been a pioneer in the development of proton radiation therapy. An overview of the proton radiation therapy program at MGH will be provided which will illustrate technological progress in proton therapy.
Materials/Methods: The initial treatment facility was in the Harvard Cyclotron Laboratory, a physics laboratory which was modified to accommodate patient treatments. Beam generated in a 160 MeV cyclotron was delivered via fixed horizontal beams. In 2001, the program was moved to a dedicated clinical facility based at the hospital, the Francis H. Burr Proton Therapy Center (FHBPTC). In 2017, an additional single room, gantry-based treatment facility will open.
Results: The FHBPTC has a 230 MeV cyclotron delivering beam to two rooms equipped with 360-degree rotational gantries and a third clinical room with a two beam-lines, one dedicated for treatment of eye tumors and the other for stereotactic intracranial radiosurgery/radiotherapy. In 2014, we delivered 13, 370 patient treatments at the FHBPTC. Currently, one of the two gantries delivers scanned proton beams including intensity modulated proton therapy. The other gantry delivers passively scattered proton treatments. We have U.S. National Cancer Institute funding to support clinical trials of intensity modulated proton therapy and to study the clinical impact of differences between proton and photon dose distributions, to optimize IMPT delivery including robust optimization, and to study proton dose perturbations caused by the heterogeneous patient and inter- and intra-factional variations. We are also active participants in ongoing NRG Oncology proton clinical trials.
Conclusions: Proton radiation therapy offers a number of potential treatment advantages to patients over photons related primarily to differences in physical dose distribution; clinical gain can be assessed in clinical trials which are currently in progress. Rapid changes in technology must be considered in designing and conducting clinical trials in this area.

62
Macrophage reprogramming for anticancer therapy
M. De Palma
The Swiss Institute for Experimental Cancer Research (ISREC), School of Life Sciences, Swiss Federal Institute of Technology Lausanne (EPFL), Lausanne, Switzerland

Tumor-associated macrophages (TAMs) are a phenotypically and functionally heterogeneous assortment of monocyte-derived cells that participate to key processes associated with tumor progression, such as angiogenesis, immunosuppression, invasion, and metastasis. Increasing studies also show that TAMs can either enhance or antagonize the antitumor efficacy of cytotoxic chemotherapy, cancer-cell targeting antibodies, and immunotherapeutic agents, depending on the tumor type, macrophage activation state, or type of treatment. TAMs can also drive reparative mechanisms in tumors after radiotherapy or treatment with antiangiogenic drugs. At the meeting, I will discuss the biological significance and clinical implications of these findings, with an emphasis on novel approaches, based on microRNA (miRNA) targeting, to reprogram TAMs into immunostimulatory cells. Indeed, we found that efficient miRNA depletion in TAMs did not alter their abundance in the tumors, but markedly reprogrammed their transcriptomes and effector functions from immunosuppressive to immunostimulatory. This enhanced cytotoxic T-cell infiltration, abated tumor progression, and increased tumor responsiveness to immune checkpoint blockade. Bioinformatics analysis of TAM transcriptomes identified a limited set of miRNAs putatively involved in TAM programming, and re-expression of Let-7 in Dicer-deficient TAMs was sufficient to rescue TAM's protumoral phenotype and abate tumor CTL infiltration. Collectively, these results have identified a mechanism of TAM programming to an immunostimulatory phenotype that may be exploited to enhance the efficacy of cancer immunotherapies.

63
The search for genetic predictors of radiotherapy response

D. De Ruysscher[1], P. Lambin[1] Maastro Clinic, Maastricht, The Netherlands

The aim of radiotherapy is to eradicate cancer, while at the same time minimizing the side effects. Although important improvements in imaging and radiotherapy techniques have enabled better target definitions and radiotherapy delivery, normal tissues are always exposed to radiation to some degree. Side effects thus still occur, but their variable degree, even when corrected for dosimetric characteristics, suggests that common genetic variants may play a role. However, similar to other human traits, radiosensitivity is considered to be a complex polygenic phenotype determined by the interaction of multiple loci.
Identifying these genetic markers will further enable precision radiotherapy in which the optimal treatment plan will take into account the genetic pre-disposition to toxicity (and of the tumour). It should not be assumed that all of the phenotypic variation is due to germ line genetic variation, but that that epigenetic changes (inherited and acquired) could also be important, including variants in mitochondrial DNA.
In response to the lack of success of candidate gene SNP studies in small studies, the focus of radiogenomics has shifted towards GWAS and big data research within international networks (1). At the same time, effort was made to establish standardized methods for reporting on radiogenomics (2). In recent years, remarkable progress has been made in the field of radiogenomics, of which some examples are cited.
Single nucleotide polymorphism genotypes were determined in female breast cancer patients from the RAPPER study, showing that patients with a high polygenic predisposition to breast cancer do not have an increased risk of radiotherapy toxicity, but that individual variants may increase risk (3). Identifying SNPs in oxidative stress-related genes associated with risk of late toxicities in breast cancer patients receiving radiation therapy, a variant allele in the base excision repair gene XRCC1 was found that could be used in combination with additional variants to predict late toxicities (4).
A GWAS study in 1742 prostate cancer patients treated with external beam radiotherapy identified the TANC1 locus (that has a role in regenerating damaged muscle) to be of significant importance in the development of late radiation-induced damage (5). It is expected that these and other improvements in genotyping together with better phenotyping of patients will be incorporated in treatment planning, decision support systems and drug development to increase the therapeutic ratio of radiotherapy.

Keywords: radiogenomics, side effects

Acknowledgement: This project has received funding from the European Union's Seventh Framework Programme for research, technological development and demonstration under grant agreement no 601826 (REQUITE).

References:
[1] Rosenstein BS, West CM, Bentzen SM, Alsner J, Andreassen CN, Azria D, Barnett GC, Baumann M, Burnet N, Chang-Claude J, Chuang EY, Coles CE, Dekker A, De Ruyck K, De Ruysscher D, Drumea K, Dunning AM, Easton D, Eeles R, Fachal L, Gutiérrez-Enríquez S, Haustermans K, Henríquez-Hernández LA, Imai T, Jones GD, Kerns SL, Liao Z, Onel K, Ostrer H, Parliament M, Pharoah PD, Rebbeck TR, Talbot CJ, Thierens H, Vega A, Witte JS, Wong P, Zenhausern F; Radiogenomics Consortium. Radiogenomics: radiobiology enters the era of big data and team science. Int J Radiat Oncol Biol Phys. 2014 Jul 15;89(4):709-13
[2] Kerns SL, De Ruysscher D, Andreassen CN, Azria D, Barnett GC, Chang-Claude J, Davidson S, Deasy JO, Dunning AM, Ostrer H, Rosenstein BS, West CM, Bentzen SM. STROGAR - STrengthening the Reporting Of Genetic Association studies in Radiogenomics. Radiother Oncol. 2014 Jan;110(1):182-8.
[3] Dorling L, Barnett GC, Michailidou K, Coles CE, Burnet NG, Yarnold JR, Elliott RM, Dunning AM, Pharoah PD, West CM. Patients with a high polygenic risk of breast cancer do not have an increased risk of radiotherapy toxicity. Clin Cancer Res. 2015 Oct 28. pii: clincanres.1080.2015. [Epub ahead of print]
[4] Seibold P, Behrens S, Schmezer P, Helmbold I, Barnett G, Coles C, Yarnold J, Talbot CJ, Imai T, Azria D, Koch CA, Dunning AM, Burnet N, Bliss JM, Symonds RP, Rattay T, Suga T, Kerns SL, Bourgier C, Vallis KA, Sautter-Bihl ML, Claßen J, Debus J, Schnabel T, Rosenstein BS, Wenz F, West CM, Popanda O, Chang-Claude J. XRCC1 Polymorphism Associated With Late Toxicity After Radiation Therapy in Breast Cancer Patients. Int J Radiat Oncol Biol Phys. 2015 Aug 1;92(5):1084-92.
[5] Fachal L, Gómez-Caamaño A, Barnett GC, Peleteiro P, Carballo AM, Calvo-Crespo P, Kerns SL, Sánchez-García M, Lobato-Busto R, Dorling L, Elliott RM, Dearnaley DP, Sydes MR, Hall E, Burnet NG, Carracedo Á, Rosenstein BS, West CM, Dunning AM, Vega A. A three-stage genome-wide association study identifies a susceptibility locus for late radiotherapy toxicity at 2q24.1. Nat Genet. 2014 Aug;46(8):891-4.

64
Combinaison of an anti HPV-E7 vaccine to radiotherapy: preclinical data in a head and neck model.

M. Mondini[1], M. Nizard[2], T. Tran [2], L. Mauge[3], M. Loi[4], C. Clémenson[1], D. Dugue[1], P. Maroun[5], E. Louvet[6], J. Adam[6], C. Badoual[7], D. Helley[3], E. Dransart[8], L. Johannes[8], M. C. Vozenin[9], J. L. Perfettini[10], E. Tartour[11], E. Deutsch[12].
[1] INSERM U1030 «Radiothérapie Moléculaire», Gustave Roussy Cancer Campus Grand Paris, Villejuif, France and Labex LERMIT.
[2] INSERM U970, PARCC (Paris Cardiovascular Research Center), Université Paris Descartes, Sorbonne Paris-Cité, Paris, France.
[3] INSERM U970, PARCC (Paris Cardiovascular Research Center), Université Paris Descartes, Sorbonne Paris-Cité, Paris, France. Service d'Hématologie Biologique, Hôpital Européen Georges-Pompidou, AP-HP, Paris, France.
[4] INSERM U1030 «Radiothérapie Moléculaire», Gustave Roussy Cancer Campus Grand Paris, Villejuif, France and Labex LERMIT. Radioterapia, Università di Firenze, Florence, Italy.
[5] INSERM U1030 «Radiothérapie Moléculaire», Gustave Roussy Cancer Campus Grand Paris, Villejuif, France and Labex LERMIT. Département de Radiothérapie, Gustave Roussy Cancer Campus Grand Paris, Villejuif, France. Université Paris Sud, Faculté de Médecine du Kremlin-Bicêtre, France.
[6] INSERM U981, Gustave Roussy Cancer Campus Grand Paris, Villejuif, France. SIRIC SOCRATE, Villejuif Cedex, France.
[7] INSERM U970, PARCC (Paris Cardiovascular Research Center), Université Paris Descartes, Sorbonne Paris-Cité, Paris, France. Service d'Anatomie Pathologique, Hôpital Européen Georges-Pompidou, AP-HP, Paris, France.
[8] Institut Curie, U1143 INSERM, UMR3666 CNRS, Endocytic Trafficking and Intracellular Delivery Group, Paris, France.
[9] INSERM U1030 «Radiothérapie Moléculaire», Gustave Roussy Cancer Campus Grand Paris, Villejuif, France and Labex LERMIT. Université Paris Sud, Faculté de Médecine du Kremlin-Bicêtre, France. Laboratoire de Recherche en Radio-Oncologie, CHUV, Lausanne, Switzerland.
[10] INSERM U1030 «Radiothérapie Moléculaire», Gustave Roussy Cancer Campus Grand Paris, Villejuif, France and Labex LERMIT. Université Paris Sud, Faculté de Médecine du Kremlin-Bicêtre, France. SIRIC SOCRATE, Villejuif Cedex, France.
[11] INSERM U970, PARCC (Paris Cardiovascular Research Center), Université Paris Descartes, Sorbonne Paris-Cité, Paris, France. Service d'Immunologie Biologique, Hôpital Européen Georges-Pompidou, AP-HP, Paris, France.
[12] INSERM U1030 «Radiothérapie Moléculaire», Gustave Roussy Cancer Campus Grand Paris, Villejuif, France and Labex LERMIT. Département de Radiothérapie, Gustave Roussy Cancer Campus Grand Paris, Villejuif, France. Université Paris Sud, Faculté de Médecine du Kremlin-Bicêtre, France. SIRIC SOCRATE, Villejuif Cedex, France. eric.deutsch@gustaveroussy.fr.

Combinaison of radiotherapy and immunomodulatory approaches is an emerging field. Beside the concurrent inhibition of immune checkpoints inhibitors, the association of anti tumor vaccines is a way to stimulate specific anti tumor immunity during radiotherapy. Here, we report an extremely effective combination of local irradiation (IR) and Shiga Toxin B (STxB)-based human papillomavirus (HPV) vaccination for the treatment

of HPV-associated head and neck squamous cell carcinoma (HNSCC). The efficacy of the irradiation and vaccine association was tested using a model of HNSCC obtained by grafting TC-1/luciferase cells at a submucosal site of the inner lip of immunocompetent mice. Irradiation and the STxB-E7 vaccine acted synergistically with both single and fractionated irradiation schemes, resulting in complete tumor clearance in the majority of the treated mice. A dose threshold of 7.5 Gy was required to elicit the dramatic antitumor response. The combined treatment induced high levels of tumor-infiltrating, antigen-specific CD8(+) T cells, which were required to trigger the antitumor activity. Treatment with STxB-E7 and irradiation induced CD8(+) T-cell memory, which was sufficient to exert complete antitumor responses in both local recurrences and distant metastases. We also report for the first time that a combination therapy based on local irradiation and vaccination induces an increased pericyte coverage (as shown by αSMA and NG2 staining) and ICAM-1 expression on vessels. This was associated with enhanced intratumor vascular permeability that correlated with the antitumor response, suggesting that the combination therapy could also act through an increased accessibility for immune cells. The combination strategy proposed here offers a promising approach that could potentially be transferred into clinical trials. The implementation of selective immunomodulatory approaches during the treatment of HPV positive tumors could eventually lead to increase anti tumor efficacy with favorable tumor versus normal tissue differential effect.

Keywords: HPV, STxB-E7 vaccine, radiation, mice

References:
[1] Mondini M et al Mol Cancer Ther. 2015 Jun;14(6):1336-45.

65

How emerging trends in basic research & technology will shape clinical research?

E. Deutsch[1,2,3]
[1] INSERM U1030 «Radiothérapie Moléculaire», Gustave Roussy Cancer Campus Grand Paris, Villejuif, France
[2] INSERM U1030 «Radiothérapie Moléculaire», Gustave Roussy Cancer Campus Grand Paris, Villejuif, France and Labex LERMIT.
[3] Département de Radiothérapie, Gustave Roussy Cancer Campus Grand Paris, Villejuif, France. Université Paris Sud, Faculté de Médecine du Kremlin-Bicêtre, France. SIRIC SOCRATE, Villejuif Cedex, France.
eric.deutsch@gustaveroussy.fr.

Radiation therapy is an ever changing discipline and technology. It has made unprecedented improvements with the incorporation of concurrent chemotherapy regimens which translated into local control and survival gains. The improvements of beam delivery techniques have led to decrease in morbidity following treatment. We are now facing an important wave of changing concepts which profoundly impact our understanding of the basic mechanistic of oncology which have had profound consequences on the perception of the biology of response to radiotherapy having both consequences for tumor and normal tissues. Interestingly these changes do not replace former concepts but rather contribute to broaden the scope of radiation biology. Direct radiation induced cell kill of tumor clonogens has now to be integrated within the concept of microenvironment. The overwhelming contribution of tumor hypoxia remains un disputed but the concept of micro environment by itself now implies the contribution of several cellular compartments which are shown to contribute to both tumor response and the generation of normal tissue damage. These findings have paved the way for a new generation of combination of clinical trials which are now emerging. The possibility that immune modulation during the course of radiotherapy could not only have impact on local control but also on distant disease is a fascinating paradigm. Technology for treatment and imaging have in parallel considerably evolved, leading to increased precision and targeting possibilities widening the use of stereotactic radiotherapy which constitutes a major change for the management of primary and secondary tumors. Routine integration of biomarkers in our tumor rounds such as HPV status for head and neck and 1p19q for brain tumors are examples of the integration of the concept of precision medecine into radiotherapy and other examples should follow.
Functional imaging and the latest developments of image texture analysis will contribute to increase the level of precision of our treatments, define the areas at risk for relapse but these images might also contains valuable biological information. Practical examples of clinical trials using novel technologies (nanoparticles), biomarkers selection and oligometastatic disease, will be used to present the practical integration and the challenges represented by these novel concepts into the clinic.

Keywords: Oligometastasis, clinical trial, immune therapy, targeted therapies, biomarkers, functional imaging.

66

First tests to implement an in-house 3d-printed photon bolus procedure using clinical treatment planning system data.

G. Dipasquale[1], R. Miralbell[1], P. Starkov[2], O. Ratib[2]
[1] Department of Radiation Oncology, Geneva University Hospital, Geneva, Switzerland
[2] Department of Nuclear Medicine, Geneva University Hospital, Geneva, Switzerland

Purpose: Additive manufacturing is becoming of interest in Radiotherapy especially for bolus creation. This study aimed to develop an in-house procedure to print photon bolus created with the treatment planning system (TPS) using small sized printers, cost effective, and logistically easy to implement in RT departments.
Material/methods: A fused deposition modeling (FDM) printer with a heated bed plate (Rova3D, Ordsolutions, Ontario, Canada), was used together with Poly-Lactic-Acid (PLA) material. Using as TPS Eclipse™ version 13 (Varian Medical Systems, Palo Alto, California) a plan was created on a Rando™ head phantom CT scan and a "digital" bolus created in the eye region with Hounsfield Units (HU) of 140, corresponding to PLA printed density of 1.12 g/cc. This bolus was exported from Eclipse and converted in STL file. Bolus creation and printing took approximately 1 hour. To verify the form of the 3D-printed bolus, its HU, and dose distribution obtained when using it, the latter was positioned on the head phantom and a CT scan was acquired. Two plans with anterior-posterior fields and 6 MV X-ray beams were created using either the "digital" or the 3D-printed bolus and plans were compared. To measure and compare the dose distribution, skin layers of 3 mm and 5 mm thickness were created, just beneath the bolus, as well as a target simulating a tumor reaching the body surface (see figure). The analytical anisotropic algorithm was used for dose calculation with a grid size of 1 mm.
Results: The first 3D-printed bolus contained some air bubbles, and had a smaller thickness (less than 0.1 cm) but properly reproduced the form (see figure). The printed bolus presented in its solid portion a density of 140-150 HU with values as low as ≈-450 HU in the bubble regions and a mean ±SD value of -32 ± 154 HU. Dosimetric comparison showed good agreement on mean doses and max doses, while volumes receiving 95% of the prescribed dose differed by ≈6% for all structures with 3D-printed bolus plans showing more coverage, (see table).
Conclusion: In conclusion, first dosimetric results look promising and further tests will be implemented to improve the bolus filling and the erosion of the surface, as well as to investigate the possibility to use soft PLA materials (likely more comfortable for patients). More sophisticated, realistic patient's plans should be tested and *in-vivo* thermo luminescent dosimetry should be used for treatment plan verification.

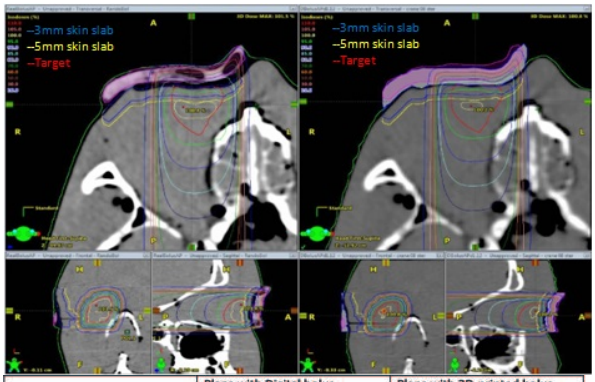

	Plans with Digital bolus	Plans with 3D-printed bolus
Mean ±Standard Deviation dose %		
Target	97±3	99±3
5mm skin slab	46±42	47±43
3mm skin slab	44±42	45±43
Dnear max (%)		
Target	100	101
5mm skin slab	99	100
3mm skin slab	97	98
Volume receiving 95% dose prescription (%)		
Target	83	89
5mm skin slab	14	20
3mm skin slab	7	13

67

Differential cross sections measurements for hadrontherapy: 50 MeV/n ^{12}C reactions on H, C, Al, O and ^{nat}Ti targets.

C. Divay[1], D. Cussol[1], M. Labalme[1], S. Salvador[1], C. Finck[2], Y. Karakaya[2], M. Vanstalle[2], M. Rousseau[2]
[1] LPC Caen
[2] IPHC Strasbourg

The increasing interest for hadrontherapy can be attributed to the great accuracy of ion beams to target the tumor while sparing the surrounding healthy tissues (due to the high dose deposition in the Bragg peak and the small angular scattering of ions) as well as the potential biological advantage of ions for some tumor types compared to photons.
To keep the benefits of carbon ions in radiotherapy, a very high accuracy on the dose location is required. The dose deposition is affected by the fragmentation of the incident ions that leads to: (i) the consumption of the projectiles with their penetration depth in the tissues, (ii) the creation of lighter fragments having a different biological effectiveness (RBE), (iii) the apparition of a fragmentation tail after the tumor. The constraints on nuclear models and/or fragmentation cross sections in the energy range used in hadrontherapy (up to 400 MeV/n) are not yet sufficient to reproduce the local dose deposition with the accuracy required in a clinical treatment.
In this context, two experiments with 95 MeV/n ^{12}C beams have been performed by our collaboration in 2011 and 2013 at GANIL [1,2] to measure the energy and angular differential fragmentation cross sections on thin targets of medical interest (H, C, Al, O and ^{nat}Ti). In March 2015, a new experiment with a 50 MeV/n ^{12}C beam on the same targets has been conducted at GANIL. The experimental set-up was made of five three stages telescopes, each composed of two Si detectors and one CsI scintillator mounted on rotating stages to cover angles from 3° to 39°.
The analysis of this new experiment is under completion. It shows that the angular cross sections for light fragments are less forward-focused at 50 MeV/n compared to 95 MeV/n, resulting in "flatter" distributions. As shown in Figure 1, protons and ^{4}He fragments are dominant on the entire angular distribution. At this beam energy, the production of alpha particles is higher than protons for angles up to 20° compared to 10° at 95 MeV/n.
However, at the most forward angles, ^{11}B fragments seem to compete with the protons production.
The energy distributions of the fragments at forward angles are peaked close to the beam energy showing an emission dominated by the quasi-projectile. Comparisons between experimental data and Geant4 simulations using different inelastic models (such as BIC, QMD and INCL++) show important discrepancies.
Final data as well as comparisons with simulations and the previous experiments will be presented during the conference.

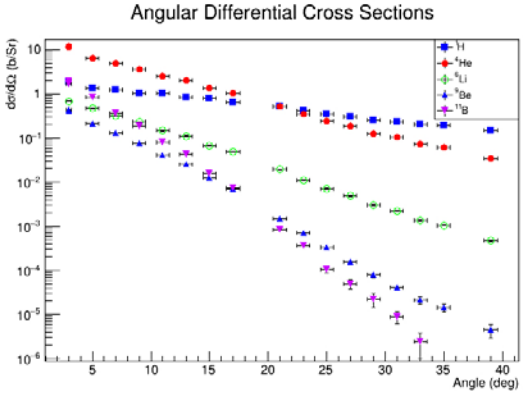

Figure 2: Preliminary angular differential cross section for various isotopes, from Z=1 to Z=5

Keywords: Hadrontherapy, Nuclear-Fragmentation, Cross-Sections

References:
[1] J. Dudouet *et al.* Physical Review C 88, 024606 (2013)
[2] J. Dudouet *et al.* Physical Review C 89, 064615 (2014)

68

Correlation of Particle Traversals with Clonogenic Survival Using Cell-Fluorescent Ion Track Hybrid Detector

I. Dokic[1,2,3], M. Niklas[1,2,3], F. Zimmermann[1,2,3], A. Mairani[2,4], P. Seidel[1,2,3], D. Krunic[5], O. Jäkel[1,2,6], J. Debus[1,2,3], S. Greilich[1,6], A. Abdollahi[1,2,3]
[1] German Cancer Consortium (DKTK), Translational Radiation Oncology, National Center for Tumor Diseases (NCT), Heidelberg Institute of Radiation Oncology (HIRO), German Cancer Research Center (DKFZ), Heidelberg, Germany
[2] Heidelberg Ion Therapy Center (HIT), Heidelberg, Germany
[3] Department of Radiation Oncology, Heidelberg University Hospital, Heidelberg, Germany
[4] National Center for Oncological Hadrontherapy (CNAO), Pavia, Italy
[5] Light Microscopy Facility, German Cancer Research Center, Heidelberg, Germany
[6] Division of Medical Physics in Radiation Oncology, German Cancer Research Center, Germany

Purpose: In radiobiology, the clonogenic survival of cells is considered the gold standard assay for assessment of cellular sensitivity to ionizing radiation. Towards further development of next generation biodosimeters in particle therapy, cell-fluorescent ion track hybrid detector (Cell-FIT-HD) previously engineered by our group [1, 2] was utilized to study its feasibility as a tool for investigating the effects of clinical beams on cellular clonogenic survival.
Materials and methods: Tumor cells were grown on the fluorescent nuclear track detector (FNTD) in cell culture, mimicking the standard procedures for clonogenic assay. Cell-FIT-HD was used to detect the spatial distribution of particle tracks within colony-initiating cells. The physical data were associated to radiation induced foci as surrogates for DNA double strand breakages (DSB), the hallmark of radiation -induced cell lethality. Long-term cell fate was monitored to determine the ability of cells to form colonies.
Results and conclusion: We showed that single cells can attach and grow as colonies on FNTD surface. Usage of the fluorescent and confocal microscopy, together with FNTD technology, enabled simultaneous analysis of the microscopic beam parameters together with the molecular events within colonies, at sub-cellular level. We report the first successful

detection of particle traverse within colony-initiating cells at subcellular resolution using Cell-FIT-HD. The current work represents a proof of principle study for correlation of particle traversal with long term colony formation using Cell-FIT-HD. The entire workflow is established and builds a solid foundation for further improvements towards population level quantitative analysis.

Keywords: cell-fluorescent ion track hybrid detector, clonogenic assay, DNA damage, ion hits

References:
[1] Niklas, M. et al. Engineering cell-fluorescent ion track hybrid detectors. *Radiation oncology* 8, 141 (2013).
[2] Niklas, M. et al. Subcellular spatial correlation of particle traversal and biological response in clinical ion beams. *International journal of radiation oncology, biology, physics* 87, 1141-1147 (2013).

69

^{43}Sc Production Development by Cyclotron Irradiation of ^{43}Ca and ^{46}Ti

K. A. Domnanich[1,2], C. Müller[3], A. Türler[1,2], N. P. van der Meulen[2]
[1] Department of Chemistry and Biochemistry, University of Bern, Freiestrasse 3, 3012 Bern
[2] Laboratory of Radiochemistry and Environmental Chemistry, Paul Scherrer Institute, 5232 Villigen PSI
[3] Center of Radiopharmaceutical Sciences, Paul Scherrer Institute, 5232 Villigen PSI

Introduction: The positron-emitter ^{43}Sc is considered to be an attractive PET radionuclidic alternative to ^{44}Sc, due to its more favourable decay properties. What is more, the lower energetic gamma line will result in a lower radiation dose burden to the patient and the operator.[1] Together with ^{47}Sc, which demonstrates therapeutic effect by emitting soft β^--particles, it can be considered as part of the "matched pair" principle, enabling tumour imaging and, following that, optimal therapy planning. The production of ^{43}Sc is described by different nuclear reactions in literature: ^{43}Ca(p,n)^{43}Sc and ^{46}Ti(p,α)^{43}Sc [1-3]. The feasibility of both production paths was tested at the PSI Injector II cyclotron.
Materials and Methods: ^{43}Ca and ^{46}Ti targets were prepared by mixing enriched ^{43}CaCO3 or ^{46}Ti powder with graphite powder, pressed and encapsulated in aluminium. Since enriched Ti is only available in oxide form, the reduction of ^{46}TiO2 to elemental ^{46}Ti powder was performed [4]. The ^{43}CaCO3 and ^{46}Ti targets were irradiated with protons at different energies. Two different chromatographic separation methods were used to separate the ^{43}Sc product from the respective target material.
Results: The production of ^{43}Ca(p,n)^{43}Sc yields ^{43}Sc with a radionuclidic purity of 66% ,while ^{44}Sc was co-produced with 33% at the end of separation (EOS). The produced ^{43}Sc was used to perform a PET phantom study, indicating promising preliminary results for ^{43}Sc being a superior imaging radionuclide to its ^{44}Sc counterpart. The labelling of the obtained ^{43}Sc with DOTANOC could be performed at a maximum specificity of 7 MBq ^{43}Sc/nmol DOTANOC with a radiochemical purity of 97 %.
The production of ^{46}Ti(p,α)^{43}Sc yielded ^{43}Sc of 98.7% radionuclidic purity at EOS. The percentage of ^{44}Sc in the final product did not exceed 1.2%. The longer-lived impurities ^{44m}Sc, ^{46}Sc and ^{48}Sc were less than 0.04%. To obtain enriched ^{46}Ti target material of higher purity, several parameters of the ^{46}TiO2 reduction process, including the amount of reducing agent, temperature profile and reaction time, were altered. Initial difficulties with the processing of the irradiated ^{46}Ti target were addressed by changing the irradiation parameters to lower beam intensity and prolonged irradiation time.
Conclusion: Successful production of ^{43}Sc was achieved utilizing two activation methods, however, the ^{43}Sc yield at end of bombardment (EOB) is significantly higher with the ^{43}Ca(p,n)^{43}Sc production route. Nevertheless, the expensive target material and a ^{43}Sc product of lower radionuclidic purity are drawbacks of this pathway. The ^{46}Ti(p,α)^{43}Sc production method yields ^{43}Sc of high radionuclidic purity. However, the ^{46}Ti preparation of reduced target material proved to be labour intensive. The significantly lower ^{43}Sc yield at EOB is the focus of further optimisation.

References:
[1] S. Krajewski et al., ichti Annual Report 2012, Warszawa, p. 35, 2013
[2] P. Kopecky et al., Appl. Radiat. Isotope. Vol. 44, No. 4, pp. 681-692, 1993
[3] EXFOR- database, version from 03.12.2014
[4] B. Lommel et al., J Radioanal Nucl Chem, s10967-013-2615-7, 2013

70

Brain motion induced artefacts in Microbeam Radiation Therapy: a Monte Carlo study

M. Donzelli[1], E. Bräuer-Krisch[1], U. Oelfke[2]
[1] European Synchrotron Radiation Facility, Biomedical Beamline ID17, Grenoble, France
[2] The Institute of Cancer Research and The Royal Marsden NHS Foundation Trust, Joint Department of Physics, London, United Kingdom

Microbeam Radiation Therapy (MRT) is a relatively new approach in radiation oncology exploiting the dose-volume effect by using orthovoltage X-rays on a microscopic scale [1]. Arrays of plane parallel beams of typically 50 µm width with spacings of a few hundred µm show extraordinary normal tissue sparing, while still being capable to ablate tumours in preclinical research [2].
Purpose: Organ motion has not been an issue in MRT, as long as preclinical research was carried out in small samples, such as cell cultures and rodents. The possible future treatment of human brain tumours using microbeam radiation however may be affected by cardio-synchronous tissue pulsation. This pulsation, with amplitudes in the order of 100 µm [3], induces translational movements of the brain tissue causing a blurring of the planned plane-parallel dose pattern of microbeams in case of extended exposure times.
Method: A Monte Carlo study to quantify these effects was performed using the Geant4 toolkit. Dose was scored in a homogeneous cubic water phantom of 15 cm size on a grid with 5 µm resolution perpendicular to the beam. The sensitive volume was chosen to have an extension of 1 mm along the beam direction in 20 mm depth from the surface, which corresponds to the reference dosimetry conditions in MRT. The relative statistical uncertainty of the dose (1 standard deviation) per voxel was between 1% and 1.5% in the peak region and between 6% and 9% in the dose valley, depending on the evaluated beam configuration and could be further reduced by appropriate binning of the raw data.
Results: Monte Carlo calculations for different geometrical microbeam configurations and employed dose rates revealed significant changes of the planned dose patterns when compared to the static case. The chosen quality indicators of our study like peak dose, peak-to-valley dose ratio (PVDR), microbeam width, spacing, and penumbra were observed to be highly degraded, e.g. the PVDR being reduced by up to 35%.
Conclusions: We have demonstrated that the effect of even small organ motions occurring at heart rate frequencies in the brain can only be tolerated at high dose rates of approx. 10 Gy/s. For example, a dose rate of 12.3 kGy/s can be given as a threshold value if one wants to apply a high peak entrance dose of 300 Gy in 3 mm depth for 50 µm wide microbeams and a primary beam size of 500 µm perpendicular to the scan direction. For lower dose rates the observed deterioration of the microbeam dose patterns is likely to destroy the intended dose sparing effect for healthy tissues.
For interlaced microbeam geometries an appropriate gating technique could be applied in the future based on the phase of the cardiac cycle.

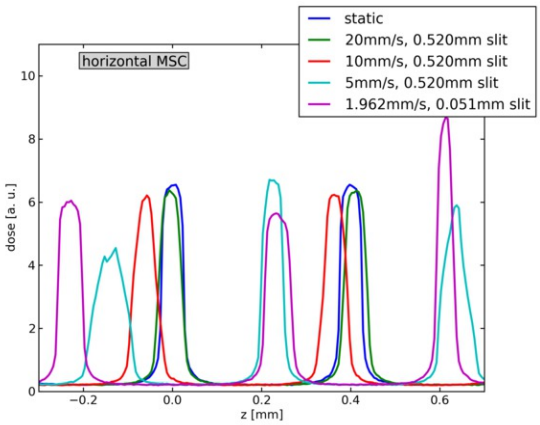

Keywords: Microbeam Radiation Therapy, brain motion, Monte Carlo

References:
[1] Bräuer-Krisch et al. Mutation Research 704 (2010) 160-166
[2] Laissue et al. International Journal of Cancer 78 (1998) 654-660
[3] Soellinger et al. Magnetic Resonance in Medicine 61 (2009) 153-162

71

Radiotherapy and the immunocytokine L19-IL2: a perfect match for an abscopal effect with long-lasting memory

L. Dubois[1], N. H. Rekers[1], A. Yaromina[1], N.G. Lieuwes[1], R. Biemans[1], B. L. M. G. Senden-Gijsbers[2], W. T. V. Germeraad[2], D. Neri[3], P. Lambin[1]
[1]Department of Radiation Oncology (MAASTRO) and [2]Department of Internal Medicine, Division of Hematology, GROW - School for Oncology and Developmental Biology, Maastricht University Medical Centre, Maastricht, The Netherlands and [3]Department of Chemistry and Applied Biosciences, Swiss Federal Institute of Technology Zurich.

Although radiotherapy (RT) is one of the major cancer treatment modalities to kill malignant cells, advanced-stage disease is often hard to control. Radiation-induced tumor cell death provides a plethora of pro-immunogenic effectors associated with inflammation. Although the potential for RT to generate anti-tumor immunity is apparent, the evidence that it does so in the clinical situation is limited. Stimulation of the immune system to assist in eliminating cancer cells within, and outside, the radiation field could be beneficial in advanced-stage or metastasized disease. Recently, it has been demonstrated that cancer patients have increased levels of cytotoxic T-cells after radiotherapy, making them eligible for immunotherapy. Interleukin-2 (IL2) is one of the essential cytokines for driving proliferation and differentiation of T-cells and NK-cells resulting in increased cytotoxic activity, eventually leading to tumor regression. Several studies have shown synergistic anti-tumor effects when combining RT with systemic IL2 administration, although this strategy was accompanied with severe adverse effects.
Monoclonal antibodies, such as the human recombinant scFv fragment L19, have been designed as "targeting vehicle" for the selective delivery of immune-stimulatory cytokines to the tumor microenvironment while sparing normal tissue. The L19 antibody selectively localizes at the tumor neovascular fibronectin extra-domain B (EDB) positive sites following systemic administration and can serve as delivery vehicle for IL2. Our lab has combined single high-dose RT with systemic L19-IL2 administration in a number of murine xenograft models and found outstanding, long-lasting complete response rates mediated by cytotoxic CD8+ T-cell (1,2) or NK-cell (3) activity depending on the tumor model. L19-IL2 is thus an immunocytokine with strong immune response enhancing properties in EDB-positive tumors.
The combination therapy resulted also in anti-tumor immune effects outside the radiation field, an effect associated with CD4+ T-cell response. Growth of secondary un-irradiated tumors was significantly delayed with even 20% cure. Similar results were found when irradiation was delivered in a fractionated manner, although without resulting in cures. An increased PD-1 expression on T-cells infiltrating these tumors suggests a more regulatory immunological phenotype after fractionated radiotherapy compared with a single high RT dose. Re-challenging cured animals with tumor cells did not result in tumor formation, associated with high CD127 expression. Our recent data show that radiotherapy combined with the immunocytokine L19-IL2 results in long-lasting complete response rates, also outside the radiation field (abscopal effect) and this effect is associated with a memory potential.

Keywords: Radiotherapy, immunocytokine, abscopal effect, memory effect

References:
[1] Zegers et al, Clin Cancer Research 2015, 21(5):1151-60
[2] Rekers et al, Oncoimmunol 2015, 4(8):e1021541
[3] Rekers et al, Radiother Oncol 2015, 116(3):438-42

72

How to produce the highest tin-117m specific activity?

C. Duchemin[1], M. Essayan[1], A. Guertin[1], F. Haddad[1,2], N. Michel[2], V. Metivier[1]
[1] Laboratoire SUBATECH, Ecoles des Mines de Nantes, Université de Nantes, CNRS/IN2P3, 4 rue Alfred Kastler, 44307 Nantes cedex 3 - FRANCE
[2] GIP ARRONAX, 1 rue Aronnax, 44817 Saint-Herblain cedex – FRANCE

Purpose: Tin-117m is a radionuclide of interest for cancer and cardiovascular disease therapies. It has a half-life of 13.6 days and emits conversion and Auger electrons. It is actually used in clinical trials, where the radiopharmaceutical is developed by Clear Vascular Inc., to treat vulnerable plaque [1]. For this application, tin-117m is produced by the irradiation of Cd-116 enriched target with alpha particles. The goal of this study is to determine the irradiation conditions to get the highest specific activity of the final product, based on this reaction.
Materials/methods: Tin-117m production study has been investigated at the ARRONAX [2] cyclotron (France) that is able to deliver alpha particles at 67.4 MeV. Production cross section measurements of tin-117m as well as radioactive contaminants have been made using the stacked-foils technique. It consists in the irradiation of a group of thin foils: target, monitor and degrader. The stacks were made of thin natural cadmium as targets and aluminum foils as degraders. Monitor foils acted also as catcher and were made of different material depending on the energy. After irradiation, the activity of each radionuclides produced in the foils has been determined by γ spectrometry [3]. Production of stable and long live isotopes has been estimated with the TALYS code [4]. From the cross section data, thick target production yields (TTY) have been calculated as well as tin-117m specific activity (SA).
Results: The production cross section values obtained for the Cd-116(α,x) reaction up to 65 MeV have been compared with the literature. From these data, Sn-117m TTY has been calculated considering a 100% Cd-116 enriched target. A TTY of 6.3 MBq/(μA.h) is obtained for 65 MeV alpha particles on a thick target. Our results are compared with the value reported by Clear Vascular Inc. at 47 MeV. A difference of only 6.3 % has been found. In order to determine the SA, the mass of stable and long live tin isotopes produced during the irradiation have been determined using the TALYS code. The figure 1 shows the tin-117m SA in kCi/g from 25 to 65 MeV. The maximum tin-117m SA is reached around 40 MeV with 41 kCi/g and corresponds to a TTY of around 4 MBq/(μA.h). Clear Vascular Inc. reported a value of 25 kCi/g at 47 MeV. This value is 28 % lower than what is expected from our calculation.

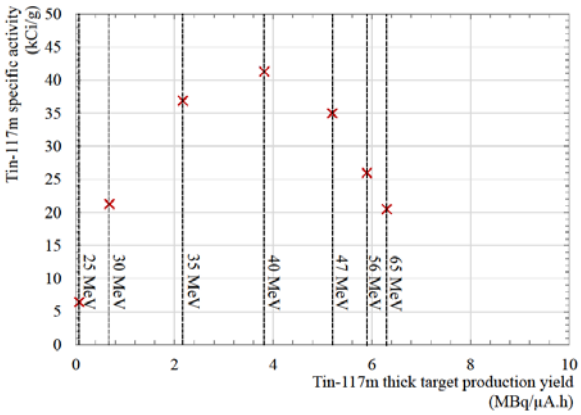

Conclusions: New experimental data have been obtained at the ARRONAX cyclotron that permits to expand the knowledge of the tin-117m TTY up to 65 MeV. The results of the TALYS 1.6 code, which reproduce correctly the tin-117m production cross section, have been used to determine the tin-117m SA taking into account the stables and long live tin isotopes produced during the irradiation. The highest tin-117m SA could be obtained using 40 MeV alpha beams which gives a TTY of 3.9 MBq/(µA.h). It is possible to get higher production yields but with a lower SA of the final product.

Keywords: tin-117m, ARRONAX cyclotron, specific activity

References:
[1] Clear Vascular Inc. Clinical stage company, http ://www.clearvascular.com/,
[2] Haddad F., Ferrer L., Guertin A., Carlier T., Michel N., Barbet J., and Chatal J.F. Arronax a high-energy and high-intensity cyclotron for nuclear medicine. Eur. J. Nucl. Med. Mol. Imaging, 35 :1377–1387, 2008
[3] Duchemin C. PhD thesis, Université de Nantes (2015).
[4] Koning A.J. and Rochman D. Modern nuclear data evaluation with the TALYS code system. Nucl. Data Sheets, 113, 2012.

73
Tb-155 production with gadolinium target: proton, deuteron or alpha beam?

C. Duchemin[1], A. Guertin[1], F. Haddad[1,2], N. Michel[2], V. Metivier[1]
[1] Laboratoire SUBATECH, Ecoles des Mines de Nantes, Université de Nantes, CNRS/IN2P3, 4 rue Alfred Kastler, 44307 Nantes cedex 3 - FRANCE
[2] GIP ARRONAX, 1 rue Aronnax, 44817 Saint-Herblain cedex – FRANCE

Purpose: Terbium is an element of growing interest for medical applications, considered as the "Swiss-knife of nuclear medicine" [1]. Indeed, four terbium radioisotopes can be used in nuclear medicine. Tb-149 is considered for alpha targeted therapy, Tb-161 for beta- targeted therapy, Tb-152 for Positron Emission Tomography (PET) and Tb-155 for Single Photon Emission Computed Tomography (SPECT). However, terbium-155 can also be used as a radionuclide that emits Auger electrons for therapy. The interest on this radioisotope is increased by the conversion electrons emitted and the possibility to follow the treatment by SPECT imaging in a theranostic approach. The Tb-155 production has been investigated using the deuteron beam delivered by the ARRONAX cyclotron [2] and natural gadolinium target, motivated by the lack of data for this reaction at the beginning of our experiments.
Materials/methods: Tb-155 production study has been considered at the ARRONAX cyclotron (France) taking advantage of the deuteron beam ranging from 15 to 35 MeV. Production cross section measurements of Tb-155 as well as radioactive contaminants have been made using the stacked-foils technique. The stacks were made of thin natural gadolinium as targets, aluminum foils as degraders and thin natural titanium as monitor foils. After irradiation, the activity of each radionuclides produced in the foils has been determined by γ spectrometry [3]. From the cross section values obtained during these experiments, the Tb-155 Thick Target production Yield (TTY) has been calculated and compared with the other Tb-155 production routes using data available in the literature. When no experimental data were available, the TALYS code [4] version 1.6 helped to estimate the TTY.
Results: In 2014, cross section values have been published for the Gd-nat(d,x)Tb-155 reaction [5]. Our set of data is in good agreement therewith. Tb-155 production cross section values for the Gd-nat(p,x) and Gd-nat(α,x) are also available in the literature. The Tb-155 TTY have been compared for each routes. Close values are obtained for the proton and the deuteron route. The Gd-nat(α,x) reaction gives the lowest TTY, whatever the incident beam energy. However, the use of a natural gadolinium target leads to the production of several contaminants and especially of Tb-156g which has the same half-life as Tb-155. Results based on calculations for two reactions using Gd-154 and Gd-155 enriched targets with, respectively, deuterons and protons as projectiles, are also discussed [3,6]. The Tb-159(p,5n)Dy-155(ε)Tb-155 reaction, with results published in 2014 [7], is also discussed as a promising production route using high energy protons.
Conclusions: New experimental data have been obtained at the ARRONAX cyclotron for the Gd-nat(d,x) reaction with a special emphasis on the Tb-155 production. The results have been compared with different production routes, using natural and enriched gadolinium target. Based on the calculations published in 2012 [6], the Gd-155(p,n) reaction seems to be the most promising for the production of Tb-155 with gadolinium as target element. However, the Tb-159(p,5n)Dy155(ε)Tb155 seems an interesting alternative.

Keywords: terbium-155, production routes, Thick Target production Yield

References:
[1] Müller C., et al. (2012). The journal of nuclear medicine, 53.
[2] Haddad F., et al. (2008). Eur. J. Nucl. Med. Mol. Imaging, 35:1377–1387.
[3] Duchemin C. PhD thesis, Université de Nantes (2015).
[4] Koning A.J. and Rochman D. Modern nuclear data evaluation with the TALYS code system. Nucl. Data Sheets, 113, 2012.
[5] Tárkányi F., et al. (2014). Applied Radiation and Isotopes, 83.
[6] Vermeulen C., et al. (2012). Nuclear Instruments and Methods in Physics
Research Section B: Beam Interactions with Materials and Atoms, 275.
[7] Steyn, et al. (2014). Nuclear Instruments and Methods in Physics Research Section B, 319.

74
RapidArc commissioning and dosimetric verification using EPID portal dosimetry system

S. Dwivedi[1], A. Jagtap[2], R. Umbarkar[3], N. Jakhotia[4], G. George[1] and M. K. Mahajan[1]
[1] Department of Radiotherapy, Advanced Cancer Diagnostic Treatment and Research Centre, Bathinda, India, [2]Department Of Radiotherapy, Camma Albless Hospital, Mumbai, India, [3]Department of Regulatory Affairs, Varian Medical Systems, India and [4]Department of Radiotherapy, Bhagwan Mahaveer Cancer hospital, Jaipur, India.

Purpose: In this study, we report the rapid arc commissioning and dosimetric verification measurements performed with the electronic portal imaging device (EPID) having portal dosimetry software.
Material and Methods: The dosimetric tests were performed on RapidArc capable Varian Unique linac, which is equipped with millennium 120 Dynamic Multi Leaf Collimators (DMLCs) and having 6 MV X-ray beam. The Varian RapidArc QA files, Eclipse treatment planning system (TPS) and EPID portal dosimetry system were used in this study. The RapidArc QA files incorporate following tests. 1) DMLC dosimetry. 2) Picket Fence (PF) test vs. gantry angle. 3) PF test during

Rapid Arc. 4) PF test during RapidArc with intentional errors. 5) Accurate control of dose rate and gantry speed during RapidArc delivery. 6) Accurate control of leaf speed during RapidArc delivery. These RapidArc QA plans were loaded on Machine and analysed using EPID portal dosimetry system.
Results and Discussion: Taking DMLC dosimetry, we measured meter reading at gantry angles 0°, 180°, 90° and 270° for a 4x10 cm DMLC field with a 0.5 cm slit, and the effect of gravity on leaf position and linac head showed maximum percentage deviation of -0.96% (± 2%). PF test at stationary gantry angles 0°, 180°, 90° and 270°, we evaluated the maximum DMLC positional shift of 0.5mm (± 1 mm). PF test during RapidArc (arc 179º-187º) has inspected the effect of gantry rotation on the MLC position, the result showed a maximum positional shift of -0.2 mm (± 1 mm). PF test during RapidArc with intentional errors have demonstrated that the test (3) can detect sub-millimetre errors during RapidArc. Accurate control of dose rate and gantry speed during RapidArc delivery has been examined by using 7 combinations of dose-rate, gantry range and gantry speed to give equal dose to seven 1.8 cm strips in a RapidArc field. When normalised to open field at same position (to exclude the beam profile influence), the dose of seven strips showed good result, with maximum mean deviation of 1.90% (< 2%). Accurate control of leaf speed during RapidArc delivery has been analysed by using 4 combinations of leaf speed (1.6, 2.4, 0.8 and 0.4 cm/s) and dose-rate to give equal dose to four strips in a RapidArc field. When normalised to corresponding open field, the dose of four strips showed good result, with a maximum mean deviation of 1.74% (< 2%). All the test results showed good agreement with manufacture and published literature stated tolerance values (written in bracket in front of each result).The RapidArc commissioning data has also obtained an approval from Atomic Energy Regulatory Board (AERB), Mumbai, India.
Conclusion: The dosimetric verification of DMLC movement, variable dose rates and gantry speed provides confidence over precision and accuracy during RapidArc delivery. These test are aimed only for commissioning and dosimetric verification of RapidArc enabled linac, and not for patient specific QA.

Keywords: Dosimetry, EPID, DMLC.

75

Dosimetric Measurement for Isocentre Blocked Boost Fields in 3D-CRT Treatment Plans

S. Dwivedi[1], R. A. Kinhikar[2], C. M. Tambe[2], A. Bargundi[3], D. D. Deshpande[2], S. K. Shrivastava[3] and M. K. Mahajan[1]
[1]Department of Radiotherapy, Advanced Cancer Diagnostic Treatment and Research Centre, Bathinda, India [2]Department of Medical Physics and [3]Department of Radiation Oncology, Tata Memorial Hospital, Mumbai, India.

Purpose: Boost fields (A small field with isocentre blocked and less beam weightage) are routinely used in three dimensional conformal radiotherapy (3D-CRT) treatment plans of oesophagus, head and neck etc for enhancing PTV coverage. Challenges for using boost fields are associated with accuracy of treatment planning system (TPS) to calculate dose distribution, normalisation and monitor units (MUs) as isocentre is blocked so dosimetric verification of boost field is essential. The purpose of this study was to measure two things; first contribution of 'Boost fields' doses to the target isocentre, second doses to the region of interest of boost field and finally compare the dosimetrically measured data with TPS calculated data.
Materials and Methods: Eclipse TPS (Version 8.6, Varian) was used for all boost fields 3D-CRT treatment plans in this study. The solid water phantom with dimension (25cmx25mx5cm), (25cmx25mx2cm) and (25cmx25mx5cm) respectively was used. The 0.65cc ionisation chamber was used for dosimetry in this study with SAD (source axis distance) setup. In boost fields study, five treatment plans of oesophagus case each having two plans with 6MV and 15MV and each plan having two boost fields (one is LPO boost field and other is RPO boost field) were performed. The contribution of boost field doses to the target isocentre for both 6MV and 15MV plans were measured with the help of ionisation chamber and also calculated in treatment planning system. The doses to the region of interest of boost field at 5cm depth in phantom were measured with help of thermoluminescence detector (TLD-100) and also calculated in treatment planning system for both 6MV and 15MV plans. Finally the measured and calculated data was compared.
Results: Mean percentage variation between TPS calculated and ionisation chamber measured boost field doses to the target isocentre was 1.53% (SD 4.12) for 6MV and 4.13% (SD 6.81) for 15MV. Maximum Percentage variation for this was 6% and 12% for 6MV and 15MV respectively. Mean percentage variation between TPS calculated and TLDs measured boost field doses of region of interest of boost field was -1.22% (SD 2.03) for 6MV and -0.4% (SD 2.84) for 15MV. Maximum percentage variation for this was 4% and 5% for 6MV and 15MV respectively. TLDs were in good agreement with TPS. Results shows that contribution of boost field doses to the target isocentre for both 6MV and 15MV were less than 1cGy.
Conclusion: Dosimetric verification of MUs delivered by boost fields is essential to verify the accuracy of TPS algorithms.

Keywords: Boost Field, 3D-CRT, Isocentre

76

The relationship between absorbed dose and DNA Damage in Lymphocytes after radionuclide therapy

U. Eberlein[1], H. Scherthan[2], C. Bluemel[1], M. Peper[2], C. Lapa[1], RA. Werner[1], AK. Buck[1], M. Port[2], M. Lassmann[1]
[1] Department of Nuclear Medicine, University of Würzburg, Germany
[2] Bundeswehr Institute of Radiobiology affiliated to the University of Ulm,
Munich, Germany

Purpose: In radionuclide therapy today mostly β^--labelled radiopharmaceuticals are used which irradiate the body internally with time-dependent dose-rate and can cause DNA double strand breaks (DSBs).
The formation of a DNA DSB in nuclear chromatin results in the rapid phosphorylation of the histone variant gamma-H2AX. DSBs also recruit the damage sensor 53BP1 to the chromatin surrounding the DSBs, which leads to 53BP1 and gamma-H2AX co-localization. By immunofluorescence staining with gamma-H2AX and 53BP1 antibodies those biomarkers can be addressed by microscopically visible foci.
The number of foci per cell represent a quantitative biomarker for DNA double strand breaks and hence for radiation exposure and radiation effects. Presently, there are only few studies, which are studying the on-set and decay of DSBs after radionuclide therapy.
The aim of our study was, therefore, to generate an in-vitro calibration curve for quantifying the dose-response of the number of radiation induced foci (RIF) after internal irradiation of blood with β^--emitters, and to describe comprehensively the dose-dependent time course of the DSB on-set and repair in lymphocytes of radiation treatment-naive patients after radiopeptide therapy with ^{177}Lu and radioiodine therapy with ^{131}I.
Material and Methods: For the in-vitro calibration with ^{131}I and ^{177}Lu blood samples were drawn from volunteers. Different activity concentrations were added, the samples were incubated for 1h to achieve absorbed doses up to 100mGy, and the number of RIF/cell was determined.
The patient studies addressed the relationship between the absorbed dose to the blood and the number and temporal behavior of radiation-induced DNA double strand breaks (RIF/cell) in multiple peripheral blood samples under radiopeptide therapy (16 patients) and under radioiodine therapy (20 patients).
Results: The in-vitro study shows that the number of RIF/cell is linearly dependent of the absorbed dose, similar to what has been observed after external irradiation.
In patients, the average number of RIF/cell showed a linear dose-response relationship within the first hours after administration of the radiopharmaceutical. Later time points were characterized by a diminishing number of radiation-

induced foci which was in accordance with the progression of DNA repair and the declining dose rates. The absorbed dose in most patients treated with ^{131}I exceeded 20mGy in the first hour, and in these patients, the on-set of a fast repair component was observed.
Conclusions: With the experimental results and model calculations presented in this work, for the first time a dose-response relationship and a description of the time course of the in-vitro and in-vivo damage response after internal irradiation of β^--emitters could be established.

Keywords: gamma-H2AX and 53BP1, radionuclide therapy, dosimetry

77

A quantitative assessment of intra-fractional tumor motion and deformation error on planned dose at conventional proton therapy

A. Ebrahimi[1], A. E. Torshabi[1]
[1] Medical Radiation Division, Department of Electrical and Computer Engineering, Graduate University of Advanced Technology, Haftbagh St. 7631133131 Kerman, Iran

Purpose: In proton therapy, two major beam delivery techniques are used which are referenced as active and passive delivery strategies. In latter case, an effective dose distribution into tumor volume is created by pencil beam extracted from the accelerator exit window. To do this aim, the modulation is performed to produce two uniform beam profiles: 1) along with beam trajectory and 2) in lateral direction vertical to beam direction. The first dose profile cover tumor volume in target depth against beam direction and the second lateral profile include tumor volume, transversely. Several passive devices are utilized to create depth dose profile known as Spread-Out Bragg Peak (SOBP) and transverse dose profiles. In proton therapy, the final purpose is to produce a three dimensional (3D) homogeneous dose distribution onto the tumor volume while minimizing the dose to the surrounding healthy tissues around the tumor. Relating to moving and deforming targets, the delivery dose is not matched with the planned dose.
Methods: Our goal in this work is to obtain a quantitative assessment of three dimensional dose distribution on the moving and deforming targets and surrounding normal tissues affected by the breathing motion. For this aim, a simulation study was performed using Monte Carlo FLUKA code. The effect of each of the parameters in a clinical passive beam scanning system on radiotherapy dosage was considered. The dose deposition from protons was simulated for fields designed for the treatment of dynamic, deformed and static tumors.
Results: Dose distribution results of Monte Carlo method simulation were compared with the results obtained during experimental process at Cyclotron and Radioisotope Center (CYRIC) in Tohoku University. Final analyzed results represent that the uniformity of dose distribution on all given tumors are up to 95% of uniformity that proves a successful dose delivery onto tumor as well according to planned dose. The results of dose distribution into tumor and surrounding healthy tissues around the tumor for static spherical case regarding with deformed tumors and moving tumors were obtained. Conclusion: In conventional proton therapy a significant dose is delivered to the normal tissues in comparison with stationary condition without getting any strategy to limit ITV region such as motion gated or real-time tumor tracking strategies. The accuracy of dose distribution increasing with decreasing magnitude of deformation, moving and stretching of the tumor.

Keywords: Proton therapy, Radiotherapy Dosage, Monte Carlo Method.

References:
[1] Goitein, M., A.J. Lomax, and E.S. Pedroni, Treating cancer with protons. Physics Today, 2002. 55(9): p. 45-51.
[2] Sessler, A.M., An Introduction to Cancer Therapy with Hadron Radiation. Online Journal], http://209.85, 2008. 229.
[3] Pedroni, E. Latest developments in proton therapy. in Proceedings of EPAC. 2000.
[4] Paganetti, H., et al., Accurate Monte Carlo simulations for nozzle design, commissioning and quality assurance for a proton radiation therapy facility. Medical Physics, 2004. 31(7): p. 2107-2118.
[5] Keall, P.J., et al., The management of respiratory motion in radiation oncology report of AAPM Task Group 76a). Medical Physics, 2006. 33(10): p. 3874-3900.
[6] Gierga, D.P., et al., Quantification of respiration-induced abdominal tumor motion and its impact on IMRT dose distributions. International Journal of Radiation Oncology* Biology* Physics, 2004. 58(5): p. 1584-1595.
[7] Langen, K. and D. Jones, Organ motion and its management. International Journal of Radiation Oncology* Biology* Physics, 2001. 50(1): p. 265-278.
[8] Shirato, H., et al., Physical aspects of a real-time tumor-tracking system for gated radiotherapy. International Journal of Radiation Oncology* Biology* Physics, 2000. 48(4): p. 1187-1195.
[9] Torshabi, A.E., Investigation of tumor motion influence on applied dose distribution in conventional proton therapy vs. IMPT; a 4D Monte Carlo simulation study. INTERNATIONAL JOURNAL OF RADIATION RESEARCH, 2013. 11(4): p. 225-231.
[10] Lambert, J., et al., Intrafractional motion during proton beam scanning. Physics in medicine and biology, 2005. 50(20): p. 4853.
[11] Battistoni, G., et al., The FLUKA code and its use in hadron therapy. Nuovo Cimento C Geophysics Space Physics C, 2008. 31: p. 69-75.
[12] Ferrari, A., et al., FLUKA: a multi-particle transport code, CERN 2005-10. INFN/TC_05/II, SLACR—773, 2005.
[13] Battistoni, G., et al., FLUKA Monte Carlo calculations for hadrontherapy application. 2012.
[14] Smith, A.R., Proton therapy. Physics in medicine and biology, 2006. 51(13): p. R491.
[15] Smith, A., et al., The MD Anderson proton therapy system. Medical Physics, 2009. 36(9): p. 4068-4083.
[16] Chesny, P., et al., GSI Annual Report 1996. GSI, 1997. 1: p. 190.
[17] Pedroni, E., et al. A novel gantry for proton therapy at the Paul Scherrer Institute. in AIP Conference Proceedings. 2001. IOP INSTITUTE OF PHYSICS PUBLISHING LTD.
[18] Zhao, L., et al., Dosimetric impact of intrafraction motion for compensator-based proton therapy of lung cancer. Physics in medicine and biology, 2008. 53(12): p. 3343.
[19] Ohara, K., et al., Irradiation synchronized with respiration gate. International Journal of Radiation Oncology* Biology* Physics, 1989. 17(4): p. 853-857.

78

A compact high current accelerator for radioisotope production

R. Barlow[1], D. Bruton[1], R. Edgecock[1] and C. Johnstone[2]
[1] University of Huddersfield, Queensgate, Huddersfield, HD1 3HD, UK
[2] Particle Accelerator Corporation, 809 Pottawatomie Tr., Batavia, IL 60510, USA

An initial design of a compact, high current Fixed Field Alternating Gradient accelerator has been made for the direct production of ^{99m}Tc and the production of a number of therapeutic isotopes that currently available only in limited quantities or not at all. These studies indicate that the FFAG could in principle accelerate a proton beam of up to 20mA to at least 30 MeV and high current alpha beams to a similar energy. This presentation will describe the FFAG and show what radioisotope yields should be possible. It will also outline the next steps in the project. It should be noted that the same basic FFAG design is being extended to the energies required for cancer therapy with light ion beams.

Keywords: FFAG; high beam current; radioisotope production; ^{99m}Tc; therapeutic isotopes

References:

R.J.Barlow et al, "PIP: A Low Energy Recycling Non-scaling FFAG for Security and Medicine", Proceedings of IPAC2013, Shanghai, China, 12-17th May 2013, pp 3711-3713

79

Proton beam irradiation inhibits cellular motility in vitro

K. Jasińska[1], M. Michalik[2], M. Sarna[1], P. Olko[3], B. Romanowska-Dixon[4], K. Urbańska[1], Z. Madeja[2], M. Elas[1]
[1]Department of Biophysics, Faculty of Biochemistry, Biophysics i Biotechnology, ul. Gronostajowa 7, Cracow, Poland
[2]Department of Cell Biology, Faculty of Biochemistry, Biophysics i Biotechnology, ul. Gronostajowa 7, Cracow, Poland
[3]Institute of Nuclear Physics, PAS, Radzikowskiego 152, Kraków, Poland
[4]Department of Ophthalmology and Ophthalmic Oncology, Jagiellonian University Medical College, Kopernika 38, Kraków, Poland
e-mail: katarzyna.jasinska87@gmail.com

Purpose: Several authors point out some substantial differences in the biological response invoked by proton beam and X-rays [1][2]. Beside differences in short-term effects such as DNA repair [3], also some long-term cellular and tissue properties are differentially affected, such as angiogenesis [4], or metastasis [5]. We aimed at studying the migratory properties of human melanoma cells after low doses of proton beam radiation.
Materials/methods: BLM human melanoma cells (derived from lung metastasis) were irradiated with 1-5 Gy of X ray (300 kVp Phillips, 1Gy/min) or proton beam (58 MeV) from Proteus C-235 cyclotron. Cells were analyzed for migratory and motility properties using time-lapse monitoring of individual cell movements, Boyden chamber assay and the wound test. To check if these effects were long-term, the same tests were performed at day 20 and 40 after irradiation. Cell stiffness was assessed using AFM method.
Results: BLM cells exhibited lower displacement after proton beam and slightly higher after X rays. Boyden chamber assay and wound test indicated lower migration rate after proton beam and higher after X rays. In agreement with these results, cells treated with proton beam revealed decreasing cell stiffeness with dose as well.
Conclusions: In contrast to X rays, low doses of proton beam irradiation inhibited the long-term migratory properties affecting their directionality and invasion potential.

Keywords: biology, melanoma, proton beam irradiation, motility

References:
[1] Tommasino F, Durante M (2015) Proton Radiobiology. Cancers (Basel) 7: 353–381. doi:10.3390/cancers7010353.
[2] Girdhani S, Sachs R, Hlatky L (2013) Biological Effects of Proton Radiation: What We Know and Don't Know. Radiat Res 179: 1–16.
[3] Grosse N, Fontana AO, Hug EB, Lomax A, Coray A, et al. (2014) Deficiency in homologous recombination renders Mammalian cells more sensitive to proton versus photon irradiation. Int J Radiat Oncol Biol Phys 88: 175–181. doi:10.1016/j.ijrobp.2013.09.041.
[4] Girdhani S, Sachs R, Hlatky L (2015) Biological effects of proton radiation: an update. Radiat Prot Dosimetry: 1–5.
[5] Romanowska-Dixon B, Elas M, Swakoń J, Sowa U, Ptaszkiewicz M, et al. (2013) Metastasis inhibition after proton beam, ß- and γ-irradiation of melanoma growing in the hamster eye. Acta Biochim Pol 60: 307–311.

80

Metal implanted multi-functional nanovectors for targeted radiotherapy and diagnostics of cancer

A. Etilé[1], A. J. Airaksinen[1], K. Helariutta[1], U. Köster[2], E. Mäkilä[3], J. Salonen[3]
[1] Laboratory of Radiochemistry, University of Helsinki, Helsinki, Finland
[2] Institut Laue-Langevin, Grenoble, France
[3] Department of Physics and Astronomy, University of Turku, Turku, Finland

The requirements for early diagnostics as well as effective treatment of cancers constantly increase the pressure on development of efficient and reliable methods for targeted radiotherapy as well as imaging of the success of the treatment. Recently, new nanotechnology-based approaches have been explored for more efficient delivery of therapeutic radionuclides. Nanocarriers allow delivery of the radionuclides not only into the tumour tissue but all the way inside the tumour cells, which increases cytotoxic efficacy of the treatment[1].
In the aim of targeted radiotherapy and imaging, new methods combining radionuclides and mesoporous silicon (PSi) nanoparticles are being developed. PSi nanoparticles present major advantages for localised radiotherapy. Indeed, mesoporous silicon can tolerate high temperatures keeping its properties, which makes it an optimal material for particle activation. Moreover, its high adsorption capacity with anti-cancer drugs combined with further modification of the nanoparticles with tumour targeting moieties allow delivery of therapeutically relevant doses into the tumour tissue with a minimum amount of particles. By selecting therapeutic radionuclides that are applicable for nuclear imaging, trafficking of the administrated chemoradiotherapy nanovectors can be followed by non-invasive imaging whether with single emission computed tomography (SPECT) or positron emission tomography (PET). In order to aim these objectives two different approaches were implemented: implantation of the nuclide of interest into the PSi nanoparticles followed by its activation or direct implantation of the radioisotope of interest into PSi
The stability of the particles in buffer solutions with different physiologically relevant pH as well as the stability of the implanted nuclei in the particles were studied. The developed methods, first results of these studies and perspectives on this new therapeutical approach will be presented here.

Keywords: Nanoparticles, chemoradiotherapy, non-invasive imaging

References:
[1] Y.D. Livney & Y.G. Assaraf, *Adv Drug Deliv Rev*, 65, (2013).

81

Development of a radioguided surgery technique with beta- decays in brain tumor resection

V. Bocci[1], E. Capparella[1,2], F. Collamati[1,2], R. Donnarumma[1,2], R. Faccini[1,2], G. Ioannidis[1,2], G. Limiti[2,3], C. Mancini Terracciano[1,2], M. Marafini[1], S. Morganti[1], A. Russomando[1,2,4], E. Solfaroli Camillocci[1,2], M. Toppi[2,5], G. Traini[1,2]
[1] INFN Roma (IT)
[2] Sapienza Universita' di Roma (IT)
[3] Istituto Superiore di Sanita' (IT)
[4] CLNS@Sapienza Istituto Italiano di Tecnologia (IT)
[5] INFN Laboratori Nazionali di Frascati (IT)

Purpose: Radio-guided surgery (RGS) is a technique adopted by the surgeon to perform a complete lesion resection, taking advantage from the uptake from the tumor of specific radiolabelled tracers. Established methods make use of γ emitting tracer and γ radiation detection probe. To extend the applicability of RGS, we are developing an innovative technique exploiting ß- radiation [1]. It penetrates only a few mm resulting both in a lower required radio-pharmaceutical activity and the possibility to apply the technique also to cases with a large uptake of nearby healthy organs. Low background rate is also correlated with low medical team exposure.
Methods: We developed and tested several prototypes of the intraoperative ß- probe, the core made of para-terphenyl scintillator. The readout electronics is portable and customized to match the surgeon needs, with

wireless data transfer to the PC. Feasibility studies have been performed on DICOM images for meningioma and glioma brain tumors and neuroendocrine tumors (NET). The technique is in validation phase by testing it on "ex-vivo" specimen of patients affected by meningioma.

Results: As first application we are investigating brain tumors. The goal is to apply the technique to glioma, but the first study case is meningioma being an efficient tracer (90Y-DOTATOC) already available for it. Preclinical tests and Monte Carlo simulations have estimated that in the case of meningioma to identify in 1s a residual of 0.1ml a radio-pharmaceutical activity of about 3MBq/kg must be administered to patient [2]. Similar studies were extended to NETs[3] Ex-vivo tests on meningioma showed excellent agreement between experimental and expected rates for lesions and healthy tissues: e.g. the bulk tumor showed signals of ~100cps, 0.2 ml residuals signals of ~40cps and healthy tissues of less than 5cps.

Furthermore, exposure measurements confirmed the low level of radioactivity in the surgical environment (<1μSv/h at 10cm from patient abdomen).

Conclusions: A very promising technique for RGS is under development. The low background would allow to extend RGS also to cases with a large uptake of nearby healthy organs where the established approach with γ radiation suffers due to the non-negligible background.

Keywords: Radioguided surgery, beta- decay, intraoperative probe

References:

[1] E. Solfaroli Camillocci et al, "A novel radioguided surgery technique exploiting ß– decays", Sci. Rep. 4, 4401 (2014)

[2] F. Collamati et al, "Toward Radioguided Surgery with Beta- Decays: Uptake of a Somatostatin Analogue, DOTATOC, in Meningioma and High- Grade Glioma" J. Nucl. Med. 56:3–8 (2015)

[3] F. Collamati et al, "Time evolution of DOTATOC uptake in Neuroendocrine Tumors in view of a possible application of Radio-guided Surgery with beta- Decays" J. Nucl. Med. 56:1501–6 (2015)

82

^{64}Cu-Labeled Folate Radioconjugate for PET Imaging of Folate Receptor-Positive Tumors

R. Farkas[1], K. Siwowska[1], N. P. van der Meulen[1,2], R. Schibli[1,3], C. Müller[1,3]

[1] Center for Radiopharmaceutical Sciences ETH-PSI-USZ, Paul Scherrer Institute, Villigen-PSI, Switzerland

[2] Laboratory of Radiochemistry and Environmental Chemistry, Paul Scherrer Institute, Villigen-PSI, Switzerland

[3] Department of Chemistry and Applied Biosciences, ETH Zurich, Zurich, Switzerland

Purpose: Folate-receptor (FR)-targeted radioconjugates are promising for the imaging of a wide variety of tumor types [1]. So far, a number of folic acid conjugates have been developed for labeling with radiometals (e.g. ^{99m}Tc, ^{111}In, ^{68}Ga) for SPECT and PET imaging [2]. The aim of this study was to synthesize a folate conjugate with an albumin-binding entity, which is known to increase the conjugate's blood circulation time, and a NODAGA-chelator for ^{64}Cu-labeling and [3]. ^{64}Cu is a promising PET radionuclide for rf42 due to its excellent β^+-energy ($E\beta^+$=278 keV) and its reasonably long half-life ($T_{1/2}$ = 12.7 h) [4]. The ^{64}Cu-NODAGA-folate (^{64}Cu-rf42) was investigated in vitro and in vivo using mice bearing FR-positive tumor xenografts.

Materials/methods: ^{64}Cu was produced via the irradiation of, and subsequent chemical separation from, a Ni target at the research cyclotron at PSI. The synthesis of the NODAGA-folate conjugate (rf42) was carried out in eight steps and the resulting product was characterized by HPLC, MS and NMR. The radioconjugate was prepared by incubation of rf42 with $^{64}CuCl_2$ in a mixture of HCl/Na-acetate (pH ~5.5) at 45°C for 15 min. ^{64}Cu-rf42 was investigated regarding its in vitro stability in PBS (pH 7.4) and in human plasma. FR-positive KB tumor cells were used for in vitro experiments. Biodistribution studies were carried out in KB tumor-bearing nude mice at 2 h, 4 h and 24 h post injection (p.i.) of ^{64}Cu-rf42. A small-animal scanner (Genisys^8) was used for the PET/CT imaging studies

Results: rf42 was synthesized with an overall yield of 5% and 95% purity. The radiochemical purity of ^{64}Cu-rf42 was >99% at a specific activity of 10 MBq/nmol. ^{64}Cu-rf42 was stable (>95%) over a period of 24 h in buffer and plasma. Cell internalization studies showed high uptake of ^{64}Cu-rf42, while co-incubation of cells with excess folic acid to block FRs reduced the uptake to less than 1%. In vivo, high accumulation of radioactivity was found in KB tumors (13.36 ± 0.82% IA/g) 2 h after injection of ^{64}Cu-rf42. As a consequence of the enhanced blood circulation time of ^{64}Cu-rf42, due to its albumin-binding properties, the tumor uptake increased over time (16.20 ± 3.58% IA/g, 24 h p.i.). Relevant uptake of ^{64}Cu-rf42 was also found in the kidneys, which also express the FR. This resulted in a tumor-to-kidney ratio of 0.55 ± 0.11 at 24 h p.i. In non-targeted tissues undesired accumulation of radioactivity decreased over time. PET/CT imaging studies allowed excellent visualization of tumor xenografts up to 60 h p.i. of ^{64}Cu-rf42.

Conclusion: The novel folate-radioconjugate, ^{64}Cu-rf42, was readily prepared and showed FR-specific accumulation in vitro and in vivo. The half-life of ^{64}Cu is well suited to the enhanced circulation time of this novel albumin-binding conjugate. Based on the excellent PET images obtained from visualizing tumors in mice, ^{64}Cu-rf42 may have the potential for future application in the clinics for diagnosis of FR-positive tumors and monitoring tumor response after therapy.

Keywords: ^{64}Cu, tumor imaging, folate-receptor

References:

[1] Sega et al. 2008, Cancer Metastasis Rev 4:655-664.
[2] Müller et al. 2011, J Nucl Med 1 :1-4.
[3] Müller et al. 2013, J Nucl Med 1 :124-131.
[4] Smith et al. 2004, J Inorg Biochem 98 :1874-1901.

83

Geant4 coupled with Comsol heat transfer simulations to determine correction factors of a novel micro-calorimeter

K. Fathi[1, 5], S. Galer[1], H. Palmans[1, 2], K. Kirkby[3], A. Nisbet[4, 5]

[1]Acoustic and Ionising Radiation, National Physical Laboratory, Teddington

[2]Medical Physics, MedAustron, Austria

[3]Institute of Cancer Sciences, Medical Health Sciences, Manchester

[4]Medical Physics, Royal Surrey County Hospital, Guildford

[5]Physics, University of Surrey, Guildford

High uncertainty in the Relative Biological Effectiveness (RBE) values of particle therapy beam, which are used in combination with the quantity absorbed dose in radiotherapy, together with the increase in the number of particle therapy centres worldwide (58 in operation, 51 proposed) necessitate a better understating of the biological effect of such modalities. The present novel study is part of

performance testing and development of a micro-calorimeter based on Superconducting QUantum Interference Devices (SQUIDs) (1). Unlike other microdosimetric detectors that are used for investigating the energy distribution, this detector provides a direct measurement of energy deposition at the micrometer scale, that can be used to improve our understanding of biological effects in particle therapy application, radiation protection and environmental dosimetry. Temperature rises of less than 1μK are detectible and when combined with the low specific heat capacity of the absorber at cryogenic temperature, extremely high energy deposition sensitivity of approximately 0.4 eV can be achieved (2).
The detector consists of 3 layers: a tissue equivalent (TE) absorber, a superconducting absorber and a silicon substrate. Ideally all energy would be absorbed in the TE absorber and heat rise in the superconducting layer would arise due to heat conduction from the TE layer. However, in practice direct particle absorption occurs in all 3 layers and must be corrected for.
To investigate the thermal behavior within the detector, and quantify any possible correction, particle tracks were simulated employing Geant4 (v9.6) Monte Carlo simulations. The track information was then passed to the COMSOL Multiphysics (Finite Element Method) software. The 3D heat transfer within each layer was then evaluated in a time-dependent model. For a statistically reliable outcome, the simulations had to be repeated for a large number of particles. An automated system has been developed that couples Geant4 Monte Carlo output to COMSOL for determining the expected distribution of proton tracks and their thermal contribution within the detector.
Preliminary results of a 3.8 MeV proton beam showed that the detector reaches the equilibrium state after 8 ns. It is estimated that 20% of the temperature rise in the superconducting absorber is due to heat conduction from the adjacent absorber which needs to be corrected for. The simulations were repeated for proton beams with energies of 2, 10, 62 and 230 MeV.

Keywords: micro-dosimetry, Monte Carlo simulations and micro-calorimeter

References:
[1] S. Galer et al. Design concept for a novel SQUID-based microdosemter Radiation *Protection Dosimetry.* Vol 143, No (2-4), 427-31, 2011.
[2] L. Hao et al. Inductive Superconducting Transition-Edge Photon and Particle Detector. *IEEE Transactions and Applied Superconductivity.* Vol 13, No 2, 2003.

84
Assessment tool to quantify and visualize treatment plan robustness regarding patient setup
M.K. Fix, W. Volken, D. Frei, D. Terribilini, D.M. Aebersold, P. Manser
Division of Medical Radiation Physics and Department of Radiation Oncology, Inselspital, Bern University Hospital, and University of Bern, Switzerland

Purpose: Nowadays, during the evaluation process of patient treatment plans in radiotherapy, the plan robustness is typically not taken into account. This evaluation of treatment plans can be improved if a user friendly and efficient tool to assess the robustness of the treatment plan is provided. Thus, the aim of this work is to develop tools and methods to quantify and visualize the robustness for treatment plans including random and systematic patient setup uncertainties.
Materials and Methods: A setup error phase-space including systematic and random setup errors for translation and rotation is explored to determine the treatment plan robustness. For this purpose a robustness-map is created based on user-defined criteria defining the robustness for the treatment plan considered. These criteria subdivide the robustness-map for the setup error phase-space into a region compatible with these criteria and into another one that is not. Several different approaches were implemented to quantify the plan robustness. One approach transforms the optimized dose distribution relatively to the patient geometry and, thus, dosimetric parameters or DVHs can be quickly estimated, but are limited with respect to accuracy. Hence, approaches using further dose calculations for the setup error phase space are needed to achieve reliable conclusions of the robustness. For this purpose, additional dose calculations using a different resolution of the setup error phase-space are performed guided by the robustness-map achieved using the dose-transformation approach. The intermediate dose distributions are determined by nearest neighbor or triangular interpolation.
Results: A graphical user interface based on QT version 5.3.1 was developed to calculate and visualize robustness-maps. These robustness-maps allow treatment plan evaluation by analyzing the corresponding dose-differences and DVHs. Additionally, correlations of all quantities can be displayed such that the user is able to efficiently view the data by scrolling through the setup error phase-space. The creation of robustness-maps is useful to assess and compare the robustness of different treatment plans and was successfully applied to plans covering different tumor-sites. For the cases investigated in this work, differences in DVH parameters using the different approaches are within 5%.
Conclusions: The developed tool for visualization and analysis of robustness-maps is an easy and efficient way to compare the robustness of treatment plans. Moreover, clinical tolerance and action levels for patient setup can be determined in order to keep specified dosimetric parameters within a certain limit. This work was supported by Varian Medical Systems.

Keywords: treatment planning, plan robustness, patient setup

85
Treatment of moving targets with active scanning carbon ion beams
P. Fossati[1], M. Bonora[2], E. Ciurlia[2], M. Fiore[2], A. Iannalfi[2], B. Vischioni[2], V. Vitolo[2], A. Hasegawa[2], A. Mirandola[2], S. Molinelli[2], E. Mastella[2], D. Panizza[2], S. Russo[2], A. Pella[2], B. Tagaste[2], G. Fontana[2], M. Riboldi[3], A. Facoetti[2], M. Krengli[4], G. Baroni[3], M. Ciocca[2], F. Valvo[2], R. Orecchia[1].
[1] European Institute of Oncology, Radiotherapy Division, Milano, Italy.
[2] Fondazione CNAO, Clinical Area, Pavia, Italy.
[3] Politecnico of Milan, Bioengineering department, Milano, Italy.
[4] University of Piemonte Orientale, Radiotherapy department, Novara, Italy.

Purpose: In this paper we report the preliminary results of clinical use of organ motion mitigation strategies in the treatment of moving target with active scanned carbon ion beams.
Material and methods: Since September 2014 25 patients with tumors located in the upper abdomen and chest were treated with active scanned carbon ion beams.
Patients were affected by pancreatic adenocarcinoma, HCC, biliary tract cancers and sarcoma of the spine retroperitoneum and heart. Tight thermoplastic mask was selected as the optimal abdominal compression device. 4D CT scan with retrospective reconstruction, with phase signal obtained with Anzai system (Anzai Medical CO., LTD), was employed for planning. Automatic assignment of raw data to respiratory phases was checked and, if necessary, modified by the medical physicist. Planning was performed using end expiration phase. Planning CT scan were visually checked for motion artifacts. Contouring was performed on end expiration phase and on the adjacent 30% expiration and 30% inspiration phases. Beam entrance was selected in order to avoid the bowel in the entrance channel. The lung diaphragm interface was contoured in the different respiratory phases and beam angles were chosen to avoid passing tangential to the lung diaphragm ITV. IMPT was used for plan optimization. Plans were recalculated in adjacent phases and if DVHs were degraded in an unacceptable way they were modified iteratively. Weekly verification 4D CT scans were performed

and, if needed, a new plan was re-optimized adaptively. Set up was verified with gated orthogonal X rays and non-gated cone beam CT in treatment room. Threshold for gate-on signal was initially set at 10% pressure signal dynamic and qualitatively adjusted in an asymmetric way according to results of plan recalculation in 30% expiration and inspiration. Gating signal was fed to the accelerator to enable beam delivery. Each slice was re-scanned 5 times to smear out possible interplay effects. Acute and early toxicity was scored according to CTCAE 4.0 scale.
Results: GTV and diaphragm excursion between end expiration and adjacent 30% phases was reduced to less than 5 mm. GTV (D95%) and critical OAR (D1%) DVH in 30% inspiration and expiration phases showed on average minimal (less than 3%) differences as compared to planning end expiration plan. Toxicity was minimal with no G3 event; 15% acute G2 and 10% G2 toxicity at 3 months was observed.
Median follow up was rather short (3 months) nevertheless in 23 patients the dose limiting OAR was either stomach or small bowel or esophagus, therefore early toxicity data are informative.
Conclusion: Active scanning with carbon ion beams for the treatment of moving target using abdominal compression, 4D simulation, robust planning gating and rescanning is feasible and safe. Longer follow up is needed to evaluate oncological outcome

Keywords: organ motion, active scanning

86

Carbon ion radiotherapy: do we understand each other? How to compare differentt RBE-weighted dose systems in the clinical setting.

P. Fossati[12], S. Molinelli[1] ,G. Magro[1], A. Mairani[1], N. Matsufuji[3], N. Kanematsu[3], A. Hasegawa[3], S. Yamada[3], T. Kamada[3], H. Tsujii[3], M. Ciocca[1], R. Orecchia[1,2]
[1] Fondazione CNAO, Pavia, Italy.
[2] European Institute of Oncology, Milnao , Italy
[3] National Institute of Radiological Sciences, Chiba, Japan

In carbon ion radiotherapy (CIRT), mainly two calculation models are adopted to define relative biological effectiveness (RBE)-weighted doses (D_{RBE}): the Japanese Kanai model and the Local Effect Model (LEM). Taken the Japanese longest-term clinical data as a reference, the use of a different RBE model, with no correction for the Gy (RBE) scale, leads to deviations in target absorbed dose (D_{abs}) with a potentially significant impact on tumor control probability. In this study we validate a conversion method linking the two D_{RBE} systems, confirming D_{RBE} prescription dose values adopted in our LEM-based protocols.
The NIRS beamline was simulated with a Monte Carlo (MC) code, according to design information about elements position, size and composition. Validation went through comparison between simulated and measured pristine and Spread Out Bragg Peaks, ridge filter based, in water. CT scan, structure set, plan and dose files of 10 treatment fields delivered at NIRS were exported in DICOM format, for prostate (3.6 Gy $(RBE)_{NIRS}$ per 16 fractions), Head & Neck (4 Gy $(RBE)_{NIRS}$ per 16 fractions) and pancreas (4.6 Gy $(RBE)_{NIRS}$ per 12 fractions) patients. Patient specific passive system geometries (range shifter, MLC, compensator, collimator) were implemented, for each field, to simulate delivered D_{abs} distributions. The MC code was then interfaced with LEM to calculate D_{RBE} resulting from the application of a different RBE model to NIRS physical dose. MC and TPS calculated D_{abs} and D_{RBE} were compared in terms of dose profiles and target median dose. Patient CT and structure sets were also imported in a LEM-based commercial TPS where plans were optimized prescribing the non-converted and converted D_{RBE} values, respectively.
The agreement between MC and measured depth dose profiles in water, in terms of particle range, peak to plateau ratio and spread out profile shape, demonstrated beamline model accuracy. Patient dose distributions were correctly reproduced by MC in the target region, with an overall target median dose difference < 2%. MC median D_{RBE} resulted 16% higher than NIRS reference, for the lower prostate dose level, 10% for head and neck and 4.5% for pancreas, in agreement with respective LEM-based prescription doses, adopted in our protocols. Deviations are expected to be close to zero around a prescription D_{RBE} = 5 Gy (RBE). Aside from unavoidable differences in dose profile shape, severe target under-dosage was shown in LEM-based optimized plans, when uncorrected D_{RBE} were prescribed.
The delivery of a voxel by voxel iso-effective plan, if different RBE models are employed, is not feasible; it is however possible to minimize differences in dose deposited in the target. Dose prescription is a clinical task which ultimately depends only on the radiation oncologist clinical decision; in this study we made an attempt to avoid systematic errors which could potentially compromise tumor control.

Keywords: Relative Biological Effectiveness, carbon ion radiotherapy, Local Effect Model

References:
[1] Jäkel O, Krämer M, Karger CP, *et al*. Treatment planning for heavy ion radiotherapy: clinical implementation and application. *Phys Med Biol* 2001;46(4):1101-16.
[2] Kanai T, Endo M, Minohara S, *et al*. Biophysical characteristics of HIMAC clinical irradiation system for heavy-ion radiation therapy. *Int J Radiat Oncol Biol Phys* 1999;44(1):201-10.
[3] Kanai T, Matsufuji N, Miyamoto T, *et al*. Examination of GyE system for HIMAC carbon therapy. *Int J Radiat Oncol Biol Phys* 2006;64(2):650-6.
[4] Krämer M, Scholz M. Treatment planning for heavy-ion radiotherapy: calculation and optimization of biologically effective dose. *Phys Med Biol* 2000;45(11):3319-30.
[5] Mairani A, Brons S, Cerutti F, *et al*. The FLUKA Monte Carlo code coupled with the local effect model for biological calculations in carbon ion therapy. *Phys Med Biol* 2010;55(15):4273-89.
[6] Fossati P, Molinelli S, Matsufuji N, *et al*. Dose prescription in carbon ion radiotherapy: a planning study to compare NIRS and LEM approaches with a clinically-oriented strategy. Phys Med Biol. 2012;57(22):7543-54.

87

Experimental study of Radiation induced DNA damage by internal Auger electron cascade compared to external γ-rays

P. M. Fredericia[1], T. Groesser[1], M. Siragusa[1], G. Severin[1], J. Fonslet[1], U. Koester[2], M. Jensen[1]
[1] Technical University of Denmark, Center for Nuclear Technologies, Copenhagen, Denmark
[2] Institut Laue-Langevin, Grenoble, France

Purpose: The aim of this study is to compare the radiation induced DNA damage done by internal Auger-electron cascades with external exposures of sparsely ionizing radiation such as γ-rays.
Background: Auger emitters decay by internal conversion (IC) or electron capture (EC) producing a number of Auger cascade electrons. These electrons are so low in energy that their range in tissue is in the order of nm-µm. This means that if the decay happens nearby the DNA, the Auger cascade electrons can produce a cluster of complex DNA damage. These clusters of DNA damage are much harder to repair and are therefore believed to be much more harmful to the cell than dispersed DNA damage, which are primarily produced by low LET radiation. Due to their short tissue range and the severe DNA damage produced, Auger emitters may be able to kill only the target cell while sparing non-targeted cells. This makes them a potential tool for radionuclide therapy(1,2,3,4).
Material/Methods: In order to compare the radiation effects by the Auger emitter to that of external γ-rays we need to be able to estimate the dose delivered. As Auger cascade electrons have a very short range the precise spatial distribution of the decays is of high importance.
We are currently working with two Auger emitters, Cs-131 and La-135. First experiments have been performed using HeLa cells, which were incubated with either Cs-131 or La-

135 for internal exposure. Theses ions seem to be taken up by the cells. However more knowledge about the bio-kinetics of these auger emitters is needed to estimate the dose rates and the dose distribution in the cell. As the cells take up the Auger emitter, the dose rate by the internal Auger decays are continuously changing as a function of cellular accumulation and half-life of the isotope.
Uptake curves are therefore produced by incubating HeLa cells with Auger-electron emitters for various amounts of time and with different levels of radioactivity to calculate the changing dose rate and accumulated dose. These conditions will be mimicked as closely as possible with external γ-rays, by moving the cells closer to the source (Cs-137). DNA damage will be assessed by flow cytometry measurements (MUSE) of phosphorylated histone H2AX (γ-H2AX) and/or the clonogenic cell survival assay.

Keywords: Auger, RBE, Internal Radiotherapy

References:
[1] Howell, R., Rao, D., Hou, D., Narra, V., & Sastry, K. (1991). The question of relative biological effectiveness and quality factor for Auger emitters incorporated into proliferating mammalian cells. Radiation Research, 128(3), 282–292. doi:1961925
[2] Howell, R. W. (2008). Auger processes in the 21st century. International Journal of Radiation Biology, 84(12), 959–75. doi:10.1080/09553000802395527
[3] Kassis, A. I. (2004). The amazing world of auger electrons. International Journal of Radiation Biology, 80(11-12), 789–803. doi:10.1080/09553000400017663
[4] Yasui, L. S. (2012). Molecular and cellular effects of Auger emitters: 2008–2011. International Journal of Radiation Biology, 88(November 2011), 1–7. doi:10.3109/09553002.2012.702296

88
Towards analytic dose calculation for MR guided particle beam therapy
H. Fuchs[1], P. Moser[1,2], M. Gröschl[2], D. Georg[1]
[1] Medical University of Vienna, Department of Radiation Oncology & Christian Doppler Laboratory for Medical Radiation Research for Radiation Oncology, Vienna, Austria.
[2] Vienna University of Technology, Institute of Applied Physics, Vienna, Austria.

Purpose: The importance of MRI steadily increases in radiation oncology not only as multimodality imaging device but also as an implemented online imaging technology. Imaging using MRI shows advantages compared to CT or CBCT offering superior soft tissue contrast without additional dose. Also in particle beam therapy integrated MR guided treatment units have great potential. A complete understanding of the particle beam characteristics in the presence of magnetic fields is required. So far, studies in this area are limited.
Material and Methods: Protons (60-250MeV) and carbon ions (120-400MeV/u) in the clinically required energy range impinging on a phantom of 35x35x50cm³ size were simulated using the MC framework GATE 7. Homogeneous magnetic fields of 0.35T, 1T and 3T perpendicular to the initial beam axis were applied. The beam deflection, shape, and the energy spectrum at the Bragg peak area was analyzed. A numerical algorithm was developed for deflection curve generation solving the relativistic equations of motion taking into account the Lorentz force and particle energy loss. Additionally, dose variations on material boundaries induced by magnetic fields were investigated for 250MeV protons.
Results: Transverse deflections up to 99mm were observed for 250MeV protons at 3T. Deflections for lower field strengths (e.g. future hybrid open-MRI proton delivery systems) yielded 12mm for 0.35T and 34mm for 1T. A change in the dose distribution at the Bragg-peak region was observed for protons. Energy spectrum analysis showed an asymmetric lateral energy distribution. The different particle ranges resulted in a tilted dose distribution, see Fig.1.The numerical algorithm successfully modeled the deflection curve, with a maximum deviation of 1.8% and calculation times of less than 5ms. For a 250MeV proton beam passing in a 3T field through multiple slabs (water-air-water), only a 4% local dose increase at the first boundary was observed in single voxels due to the electron return effect, more than a factor 10 lower compared to a photon beam [1].

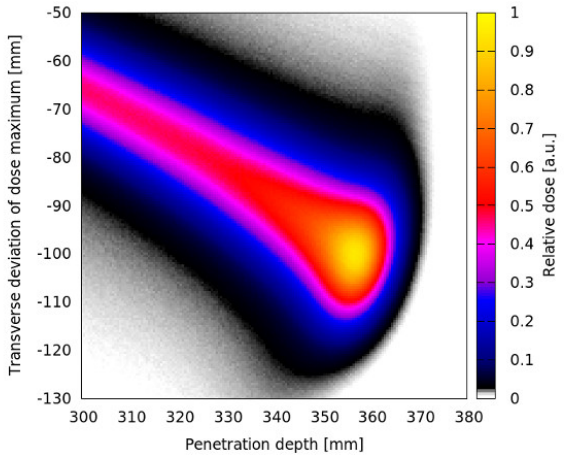

Fig1: Deformed 2D dose distribution at the Bragg peak area for a 250MeV proton beam in a 3T field

Conclusion: Beam deflections in magnetic fields could be described by a numerical algorithm. The observed change in dose distribution in the Bragg-peak region has to be taken into account in future dose calculations. However, local dose changes due to boundary effects seem to be negligible for clinical applications. Current work in progress deals with the inclusion of magnetic field effects in a dose calculation algorithm for particles.

Keywords: particle therapy, Monte Carlo, Magnetic Resonance Imaging

References:
[1] Raaijmakers et al., Magnetic-field-induced dose effects in MR-duided radiotherapy systems: dependence on the magnetic field strength, Physics in Medicine and Biology, 53(4):909,2008

89
The Biology of Single Dose Radiotherapy
Zvi Fuks
Memorial Sloan Kettering Cancer Center
New York, NY USA

The mechanism of tumor cure by ionizing radiation is regarded tumor cell autonomous, effected by misrepair of radiation-induced DNA double strand breaks (DSBs), to a large extent *via* the function of error prone non-homologous end joining (NHEJ). This model prevails at the low dose range, with cure depending on tumor phenotypic propensity for NHEJ misrepair, and requires repeated exposures for tumor ablation. Here we report high (>10Gy) single dose radiotherapy (SDRT) employs an alternative dual target model, inducing in addition to DSBs also an early wave of acid sphingomyelinase (ASMase)-mediated microcirculatory ischemia/reperfusion (I/R) injury. Reactive oxygen species (ROS) induced therein in parenchymal tumor cells disrupt activation of homology-directed repair (HDR), leading to catastrophic reprograming of DSB repair. We show Ku- and 53BP1-mediated NHEJ are not affected, although MDC1/53BP1 resolution is delayed, while engagement of the HDR mediator cluster in DSB repair is aborted, promoting a divergent DSB repair pathway, generation of massive chromosomal alteration and reproductive tumor clonogen demise. Scavenging of ROS with the SOD-mimetic tempol reversed the loss-of-function HDR and tumor cell lethality, aborting tumor cure by SDRT. We define I/R-mediated loss-of-function HDR as the detrimental SDRT damage response,

conferring synthetic tumor clonogen lethality, with far reaching clinical implications.

90

Multiple Code Comparisons of Proton Interactions in the Presence of Gold Nanoparticles in the Human Eye

M.F. Samavat[1], S. Asadi[1], S. Gaeeni[1], H. Tavassoli[1]
[1] K.N. Toosi University of Technology, Faculty of Physics

Purpose: The main focus of the present study is to investigate dose enhancement effects in presence of gold nanoparticles (AuNPs) in proton delivery site of the ocular melanoma by the use of fixed pencil beam method associated with the Harvard ocular nozzle in a series of Monte Carlo simulations. Moreover, this paper also aims to present a comparison of the obtained results between the actual eye model, consisting of all sections of the eye and realistic compositions in the presence of AuNPs, and in the exact same organ, albeit in privation of the mentioned material.
Materials and Methods: Previous Monte-Carlo simulations have strained to acquire the same results obtained through latest experiments that have considered dose enhancement effects of proton treatments with existence of AuNPs, but to no avail; thus, multiple simulation codes such as MCNP, GEANT4, and FLUKA have been taken into account to insure the least possible deviation from in vivo findings. Rigorous libraries and models have been used, and all physical processes involved have been accounted for.Furthermore, for the sake of accuracy, the production of the most probable secondary particles due to interactions with matter has also been examined.Contribution to dose enhancement effects are due to stopping losses, coulomb interactions, and elastic and non-elastic collisions of proton itself, as well as from secondary particles that are produced in mentioned processes.
Results and Conclusions: The attempt of such paper is to shed light on the endless possibilities of escalating the efficiency of medical endeavors through interdisciplinary methods which combine various aspects of science and technology to attain desired results.

Keywords: Proton-therapy, AuNPs, MC Simulations

91

Characterization of the immune component in the lung of KP mouse with pulmonary adenocarcinoma: from infiltrated immune cells to tertiary lymphoid structures.

B. Gael[1*], J. Faget[2*], J. Bourhis[1], E. Meylan[2°] and M-C. Vozenin[1°].
[1] Unil-CHUV
[2] EPFL ISREC
* and ° Contributed equally

Introduction: In this preliminary work, we developped a method to phenotype and analyse the tumour infiltrating immune cells (TIICs) and identified tertiary lymphoid structures (TLS) as potential immune reservoir in lslKrasG12D P53fl/fl mice model. As radiotherapy as been described to act on the recruitment, removal, reorganisation, repolarisation and activation of immune cells (1), our final goal will be to define optimal radiotherapy scheme to stimulate immune response.
Material & method: lslKrasG12D P53fl/fl mice were used and tumours genenerated by intratracheal admnistration of LentiCre to generate numerous widespread lung autochonous tumours. Those were macrodissected, weighed and measured to analyse TIICs with a 16 colours facs pannel. TLS were identified, anayzed in serial lung sections and the TLS/ tumors ratio was assessed. Both TIICs and TLS were studied with IHC and/or IF. (B220, LY6G, CD3, Lyve1, Prox1, CD163, CD68, KI67, CXCR4, Ecadhérin, CD205).
Results: Size of tumors positively correlated with high amount of CD80- macrophages/monocytes, MDSCs and Tregs, but was inversely proportionnal with the amount of NK1.1+, B220+, Ly6g+ cells and CD8/FoxP3 ratio. Histological analysis showed that immune cells were not strongly infiltrating tumors but located in aggregates defined as TLS in the vincinity of tumours and were mostly composed of B220+ cells and CD163+ macrophages.. TLS were approximately 50 uM sized and the tumour/TLS ratio was heteroeneous on 4um section, ranging from 0,5 to 6,6. However, TLS were not observed in tumour-free control KP mouse.
Conclusion: TLS are a known good prognosis factor in human lung cancer (2) and consistently with a recent publication (3) we report TLS infiltrates in tumour bearing KP mouse. Our hypothesis is that TLS may promote anti-tumour immunity upon radiotherapy and is currently being tested using conventionnal and flash radiotherapy.

Bibliography:
[1] Silvia C Formenti et al, Myeloid-Derived Cells in Tumors: Effects of Radiation. Seminar in radiation oncology 2015
[2] Dieu Nos-Jean MC et al, Long-Term Survival for Patients With Non–Small-Cell Lung Cancer With Intratumoral Lymphoid Structures. Journal of Clinical Oncology, sept 20.2008.
[3] Joshi, Nikhil S. et al, Regulatory T Cells in Tumor-Associated Tertiary Lymphoid Structures Suppress Anti- tumor T Cell Response. Immunity , Volume 43 , Issue 3 , 579 – 590

92

Detectors for quality assurance of pencil beam scanning gantries for proton therapy

F. Gagnon-Moisan, R. van der Meer, Z. Chowdhuri, M. Eichin, S. Koenig, F.-J. Schmid, D. C. Weber
Paul Scherrer Institut, Center for Proton Therapy, 5232 PSI-Villigen, Aargau, Switzerland

Purpose: The Center for Proton Therapy (CPT) of the Paul Scherrer Institute has a long history of technical innovation and development in the field of proton therapy and related quality assurance (QA) [1]. The unique integration of QA equipment for the second proton pencil beam scanning (PBS) gantry built at the CPT [2], Gantry2, allows extensive diagnostic of the treatment unit for performance improvement. Here we present our latest developments in detection systems and their performance for daily QA for PBS.
Method: The daily QA equipment developed for Gantry2 consists of a multi-layer ionization chamber (MLIC), a strip ionization chamber and two calibrated ionization chambers for dose measurement. The signals from the MLIC and strip monitor are first digitized by a multi-channel current-to-frequency converter (TERA06 chip [3]) and then processed by detector specific electronics (DSE) modules designed at CPT. The DSE is fully integrated into the Gantry2 system, allowing recording of the data from external detectors for each delivered spot. The data recorded from November 2013 to October 2015 with Gantry2 consists of a set of comprehensive daily measurements for the proton energies, spots delivery parameters (size, shape, and parallelism) and dose measurements.
Results: The results from the different detectors provide critical information about the performance of our treatment system. The range measurement shows a deviation of less than 0.5 mm water equivalent thickness (WET) over 115 energies between 70 MeV and 230 MeV on a daily basis. This illustrates the good reliability of the beam delivery system. We compare two different MLIC systems with a water-based range measurement device as reference. The mean deviation of range between the devices is lower than 0.8 mm WET. The spot position during delivery provides crucial information about the stability of the gantry massive structure. Correlation between the gantry angle and the position of spots are clearly established. The results are all well within clinical tolerances.
Conclusions: The in-house developed QA detectors and their integration into the Gantry2 system has provided unique possibilities for comprehensive and efficient daily QA. The results show the strong points of both the Gantry2 systems and the equipment developed in-house, such as the stability of the daily range measurements. The results are being used to draft the next, improved generation of QA devices at the CPT for new PBS techniques.

Keywords: Proton therapy, ionization chambers, quality assurance

References:
[1] L. Shixiong et al., Med. Phys. 36, 5331 (2009)
[2] E. Pedroni et al., Eur. Phys. J. Plus 126, 66 (2011)
[3] A. La Rosa et al., Nucl. Instr. & Meth. in Phys. Res. A 586, 270 (2008)

93

A novel method for assessment of nuclear interactions of therapeutic helium-ion beams using the Timepix detector

R. Gallas[1,2], G. Arico[1,2,3], T. Gehrke[1,2,3], O. Jäkel[1,2,3,4], M. Martisikova[1,2,3]
[1] German Cancer Research Center DKFZ, Heidelberg, Germany
[2] Heidelberg Institute for Radiation Oncology (HIRO), National Center for
Radiation Research in Oncology, Heidelberg, Germany
[3] University Clinic Heidelberg, Heidelberg, Germany
[4] Heidelberg Ion-Beam Therapy Center, Heidelberg, Germany

Purpose: Ion beam radiotherapy exploits the advantageous shape of the Bragg curve, resulting in conformal dose distributions. Helium ions, being heavier than protons, exhibit lower scattering than protons. Moreover, their lower charge leads to lower biological effectiveness when compared to carbon ions. These characteristics make helium ions attractive for future radiotherapy, especially for pediatric patients. However, before helium ions can be implemented in the clinical practice, it is necessary to obtain further information on the nuclear interactions between beam particles and patient tissues. Particularly important factors are the attenuation of primary ions fluence and the amount of arising secondary fragments. This information is an important input for biological models employed in treatment planning. In this contribution we present a novel method for measurement and identification of ions in mixed helium beams.
Materials and methods: Measurements were performed at the Heidelberg Ion-Beam Therapy Center (HIT) in Germany. Abundance of helium ions and lighter fragments arising in PMMA, water, and different tissue-equivalent materials were investigated. Single particles were detected using the highly pixelized (55 µm) semiconductor detector Timepix [1], developed by the Medipix Collaboration at CERN. Its sensitive volume consists of a 300 µm thick silicon layer with an area of 1.4x1.4 cm². Timepix detectors were placed perpendicular to the helium beam. The first of them in front of the target served for monitoring of single incoming particles. The second one behind the target was used to register helium ions and fragments. The information on the time coincidence between the two detectors enabled us to relate the outcoming particles to single incoming helium ions.
Results: Pattern recognition [2] of the single particle signals was found to be capable of distinguishing between helium ions and lighter fragments, as shown in Fig.1.
The numbers of helium ions and fragments behind the used targets were quantified. As expected, we found an increasing amount of fragments and a decreasing amount of helium ions for increasing the thickness of PMMA targets. Furthermore, a comparison of measurements behind PMMA and water targets, with the same water-equivalent thicknesses, shows that the numbers of helium ions and fragments agree rather well for thin targets while greater differences were found for thicker targets.
Conclusion: The small and versatile Timepix detectors allow to investigate the abundance of different ion types in helium ion beams. The whole setup is about two orders of magnitude smaller than previously used apparati based on time-of-flight measurements. This method is promising to acquire large data sets on helium nuclear interactions and thus improve the treatment planning in helium radiotherapy.

Keywords: Helium ion radiotherapy, single particle detection, semiconductor Timepix detectors

Acknowledgments: Medipix Collaboration and HIT, German Cancer Aid for funding.

References:
[1] Llopart X, Ballabriga M, Campbell M, Tlustos L, Wong W. Timepix, a 65k programmable pixel readout chip for arrival time, energy and/or photon counting measurements. Nucl. Instrum. Meth. A. 2007;581:485-494.
[2] Hartmann, B. A Novel Approach to Ion Spectroscopy of Therapeutic Ion Beams Using a Pixelated Semiconductor Detector. PhD thesis, University of Heidelberg, 2013.

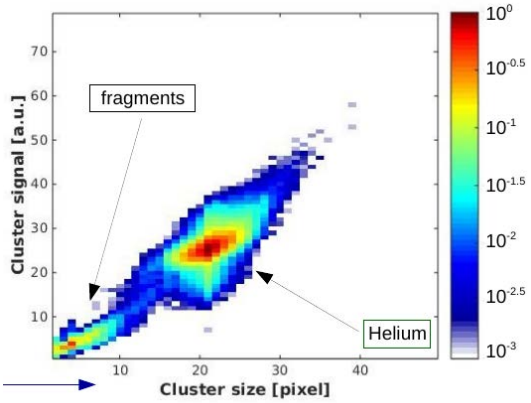

Fig. 1: "Pattern recognition" analysis of a mixed helium ion beam, with an initial energy of 220 MeV/u, arising behind a PMMA phantom of 24.5 cm thickness.

94

Image-guided and adaptive radiotherapy: medical physics challenges ahead

D. Georg
[1] Department of Radiation Oncology, Medical University Vienna/AKH Wien
[2] Christian Doppler Laboratory for Medical Radiation Research for Radiation Oncology, Medical Univ. Vienna

During the last two decades spectacular advances in medical imaging of anatomy and physiology, and medical radiation physics as well as in computer sciences have made it possible to deliver radiation doses to a predefined target with unprecedented precision. This holds for both photon and ion-beam therapy with fluence modulation. The latest generation of ion-beam delivery systems based on pencil beam scanning, which is the new standard, combines highest conformity with optimal organ at risk sparing. On the other hand, an essential characteristic of ion treatment plans is their intrinsic sensitivity to temporal anatomic changes since tissue density can deteriorate a good proton or ion dose distribution.
The multifaceted new paradigms of image guided and (biologically) adaptive radiotherapy motivated many recent technological developments or new treatment concepts. For example, image guidance by magnetic resonance imaging (MRI) has lead to new beam delivery units where an MR is combined with a linear accelerator or a cobalt sources for photon beam therapy. The MR guidance paradigm from photon beam therapy is also influencing proton beam research. The new treatment concept of dose painting, where tumor sub-volumes with a potential resistance are visualized via functional imaging and are boosted with an extra dose, has also its origin in the photon community but ion-beam are probably the ultimate brushes for dose painting.
One great challenge in image guided and (biologically) adaptive radiotherapy remains however to detect, assess, delineate, and track this target with the same precision and to respond to changes in the target volume during the course of the treatment, both with respect to changes in time and space. In this context medical image processing has become an important research field. Moreover, "missing links" have hampered the widespread clinical implementation and validation of new developments.

Another challenge for the clinical implementation of adaptive treatments is linked to treatment planning and quality assurance, with the associated workload that is directly linked to the patient numbers. For treatment planning, first generation systems for automated planning already exist, with minimal user interaction tested under clinical scenarios. With respect to quality assurance there is a move from patient specific QA towards more stringent machine specific QA, and from reactive to proactive procedures utilizing electronic data. Verifying range in ion-beam therapy is a very specific QA procedure but complementary.
The overarching challenges ahead for image guided and (biologically) adaptive radiotherapy are similar for both photon and ion-beam therapy, although each branch has its own detailed issues to be solved. The era of technological developments turns into the era of clinical implementation, which necessitates the intensification of interdisciplinary collaboration.

Keywords: advanced photon beam therapy, ion-beam therapy, MR guidance, dose painting, quality assurance, image processing

95

Geometrical interpretation of TOF PET raw data in commercial PET-CT scanner for SNR optimization

C. Gianoli[1], E. De Bernardi[2], C. Kurz[1], M. Riboldi[3], G. Baroni[3], K. Parodi[4]
[1]Department of Experimental Physics - Medical Physics and Department of Radiation Oncology, Ludwig Maximilian University of Munich, Germany; Department of *Department of Radiation Oncology,* Heidelberg University Hospital, Germany
[2]Medicine and Surgery Department – Tecnomed Foundation, University of Milano-Bicocca, Milan, Italy
[3]*Dipartimento di Elettronica, Informazione e Bioingegneria* (DEIB)*, Politecnico di Milano, Italy*
[4]*Department of Experimental Physics - Medical Physics, Ludwig Maximilian University of Munich, Germany; Heidelberg Ion-Beam Therapy Center* (HIT), Germany

Purpose: The purpose of this work is the understanding of image partitioning due to Time of Flight (TOF) in PET raw data, as extracted from commercial PET-CT scanners without confidential information from the vendors. The work complements the geometrical characterization of PET raw data in terms of image and sinogram correspondence, as reported in [1]. This characterization enables implementation of vendor independent TOF 3D reconstruction algorithms for Signal to Noise Ratio (SNR) enhancement in extremely low count statistics imaging scenarios, as encountered in off-line PET-based treatment verification in ion beam therapy [2]
Materials/methods: Seven point sources, placed in different trans-axial positions *(x,y)* of the Field of View (FOV) are acquired with a commercial PET-CT scanner (Siemens Biograph mCT*)* installed at the Heidelberg Ion Beam Therapy Center (Germany). PET raw data are organized in *b* TOF bins, where *b=1:13*. Each TOF bin is a sinogram parameterized in *(p,θ,φ)*, collecting PET counts as a function of projection line *p*, azimuthal projection angle *θ* and polar angle *φ*. The method relies on the hypothesis that the unknown image partitioning coincides with half ring-shaped regions within the FOV, in addition to the first TOF bin that corresponds to the central full ring-shaped region, as depicted in Fig. 1 (Panel B). Hence, given a point source in *(x,y)*, the image partitioning is exclusively encoded in the projection angle *θ*. For each point source, the fraction of PET counts in each *b* as a function of *θ* is calculated ($f_b(\theta)$). The intersection of $f_b(\theta)$ along *θ* for adjacent *b* defines the projection angle encoding the region interface. Then, the radial position

$$d(\theta) = x \times cos\left(\theta + \frac{\pi}{2}\right) + y \times sin\left(\theta + \frac{\pi}{2}\right)$$

relevant to the interface is calculated according to the source-to-detector distance ($d(\theta)$):
Median and standard deviations of $d(\theta)$ for the different point sources are calculated.
Results: In Fig. 1 (Panel A), $f_b(\theta)$ is reported for four different point sources. The mean values of radial partitioning resulted in ≈26 pixels for the first TOF bin, which coincides with the ray of the central full ring-shaped region, and ≈46 pixels for the second and the third TOF bins. The approximation depends on the adopted fitting to determine the $f_b(\theta)$ intersections. For external TOF bins, the estimation resulted affected by large standard deviations because of noise due to reduced number of PET counts.
Conclusions: In PET-based treatment verification, PET activity is distributed in proximity of the tumor target, which is typically centered in the FOV. In future investigations, to additionally increase the SNR of the image obtained from TOF 3D reconstruction, external TOF bins (b>5) will be intentionally neglected since they contain noisy PET counts coming from scatter (which has a TOF dependency [3]) and random contributions.

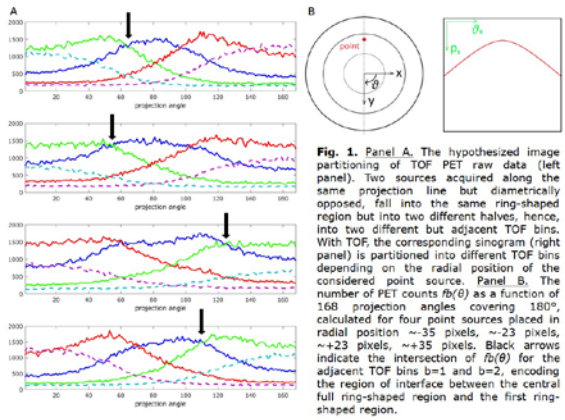

Fig. 1. Panel A. The hypothesized image partitioning of TOF PET raw data (left panel). Two sources acquired along the same projection line but diametrically opposed, fall into the same ring-shaped region but into two different halves, hence, into two different but adjacent TOF bins. With TOF, the corresponding sinogram (right panel) is partitioned into different TOF bins depending on the radial position of the considered point source. Panel B. The number of PET counts $f_b(\theta)$ as a function of 168 projection angles covering 180°, calculated for four point sources placed in radial position ~-35 pixels, ~-23 pixels, ~+23 pixels, ~+35 pixels. Black arrows indicate the intersection of $f_b(\theta)$ for the adjacent TOF bins b=1 and b=2, encoding the region of interface between the central full ring-shaped region and the first ring-shaped region.

Keywords: Commercial Time of Flight PET-CT scanner, Signal to Noise Ratio, PET-based treatment verification in ion beam therapy

Acknowledgments:
FP 7 EU ENVISION (N.241851)

References:
[1] Gianoli C et al (2014). *Comput Med Imaging Graph*, *38*(5), 358-368.
[2] Kurz C et al (2015). *Med Phys*, *42*(7), 3979-3991.
[3] Moses (2003). *IEEE Trans Nucl Sci 50*(5), 1325-1330.

96

Spatial Resolution Enhancement in Integration-Mode Detectors for Proton Radiography and Tomography

C. Gianoli[1,2], S. Meyer[1], L. Magallanes[1,3], G. Dedes[1], G. Landry[1], R. Nijhuis[2], U. Ganswindt[2], C. Thieke[2], C. Belka[2], K. Parodi[1]
[1]Department of Experimental Physics - Medical Physics, Ludwig Maximilian University of Munich, Germany
[2]Department of Radiation Oncology, Ludwig Maximilian University of Munich, Germany
[3]*Department of Radiation Oncology, Heidelberg University Hospital, Germany*

Purpose: This work proposes a novel method for spatial resolution enhancement of proton radiographies acquired with raster scanning and integration-mode detectors. The method, called enhanced integration-mode (EI-mode), simply relies on statistical interplay between adjacent raster points due to finite beam spot size and multiple Coulomb scattering (MCS). The aim is to investigate the performance of the proposed method for a simple and cost-effective integration-mode configuration as alternative to widely investigated list-mode detectors with broad beams.
Materials/methods: With integration-mode the residual range information, or water equivalent thickness (WET), is obtained from multiple ions belonging to the same pencil beam, without single particle tracking. The integrated signal is

numerically modeled as a combination of multiple Bragg peak signals and linear decomposition can disentangle different WET contributions, thus building up WET histogram at each raster point.
The Gaussian model of the lateral pencil beam profile is calculated for each raster point as convolution between beam spot and MCS models, thus defining a neighborhood on the radiography space. The MCS model is based on WET with maximum probability, typically considered in integration-mode. The integral of the WET histogram is normalized to unity, thus expressing WET probability. The WET probability, originally assigned to the raster point, is spatially distributed based on corresponding WET probabilities of adjacent raster points, weighted according to the Gaussian model of beam intensity.
Quantification is performed in comparison with list-mode in radiography space, prior to image reconstruction. Analytical and Monte Carlo simulations of proton radiographies for phantom and Computed Tomography (CT) patient data are considered.
Results: The enhancement of spatial resolution from IE-mode with respect to list-mode is observable in Fig.1. The method does not modify the typical integration-mode radiography based on WET with maximum probability for each raster point, unless at the edges where the neighborhood is not centered at the raster point position (Fig.1). On analytical simulations, WET root mean square difference of IE-mode with respect to list-mode is 9.39±0.83 mm. On Monte Carlo simulations of patient data this difference is reduced down to 3 mm because of absence of sharp anatomical details in CT data.
Conclusions: The redundancy of information collected by integration-mode detector offers possibilities to enhance spatial resolution. Similar to list-mode radiographies, the spatial resolution will be optimized by tomographic image reconstruction algorithms embedding this spatial information. Quantification will be performed in both radiography end tomography spaces, with respect to MCS-free gold standard.
Keywords: Proton radiography and tomography, integration-mode and list-mode configurations, spatial resolution

Acknowledgments
BMBF (01IB13001, SPARTA); DFG (MAP); DFG (VO 1823/2-1)

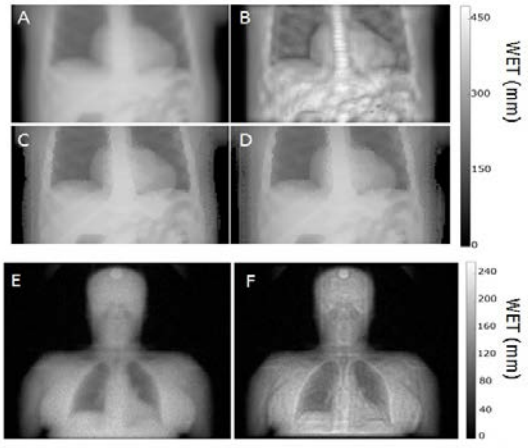

Fig.1. Analytical simulation in phantom: list-mode radiography (A), integration-mode radiography corresponding to the maximum WET probabilities (C), enhanced integration-mode radiography (B) and its maximum WET probabilities (D). Monte Carlo simulation in patient data: list-mode radiography (E) and enhanced integration-mode radiography (F).

97

Hybrid TOF-PET/MRI local transceiver coil

B. Głowacz[1,@], M. Zieliński[1] D. Alfs[1], T. Bednarski[1], P. Białas[1], E. Czerwiński[1], A. Gajos[1], M. Gorgol[2], B. Jasińska[2], D. Kamińska[1], Ł. Kapłon[1,3], G. Korcyl[1], P. Kowalski[4], T. Kozik[1],W. Krzemień[5] , E. Kubicz[1], M. Mohammed[1], M. Pawlik-Niedźwiecka[1] , S. Niedźwiecki[1], M. Pałka[1], L. Raczyński[4], Z. Rudy[1], O. Rundel[1], N. G. Sharma[1], M. Silarski[1], A. Słomski[1], A. Strzelecki[1], A. Wieczorek[1,3], W. Wiślicki[4], B. Zgardzińska[2], P. Moskal[1]
[1]Faculty of Physics, Astronomy and Applied Computer Science, Jagiellonian University, S. Łojasiewicza 11, 30-348 Kraków, Poland,
[2]Department of Nuclear Methods, Institute of Physics, Maria Curie Sklodowska University, Pl. M. Curie-Sklodowskiej 1, 20-031 Lublin, Poland
[3]Institute of Metallurgy and Materials Science of Polish Academy of Sciences, W. Reymonta 25, 30-059 Kraków, Poland
[4]Świerk Computing Centre, National Centre for Nuclear Research, A. Soltana 7, 05-400 Otwock-Świerk, Poland
[5]High Energy Physics Division, National Centre for Nuclear Research, A. Soltana 7, 05-400 Otwock-Świerk, Poland
[@] - bartosz.glowacz@cern.ch

Purpose: Nowadays devices based on the detection of nuclear and electromagnetic radiation are in common use for the diagnosis of the interior of the human body. The most technologically advanced are positron emission tomography (PET), computed tomography (CT) and magnetic resonance imaging (MRI). In order to enhance diagnostic capabilities PET and MRI devices were combined into a single hybrid device providing an access to both metabolic and morphological information during a single examination. Typically the PET detectors are placed inside the diagnostic tunnel of the MR scanner. In spite of a possibility of the whole body and simultaneous PET and MR imaging the problem of the local MR transmit-receiver (transceiver) coils use still remains. Such coils are designed to be close to the imaged object, thus enhancing the MR image quality in comparison to the whole body coil use that is built in the MR scanner.
The coils are made of plastic parts and metal conductors which are on the way of gamma quanta flying from the annihilation point in the patients body to the scintillating material. This fact could cause the worsening of a spatial resolution of the PET diagnostic images, as the field-of-view (FOV) for the PET detectors is limited and gamma quanta scattering increases.
Material and methods: Therefore, it would be favorable to construct a single device consisting of a wire transmit-receive MR antenna integrated with the PET detectors that are able to register gamma quanta simultaneously with the magnetic resonance scan without mutual disturbance between the two detection systems and limiting the loses of images quality met so far.
We propose a solution based on a strip TOF-PET tomograph concept [1] comprising multiple PET detection modules, built from polymer scintillation strip ended with silicon photodetectors, arranged circumferentially inside the working volume of the MRI local transceiver coil. The adaptive of the polymer scintillators in both shape and size properties allows for a use of a standard MRI coils constructions to be combined with PET detection system with only a minor changes in the overall MRI coil dimensions, that do not influence the coil shape, geometry and material properties optimized so far.
The detection electronics based on silicon photodetectors and digital signal processing system [2] will operate in high static magnetic fields as well as radiofrequency waves environment of MR scanner, for instance. Such hybrid coil could be used in existing MRI systems extending its functionality by the PET imaging feature.
Conclusions: In the presentation the problem of local MR coils use in PET detectors will be introduced referring to the technology developed so far, underlying its weaknesses and limitations. Starting with the strip TOF-PET concept the idea of hybrid PET/MR local coil construction will be presented in details emphasizing the advantages over the former solutions [3].

Keywords: PET-MR, hybrid PET-MR coil, strip-PET

References:

[1] "STRIP-PET: Concept of TOF-PET scanner based on polymer scintillator strips", P.Moskal et al. Nuclear Medicine Review 15 (2012) A61-A63
[2] "A novel method based solely on FPGA units enabling measurement of time and charge of analog signals in Positron Emission Tomography". M.Pałka el al. Bio-Alg. and Med-Systems Vol. 10, 1,(2014) 41-45
[3] "Hybrid TOF-PET/MRI transceiver coil", B.Glowacz, M.Zielinski, P.Moskal, Patent application PZ/3256/RW/PCT (2015)

98

Treatment outcome in patients treated with single-dose irradiation (SDRT) for oligometastatic disease

Carlo Greco [1]
[1] Department of Radiation Oncology, Chamapalimaud Centre for the Unknown, Lisbon

Purpose: to analyze treatment outcome following Single-Dose Image-Guided Radiotherapy (SDRT) using PERCIST criteria based on 18-F-fluoro-2-deoxy-D-glucose PET Standardized Uptake Value (SUV_{max}) assessments in patients with limited extra-cranial metastatic disease.
Methods and Materials: 259 lesions in 101 consecutive patients with early metastatic disease with less than five lesions at initial presentation (mean 2.1, range 1-5 lesions) were treated between November 2011 and March 2015 with SDRT. Mean and median PTV volume were 40.6 and 18.1 cm^3 (range, 1.3-339), respectively. PTV prescription dose was 24Gy. Of the 101 patients, 56 (55%) of had a solitary metastasis at the time of first treatment. While the majority of the patients received only one treatment, 27% (27/101) received additional treatments (mean 1.4, median 1 range, 1-7) for relapses elsewhere. Thus, the mean number of lesions for the entire population was 2.6 (range, 1-13). SUV_{max} were acquired at the time of FDG-PET/CT planning before SDRT, at 3 and 6 months post-treatment and every 6 months thereafter. Treatment outcome was assessed by PERCIST criteria, with metabolic relapse defined as any increase of SUV_{max} >20% above nadir level. All metabolic relapses were confirmed by morphologic imaging. Lesions had a minimum of 2 post-treatment scans (mean 4; range 2-11) with a minimum follow-up of 6 months.
Results: actuarial 2- and 3-year overall survival for this cohort were 71% and 64%, respectively. At a median follow-up of 16.1 months (range, 6.7- 43.5 months), 6% (15/259) of lesions developed PERCIST failure within the irradiated region yielding a 3-year actuarial freedom of local relapse of 90%. Mean time to local relapse was 9 months. All recurrences occurred within the first 19 months. The mean percentage increase in SUV_{max} in relapsing lesions was 429% (range, 28% - 2530%). The mean and median baseline SUV_{max} were 8.9 and 6.9, respectively (range, 0.7-52.0). At 3 months post-SDRT, 15% (40/259) of the lesions had a >90% reduction in SUVmax (PERCIST complete metabolic response). SUV_{max} declines >75% ($\Delta SUV_{max\ >75\%}$) was significantly associated with freedom from metabolic relapse at 3 years ($p = 0.02$). Lesions with with $\Delta SUV_{max\ >75\%}$ had 94% local control at 36 months *vs*. 77% for $\Delta SUV_{max\ \leq 75\%}$. On univariate analysis, no correlation was found with primary tumor histology, metastasis site, PTV volume or ongoing systemic treatment and the likelihood of local relapse free survival.
Conclusion: These results confirm that high dose SDRT provides long-term local relapse-free survival using objective PERCIST therapeutic response criteria in patients with early metastatic disease. Additionally, they provide preliminary evidence that an early evaluation in metabolic changes post-SDRT may serve as a useful prognostic tool in the assessment of lesions treated with ablative intent.

99

How to produce scandium-44 efficiently?

C. Duchemin[1], A. Guertin[1], F. Haddad[1,2], N. Michel[1,2], V. Metivier[1]
[1] Laboratoire SUBATECH, Ecoles des Mines de Nantes, Université de Nantes, CNRS/IN2P3, 4 rue Alfred Kastler, 44307 Nantes cedex 3 - FRANCE
[2] GIP ARRONAX, 1 rue Aronnax, 44817 Saint-Herblain cedex – FRANCE

Purpose: Among the large number of radionuclides of medical interest, Sc-44 is promising for PET imaging. Either the Sc-44g or the Sc-44m can be used for such applications, depending on the molecule used as vector. This study compares the production rates of both Sc-44 states, when protons or deuterons are used as projectiles on an enriched calcium-44 target for 3 scenarios: the production of Sc-44g for conventional PET imaging, its production for the new 3 γ imaging technique developed at the SUBATECH laboratory and the production of Sc-44m to be used as Sc-44m/Sc-44g in vivo generator for antibody labelling.
Materials/methods: Experimental production cross section have been measured up to 34 MeV for the Ca-44(d,2n)Sc-44m,Sc-44g reactions, using the stacked-foil technique [1] and gamma-spectrometry, at the ARRONAX cyclotron [2]. The stacks were made of $Ca\text{-}44CO_3$ as targets and aluminum foils as degraders. Monitor foils were made of natural titanium in order to use the IAEA recommended cross section of the Ti-nat(d,x)V-48 reaction. Some results on the production of K-42,43 and Sc-43 have also been obtained but not in all the targets as the main objective was first to properly measure the activity of Sc-44m and Sc-44g. The results are compared with the TALYS code [3] version 1.6. Based on these experimental data, the Thick-Target production Yields (TTY) of Sc-44m and Sc-44g are calculated and compared with those for the proton route for the 3 scenarios [4].
Results: Experimental cross section values have been obtained for the first time for Ca-44(d,2n)Sc-44m,Sc-44g reactions with some information on Sc-43 and K-42,43 also produced during the irradiation. The TALYS results are close to the experimental values for the Ca-44(p,n) and Ca-44(d,2n) reactions whereas it is not able to reproduce the data for the production of potassium isotopes. Our new experimental results have shown that the Sc-44m/Sc-44g cross section and TTY ratios are higher with deuterons than with protons, whatever the incident beam energy.
Conclusions: This study shows that the use of a proton beam is the best choice, as compared to deuterons, to produce Sc-44g for PET imaging using peptides or small molecules with rapid distribution in the body. For the 3 γ imaging technique, Sc-44g has to be produced with protons of 15 MeV to limit the background generated by Sc-44m and Sc-43 decay. The production of the Sc-44m to be used as Sc-44m/Sc-44g in vivo generator for antibody labelling required the highest Sc-44m production rate, with a limited amount of Sc-44g directly produced. The production of Sc-44m is advantageous with deuterons as projectiles, using a calcium-44 carbonate target. Sc-44m can be produced with a 15 MeV deuteron. A higher amount of Sc-44m is produced with a 30 MeV deuteron beam and some cooling time, before the extraction and separation processes, allows to significantly reduce the contribution of directly produced Sc-44g and Sc-43.

Keywords: Sc-44g for PET, 3γ imaging, Sc-44m/Sc-44g in vivo generator

References:
[1] Duchemin C, Guertin A, Haddad F, Michel N and Métivier V. Cross section measurements of deuteron induced nuclear reactions on natural tungsten up to 34 MeV. Appl. Radiat. Isot. 97 52–8, 2015
[2] Haddad F., Ferrer L., Guertin A., Carlier T., Michel N., Barbet J., and Chatal J.F. Arronax a high-energy and high-intensity cyclotron for nuclear medicine. Eur. J. Nucl. Med. Mol. Imaging, 35:1377–1387, 2008
[3] Koning A.J. and Rochman D. Modern nuclear data evaluation with the TALYS code system. Nucl. Data Sheets, 113, 2012
[4] Duchemin C, Guertin A, Haddad F, Michel N and Métivier V. Production of scandium-44m and scandium-44g with deuterons on calcium-44: cross section measurements and production yield calculations. Phys. Med. Biol. 60 (2015) 6847–6864, 2015

100

Is there an interest to use deuteron beams to produce non-conventional radionuclides?

C. Alliot[1,2], N. Audouin[1], J. Barbet[1,2], A. C. Bonraisin[1], V. Bossé[1,2], C. Bourdeau[1], M. Bourgeois[1,2], C. Duchemin[3], A. Guertin[3], F. Haddad[1,3*], S. Huclier-Markai[3], R. Kerdjoudj[3], J. Laizé[1], V. Métivier[3], N. Michel[1,3], M. Mokili[1,3],M. Pageau[1], A. Vidal[1].

[1] GIP ARRONAX, 1 rue Aronnax, 44817 Saint-Herblain cedex – FRANCE

[2] CRCNA, Inserm, CNRS, Université de Nantes, 8 quai Moncousu, 44007 Nantes cedex 1, France.

[3] Laboratoire SUBATECH, Ecoles des Mines de Nantes, Université de Nantes, CNRS/IN2P3, 4 rue Alfred Kastler, 44307 Nantes cedex 3 - FRANCE

Purpose: With the recent interest on the theranostic approach, there has been a renewed interest for alternative radionuclides in nuclear medicine. They can be produced using common production routes using protons accelerated by biomedical cyclotrons or neutrons produced in research reactors. However, in some cases, it can be more valuable to use deuterons as projectiles.

The aim of this study is to illustrate the interest of using deuterons as projectiles to produce alternative radionuclides for medical applications. For that purpose, three examples have been chosen according to the fact that these radionuclides are produced using deuterons: production of Cu-64, Sc-44m and Re-186.

Materials/methods: For each radionuclide of interest, production yields have been calculated using experimental data from the literature when they exist or calculated value obtained using the TALYS 1.6 code [1] when no experimental data is available or for stable element. In some cases, new experimental production cross section have been measured [2, 3] at our facility [4].

Results: New set of cross sections have been obtained for $^{nat}W(d,x)^{186}Re$ and for $^{44}Ca(d,n)^{44}Sc$ using the stacked foil technique. Thick target yield for deuteron induced and proton induced reaction have been calculated and compared with yield obtained real production run.

In the case of Cu-64, smaller quantities of the expensive target material, Ni-64, are used with deuterons as compared with protons for the same produced activity. For the Sc-44m/Sc-44g generator, deuterons afford a higher Sc-44m production yield than with protons. Finally, in the case of Re-186g, deuterons lead to a production yield three times higher than protons.

Conclusions: These three examples show that it is of interest to consider not only protons or neutrons but also deuterons to produce alternative radionuclides. At the Arronax facility where deuteron beams are available with energy ranging from 15 MeV to 34 MeV, Cu-64 and Sc-44 are produced using 16 MeV deuterons. In the future Re-186 will also be considered for production using deuteron beams.

Keywords: deuteron induced production

References:

[1] Koning A.J. and Rochman D. Modern nuclear data evaluation with the TALYS code system. Nucl. Data Sheets, 113, 2012

[2] Duchemin C, Guertin A, Haddad F, Michel N and Métivier V. Production of scandium-44m and scandium-44g with deuterons on calcium-44: cross section measurements and production yield calculations. Phys. Med. Biol. 60 (2015) 6847–6864, 2015

[3] Duchemin C, Guertin A, Haddad F, Michel N and Métivier V., Cross section measurements of deuteron induced nuclear reactions on natural tungsten up to 34 MeV, Appl. Rad. Isot. 97(2015)52–58

[4] Haddad F., Ferrer L., Guertin A., Carlier T., Michel N., Barbet J., and Chatal J.F. Arronax a high-energy and high-intensity cyclotron for nuclear medicine. Eur. J. Nucl. Med. Mol. Imaging, 35:1377–1387, 2008

101

Disruption of telomere equilibrium sensitises human cancer cells to DNA repair inhibition and radiation

S. Venkatesan[1], R. Lal Gurung[1], S. Sameni[1], S. Sethu[1,2] and M. P. Hande [1,3,4]

[1] Department of Physiology, Yong Loo Lin School of Medicine, National University of Singapore, Singapore

[2] Narayana Nethralaya, Bangalore, India

[3] Tembusu College, National University of Singapore, Singapore

[4] Applied Radiation Biology and Radiotherapy Section, Division of Human Health, International Atomic Energy Agency, Vienna, Austria

Telomerase reactivation is essential for telomere maintenance in human cancer cells ensuring indefinite proliferation. Targeting telomere homeostasis has become one of the promising strategies in the therapeutic management of tumours. One major potential drawback, however, is the time lag between telomerase inhibition and critically shortened telomeres triggering cell death, allowing cancer cells to acquire drug resistance. Dysfunctional telomeres, resulting from the loss of telomeric DNA repeats or the loss of function of telomere-associated proteins trigger DNA damage responses similar to that observed for double strand breaks. We have recently shown that inhibition of DNA repair protein and telomerase renders cells more sensitive to DNA damaging agent. In addition to the disruption of telomere length maintenance, telomerase inhibition decreased tumour cell viability, induced cell cycle arrest and DNA damage. Repair of telomerase inhibitor-induced DNA damage involved activation of DNA-PKcs protein with inhibition of DNA-PKcs activity causing delay in the repair of induced DNA damage. Additionally, telomere dysfunctional foci were more detectable in DNA-PKcs deficient cancer cells as compared to DNA-PKcs proficient cells. The observed therapeutic potential in the cancer tumour cells improved when they were combined with the inhibition of certain selective DNA repair factors (such as PARP-1 and DNA-PKcs). We have also observed the radio-sensitisation potential of these telomerase inhibitors in selected human tumour cells. Taken together, our in vitro studies in cancer cells demonstrate that inhibition of DNA repair pathways and that of telomerase could be an alternative strategy to enhance anti-tumour effects and circumvent the possibility of drug resistance.

Keywords: Biology, Telomerase Inhibition, DNA repair inhibition, Experimental cancer therapeutics.

102

Pelvic tumor irradiation: new tools to reduce toxicity: from technology to drugs.

I. Joye[1,2], K. Haustermans[1,2]

[1] KU Leuven - University of Leuven, Department of Oncology, B-3000 Leuven, Belgium

[2] University Hospitals Leuven, Department of Radiation Oncology, B-3000 Leuven, Belgium

Radiotherapy plays an important role in the treatment of pelvic tumors. The advances in patients' prognosis come at the expense of radiation-induced toxicity. Progressive cell depletion and inflammation are the leading mechanisms of acute toxicity which is observed during or shortly after treatment. The pathogenetic pathways of late toxicity, developing 90 days after the onset of radiotherapy, are more complex and involve processes such as vascular sclerosis and fibrosis. Since many patients have become long-term survivors, awareness and recognition of treatment-related toxicity has gained in importance and increased efforts are made for its prevention and management.

Technical innovations contribute to a reduction in radiotherapy-associated toxicity. The steep dose gradients of highly-conformal radiotherapy techniques allow for an accurate dose delivery with optimal sparing of the normal tissues. Several studies have demonstrated the dosimetrical benefit of intensity-modulated radiotherapy (IMRT) and volumetric modulated radiotherapy (VMAT) compared to

conventional radiotherapy techniques. It has been shown that the dosimetrical benefit of IMRT translated into a clinically significant reduction in lower gastrointestinal toxicity compared with three-field conventional radiotherapy. MRI-linacs and proton therapy are likely to broaden the therapeutic window further in the near future. Prone positioning on a bellyboard reduces small bowel toxicity by pushing away the small bowel loops from the high dose region. Image-guided radiotherapy allows for an accurate definition, localization and monitoring of tumor position, size and shape before and during treatment and may help to reduce set-up margins.
Small randomized controlled trials have shown that the administration of several agents might have a beneficial effect for the prevention of acute (e.g. intrarectal amifostine, oral sulfasalazine and balsalazide) and/or late-onset radiation-induced toxicity (intrarectal beclomethasone and oral probiotics). Once severe toxicity develops, total replacement of the diet with elemental formula may be appropriate. Probiotics influence the bacterial microflora and seem promising in reducing the incidence and severity of radiation-induced diarrhea. Currently there is insufficient evidence for cytoprotective and anti-inflammatory drugs in the management of radiation-induced toxicity. Future challenges lie in the prediction of treatment-related toxicity, which might be a promising step towards an individualized risk-adapted treatment.

103
Lessons from translational research in EORTC glioma trials
M. E Hegi
Laboratory of Brain Tumor Biology and Genetics
Neurosurgery & Neuroscience Research Center
Department of Clinical Neurosciences
University Hospital Lausanne, Iausanne Switzerland

Glioblastoma (GBM) is the most common and most malignant primary brain tumor in adults with a dismal prognosis of 15 to 18 months and few therapeutic options. GBM are notorious for their resistance to therapies, likely due to a plethora of genetic and epigenetic alterations affecting multiple cancer relevant pathways conferring enhanced adaptive plasticity to tumor cells. The addition of concomitant and adjuvant temozolomide to radiotherapy has been introduced 10 years ago based on the pivotal EORTC-NCIC trial. At the same time, the predictive value of promoter methylation of the repair gene *MGMT* for benefit from the alkylating agent temozolomide has been established. Despite efforts in developing targeted agents this combination therapy is still the current the standard of care. Clinical trials have used the combination therapy as backbone and added new drugs, immunotherapies, or use of devices. Or, in a second strategy, patients were selected according to their *MGMT* status. *MGMT* unmethylated patients who basically do not profit from alkylating agent therapy can be entered into trials omitting temozolomide. This allows avoiding unnecessary toxicity, thereby enhancing chances for new drugs and providing new options for patients with a particularly bad prognosis. Advances of molecular techniques have led to discovery of new genetic and epigenetic alterations with prognostic and predictive value that have changed tumor classification, in particular in lower grade gliomas. This emphasizes the importance of collection of tumor tissue within clinical trials to test respective markers that need to be taken into account when analyzing completed trials or devising new strategies for clinical trials. Druggable mutations are usually only present in a relatively small subset of patients, a fact that is observed across tumor types. Therefore, in a new strategy the EORTC has launched the SPECTA program – allowing for efficient biomarker screening across all tumor types for improving access to molecularly driven and transversal clinical trials. SPECTAbrain will open in January.

104
Vascular disrupting agents: a new avenue of research
M. R. Horsman[1]
[1] Department of Experimental Clinical Oncology, Aarhus University Hospital, Aarhus, Denmark

The growth and development of solid tumours requires an adequate supply of oxygen and nutrients. Initially this is obtained from the vascular supply of the normal tissue in which the tumour arises. However, the demands of the growing tumour mass soon exceed the supply from this source and further growth is only possible if the tumour forms its own blood supply from the host vessels via the process of angiogenesis. This significance of the tumour neo-vasculature makes it an excellent target and two approaches have now emerged. These are the more popular use of drugs that inhibit the angiogenesis process and the less popular use of agents that disrupt the already established tumour vasculature. This latter approach actually has a much longer history than angiogenesis inhibitors. Indeed, the first vascular disrupting agent (VDA) investigated as an anti-tumour agent was colchicine back in the 1930s. Although it was shown to possess significant anti-tumour activity in both pre-clinical and clinical studies, it was also found to have substantial systemic toxicity. Later agents with VDA activity were also very toxic. This changed in the 1980s when combretastatin A-4 phosphate (fosbretabulin) was developed from products isolated from the bark of the African Bush Willow and found to have anti-tumour activity at doses well below those that caused systemic toxicity. Numerous other VDAs have since been developed with similar anti-tumour/toxicity profiles and many are under clinical evaluation. These include fosbretabulin, ombrabulin, crinobulin, and plinabulin. Although the vascular damage induced by VDAs can be severe and translates into a significant inhibition of tumour growth, it is never sufficient to induce tumour control, thus the potential of VDAs is not when used alone but when combined with conventional radiation or chemotherapy. Drug, timing, and sequencing are critical in such combinations. For radiation, pre-clinical studies performed using optimum conditions have shown a variety of different VDAs to be capable of significantly improving tumour response when the radiation is administered either as single treatments or in more clinically relevant fractionated and stereotactic schedules. Limited normal tissue studies, using both early and late responding endpoints, suggest no enhancement of radiation damage, thus a therapeutic benefit is observed. In this review we will briefly discuss the development of VDAs and the current status of both pre-clinical and clinical studies.
Key words: Vascular disrupting agents, radiation, pre-clinical/clinical studies.

105
The influence of chemical composition on quenching in proton irradiation of a new deformable 3D dosimeter
E. M. Høye[1], P. S. Skyt[1], P. Balling[2], L. P. Muren[1], J. Swakoń[3], G. Mierzwińska[3], M. Rydygier[3], V. Taasti[1] and J. B. B. Petersen[1]
[1] Department of Medical Physics, Aarhus University Hospital, Denmark
[2] Department of Physics and Astronomy, Aarhus University, Denmark
[3] Institute of Nuclear Physics, Polish Academy of Sciences, Poland

Purpose: In proton therapy, anatomical changes may cause considerable deterioration of the delivered dose distributions. Transmission-based treatment verification is generally not possible, making three-dimensional (3D) dosimetry a promising tool for verification of the delivered dose. However, solid state 3D detectors have shown significant problems related to linear-energy-transfer dependent quenching in particle beams – an under-response of the signal in the Bragg peak. A new deformable, silicone-based, radiochromic 3D dosimeter has recently been developed by our group. The aim of this study was to perform the first proton beam experiments with this detector. Special attention was given to the quenching and dose-rate dependencies in general, relating these effects to the chemical composition of the dosimeter.

Material/methods: Dosimeters (1 x 1 x 4.5 cm^3) of varying chemical compositions were produced. They contained leuco-malachite green (LMG) dye as the active component, chloroform and silicone elastomer.
Twelve different batches were irradiated with 60 MeV proton beams, using a 40 mm circular collimator, to different doses (0 – 30 Gy). Irradiations were performed with both a low and a high dose rate (0.23 and 0.55 Gy/s). For comparison, depth–dose distributions were measured in water with a Markus-type, plane-parallel ionization chamber. Simultaneously, dosimeters from the same batches were irradiated with 6 MV photon beams in a 10 cm square field on a linear accelerator.
All dosimeters were read out before irradiation and four hours after, at a wavelength of 635 nm. The read-out was performed with a home-built 1D-scanner with a depth resolution of 0.2 mm for the proton irradiated dosimeters, while a spectrophotometer was used for the photon read-out. The dose-rate dependency was compared for proton and photon irradiations. The ratio of Bragg-peak to plateau response (at 1 cm) was compared between batches.
Results: The effect of lowering the dose rate was similar for proton and photon beams, although the beam qualities were different. The dose response was higher at a low dose rate, but at increasing dye concentration the effect was reduced.
Significant under-response was observed in the Bragg peak. The peak-to-plateau ratio was improved from (2.5 ± 0.1) to (3.0 ± 0.04) by increasing the dye concentration from 0.1 to 0.3 % (w/w). By increasing the curing-agent concentration from 5 to 9 % (w/w), the ratio further improved to (3.7 ± 0.4) and (3.5 ± 0.1) for the same respective dye concentrations.
Conclusion: The 3D radiochromic silicone based dosimeter has for the first time been investigated in proton beams, and it was demonstrated that chemical modifications could influence the dosimeter response.

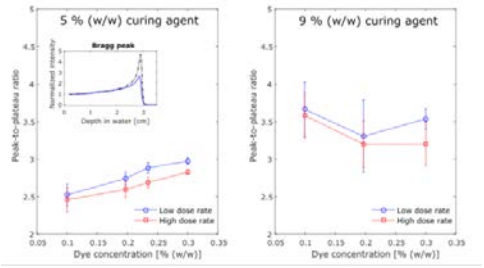

The peak-to-plateau ratio measured for dosimeters containing different dye concentrations. All dosimeters contained 1.5 % (w/w) chloroform, while the curing agent concentration was 5 % (w/w) in the figure to the left and 9 % (w/w) in the figure to the right. The measurements have been separated into low dose rate (blue circles) and high dose rate (red squares). The ionization chamber showed a peak-to-plateau ratio of 4.82 ± 0.01. The inset shows one example of a measured proton depth–dose profile (blue full line), which has been normalized to the ionization chamber measurement (black dashed line) at a depth of 13.1 mm. The example given here is from a batch irradiated with protons at 0.23 Gy/s, where the dosimeters contained 0.23 % (w/w) dye, 1.5 % (w/w) chloroform and 5.0 % (w/w) curing agent.

Keywords: 3D dosimetry, proton therapy, quenching

106
Accelerated Prompt Gamma estimation for clinical Proton Therapy simulations
B. F . B. Huisman[1,2], J. M. Létang[1], É. Testa[2], D. Sarrut[1]
[1] CREATIS, Université de Lyon; CNRS UMR5220; INSERM U1044; INSA-Lyon;
Université Lyon 1; Centre Léon Bérard, Lyon, France
[2] IPNL, Université de Lyon; CNRS/IN2P3 UMR5822; Université Lyon 1 Lyon, France

Purpose: There is interest in the particle therapy community to use prompt gammas (PG), a natural byproduct of particle treatment, for range verification and eventually dose control (Knopf *et al.* 2015). However, PG production is a rare process and therefore estimating PGs exiting a patient during a proton treatment plan executed by a Monte-Carlo simulation converges slowly. Recently, different approaches to accelerating the estimation of PG yield have been presented. Sterpin *et al.* (2015) described an analytic method that is about to be implemented in a commercial product, but has as drawback sensitivity to heterogeneities. Kanawati *et al.* (2015) described a variance reduction method (pgTLE) that accelerates the PG estimation by precomputing PG production probabilities as a function of energy and target materials, but has as drawback that it only works for analytical phantoms.
Materials/Methods: We present a two-stage method, voxellized pgTLE (vpgTLE) that extends pgTLE to voxellized volumes. PG production probabilities are precomputed once, stored, and reused. In stage one, we simulate the interactions between the treatment plan and the patient CT with low statistic MC to obtain the spatial and spectral distribution of the PGs. As primary particles are propagated throughout the patient CT, the PG yields are computed in each voxel from the initial database, as function of the current energy of the primary, the material in the voxel and the step length. The result is a voxellized PG yield image, normalized to a single primary. The second stage uses the intermediate PG image as a source to generate and propagate PGs throughout the rest of the scene geometry, e.g. into a detection device, proportional to the number of primaries desired.
Results: We have achieved a global speed-up of around 10^3 for a heterogeneous phantom, for a 2% relative uncertainty on the PG yield. The method agrees with a reference Monte Carlo simulation to within 1% at the level of 2% relative uncertainty on the PG. Preliminary work on a full simulation of a clinical spot-scanning treatment plan and a patient CT image indicates a similar gain factor. Gains per voxel range from 10^2 to 10^5.
Conclusion: We presented a generic PG yield estimator, drop-in usable with any geometry and beam configuration. We showed a gain of around three orders of magnitude compared to analog MC. With a large number of voxels and materials, memory consumption may be a concern and we will discuss the consequence and possible trade-offs. The method will be available in the next release of Gate.

Keywords: variance reduction, track length estimator, Monte Carlo simulation, clinical proton therapy, particle therapy, proton therapy, hadron therapy, vpgTLE

References:
[1] Knopf *et al.* (2015) Phys. Med. Biol.
[2] Kanawati *et al.* (2015) Phys. Med. Biol.
[3] Sterpin *et al.* (2015) Phys. Med. Biol.

107
Correlation of Gross Tumour Volume and metabolic Tumour Volume for non-small cell lung cancer patients
M.G. Jameson[1,3,4], A.J. Oar[1,2],M. Field[3,4] , I. Ho-Shon[5,6], P. Phan[1], D. Wang[5], J. Descallar[3,5], A. Pramana[8], S. Vinod[1,2,5], E. Koh[1,2,3], L.C. Holloway[1,3,4,5,7]
[1] Liverpool and Macarthur Cancer Therapy Centres, Sydney, Australia
[2] University of Western Sydney, Sydney, Australia
[3] Ingham Institute of Applied Medical Research, Liverpool Hospital, Sydney, Australia
[4] Institute of Medical Physics, School of Physics, University of Sydney, Sydney, Australia
[5] University of New South Wales, Sydney, Australia
[6] Department of Nuclear Medicine and PET, Liverpool Hospital, Sydney Australia
[7] Centre for Medical Radiation Physics, University of Wollongong, Wollongong, Australia
[8] St George Cancer Care Centre, Sydney, Australia

Metabolic Tumour Volume (MTV) is defined as the volume on FDG-PET/CT with increased FDG uptake. MTV has been shown to be of superior prognostic value compared to SUVmax in NSCLC. This study aims to explore the spatial overlap between CT-derived Gross Tumour Volume (GTV) and FDG-PET/CT derived MTV. The second aim was to investigate the impact of this overlap on progression-free survival (PFS) and overall survival (OS).
This was a single institution review performed in South Western Sydney, Australia. Inclusion criteria included proven NSCLC, stage I-III disease, radical radiotherapy and received PET imaging no more than 105 days before Tx. All FDG-PET

scans were from the mid-brain to proximal femora using a dedicated Philips Gemini GXL PET/CT scanner. If a patient underwent more than one FDG-PET/CT scan, the most recent available study was used for analysis. All FDG-PET/CT data was reviewed on OsiriX (version 5.1.2). All metabolically active disease regions on FDG-PET/CT studies were manually contoured by consensus between a nuclear medicine physician and a radiation oncologist. Spatial overlap between MTV and GTV was measured using the Dice similarity coefficient (DSC) which was calculated in Matlab with CERR and in house scripts. The value of a DSC ranges from 0, indicating no spatial overlap between two volumes in spaces, to 1, indicating complete spatial overlap. Other geometric descriptors were also calculated including volume, centre of mass and dimension. Univariate Cox regression was used to determine whether DSC was associated with OS and PFS.
Forty three patients were included in the study with a median age of 69 years (51-91). Median follow-up was 1.8 years (0.6-6.1) with 29 patiens experiencing relapse, there were 13 patients alive at the time of analysis and 30 deceased. The median value for the treated GTV volumes and the DSC was 77.4 (3.7-387.3) and 0.63 (0.18-0.86) respectively. The DSC was not found to be associated with PFS (p=0.85) or OS (p=0.70).

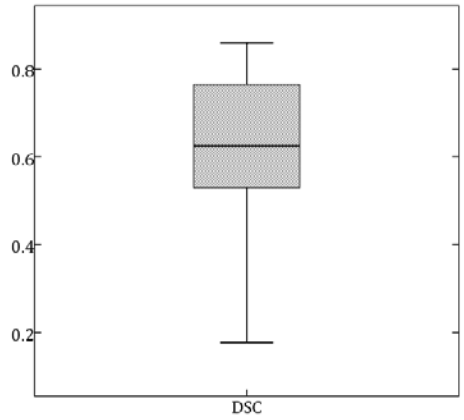

Figure 2 Boxplot displaying values of Dice similarity coefficient for MTV and GTV

Results in a small cohort show a moderate overlap between GTV and MTV, as represented by the DSC and that there is limited correlation between this and OS or PFS. Further investigation in a larger sample with modern treatment techniques (i.e. IMRT, VMAT and SBRT) will aid in clarifying the relationship, if any, between known clinical prognostic factors, novel metabolic parameters and the end-points of progression-free survival and overall survival.

Keywords: GTV, MTV, NSCLC

References:
[1] Deasy, Joseph O., Angel I. Blanco, and Vanessa H. Clark. "CERR: a computational environment for radiotherapy research." *Medical physics* 30.5 (2003): 979-985.
[2] El Naqa, Issam, et al. "Exploring feature-based approaches in PET images for predicting cancer treatment outcomes." *Pattern recognition* 42.6 (2009): 1162-1171.

108
Radiation induced DNA damage in human uveal melanoma cells.
K. Jasińska[1], K. Berniak[2] P. Olko[3], B. Romanowska-Dixon[4], K. Urbańska[1], J. Dobrucki[2], M. Elas[1]
[1] Department of Biophysics, Faculty of Biochemistry, Biophysics i Biotechnology, ul. Gronostajowa 7, Cracow, Poland
[2] Laboratory of Cell Biophysics, Faculty of Biochemistry, Biophysics i Biotechnology, ul. Gronostajowa 7, Cracow, Poland
[3] Institute of Nuclear Physics, PAS, Radzikowskiego 152, Kraków, Poland
[4] Department of Ophthalmology and Ophthalmic Oncology, Jagiellonian University Medical College, Kopernika 38, Kraków, Poland
e-mail: katarzyna.jasinska87@gmail.com

Purpose: Biological effects of proton beam irradiation, despite their wide clinical use, are not well understood. In recent years some differences in DNA repair mechanisms[1][2], angiogenesis and metastatic potential between proton beam and X-ray radiation were described[3,4].
Materials/methods: Mel270 human uveal melanoma cells, derived from primary tumor, were irradiated with 1 – 5 Gy of X ray (300 kVp Phillips, 1Gy/min) or proton beam (58 MeV) from Proteus C-235 cyclotron. Cells were analysed for survival using both rate of proliferation and clonogenic assay. DNA damage was evaluated after 4 and 8 hours using immunofluorescence staining of γ-H2AX, 53BP1 (for double strand breaks) and XRCC1 (for single strand breaks) and detection with confocal microscopy.
Results: Mel270 proliferation was slightly inhibited after 1 Gy, and strongly inhibited after 5 Gy. RBE value for Mel270 cells was determined. Staining of proteins showing DNA damage present several distinctive features.The foci of γ-H2AX were bigger than the others. Two kinds of foci could be distinguished:1) with high colocalization preference, below 1μm between foci; 2) random distribution, above 1μm between foci. The number of SSBs foci is higher at 4 than at 8 h after irradiation.
Conclusions: Low doses of proton beam irradiation and X rays damage DNA affecting the formation of foci indicating single and double strand breaks. The number of SSBs decreases with time.

Keywords: biology, melanoma, proton beam irradiation, DNA damage

References:
[1] Ugenskiene R, Prise K, Folkard M, Lekki J, Stachura Z, et al. (2009) Dose response and kinetics of foci disappearance following exposure to high- and low-LET ionizing radiation. Int J Radiat Biol 85: 872–882.
[2] Tommasino F, Durante M (2015) Proton Radiobiology. Cancers (Basel) 7: 353–381.
[3] Girdhani S, Sachs R, Hlatky L (2015) Biological effects of proton radiation: an update. Radiat Prot Dosimetry: 1–5.
[4] Girdhani S, Sachs R, Hlatky L (2013) Biological Effects of Proton Radiation: What We Know and Don't Know. Radiat Res 179: 1–16.

109
Production of and research on medical radioisotopes at the heavy ion laboratory, University of Warsaw
J. Jastrzębski[1], J. Choiński[1], A. Jakubowski[1], M. Sitarz[1,2], A. Stolarz[1], K. Szkliniarz[3], A. Trzcińska[1], W. Zipper[3]
[1] Heavy Ion Laboratory, University of Warsaw, Pasteura 5a, 02-093 Warszawa, Poland
[2] Faculty of Physics, University of Warsaw, Pasteura 5, 02-093 Warszawa, Poland
[3] Institute of Physics, Department of Nuclear Physics, University of Silesia, 40-007 Katowice, Poland
(jastj@slcj.uw.edu.pl)

Two charged particle accelerators are currently in operation at the Heavy Ion Laboratory, University of Warsaw (HIL UW): a K=160 isochronous cyclotron accelerating gaseous ions from He to Ar to energies from 2 to 10 MeV/nucleon and a high current medical p/d cyclotron, accelerating protons to an energy of 16 MeV and deuterons to an energy of 8 MeV. The alpha particle beam from the isochronous cyclotron and protons and deuterons from the medical cyclotron are currently used to produce research quantities of therapeutic and diagnostic radioisotopes. Occasionally, the C30 proton cyclotron at Świerk at National Centre for Nuclear Research is also employed.
The present research program includes the production of the Targeted Alpha Therapy isotope ^{211}At, the prospective PET radioisotopes ^{43}Sc,^{44}Sc and ^{44m}Sc and the positron generator

^{72}Se/^{72}As. An important research strand is also devoted to the alternative (in opposition to the classical reactor route via ^{99}Mo generator) accelerator production method of the most popular nuclear medicine radioisotope, ^{99m}Tc. The research on accelerator produced medical radioisotopes based on the HIL cyclotrons is conducted within a large collaboration, involving the Heavy Ion Laboratory, the University of Silesia, the Institute of Nuclear Chemistry and Technology (INCT), POLATOM at the National Centre for Nuclear Research, the Centre of Biological and Chemical Research of the University of Warsaw and the Institute of Nuclear Physics in Kraków. After target preparation and irradiation the properties of the produced radioisotopes are first investigated at HIL via gamma-ray spectroscopy techniques and subsequently transported to INCT or POLATOM for further chemical investigations. Table below shows some of the obtained results.

This research was supported by the Polish Founding Agency NCBiR grants ALTECH and SCANDPET. Discussion with and suggestions from Aleksander Bilewicz are greatly appreciated. Our thanks are also due to Jola Wojtkowska and Maciek Kisieliński for their help in the proton irradiations in Świerk.

Keywords: medical radioisotopes

TABLE I
Investigated radioisotopes

Isotope	Target	Energy [MeV]	TTY* [MBq/μAh]	Comment
^{211}At	^{209}Bi	α 29	37(6)	(a)
^{72}Se	$^{nat}GeO_2$	α 30	0.19(3)	(a)
^{72}As			2.7(1)	
^{43}Sc	$^{nat}CaCO_3$	α 20	84(4)	(b)
^{44gd}Sc	$^{42}CaCO_3$ (95.9%)	α 29	44(7)	(b)
^{44m}Sc			4.7(8)	
^{99m}Tc	^{100}Mo (99.815%)	p 16 p 25	372(25) 806(133)	-
^{99}Mo		p 16 p 25	2.4(6) 18(7)	-

* Thick Target Yield
(a) From K. Szkliniarz et al. Acta Phys. Pol. A127, 1471
(b) From K. Szkliniarz et al. submitted for publication

110
Comparison of the various paths of ^{44}Sc isomeric pair production

J. Jastrzębski[1], K. Szkliniarz[2], M. Sitarz[1,3], R.Walczak[4], A. Bilewicz[4], J. Choiński[1], A. Jakubowski[1], A. Majkowska[4] , A. Stolarz[1],
A. Trzcińska[1], W. Zipper[2]
[1] Heavy Ion laboratory, University of Warsaw, 02-093 Warszawa, Poland
[2] Institute of Physics, Department of Nuclear Physics, University of Silesia, 40- 007 Katowice, Poland
[3] Faculty of Physics, University of Warsaw, 02-093 Warszawa, Poland
[4] Institute of Nuclear Chemistry and Technology, 03-195 Warszawa, Poland
(jastj@slcj.uw.edu.pl)

The ^{44}Sc isomeric pair has attracted a lot of attention in recent years as a candidate for various applications in nuclear medicine [1-6]. Colloquially speaking, this pair can be considered as an "ARRONAX" isotope, with applications in Three Photon PET techniques already suggested in 2007[1], and the 58 h high spin (6+) isomeric state, decaying by 99% IT to the 4 h (2+) ground state, as an *in vivo* generator discussed recently in Refs [4-6]. This ground state undergoes in turn predominantly the β^+ decay to the 1157 keV excited state in ^{44}Ca. The previously investigated production of ^{44m}Sc using the deuteron beams is extended to alpha particle projectiles in the present work. It is well known that due to its larger mass and higher bombarding energy, the alpha particle transfers to the compound nucleus a larger angular momentum than lighter projectiles. Although the production efficiency (Thick Target Yield) of the high spin isomer is not much augmented with this projectile, the isomeric ratio is substantially increased (from 2.2% up to 10.9%, see table below) which should allow this isomer to be produced with a much lower contribution of the directly formed ground state decay; as discussed in previous references, this is very important for synthesis of the *in vivo* ^{44}Sc generator.

This research was supported by the Polish Funding Agency NCBiR grant SCANDPET.

Keywords:
medical radioisotopes

References:
[1] C. Grignon et al. *Nucl. Inst. Meth. in Phys. Res. A 571 (2007) 142*
[2] G.W. Severin et al. *Appl. Rad. Isot. 70 (2012) 1526*
[3] H.F. Valdovinos et al. *Appl. Rad. Isot. 95 (2015) 23*
[4] S. Huclier-Markai et al. *Nucl. Med. Biol. 41 (2014) e36*
[5] C. Alliot et al. *Nucl. Med. Biol. 42 (2015) 524*
[6] C. Duchemin et al. *Phys.Med. Biol. 60 (2015) 6647*

TABLE I
Thick Target Yield of ^{44gd}Sc ($^{42}CaCO_3$ or ^{41}KCl targets) and the ratio of TTY of ^{44m}Sc/^{44gd}Sc for p, d and α projectiles estimated from Refs. 2-5 and the present work.

Projectile	p	d	α	α	α
Projectile energy (MeV)	15.6	14.9	20	29	50
Target	^{44}Ca (98%)	^{44}Ca (96.9%)	^{41}K (95.4%)	^{42}Ca (95.9%)	^{42}Ca (95.9%)
TTY* ^{44gd}Sc (MBq/μAh)	630[a]	220	60(9)	44(7)	54[d]
TTY m/g % (exp)[b]	0.54	2.21	5.0(5)	10.9(1.4)	-
TTY m/g % (exp EXFOR)[c]	0.55	-	3.8	10.6	12.1
TTY m/g % (th)[d]	0.5	2.34	5.3	15.2	18.2

* Thick Target Yield
(a) Metallic target experimental data converted to $CaCO_3$
(b) From the thick target data
(c) From the experimental cross-sections and SRIM stopping powers
(d) Calculated using EMPIRE cross sections and SRIM stopping powers

111
Distributed learning: predictive models based on data from multiple hospitals without data leaving the hospital

A.T.C. Jochems[1], T.M. Deist[1,2], J. van Soest[1,2], M. Eble[3], P. Bulens[4], P. Coucke[5], W. Dries[6], P. Lambin[1,2], A. Dekker[1]
[1] Department of Radiation Oncology (Maastro Clinic), Dr. Tanslaan 12, Maastricht, The Netherlands
[2] GROW - School for Oncology and Developmental Biology, Maastricht University Medical Centre, Minderbroedersberg 4-6, Maastricht, The Netherlands
[3] Klinik für Strahlentherapie (University clinic Aachen), Pauwelsstraße 30, Aachen, Germany
[4] Department of Radiation Oncology (Jessa hospital), Stadsomvaart 11, Hasselt, The Netherlands
[5] Departement de Physique Medicale (CHU de Liège), Bâtiment B 35, Liège, Belgium
[6] Catharina-Hospital Eindhoven, Michelangelolaan 2, Eindhoven, The Netherlands

Purpose: Personalized medicine is greatly facilitated by predictive models. In order to successfully train predictive models, large volumes of patient data are required. These data are readily available from hospitals worldwide, however, sharing these data is hampered by ethical, political, administrative and legal boundaries. A method by which these boundaries can be circumvented is distributed learning. In a distributed learning approach, the model application is sent to each individual hospital that contains data. The model learns from the data at the hospital. Subsequently, the models are sent back from the hospitals to a central location. At the central location, the models are combined to form a model that has been trained on all data.
In this work, we show that it is possible to train a Bayesian network using distributed learning on data from multiple

hospitals. The model predicts dyspnea, which is a common side effect of radiotherapy treatment of lung cancer.
Materials/methods: Clinical data from 229 lung cancer patients, treated with curative intent with chemoradiation (CRT) or radiotherapy (RT) alone were collected and stored in 5 different medical institutes (123 patients at Maastro (Netherlands, Dutch), 24 at Jessa (Netherlands, Dutch), 34 at Liege (Belgium, Dutch and French) and 48 at Aachen (Germany, German)). None of the patients received stereotactic body radiotherapy. Patients were treated for their primary lung tumor and had not had another tumor in the 5 years before treatment.
A Bayesian network model was trained on these data. Structure learning was done using the PC-algorithm at each hospital[1]. Network structures were transmitted to the central location, and using a voting algorithm, the optimal network structure was determined. Conditional probability tables were learned using the EM-learning algorithm[2]. Performance of the model was compared for a structure that was learned from multiple hospitals against a structure that was learned locally. The models were trained on data from Aachen, Liege and Jessa and validated on the data at Maastro. Performance was assessed using the area under curve (AUC) of the receiver operator characteristic. ROCs were compared using a method described by DeLong et al [3].
Results: The network structure of the globally learned Bayesian network can be observed in figure 1. The model performed above chance level for making predictions (AUC = 0.69, 95% CI: 0.58-0.80). The model that used a structure originating from local learning also performed above chance level (AUC = 0.67, 95% CI: 0.55-0.79). The globally learned structure allows the Bayesian network to perform marginally better (AUC of 0.69 vs 0.67), however, this improvement is not significant (p = 0.69).
Conclusions: In this work we show that it is possible to train a Bayesian network in a distributed setting, making a big stride forward to enabling personalized medicine in radiotherapy.

Keywords: Dyspnea, Bayesian networks, Distributed learning

References:
[1] Spirtes P, Glymour CN, Scheines R. Causation, prediction, and search. MIT press 2000.
[2] Lauritzen SL. The EM algorithm for graphical association models with missing data. Comput Stat Data Anal 1995;19:191–201.
[3] DeLong ER, DeLong DM, Clarke-Pearson DL. Comparing the areas under two or more correlated receiver operating characteristic curves: a nonparametric approach. Biometrics 1988;44:837–45.

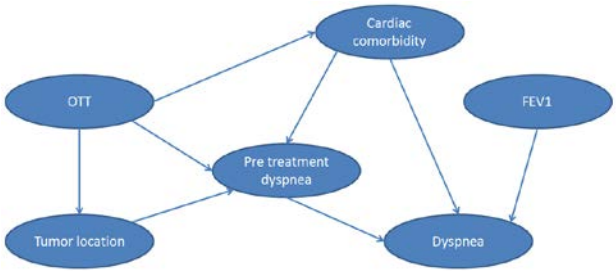

Figure 1: Network structure of the Bayesian network model. The Bayesian network uses, tumor location (right lower lobe, right middle lobe, right hilus, right upper lobe, left lower lobe, left upper lobe, left hilus, mediastinum), FEV1 (forced expiratory volume in 1 second, in %, adjusted for age and gender; measured prior to medication), pre-treatment dyspnea score (CTCAE grade < 2), baseline dyspnea score (CTCAE grade < 2), OTT (overall treatment time) and cardiac comorbidity (Non-hypertension cardiac disorder (at baseline)) to classify acute dyspnea.

112
RSI: A genomic signature of radiosensitivity
P. Johnstone[1], J. Scott[1,2], S. Eschrich[3], J. Torres-Roca[1]

[1] Radiation Oncology, Moffitt Cancer Center, Tampa, FL USA
[2] Integrated Mathematical Oncology, Moffitt Cancer Center, Tampa, FL, USA.
[3] Bioinformatics, Moffitt Cancer Center, Tampa, FL, USA.

Most cancer patients receive radiation therapy (RT) during their illness. Virtually all RT courses are based on techniques and fractionation schemes determined by trial and error, often decades ago. Thus there is a pressing and urgent need for a molecular diagnostic to inform personalized RT delivery. Our team developed a molecular fingerprint of tumor radiosensitivity (RSI), and has subjected it to extensive clinical and analytical validation (1-5). RSI score distribution across disease sites is consistent with their known clinical radio-responsiveness as defined by the surviving fraction after 2 Gy (SF2), and has been validated in 2,200 patients in 12 independent datasets across several disease sites. We have shown that RSI correlates with outcome only in patients treated with RT; it is not prognostic but predictive. The National Cancer Institute designed the Clinical Assay Development Program (CADP) to assist with the development of assays that may predict therapy response or prognostic behavior of a diagnosed cancer; RSI has undergone further development through CADP.
Using RSI and the linear quadratic model, our team next modeled the genomically adjusted dose (GAD) to predict RT dose effect at the individual patient level. RSI/GAD has predicted cancer cohorts that will specifically benefit from RT-dose escalation, such as radioresistant luminal lesions in breast cancer (6) and some glioblastomas (7). Current data have also revealed that metastatic lesions have markedly different RSI than the primary lesion, which is further modified by the site of metastasis (8).
We will discuss current knowledge of RSI/GAD and describe ongoing current research plans to incorporate RSI, as a predictive biomarker of radiosensitivity, into personalized therapy options for RT patients.

References:
[1] Eschrich S, Zhang H, Zhao H, Boulware D, Lee JH, Bloom G, Torres-Roca JF. Systems biology modeling of the radiation sensitivity network: a biomarker discovery platform. Int J Radiat Oncol Biol Phys 2009 Oct 1;75(2):497-505.
[2] Eschrich SA, Fulp WJ, Pawitan Y, Foekens JA, Smid M, Martens JW, Echevarria M, Kamath V, Lee JH, Harris EE, Bergh J, Torres-Roca JF. Validation of a radiosensitivity molecular signature in breast cancer. Clin Cancer Res 2012 Sep 15;18(18):5134-43.
[3] Eschrich SA, Pramana J, Zhang H, Zhao H, Boulware D, Lee JH, Bloom G, Rocha-Lima C, Kelley S, Calvin DP, Yeatman TJ, Begg AC, Torres-Roca JF. A gene expression model of intrinsic tumor radiosensitivity: prediction of response and prognosis after chemoradiation. Int J Radiat Oncol Biol Phys 2009 Oct 1;75(2):489-96.
[4] Torres Roca JF. A molecular assay of tumor radiosensitivity: a roadmap towards biology-based personalized medicine. Pers Med 2012;9(5):547-57.
[5] Torres-Roca JF, Eschrich S, Zhao H, Bloom G, Sung J, McCarthy S, Cantor AB, Scuto A, Li C, Zhang S, Jove R, Yeatman T. Prediction of Radiation Sensitivity Using a Gene Expression Classifier. Cancer Res 2005 August 15, 2005;65(16):7169-76.
[6] Torres-Roca JF, Fulp WJ, Caudell JJ, Servant N, Bollet MA, van de Vijver M, Naghavi AO, Harris EE, Eschrich SA. Integration of a Radiosensitivity Molecular Signature Into the Assessment of Local Recurrence Risk in Breast Cancer. Int J Radiat Oncol Biol Phys. 2015 Nov 1;93(3):631-8.
[7] Ahmed KA, Chinnaiyan P, Fulp WJ, Eschrich S, Torres-Roca JF, Caudell JJ. The radiosensitivity index predicts for overall survival in glioblastoma.Oncotarget. 2015 Oct 3
[8] Ahmed KA, Fulp WJ, Berglund AE, Hoffe SE, Dilling TJ, Eschrich SA, Shridhar R, Torres-Roca JF.Differences Between Colon Cancer Primaries and Metastases Using a Molecular Assay for Tumor Radiation Sensitivity Suggest Implications for Potential Oligometastatic SBRT Patient Selection. Int J Radiat Oncol Biol Phys. 2015 Jul 15;92(4):837-42

113

Further Development of Spinal Tissue Radiotherapy Re-treatment Modelling, with inclusion of Hadrontherapy.

J. Belmonte-Beitia[1], G. Fernandez Calvo[1], E. A. Gaffney[2], J. Hopewell[3], B. Jones[4], T. E. Woolley[2].
[1] Department of Mathematics, U. Castilla-La Mancha, Ciudad Real, Spain
[2] Wolfson Centre for Mathematical Biology, U. Oxford, UK
[3] Particle Therapy Cancer Research Institute and Green Templeton College, U. Oxford, UK
[4] Gray Laboratory, CRUK/MRC Oxford Institute for Radiation Oncology, U. Oxford, UK

Purpose: Radiotherapy retreatment (radical or palliative) is useful in selected patients. Two recent publications provided methods for estimating changes in spinal radio-tolerance with time between initial radiotherapy and retreatment, but with important limitations.
Materials and methods: A model was developed to find a temporal relationship between the percentages of the tolerance biological effective doses (%BED) for two treatment courses. The primate data of Ang et al (2010), isoeffective for a 10% incidence of myelitis, with re-treatment intervals of 1, 2 and 3 years provided the fitting parameters. As summarised in Jones and Hopewell (2014), rodent studies used shorter intervals (~ 6 months), spinal tissue recovery starts around 70 days after first treatment courses, and appears dose related (experiments showed little or no recovery six months after initial low dose treatments around 20-30% of %BED tolerance).
Thus recovery displays different time scales contingent on the initial dose. In the longer term, slow normal tissue turnover may allow recovery after low initial doses. This is consistent with lack of reported clinical experience of severe effects in low dose regions of the central nervous system, away from the primary target volume of the initial treatment, when compared with fully treated volumes at extended re-treatment times.
Results: The previous work is modified to incorporate the above processes to yield estimates for BED_2, the %tolerance BED after an elapsed time, t, and BED_1, the initial %tolerance BED dose. The Probit model is used to extrapolate from primate data to the clinical situation, where the incidence of myelitis is much lower.

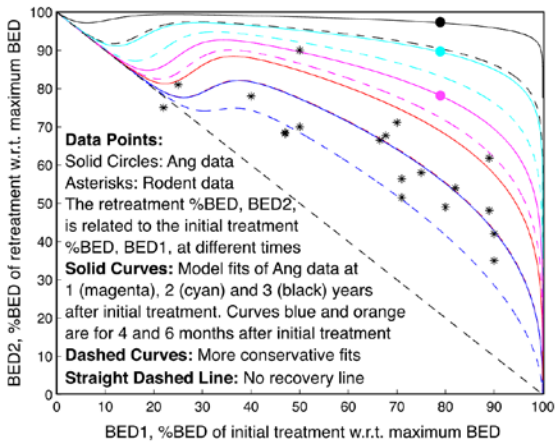

The fitted solid curves, with more conservative hatched curves, are presented in the Figure, with a superposition of both the primate (circles) and rodent data sets (asterisks), the latter isoeffective for a 50% incidence of myelitis. This is the best available quantitative model, though it must be used cautiously in humans where greater longevity and other causes for reduced spinal tolerance may concur. So, human doses should be below the curves shown.
A further challenge is to use RBE models to allocate the BEDs for charged hadron therapy (protons or ions), which may further spare normal tissues and be useful in re-treatments. Two examples are given in the table.

Table 1. Estimated proton and carbon ion retreatment doses per fraction (d) and total doses (TD) 2 years after previous photon dose of 54 Gy in 28 to cortical brain (tolerance 60 Gy in 30 fractions).

Number of fractions	Proton dose estimates (Gy)	Carbon ion estimates (Gy)
10	d = 3.17 TD = 31.7	d = 1.47 TD = 14.7
25	d = 1.70 TD = 42.5	d = 0.68 TD = 17
30	d = 1.48 TD = 44.4	d = 0.58 TD = 17.4

Assumptions: Available tolerance= 81.53% of tolerance BED at 2 years proton RBEmax=1.4, RBEmin=1.05; carbon ion RBEmax=5, RBEmin=1.5 CNS α/β=2 Gy.
The estimated maximum photon retreatment dose would be 54 Gy in 28 fractions. In clinical practice more cautious doses are advised.

Conclusions: The new model allows re-treatment dose estimation within the time window of 70 days to three years after the initial course, and can be adapted for hadrontherapy. It should be used cautiously in clinical practice by choosing doses lower than predicted.

References:
[1] Ang KK et al. 2001. Int J Radiat Oncol Biol Phys 50:1013–1020.
[2] Jones B, Hopewell JW. 2014. Int J Radiat Biol 90:731-741.

114

Measurement of Acoustic Emissions Generated by a Pulsed Proton Beam from a Hospital-Based Clinical Cyclotron

K. C. Jones[1], F. Vander Stappen[2], C. R. Bawiec[3], G. Janssens[2], P. A. Lewin[3], D. Prieels[2], T. D. Solberg[1], C. M. Sehgal[4], S. Avery[1]
[1] Department of Radiation Oncology, University of Pennsylvania, Philadelphia, Pennsylvania
[2] Ion Beam Applications SA, Louvain-la-Neuve, Belgium
[3] School of Biomedical Engineering, Drexel University, Philadelphia, Pennsylvania
[4] Department of Radiology, University of Pennsylvania, Philadelphia, Pennsylvania

Heating caused by pulsed proton beam energy deposition generates a thermoacoustic signal. Based on time-of-flight (TOF) calculations, the arrival time of the acoustic waves can be used to verify the range of the proton beam(1, 2). The goal of this work is to assess the clinical potential of the technique by experimentally measuring the acoustic signal generated by a proton beam from a hospital-based source and to measure the accuracy of the TOF range verification.
To create a short, intense pulsed proton beam in a hospital setting, an electronic function generator was used to modulate the IBA C230 isochronous cyclotron at the University of Pennsylvania's Roberts Proton Therapy Center. A submerged hydrophone measured the acoustic emissions generated by the proton beam in water. The acoustic measurements were repeated with variable proton current and increasing distance between detector and beam. To model the expected acoustic signal, simulations were performed and compared to experimental results.
The cyclotron produced proton spills with pulsewidths of 18 µs and a maximum measured instantaneous proton current of 790 nA. The collected acoustic signal was on the order of mPa, and the pressure amplitude increased monotonically with increasing proton current. Based on the observed relationship between detector distance and acoustic arrival time, the measured signal originated in the proton beam dose deposition volume. The acoustic frequency spectrum peaked at 10-20 kHz. At a single detector position, the arrival time can be measured with a standard deviation of 0.6 µs (1 mm). The difference between simulated and measured acoustic arrival times has a standard deviation of 0.9 µs (1.4 mm).
We report the first observation of acoustic emissions generated by a proton beam from a hospital-based clinical cyclotron. Based on the methods presented, acoustic-based techniques may provide <2 mm (standard deviation) accuracy in verification of proton range.

Keywords: Proton range verification, acoustics, time-of-flight

References:
[1] Jones KC, Witztum A, Sehgal CM, & Avery S (2014) Proton beam characterization by proton-induced acoustic emission: simulation studies. Physics in Medicine and Biology 59(21):6549-6563.
[2] Assmann W, et al. (2015) Ionoacoustic characterization of the proton Bragg peak with submillimeter accuracy. Medical Physics 42(2):567-574.

115
Water based 3D optical dose imaging for particle therapy
O. Kavatsyuk[1], M. J. van Goethem[1,2], A. A. van 't Veld[2], S. Brandenburg[1]
[1] KVI-CART, University of Groningen, Groningen, Netherlands
[2] Department of Radiation Oncology, UMCG, Groningen, Netherlands

Purpose: Scanned ion-beam delivery offers the highest conformation of target dose in external beam radiotherapy. However, fast and accurate patient-specific quality assurance is challenging. The current clinical standard for verification of dose distributions with a 2D array of ionization chambers (ICs) is slow and not very suitable for dose delivery using scanned ion-beams because the response of the ICs is not necessarily independent of beam size and position with respect to the IC.
At present, no suitable method for rapid verification of dose distributions for scanned ion-beam delivery is commercially available.

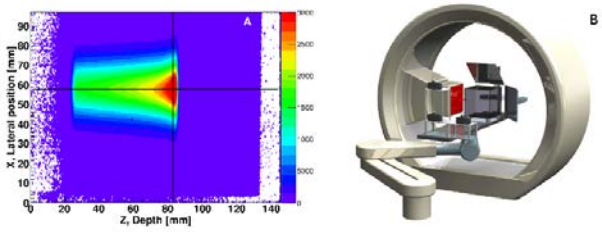

Figure 1. A. Imaging principle: raw 2D image measured with a 360 MeV ^{4}He-beam. B. Schematic drawing of the set-up with the proton gantry nozzle.

Materials/methods: We are developing a fast QA technique based on the UV light produced by swift ions in water (Fig.1A). Using fast, UV sensitive CCD cameras we measure the light distributions from which the dose distribution is reconstructed [2]. The system consist of a water tank in which ion beams are stopped and low noise, high sensitive CCD cameras (Fig.1B), which register the light distribution produced by each of the many subsequent ion beams that compose the treatment plan. Data can be taken in two modes: integral and differential (synchronized with beam delivery), thus allowing the detailed reconstruction of the contribution of each individual beam to the dose distribution.
Results: We have built a prototype optical dose imaging system to demonstrate the potential of this method for 3D dose scanning in clinical conditions (to verify actual treatment plans in particle therapy clinics). We demonstrated the feasibility of optical imaging of the full 3D dose distribution in water with a small (<1% by weight) admixture of a nontoxic , low-cost fluorescent emitting visible light. In experiments with 90 MeV proton beams approx. 50 photons/MeV were produced in the solution, allowing for high quality imaging. Bragg curves measured in pure water show a good agreement with those of an ionisation chamber, while those measured with the fluorescent show some concentration dependent quenching.
Conclusions: The presented novel method resolves the issues of the QA techniques currently used in particle therapy: it has high position resolution in three dimensions, features direct measurement in the reference material water, and is fast as the whole dose distribution is imaged in a single dose delivery.

Keywords: particle therapy, Quality Assurance, 3D dosimetry

References:
[1] B. Arjomandy et al., Med.Phys 37 (2010) 5831.
[2] Dutch Patent Application No. 2014012.

116
Low-dose-rate irradiation induces up-regulation of genes involved in suppression of cancer progression
H-S. Kim
Radiation Health Institute, Korea Hydro and Nuclear Power Co., Ltd., Seoul 132-703, Republic of Korea

Chronic low-dose rate irradiation has been shown to be beneficial in a variety of animal models including cancer. To assess the specific transcriptional changes that tumor-bearing mice would have manifested upon LDR in comparison with that of normal mice undergoing LDR irradiation, we investigated the expression of DNA repair and damage-associated genes in the thymus of naturally occurring tumor-bearing AKR/J and normal ICR mice following low-dose-rate (LDR, Cs-137, 0.7 mGy/h, a cumulative dose: 1.7 Gy) irradiation. Thymuses were collected at 100th day post irradiation and analyzed using whole-genome microarray, quantitative reverse transcription polymerase chain (qPCR), and western blot. The thymus weight was decreased and survival rate was increased in LDR irradiated AKR/J mice while no significant changes were found in normal ICR mice. qPCR analysis demonstrated Serpina1a, Mmp3, Gzmc, Neil2, Plxnc1, Rnd3, Cyp11a1, Ptgs2 were specially altered in LDR-irradiated AKR/J mice but not in ICR mice. By performing Western blot, we found that Plxnc1 and Rnd3, genes involved in suppression of melanoma progression, were upregulated while Cyp11a1, a gene contributes to tumor immune escape, was downregulated in LDR-irradiated AKR/J mice, but not ICR mice. These results suggest that LDR γ-radiation suppressed early stage of carcinogenesis and removed cancer cells from body by stimulating apoptosis and immune-mediated mechanisms. Therefore, LDR may offer significant benefit for the patients with solid cancer, which has traditionally been thought to be a relatively radiotherapy-resistant tumor.

Keywords: Low-dose-rate, Radiation, mice, cancer suppression, genes

References:
[1] Bong, J.J., Kang, Y.M., Shin, S.C., Choi, S.J., Lee, K.M., et al., (2013) Identification of radiation-sensitive expressed genes in the ICR and AKR/J mouse thymus. Cell Biol. Int. 37, 485-494.
[2] Bong, J.J., Kang, Y.M., Shin, S.C., Choi, S.J., Lee, K.M., et al. (2013) Differential expression of thymic DNA repair genes in low-dose-rate irradiated AKR/J mice. J. Vet. Sci. 14, 271-279.
[3] Shin, S.C., Kang, Y.M. and Kim, H.S. (2010) Life span and thymic lymphoma incidence in high- and low-dose-rate irradiated AKR/J mice and commonly expressed genes. Radiat. Res. 174, 341-346.
[4] Shin, S.C., Lee, K.M., Kang, Y.M., Kim, K.H., Lim, S.A., et al. (2011) Differential expression of immune-associated cancer regulatory genes in low- versus high-dose-rate irradiated AKR/J mice. Genomics 97, 358-363.

117
Fast dose modulation in proton therapy with continuous line scanning
G. Klimpki[1], S. Psoroulas[1], P. Fernandez[1], C. Bula[1], D.C. Weber[1,2], D. Meer[1], A. Lomax[1]
[1] Center for Proton Therapy, Paul Scherrer Institute, 5232 Villigen PSI, Switzerland
[2] University of Zurich, UniversityHospital, Rämistrasse 100, 8091 Zurich, Switzerland

Purpose: The accuracy of scanned proton therapy suffers from respiratory or cardiac motion during irradiation: The discrete scan pattern can interfere with the induced motion of the target yielding regions of over- and underdosage [1]. Applying the same field multiple times with proportionally reduced dose – commonly referred to as rescanning – can help averaging out such interferences [2]. However, dead

times in delivery accumulate with increasing number of rescans for all discrete scanning techniques, especially for spot scanning. Thus, efficient rescanning requires fast lateral scanning; yet the flexibility to deliver highly modulated fields must be preserved. For this purpose, we pursue the implementation of a novel delivery technique, in which we scan the beam continuously along straight lines while quickly modulating the scan speed and/or beam current to shape the dose profile [3].

Method: Our Gantry 2 beamline provides the necessary prerequisites for this technique: (a) the extracted cyclotron current can be adjusted in less than 1 ms [4] and (b) the proton beam can be scanned with up to 2 cm/ms in lateral direction [5]. Thus, the frequency of speed and current modulation along a line can be remarkably high, which allows us to deliver both uniform and highly modulated fields. To do so, we divide each iso-energy layer in parallel lines and each of those lines in small segments (sub-mm resolution). The planned dose profile defines the scan speed and beam current of each segment. Since delivery accuracy strongly depends on the stability of the beam current, we installed a feedback system, in which the current measured in the gantry nozzle controls the output of the cyclotron in real-time.

Results: We found that scan speed modulation is favorable over beam current modulation for two reasons: (1) accuracy – we can control the scanner magnets with higher precision and shorter response time than the extracted cyclotron current – and (2) efficiency – scanning lines with a high current minimizes the overall beam-on time. Thus, the beam current is set to its maximum and lowered only in regions, where pure speed modulation fails to decrease the delivered dose sufficiently. This preserves full flexibility on dose modulation. We verified this approach by comparing highly modulated dose profiles delivered with both spot and line scanning (*cf.* figure 1). While the lateral penumbra of the line scan is slightly worse (less than + 0.1 mm on both sides), its delivery time is 20% smaller. We expect the reduction in delivery time to be even larger when rescanning multiple times.

Conclusion: Line scanning is a fast scanning technique that offers the possibility to deliver arbitrary dose distributions by quickly modulating the scan speed and beam current. Thus, we consider line scanning a well-suited technique to realize efficient and accurate rescanning of moving tumors.

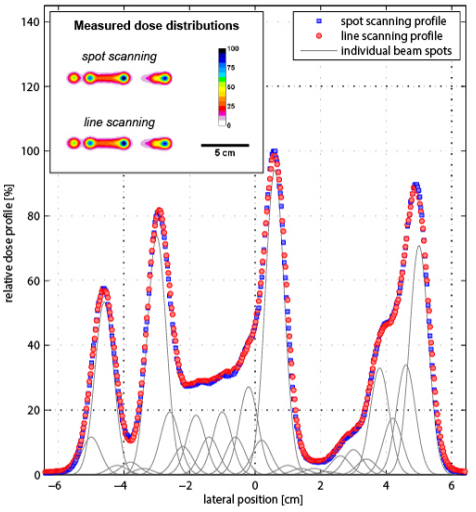

Figure 1: Comparison of a highly modulated dose distribution painted with spot and line scanning. The spot scanning profile (blue squares) was delivered by superimposing 26 individual beam spots (grey curves) with weights between 10^8 and 10^8 protons/spot. The line scanning profile (red circles) was delivered by modulating the scan speed only. The enclosed graphic shows the corresponding lateral dose distributions.

Keywords: organ motion, rescanning, dose delivery

References:

[1] Phillips et al., *Phys. Med. Biol.* 37(1) (1992). DOI: 10.1088/0031-9155/37/1/016
[2] Knopf et al., *Phys. Med. Biol.* 56(22) (2011). DOI: 10.1088/0031-9155/56/22/016
[3] Schätti et al., *Phys. Med. Biol.* 59(19) (2014). DOI: 10.1088/0031-9155/59/19/5707
[4] Schippers et al., *Proceedings of the 19th International Conference on Cyclotrons and their Applications* (2010).
[5] Pedroni et al., *Eur. Phys. J. Plus* 126(66) (2011). DOI: 10.1140/epjp/i2011-11066-0

118

Criteria of spot asymmetry in proton radiotherapy pencil beam scanning – a Monte Carlo study

M. Kłodowska[1], J. Gajewski[1], K. Skowrońska[1], P. Olko[1]
[1]Institute of Nuclear Physics Polish Academy of Sciences, Radzikowskiego 152, PL 31-342 Kraków, Poland

Cancer treatment in hadron therapy facilities equipped with pencil beam scanning (PBS) is based on delivering each energy layer, spot by spot in the plane perpendicular to the beam axis. Uniform and robust treatment plan depends on the correct values defining horizontal and vertical spot size (*i.e.* σ_x, σ_y) introduced to the Treatment Planning System (TPS) like Eclipse (Varian). In TPS these values are, however, assumed to be constant for a given layer, moreover the influence of the spot rotation on the spot dimensions is not taken into account (Fig.). The purpose of this study was to propose criteria of spot asymmetry within which target dose conformity is preserved.

In the Eclipse for Proton TPS a conformal field of 3 x 3 x 3 cm^3 was planned to cover the whole target volume with at least 95% dose. A dedicated tool was developed to convert the treatment plan into the simulation input file. Simulations were performed with FLUKA transport code [1,2] with uncertainty level kept below 1%, by using computational PL-Grid Infrastructure.

Dedicated beam model for proton scanning beam in the gantry-1 room at the Bronowice Cyclotron Centre (IFJ Kraków) was used. Preserving the 2D Gaussian spot shape (volume integral) and spot weight, spot σ up to 50% and spot rotation up to 45° were investigated. 1D and 2D analysis of dose distribution was carried out.

For asymmetrical spots field width differences were observed together with larger lateral penumbra (the factor of 1.5 obtained for maximal spot asymmetry), which resulted in target volume decrease [3]. Perturbed field flatness did not exceed the accepted level of 5% difference. By spot rotation implemented to all spots whole target region skewness was observed.

The tool for treatment plan conversion into a Monte Carlo input file has been created to consider spot deformation indistinct to the TPS dose calculation. Observed field dose non-uniformity may be the origin of hot and cold spots inside and outside the target volume. Considered spot asymmetry criteria allow to preserve optimal target dose distribution with regard to the spot size changes. As such spot deformation can differ for different gantry angles, accurate gantry-angle-dependent spot shape measurements with 2D detectors such as films or 2D foils are considered.

Spot sizes are obtained from the horizontal and vertical profiles, not taking into account the influence of the spot rotation by the angle α, resulting in different spot sigma values (here $\sigma_{x'}$, $\sigma_{y'}$).

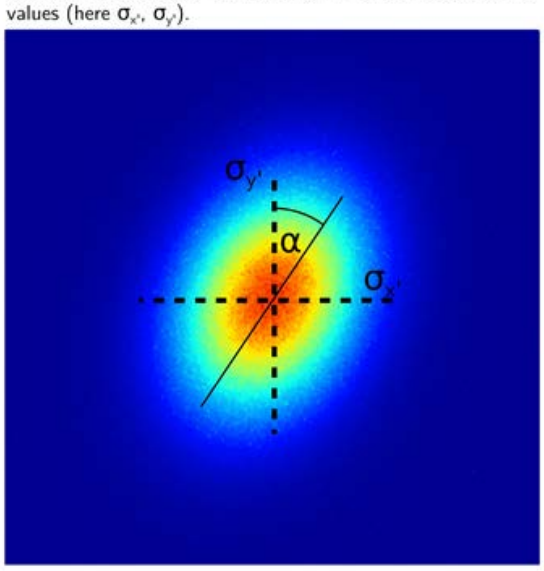

Keywords: proton radiotherapy, spot asymmetry, Monte Carlo

References:
[1] V. Bohlen, *et al.*, Nuclear Data Sheets 120, 211-214 (2014)
[2] A. Ferrari, *et al.*, CERN-2005-10, INFN/TC_05/11, SLAC-R-773 (2005)
[3] K. Parodi, *et al.*, Phys. Med. Biol. 55 (2010) 5169–5187

119

^{191}Os – revival of an out-of-favor radionuclide?

U. Köster[1], B. Lee[2],
[1] Institut Laue-Langevin, Grenoble, France
[2] Australian National University, Canberra, Australia

Purpose: Novel osmium anticancer drugs are under evaluation that promise superior properties with respect to traditional Pt based drugs [1]. Even selective action against cancer stem cells has been reported [2]. Radiotracer and nuclear medicine techniques could help in the development and application of these drugs. ^{191}Os is an osmium radioisotope well suited for this purpose with excellent properties for imaging and therapy. We discuss calculated Auger electron spectra, production methods and prospects of applications of ^{191}Os.

Methods: ^{191}Os ($T_{1/2}$=15.4 d) decays to short-lived ($T_{1/2}$=4.9 s) ^{191m}Ir that emits 129 keV γ rays (26.5% intensity) well suited for SPECT imaging. In the past ^{191}Os/^{191m}Ir generators [3] were used to provide ^{191m}Ir for first pass radionuclide angiocardiography [4] or studies of renal blood flow [5], but no direct use of ^{191}Os has been reported so far. Among all known β-emitters with days to weeks half-life ^{191}Os sticks up with the lowest β decay energy of only 38 keV on average (114 keV maximum), corresponding to a range of about one cell diameter. This β radiation is supplemented by abundant emission of short-range conversion and Auger electrons (< 60 keV). Consequently ^{191}Os has also potential as therapeutic isotope. The Auger electron spectrum of this decay was calculated using the methodology described in Ref. [6].

Results: The figure shows the calculated electron energy spectrum in the β^- decay of ^{191}Os (red, left scale) and in the internal transition decay of ^{191m}Ir (blue and yellow, right scale).

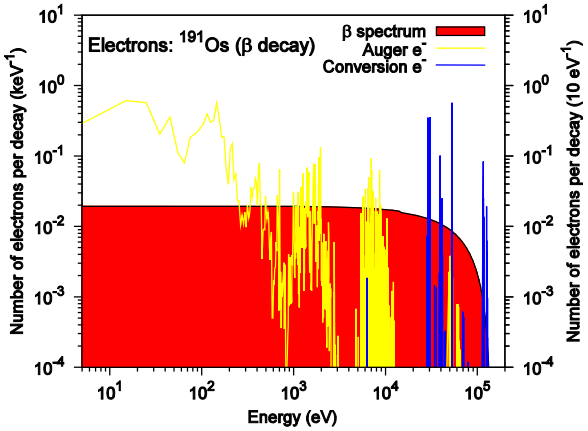

Upon β^- decay of ^{191}Os the nuclear recoil of ^{191m}Ir is <0.4 eV, thus avoiding breakage of chemical bonds and uncontrolled translocation of ^{191m}Ir, provided the chemical valency change is tolerated.

Direct production by ^{190}Os(n,γ)^{191}Os in a high thermal neutron flux of $1.5{\cdot}10^{15}$ n.cm^{-2}s^{-1} in ILL's high flux reactor [7] reaches specific activities of ≈10 GBq/mg (≈2 MBq/μmol) after 5 days of irradiation.

For Os drug dosages similar to cisplatin dosage this specific activity is by far sufficient for preclinical and clinical SPECT imaging. Even shorter irradiation times can be used to minimize co-produced activities (^{192}Ir, etc.).

Conclusions: Reactor-produced ^{191}Os has great potential as radiotracer for in vitro studies of sub-cellular distribution of Os based drugs, for preclinical and clinical in vivo studies of pharmacokinetics of Os based drugs and eventually even for combined radionuclide-chemotherapy against particularly resistant tumors.

Keywords: osmium-based chemotherapy drugs, SPECT, Auger emitter

References:
[1] M Hanif et al. Drug Discov Today 2014;19:1640.
[2] K Suntharalingam et al. J Am Chem Soc 2014;136:14413.
[3] C Brihaye et al. J Nucl Med 1986;27:380.
[4] PR Franken et al. J Nucl Med 1989;30:1025.
[5] S Treves et al. Eur J Nucl Med 1999;26:489.
[6] B Lee et al. Comp Math Meth Med 2012;651475.
[7] U Köster et al. Radiother Oncol 2012;102:S170.

120

A dose response analysis of the patients treated with Boron Neutron Capture Therapy (BNCT) in Finland in 1999 to 2011

H. Koivunoro[1,2,3], S. González[4,5], L. Provenzano[4,5], G. Santa Cruz[4], L. Kankaanranta[3] S. Savolainen[1,2] and H. Joensuu[3]
[1] HUS Helsinki Medical Imaging Center, Helsinki University Hospital, Finland
[2] Department of Physics, University of Helsinki, POB 64, FI-00014, Finland
[3] Comprehensive Cancer Center, Helsinki University Hospital, and Department of Oncology, University of Helsinki, Helsinki, Finland
[4] Comisión Nacional de Energía Atómica (CNEA), Argentina
[5] Consejo de Investigaciones Científicas y Técnicas (CONICET), Argentina

In 1999 to 2011, 249 cancer patients received boronophenylalanine (BPA)-mediated boron neutron capture therapy (BNCT) in Finland. Over one hundred of these patients were treated within the context of clinical trials. The purpose of the trials was to investigate the efficacy and safety of BNCT in the treatment of malignant gliomas (newly diagnosed or gliomas that progressed after surgery and radiotherapy) [1,2], and inoperable head-and-neck cancers that had recurred locally after external radiotherapy [3,4].

In BNCT, the absorbed radiation dose results from four main components: 1) the therapeutically desired high-LET

radiation dose from the $^{10}B(n,\alpha)^{7}Li$ reaction, 2) the intermediate-LET proton dose released from the $^{14}N(n,p)^{14}C$ reaction in tissue, 3) the intermediate-LET protons released from the $^{1}H(n,n')p$ reaction in tissue, and 4) the low-LET *photon dose* mainly from the $^{1}H(n,\gamma)$ reaction in tissue, but in part also from minor photon contamination in the neutron beam.

Conventionally, the biologically effective "photon radiotherapy equivalent" dose has been derived from multiplying each dose component by a constant relative biological effectiveness (RBE) factor, or in the case of the boron dose, the compound biological effectiveness (CBE) factor. The estimations for the RBE and the CBE are obtained from cell culture studies and irradiation with photons, BNCT beam alone, and the beam in the presence of the boron compound [5]. The RBE and CBE factors are applied as fixed, although they depend on the cumulative irradiation time and the dose rate, and, ideally, they should be derived for each irradiation component individually. Furthermore, the radiation dose components have synergistic effects. The conventional fixed RBE-based dose calculation in BNCT tends to lead to unrealistically high estimated tumor doses, which may not be reflected in clinical outcomes and may not be comparable with photon irradiation data.

Recently, an alternative method for calculating the effective dose was proposed [6]. The photon-isoeffective dose calculation formalism takes into account the dose rate and the cumulative dose per fraction in a modified linear-quadratic model, and it also considers the synergistic interactions between different radiation components. The isoeffective dose calculation formalism predicted the response of melanoma lesions to BNCT better than the fixed RBE approach.

In this study the tumor doses calculated with the RBE model and using the photon-isoeffective formalism are correlated with the clinical responses of the patients treated with BNCT in Finland. For glioma patients, the doses are compared with the overall survival time, whereas for patients with head-and-neck cancer, tumor responses are evaluated. The BNCT dose response rates are compared with those obtained with conventional radiotherapy and responses reported in similar patient groups.

Keywords: BNCT, neutron, dosimetry, glioma, head and neck cancer

References:

[1] H. Joensuu et al. J. Neurooncol. 62, 2003
[2] Kankaanranta et al. Radiother Oncol. 80, 2011
[3] Kankaanranta et al. Radiother Oncol. 69, 2007
[4] Kankaanranta et al. Radiother Oncol. 82, 2012
[5] Coderre et al. IJROBP 27, 1993
[6] González and Santa Cruz, Rad Res. 178, 2012

121

Human Sphingolipid Biomarkers of Single Dose Radiotherapy: A Clinical trial

R. Kolesnick
Sloan-Kettering Institute
NYC, NY USA

Single dose radiotherapy (SDRT), facilitated by image guidance and intensity modulation technologies that improve precision in tumor targeting to reduce risk of normal tissue toxicity, has revolutionized cancer treatment with local control rates ≥90%, even in tumors resistant to conventional fractionation. While classic radiobiology focuses on response of tumor cells rather than non-tumor microenvironmental cells, initial pre-clinical studies in our lab found disruption of tumor vasculature obligate for SDRT cure. This endothelial cell dysfunction results from activation of acid sphingomyelinase (ASMase), converting sphingomyelin to the second messenger ceramide in endothelial plasma membranes, events inhibitable by VEGF-121 or VEGF-165. Conversely, precisely timed delivery of anti-angiogenic agents, such as anti-VEGFR2 Ab DC101 (Imclone), de-represses ASMase activity, synergistically increasing SDRT-induced ceramide elevation, enhancing endothelial dysfunction. That ceramide is critical for anti-angiogenic radiosensitization is evidenced by □n□-ceramide Ab inhibition of DC101-enhanced endothelial damage and radiosensitization. These results translate *in vivo*, as anti-VEGFR2 DC101 or anti-VEGF G6-31 (Genentech) synergistically increase SDRT-induced endothelial injury in numerous solid tumor types, only if delivery timed to maximally enhance ASMase signaling. In contrast, tumors in *asmase*$^{-/-}$ mice, which provide damage-resistant vasculature, are radioresistant and unaffected by either anti-angiogenic agent. This presentation will review fundamentals of this "New Biology" and present unpublished data that define mechanism of coupling of ceramide-driven endothelial dysfunction to DNA repair in tumor cells.

122

Targeted Treatment for the Non- Small Cell Lung Cancer

R. Komaki
Department of Radiation Oncology
University of Texas MD Anderson Cancer Center
rkomaki@mdanderson.org

Lung cancer is the leading cause of cancer-related death in the United States and throughout the world. Although overall mortality rates from lung cancer in the United States have dropped from 85% two decades ago to 70% in 2015, tumor control and survival outcomes after standard therapy are still poor.

Early detection involving the use of low-dose spiral computed tomography (CT) among former or current smokers led to a 20% reduction in the rate of lung-cancer death in these individuals. Early stage lung cancer can be cured in some patients by stereotactic body radiation therapy SBRT). Advancement of sophisticated radiation treatment equipment and understanding physics of utilization of the equipment for SBRT rapidly became clinical application for the primary lung or hepatic lesions as well as or other metastatic lesions. Because of high dose per fraction, technical aspects and quality assurance to deliver the radiation to the tumor precisely and avoid high dose of radiation to the critical surrounding normal tissue are critical issues for SBRT.

To understand tumor motion and control tumor motion have been major challenge for mainly lung lesions. To visualize hepatic lesion or other metastatic lesions e.g pancreas or soft tissue can be difficult without contrast enhancement or fiducial markers. The most challenging part of SBRT in addition to controlling tumor motion is lesions to be treated by this technique close to the critical organs e.g. blood vessels, brachial plexus, esophagus, major air way etc.

Technologic advancements of imaging and radiotherapy to conform the gross target volume(GTV) with tighter margins but adequate clinical targeted volume (CTV) and planning tumor volume (PTV) considering daily set up variations which are supposed to minimize the dose to nearby normal tissues. Thus the technical advancement such as intensity modulated radiotherapy (IMRT) compared to 2 or 3 dimensional radiotherapy improved outcomes among patients with locally advanced lung cancer, as has the addition of concurrent chemotherapy to radiation therapy. Further improvements are expected from the use of charged particle therapy with protons or other particles; randomized comparisons of proton therapy vs. intensity-modulated photon radiation therapy for lung cancer are underway in the United States.

Approximately 50% of Non-Small Cell Lung Cancer patients have Adenocarcinoma Histology.

Among the patients with Adenocarcinoma of Lung, 50% of them have genetic mutation. If they have ALK, EGFR, K-Ras or B-Raf mutation, we can target the mutated genes.

For many years, immunomodulation or immunotherapy as a means of cancer therapy has been studied. Cancer cells are well known to have the ability to bypass immune surveillance through a variety of different mechanisms, including reduced expression of tumor antigens, downregulation of major histocompatibility complex (MHC) class I and II molecules for tumor antigen presentation, secretion of immunosuppressive cytokines such as tumor growth factor-beta (TGF-ß), recruitment or induction of immunosuppressive cells such as

T-regulator cells or myeloid-derived suppressor cells, and overexpression of certain ligands (e.g., programmed death ligand-1 [PDL-1]) that inhibit the host's existing antitumor immunity. The latter effect is thought to take place by the cancer cells' overexpressing ligands that can bind inhibitory co-receptors expressed by T lymphocytes (also known as "immune checkpoints"). Recent advances in melanoma research have led to the development of immunotherapies that have substantial antitumor effects in other types of cancer as well, including lymphoma, renal cell carcinoma, and non-small lung cancer (NSCLC). These advances have been paradigm-shifting for several reasons. For example, the observed immune response patterns have led to marked deep tumor regression that often outlasted the period of study. Such responses are unprecedented for disease that has been refractory to other types of treatment. Second, these new forms of immunotherapy have shown activity in tumors traditionally viewed as unresponsive to immune therapies, raising hopes that any type of cancer might be "targetable" by immunotherapies if the right agent can be found. This antitumor activity has been most impressive in NSCLC, particularly among patients with unresectable disease treated with primary radiation therapy, a modality known to stimulate antigen production. It is conceivable that treatment such as this acts as a type of "in situ vaccine" to prime the immune response. Nascent preclinical and early clinical findings have supported this possibility, suggesting that radiation, through its immune-stimulating properties, may eventually be useful as a form of systemic therapy in addition to a means of local tumor control.

123

Prompt Gamma-ray Timing experiment during different modalities of proton beam delivery

T. Kormoll[1] , A. Duplicy[2], W. Enghardt[1], C. Golnik[1], R. Loeschner[2], J. Petzoldt[1], T. Werner[1] and G. Pausch[1]
[1] OncoRay – National Center for Radiation Research in Oncology, Dresden, Germany
[2] IBA Proton Therapy, Ottignies-Louvain-la-Neuve, Belgium

Purpose: Prompt Gamma-ray Timing (PGT) is a method for range verification in hadron therapy which requires only minor or no interference with clinical routine due to a very low hardware footprint. The principal feasibility of the method for range verification has already been shown in theoretical considerations [1] and in proof-of-pricipal experiments [2]. Further considerations of the clinical feasibility show that a high-throughput data acquisition system is crucial [3]. In this work, PGT measurements during phantom irradiation with clinical beam currents – both during pencil beam scanning (PBS) and passive beam formation (double scattering, DS) are presented.
Materials and Methods: By exploiting the time structure of the beam on the nanosecond scale, it is possible to measure the duration of the emission of secondary photons. This duration is linked with the transit time of the projectiles in the target. Longer transit times reflect a larger range. Since no direct start signal is available, a classical time-of-flight measurement against the accelerator RF is used. Experiments were conducted at the University Proton Therapy Dresden (UPTD) center where an IBA Cyclone 230 isochronous cyclotron is installed with a fixed RF frequency of 106 MHz. For actual clinical application, it is required that the bunch width and phase remain constant or are monitored. The shown data do not incorporate any kind of bunch timing correction and the conditions are assumed to be constant.
As a photon detector, a $CeBr_3$ crystal in the extends of ø2"×1" coupled to a PMT is used. It is either read out with a CAEN DT5730 waveform digitizer or with a Target Systemelektronik U100 dedicated system which is also a sampling ADC based readout module. Online pulse processing algorithms are applied in both cases to achieve a high throughput rate. The ADCs were synchronized to the RF.
Experiments during DS were conducted parasitically during the workflow training with an anthropomorphic phantom. For the PBS measurements dedicated beam time could be scheduled at the therapeutic treatment room. A rectangular dose distribution was impinged on a homogeneous PMMA target. In DS mode, a lead shielding was placed between the detector and the nozzle in order to reduce background radiation which originates from the nozzle.
Results: In both cases, it was possible to identify the individual phases of beam delivery. In DS mode, the periodic modulation at 600 Hz which is synchronized with the beam formation equipment can be seen. In PBS, single layers and single spots can be recognized (figure 1). After data selection, the beam microstructure is revealed in PBS as well as in DS mode although it is considerably less clear in the DS case.
Conclusions: The experimental techniques which are required for a clinical implementation of PGT are being evaluated under clinical beam conditions. The beam delivery mode has major impact on the data quality.

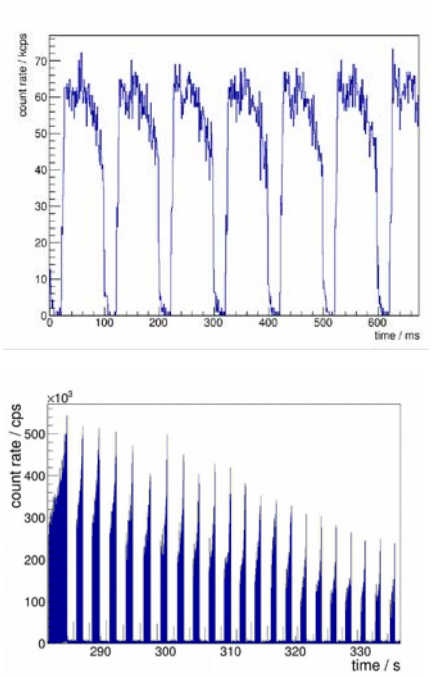

Figure 1: Count rate over time during DS (left) and PBS (right), recorded at 2 Gy/min at different distances.

Keywords: Prompt Gamma-ray Timing, Range Verification, Hadron Therapy

References:
[1] C. Golnik et al. "Range assessment in particle therapy based on prompt γ-ray timing measurements." Physics in Medicine and Biology 59 (2014): 5399.
[2] F. Hueso-González et al. "First test of the prompt gamma ray timing method with heterogeneous targets at a clinical proton therapy facility." Physics in Medicine and Biology 60 (2015): 6247.
[3] G. Pausch et al. "Scintillator-Based High-Throughput Fast Timing Spectroscopy for Real-Time Range Verification in Particle Therapy", SCINT Proceedings, 2015.
[4] T. Kormoll et al. "Prompt Gamma Timing Range Verification for Scattered Proton Beams", ANIMMA Conference Record, 2015.

124

Proton Beams for Physics Experiments at OncoRay

S. Helmbrecht[1], F. Fiedler[1], M. Meyer[1], P. Kaever[1] and T. Kormoll[2]

[1]Helmholtz-Zentrum Dresden-Rossendorf, Dresden, Germany
[2]OncoRay – National Center for Radiation Research in Oncology, Dresden, Germany

Purpose: At the OncoRay center in Dresden at proton therapy facility is in operation. The first patient was treated in December 2014. The system is driven by an IBA (IBA Proton Therapy, Louvain-la-Neuve, Belgium) Cyclone 230 isochronous cyclotron with a maximum proton energy of 230 MeV. Patients are treated in one room equipped with a 360° rotating gantry. Besides patient treatment a strong focus is on research. A dedicated experimental room is part of the facility. In the current state of expansion this room is equipped with a fixed beam line. Beam energies between 70 and 230 MeV and currents up to about 120 nA at 230 MeV can be provided.
Materials and Methods: An in house developed control system (figure 1) allows for a parallel operation of the treatment and the experimental beamline. Absolute priority for the treatment room is ensured by the control software.
The beam current is controlled by a dedicated hardware directly. Continuous wave beams as well as pulsed beams with repetition rates up to 333 Hz with variable duty cycles are available. The beam is monitored by means of a segmented ionization chamber. The beam can be activated manually, for a defined time or until a certain charge has been reached at the beam exit. A direct continuance after a beam switch to the treatment room is possible.
Results: The proton therapy system itself is operated by an IBA team, that ensures excellent beam stability and availability. Since only one treatment room is present, experiments can be performed conveniently during the day shifts. Requests from the treatment room cause interruptions of 1-2 min duration in intervals of about 20 min.
Conclusions: In summary, the OncoRay center is equipped with an experimental beamline that combines the reliability and beam quality of a commercial clinical proton therapy system with the flexibility of an in house developed control system whose design parameters are governed by the needs of physical and translational research.

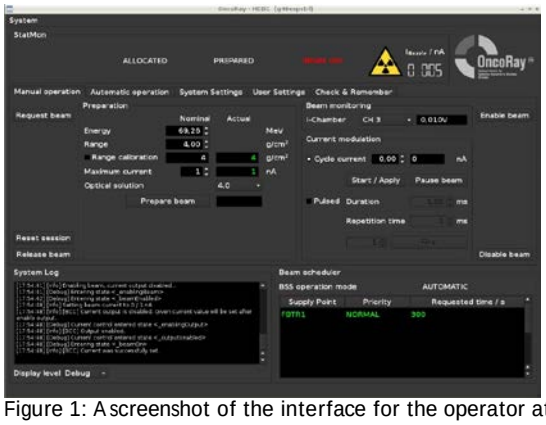

Figure 1: A screenshot of the interface for the operator at the control room for the experimental area.

Keywords: Cyclotron, hadron therapy, radiation research

125
Nanoparticle Enhanced MRI-Guided Radiation Therapy: Final proof of concept before phase I trial.

S. Kotb[1], F. lux[1], Claire-Rodriguez-Lafrasse[2], O. Tillement[1], L. Sancey[1].
[1] Institut Lumière Matière, UMR5306, Université Claude Bernard Lyon1-CNRS, 69622 Villeurbanne Cedex, France.
[2] Laboratoire de Radiobiologie Cellularie et Moléculaire, EMR3738, Faculté de Médecine Lyon-Sud, Université Lyon 1, Oullins, France.

Purpose: Radiation therapy is currently prescribed to more than 60 % of cancer patients[1]. However, effective treatment is often limited by tumor visualization and collateral damage of healthy tissues. One possibility to overcome this problem, besides using a local approach such as stereotactic radiosurgery, is combining radiation with nanoparticles containing high-Z elements which are known to boost locally the efficacy of radiation exposure during cancer therapy. In this context, we developed gadolinium-based nanoparticles named AGuIX (Activation-Guided Irradiation by X-ray) for MRI-guided radiotherapy.
Material and methods: (AGuIX) nanoparticles were obtained as previously described[2]. We performed *in vitro* radiosensitization clonogenic assay with 220kVp X-ray at doses ranging from 0 to 6 Gy on B16F10 mouse melanoma cell line, in addition to cell uptake characterization using TEM and confocal microscopy. *In vivo*, B16F10 mouse melanoma cells were orthotopically grafted into mouse brains to mimic human melanoma brain metastases. After intravenous injection of 10 μmol of (AGuIX) into mice bearing B16F10, MR and intravital two photon microscopy imaging were performed to determine the maximum tumor uptake, and tumor vs. healthy tissue ratio before radiation therapy. Similar to the clinical workflow, an image guided cone-beam CT (CBCT) was performed prior to irradiation exposure to calculate the delivered dose during whole brain radiotherapy (WBRT) to the brain, the metastases and other organs at risk.
Results: Radiosensitization shows a significant effect ($P<0.05$) when the (AGuIX) are combined with 220 kVp X-rays exposure *in vitro*. The percentage enhancement factor at 2 Gy (%EF 2 Gy) was 60 % compared with that for radiation alone, with a significant increase in DNA double strand breaks ($P<0.01$). *In vivo* the (AGuIX) nanoparticles accumulate passively in brain tumors; such phenomenon has previously been reported in brain-tumor bearing animals[3]. After radiation exposure, the increase in life spans (ILS) compared to control group was 8.3% for the animals that were only irradiated and increased to 25% with pre-injection of (AGuIX) nanoparticles; such increase corresponds to 15.4% compared to irradiated animals ($P=0.0025$). Histological observation of the brains indicated the presence of large metastases for the control and irradiated only group compared to the group treated by the combination of irradiation with nanoparticles[4,5].
Conclusion: (AGuIX) nanoparticles are not only potential radiosensitizing agent, but it also acts as positive contrast agent for MRI, which allows accurate delineation of the tumor region instead of using conventional CT. Regulatory toxicity investigations demonstrated the absence of any side effects, even at repeated injections. A clinical trial phase I on patients with multiple brain metastases will be launched in France winter 2016.

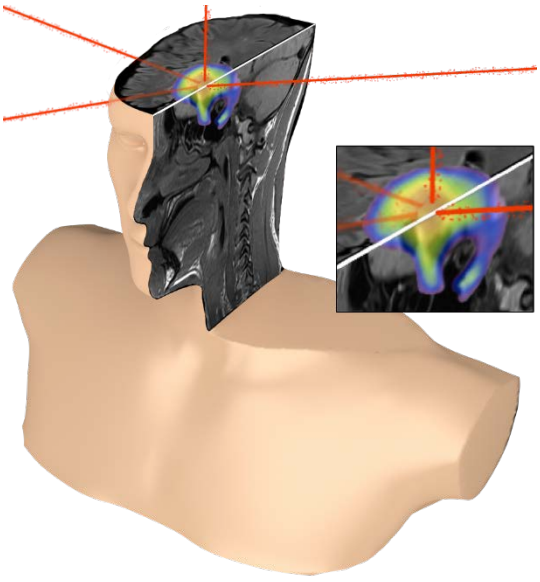
Fig. 1. Guided and enhanced radiotherapy with (AGuIX) nanoparticles.

Keywords: AGuIX nanoparticles, imaged-guided radiotherapy, radiosensitization.

References:
[1] Siegel RL, Amos RA, Jemal A. Cancer Statistics, 2015. CA Cancer Jan 1;65(1)5-29.
[2] Lux F, Mignot A, Mowat P, et al. Ultrasmall rigid particles as multimodal probes for medical applications. Angewandte chemie 50(51) :12299-12303.
[3] Sancey L, Lux F, Kotb S, et al. The use of theranostic gadolinium-based nanoprobes to improve radiotherapy efficacy. Br J Radiol.2014.
[4] Sancey L & Kotb S, Truillet C, et al. Long-term in vivo clearance of gadolinium-based AGuIX nanoparticles and their biocompatibility after systemic injection. ACS Nano. 2015 Mar 24;9(3):2477-88.
[5] Kotb S, Detappe A, Lux F, et al. Gadolinium-based nanoparticles and radiation therapy for multiple brain melanoma metastases: proof of concept before phase I trial. Theranostics (under consideration).

126

Development of the Flair tool for FLUKA Treatment Planning Verification

W. Kozłowska[1,2], T. Böhlen[3], A. Ferrari[1], D. Georg[2,4], A. Mairani[5,6] , P. Sala[1,7], V. Vlachoudis[1]
[1] CERN, Geneva, Switzerland
[2] M Department of Radiation Oncology, Division of Medical Radiation Physics Medical University of Vienna, Vienna, Austria
[3] EBG MedAustron GmbH, Wiener Neustadt, Austria
[4] Christian Doppler Laboratory for Medical Radation Research, Medical University of Vienna/AKH Vienna, Austria
[5] CNAO, Pavia, Italy
[6] HIT Heidelberg, Germany
[7] INFN Sezione di Milano, Milan, Italy

Outcome of radiation therapy depends on accurate, robust and verified calculations of the planned dose. Monte Carlo (MC) is considered as the gold standard for dosimetric calculations, however its popularity in a clinical environment is still limited. One of the reasons is the typically complex procedure of setting the patient models and beam parameters. The focus of physical models development in the FLUKA [1][2] MC code, since many years, is put on the medical area, making it an ideal tool applicable for the nuclear medicine and hadron-therapy simulations. It is already used in the clinical environment in HIT and CNAO for generating Treatment Planning System (TPS) databases and offline treatment verification. The aim of this work is to present the recent improvements of FLUKA and its Graphical User Interface - Flair [3] providing a fully-functional and easy-to-use tool for quality assurance (QA) of treatment plans for protons, carbon and other light ion species.
In this study we present the most recent developments, based on several re-calculations of complete proton/ion treatment plans from different TPS and facilities using Flair and FLUKA. FLUKA recently was enhanced with the RBE estimator and dedicated PET, prompt-gamma and charged particles scoring for beam range verification. To better utilize these advantages, Flair facilitates the application of the treatment scheme into the simulation procedure. It is able to import the CT DICOM images creating the voxel-phantom geometries based on parameterization according to Schneider et al[4]. Flair allows importing the entire treatment scheme directly from the RT DICOM files, such as RTSTRUCT, RTDOSE and RTPLAN. To better comply with the real irradiation settings, Flair incorporates also the basis characteristics of the beam delivery system with the minimal effort from the user point of view.
Several comparisons were made between the TPS and the FLUKA simulation scheme. The DVH plots for the PTV/OAR shows good agreement for the presented cases; some dose deposition differences in various tissues are noticeable, especially in the end of the ranges of the beam particles. FLUKA physical models were thoroughly validated, hence, quantification and identification of the discrepancies, especially taking into consideration more complex cases – like patients/organs with the more heterogeneous structures, may bring a great value for the treatment quality. Additional, independent re-calculation is always an asset, and usage of FLUKA and its efficient graphical user interface Flair, can enhance the popularity of the MC in the clinical environment for both research and QA purposes.
The presented results will be used for further work on the tool development, assuring the quality of the treatment plans and providing the user with the guidelines for the treatment plan optimization.

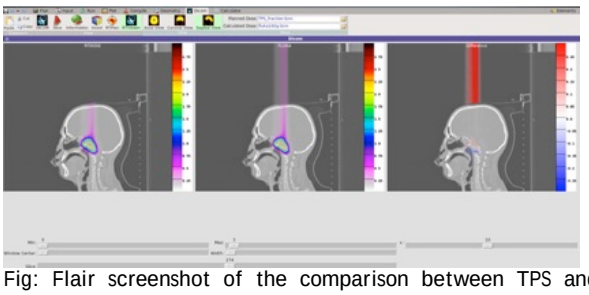

Fig: Flair screenshot of the comparison between TPS and FLUKA simulations

Keywords:
Treatment Planning System, Quality Assurance, FLUKA

References:
[1] Böhlen, T. T., Cerutti, F., Chin, M. P. W., Fassò, A., Ferrari, A., Ortega, P. G., Mairani, A., Sala, P. R.,Smirnov, G., Vlachoudis, V. (2014). *The FLUKA Code: Developments and challenges for high energy and medical applications*. Nuclear Data Sheets, 120, 211-214
[2] Ferrari, A., Sala, P. R., Fasso, A., & Ranft, J. (2005). *FLUKA: A Multi-Particle Transport Code*. CERN 2005-10 (2005), INFN/TC_05/11, SLAC-R-773
[3] Vlachoudis, V. (2009). *FLAIR: A Powerful But User Friendly Graphical Interface For FLUKA*. Proc. Int. Conf. on Mathematics, Computational Methods & Reactor Physics (M&C 2009), Saratoga Springs, New York
[4] Schneider W., Bortfeld T., Schlegel W. (2000). *Correlation between CT numbers and tissue parameters needed for Monte Carlo simulations of clinical dose distributions.* Physics in Medicine and Biology, 45(2), 459-78

127

Improved patient-specific optimization of the stopping power calibration for proton therapy planning using a single optimized proton radiography

N. Krah[1], M. Testa[2,3,4], I. Rinaldi[4]
[1] Heidelberg Collaboratory for Image Processing, Heidelberg University, Speyerer Str. 6, 69115 Heidelberg, Germany
[2] Department of Radiation Oncology, Massachusetts General Hospital, Boston, USA
[3] Department of Radiation Convergence Engineering, Yonsei University, Wonju, South-Korea
[4] Lyon 1 University and CNRS/IN2P3, UMR 5822, 69622 Villeurbanne, France

Purpose: We present an improved method to calculate patient-specific calibration curves to convert X-ray computed tomography (CT) Hounsfield Unit (HU) to relative stopping powers (RSP) for proton therapy treatment planning. We introduce also an optimization method to improve the spatial resolution and the water equivalent thickness (WET) accuracy of proton radiographies [1].
Materials/Methods: By optimizing the HU-RSP calibration curve, the difference between a proton radiographic image and a digitally reconstructed X-ray radiography (DRR) is minimized. The feasibility of this approach has previously been demonstrated [2,3]. This scenario assumes that all discrepancies between proton radiography and DRR originate from uncertainties in the HU-RSP curve. In reality, external factors cause imperfections in the proton radiography, such as misalignment compared to the DRR and unfaithful representation of geometric structures (“blurring”). We

analyze these effects based on synthetic datasets of anthropomorphic phantoms and suggest an extended optimization scheme which explicitly accounts for these effects. Performance of the method is been tested for various simulated irradiation parameters.
We also investigate the use of a special optimization method to enhance the spatial resolution and the WET accuracy of proton radiographies prior to the HU-RSP re-calibration. The optimization method is designed for imaging systems measuring only the residual range of protons without relying on tracker detectors to determine the beam trajectory before and after the target.
The ultimate purpose of the optimization is to minimize uncertainties in the HU-RSP calibration curve. We therefore suggest and perform a thorough statistical treatment to quantify the accuracy of the optimized HU-RSP curve.
Results: We demonstrate that without extending the optimization scheme, spatial blurring (equivalent to FWHM=3mm convolution) in the proton radiographies can cause up to 10% deviation between the optimized and the ground truth HU-RSP calibration curve. Instead, results obtained with our extended method reach 1% or better correspondence, as shown in Figure 1. We have further calculated gamma index maps for different acceptance levels. With DTA=0.5mm and RD=0.5%, a passing ratio of 100% is obtained with the extended method, while an optimization neglecting effects of spatial blurring only reach ~90%.
Conclusions: Our contribution underlines the potential of a single optimized proton radiography to generate a patient-specific calibration curve and to improve dose delivery by optimizing the HU-RSP calibration curve as long as all sources of systematic incongruence are properly modeled.

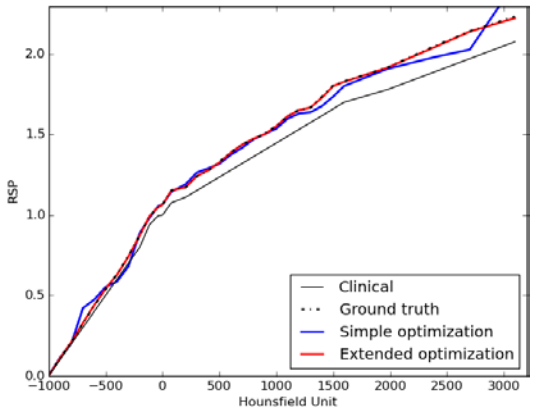

Figure 1: Comparison of optimized conversion curves.

Keywords: proton therapy, proton radiography, image processing

References:
[1] Krah, N. et al. 2015, *An advanced image processing method to improve the spatial resolution of ion radiographies,* Physics in medicine and biology, 60(21), pp.8525–8547
[2] U. Schneider et al. 2005, *Patient specific optimization of the relation between CT-Hounsfield units and proton stopping power with proton radiography,* Med Phys 32 195
[3] P. J. Doolan et al. 2015, *Patient-specific stopping power calibration for proton therapy planning based on single-detector proton radiography,* PMB 60 1901

128
Overcoming Cancer Radioresistance
Factors of radioresistance in prostate cancer
M. Krause[1,2,3,4], A. Dubrovska[1,2,3], M. Baumann[1,2,3,4]
[1] German Cancer Consortium (DKZK) Dresden and German Cancer Research Center (DKFZ) Heidelberg
[2] Dept. of Radiation Oncology, Faculty of medicine and University Hospital C.G. Carus, Technische Universität Dresden
[3] OncoRay – National Center for Radiation Research in Oncology (NCRO), Faculty of medicine and University Hospital C.G. Carus, Technische Universität Dresden and [4]Helmholtz-Zentrum Dresden – Rossendorf

Prostate Cancer is one of the leading cancer entities in men, however. In this disease, radiotherapy leads to comparable cure rates compared to surgery. Overall, survival and cure rates of patients with prostate cancer are on average much higher than in many other cancers. Despite this fact, biological individualization of treatment is also an important research topic in this disease. Specifically in the field of personalized radiation oncology important research questions include: 1) pre-treatment identification of patient subgroups with individually very radioresistant tumours that would have a high risk of recurrence after standard radiotherapy alone. 2) pre-treatment identification of subgroups that have a high chance of tumour cure after radiotherapy alone 3) identification of subgroups with a high risk of distant metastasis after local treatment
Definition of biomarkers to identify such patient subgroups need to consider biochemical failure, local recurrences and distant metastases. Biomarkers will in future help to individualize radiation dose, but also combined radiation and systemic treatments. All endpoints need to be compared with surgical patient groups, with the mid-term aim to find decision parameters between the two treatment approaches. The talk will give an overview over current candidate biomarkers in preclinical and translational research.

Keywords: prostate cancer, radiotherapy, personalized treatment, biomarker

129
Front-end electronics and hit position reconstruction methods for the J-PET scanner
W. Krzemień[1*], D. Alfs[2], T. Bednarski[2], P. Białas[2], E. Czerwiński[2], A. Gajos[2],
B. Głowacz[2], M. Gorgol[3], B. Jasińska[3], D. Kamińska[2], Ł. Kapłon[2,4], G. Korcyl[2],
P. Kowalski[5], T. Kozik[2], E. Kubicz[2], M. Mohammed[2], Sz. Niedźwiecki[2],
M. Pałka[2], L. Raczyński[5], Z. Rudy[2], O. Rundel[2], N. G. Sharma[2],M. Silarski[2],
A. Słomski[2], A. Strzelecki[2], A. Wieczorek[2,4], W. Wiślicki[5], B. Zgardzińska[3],
M. Zieliński[2], P. Moskal[2]
[1]High Energy Physics Division, National Centre for Nuclear Research,
A. Soltana 7, 05-400 Otwock-Świerk, Poland
[2]Faculty of Physics, Astronomy and Applied Computer Science,
Jagiellonian University, S.Łojasiewicza 11, 30-348 Kraków, Poland
[3] Department of Nuclear Methods, Institute of Physics, Maria Curie Sklodowska University, Pl. M. Curie-Skłodowskiej 1, 20-031 Lublin, Poland
[4]Institute of Metallurgy and Materials Science of Polish Academy of Sciences, W. Reymonta 25, 30-059 Kraków, Poland
[5]Świerk Computing Centre, National Centre for Nuclear Research, A. Soltana 7, 05-400 Otwock-Świerk, Poland
email: wojciech.krzemien@ncbj.gov.pl
tel:+48 22 5532265
fax:+48 22 5532265

Purpose: The J-PET collaboration is developing a novel TOF-PET, whole-body tomography scanner based on polymer scintillators [1-4]. The scanner barrel is made of long scintillators, axially positioned, which are readout from both sides by photomultipiers. This novel approach relies mainly on the timing of the signals instead of their amplitudes for the reconstruction of the Lines-of-Response, therefore a very precise time resolution is one of the main challenges of the project.
Material and methods: For this purpose, novel ultrafast front-end electronics (FFE) allowing for sampling in the voltage domain of the signals with a duration of few nanosecond was developed [5]. The FEE solution is a purely digital implementation, based solely on a FPGA (Field Programmable

Gate Array) device and few satellite discrete electronic components. An additional advantage of the FPGA solution is a very low cost. At present, in the prototype phase, one sample together with digitization costs only about 10 Euro.
Results: The proposed solution provides very good time measurement properties, allowing to probe the signal in the voltage domain with an accuracy below 20 ps (σ) [5]. The input signals are amplified and split into four paths, each having an individual threshold level. This multi-level threshold technique is well suited for the application of reconstruction methods of the hit position of gamma quanta in the scintillator, which results in the improvement of the TOF resolution. We developed several hit reconstruction methods, e.g. compressive sensing technique allows for the recovery of the full signal shape and amplitude based on the samples registered in the PMTs. This information can be used to improve the precision of the hit position reconstruction [6]. Other methods are based on the comparison of detector signals with results stored in a library of synchronized model signals registered for a set of well-defined positions of scintillation points. The hit position is reconstructed as the one corresponding to the signal from the library, which is more similar to the measurement signal. A degree of similarity between measured and model signals is defined as the distance between points representing the measurement- and model-signal in a multidimensional measurement space [7] or as the Mahalonobis distance[8].
In this talk, the developed front-end electronics will be described. Also, the application of the multi-threshold measurement to the hit reconstruction methods will be presented.

Keywords: PET, FEE, hit reconstruction methods

References:
[1] P. Moskal el al. Radiotheraphy and Oncology 110, S69 (2014)
[2] P. Moskal el al. Nuclear Medicine Review 15, C68 (2012)
[3] P. Moskal, Patent granted in 2014, N. EP2454612B1, WO2011008119, 1 EP2454611, WO2011008118
[4] P. Moskal el al. Nucl. Instr. and Meth. A 764 (2014) 317-321
[5] M. Pałka el al. Bio-Alg. and Med-Systems Vol. 10, 1,(2014) 41-45
[6] L. Raczyński el al. Nucl. Instr. And Meth. A 786 (2015) 105-112
[7] P. Moskal el al. Nucl. Instr. and Meth. A 775 (2015) 54-62
[8] P. Moskal el al Acta Phys. Pol A127 (2015) 1495-1499

130
Utilizing CBCT data for dose calculation in adaptive IMPT
C. Kurz[1,2], F. Kamp[1], Y.K. Park[3], B.A. Winey[3], G.C. Sharp[3], S. Rit[4], D. Hansen[5], M. Reiner[1], R. Nijhuis[1], U. Ganswindt[1], C. Thieke[1], C. Belka[1], K. Parodi[2], G. Landry[2]
[1] Department of Radiation Oncology, Ludwig-Maximilians-University, Munich, Germany
[2] Department of Medical Physics, Ludwig-Maximilians-University, Munich, Germany
[3] Department of Radiation Oncology, Massachusetts General Hospital, Boston MA, USA
[4] Université de Lyon, CREATIS, CNRS UMR5220, Inserm U1044, INSA-Lyon, Université Lyon 1, Lyon, France
[5] Department of Oncology, Aarhus University Hospital, Aarhus, Denmark

Purpose: In intensity modulated proton therapy (IMPT), inter-fractional anatomical changes can substantially compromise the treatment quality for cranial and pelvic lesions [1,2], motivating treatment adaptation. The increasing availability of in-room cone beam computed tomography (CBCT) in proton centers enables frequent acquisition of 3D imaging data which may be used for dose calculation and plan adaptation. This work investigates and compares two complementary approaches for correcting CBCT image intensity for dose calculation in adaptive IMPT for head and neck (H&N) and prostate cancer. For H&N patients a mid-treatment replanning CT was used for validating the correction methods.

Material and methods**:** CBCT images and corresponding projections of 3 H&N and 3 prostate cancer patients were used in this study. In the first approach, a so-called virtual CT (vCT) was generated by deformable image registration (DIR) of the corresponding planning CT to the pre-treatment CBCT [3]. In the second approach, the vCT was used as prior for scatter correction of the raw CBCT projections, following the approach of Park *et al.*[4] Reconstruction of the corrected projections yielded a corrected CBCT image ($CBCT_{cor}$). Both approaches were evaluated for CT number accuracy using phantom scans and compared by means of beam eye view 2D range maps of single field uniform dose (SFUD) plans in all patients. For prostate cases, the geometric accuracy of target and OAR structures was also evaluated qualitatively.
Results: For H&N cases, no considerable differences between SFUD dose calculations on vCT and $CBCT_{cor}$ were found, with 97.3% to 99.8% of the 2D range maps showing a range difference below 3 mm (Table 1). Median range differences compared to a diagnostic quality replanning CT acquired within 3 days of the CBCT were below 0.5 mm. For prostate cases, an even higher agreement of SFUD beam ranges between vCT and $CBCT_{cor}$ was observed (Table 1). However, the analysis also showed that the DIR-based vCT approach exhibits inaccuracies in the pelvic region due to the very low soft-tissue contrast in the CBCT. The $CBCT_{cor}$ approach yielded results closer to the original CBCT (Figure 1), promising an improved accuracy in delineation. In general, the $CBCT_{cor}$ approach was not affected by inaccuracies of the DIR used during the generation of the vCT prior. An enhanced agreement of bowel filling with respect to the original CBCT image was observed on the $CBCT_{cor}$.
Conclusions: A DIR-based CBCT intensity correction has been compared to a scatter correction method on basis of the CBCT projections. Both techniques yield 3D CBCT images with intensities equivalent to diagnostic CT and appear to be suitable for dose calculation in adaptive IMPT. For H&N cases, no considerable differences between the two techniques were found, while improved results of the $CBCT_{cor}$ were observed for pelvic cases due to the reduced sensitivity to registration inaccuracies. A detailed quantification based on delineation accuracy using vCT and $CBCT_{cor}$ is under way.

Keywords: IMPT, Adaptive Radiotherapy, CBCT imaging

Acknowledgements: BMBF (01IB13001, SPARTA); DFG (MAP)

Patient	SFUD angle	RD < 3mm (%)	RD < 2mm (%)	Median RD (mm)	IPR RD (mm)
PatHN1	315°	99.7	98.9	0.1	1.1
PatHN2	0°	97.3	91.3	0.1	2.2
PatHN3	270°	99.8	99.2	0.3	1.1
PatPR1	0°	100.0	100.0	0.0	0.6
	270°	100.0	100.0	0.2	0.5
PatPR2	0°	99.8	99.8	0.2	0.7
	270°	100.0	100.0	0.0	0.9
PatPR3	0°	100.0	100.0	-0.3	0.7
	90°	100.0	100.0	-0.1	0.4

Table 1: SFUD BEV range comparison of vCT and $CBCT_{cor}$ for the investigated H&N (PatHN1-3) and prostate (PatPR1-3) patients. The percentage of 2D range maps with a range difference (RD) below 3mm and 2mm is given together with the median range difference and half the 2.5% to 97.5% inter-percentile range (IPR). The SFUD angle is given according to the IEC scale.

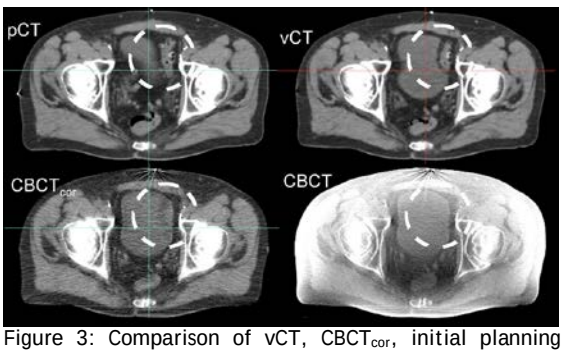

Figure 3: Comparison of vCT, $CBCT_{cor}$, initial planning CT (pCT) and the original CBCT of PatPR3, using the same window for displaying. The original CBCT shows inaccurate

CT numbers, thus demonstrating the need for CBCT corrections as investigated in this work. The DIR inaccurately matches the outline of the bladder (see dashed circle), leading to a wrong anatomy in the vCT. In contrast, the $CBCT_{cor}$ bladder anatomy agrees well with the original CBCT.

References:
[1] Barker JL et al, Quantification of volumetric and geometric changes occurring during fractionated radiotherapy for head-and-neck cancer using an integrated CT/linear accelerator system, 2004, IJROBP 59
[2] Zhang X et al, Effect of anatomic motion on proton therapy dose distributions in prostate cancer treatment, 2007, IJROBP, 67
[3] Landry G et al, Investigating CT to CBCT image registration for head and neck proton therapy as a tool for daily dose recalculation, 2015, Med. Phys. 42
[4] Park YK et al, Proton dose calculation on scatter-corrected CBCT image: Feasibility study for adaptive proton therapy, 2015, Med. Phys. 42

131

MRI for external beam radiotherapy guidance

J.J.W. Lagendijk, B.W. Raaymakers, M. van Vulpen
Department of Radiotherapy, Centre for Image Sciences, UMC Utrecht, The Netherlands

Its excellent soft tissue contrast makes MRI extremely well suited for guidance of external beam radiotherapy.
In recent years, using cone beam CT-linac radiotherapy systems, great success has been realized in the minimal invasive treatment of prostate tumours, stereotactic ablative body radiotherapy of lung tumours and stereotactic treatment of tumours of the brain. For these tumours, there is good visualization of the tumour itself or there is a good visualization of tumour related structures or fiducial markers. There is a clear trend towards better targeting with less normal tissue involvement and thus less toxicity, less surgery and less fractionation. However, for most other tumour locations the limited visualization using cone beam CT and the lack of dynamic information hinders this development. On-line and real-time MRI guidance may offer the possibility to implemented this stereotactic revolution for most remaining tumour locations like radiotherapy of tumours of the rectum, oesophagus, pancreas, kidney, individual lymph nodes, etc. This may provide a breakthrough in the application of radiotherapy and redefine the relation radiotherapy and surgery.
Essential is the availability of high quality MRI (e.g.1.5T Philips Ingenia) during the actual treatment process. The design of the experimental UMCUtrecht/Elekta MRI-Linac combination has been described in Lagendijk et al. [2008] and Raaymakers et al. (2009). The MRI accelerator facilitates good soft tissue visualization and continuous patient anatomy updates regarding translations, rotations and deformations of targets and organs at risk. Accounting for this, demands high speed, online intensity-modulated radiotherapy re-optimization. The MRI must supply real-time information about the actual position of the tumour and organs at risk and the on-line treatment planning must be able to deal with this. Dedicated sequences and correction protocols are being developed to guarantee extreme fast and geometrically correct MR imaging. Essential is that the complete 3D anatomy can be followed in real-time. Treatment planning procedures are being developed which can optimize the dose delivered on the actual anatomy.
The radiation dose is being delivered with the patient in a 1.5T magnetic field. The actual dose deposition, beam characteristics and absolute dosimetry must be evaluated for this magnetic field environment.
The clinical introduction of the MRL system is being organized within an international consortium. Within this consortium structure imaging protocols are being optimizes, 'blue sky' approached are being discussed for several tumour groups and the actual clinical trials are being designed.

Keywords:
MRI, on-line, adaptive

References:
Lagendijk JJW et al. Radiother Oncol. 2008; 86(1), 25-9
Raaymakers BW et al. Phys Med Biol. 2009; 54(12), N229-37

132

Current status of particle therapy in the Netherlands

J.A. Langendijk

In 2009, the Health Council of Ministry of Health published the Horizon Scanning Report Proton Radiotherapy, which paved the way for the clinical introduction of proton therapy in the Netherlands. In this report, four categories of indications were identified, including: standard indications (e.g. pediatric patients), prevention of secondary tumors in young patients with favorable prognosis (e.g. Hodgkin lymphoma), potential indications (i.e. dose escalation without enhancing toxicity) and the model-based indications (i.e. prevention of side effects). The model-based indications are the largest group of indications. In this category, patients will only be selected for proton therapy after an individual planning comparison and if the difference in dose translates in a minimal difference in NTCP (ΔNTCP). This model-based approach has been recognized by the Health Insurance Board as well, which means that patients selected for proton therapy according to this approach will receive reimbursement for their treatment.
In addition to this, the Ministry of Health, together with the proton therapy initiatives launched a national plan for proton therapy, which includes the realization of four small to medium sized proton therapy centers, with a geographic distribution over the country that foresees optimal accessibility of proton therapy for all eligible patients in the Netherlands. The maximum capacity to be created is 2,200 patients per year, divided among these four centers. These centers are now under construction.
Consensus has been reached on a national level regarding the threshold for ΔNTCP to be selected for proton therapy. More detailed indication protocols are now developed coordinated by the National Proton Therapy Platform, in which all radiotherapy departments are represented.
In addition, the four initiatives closely collaborate to create a national prospective data registry program to create a rapid learning health care system which can be used to develop and externally validate NTCP-models and to validate the added value of proton therapy to reduce radiation-induced side effects.
In this way, the Netherlands is one of the first countries worldwide that will realize a well balanced national plan for proton therapy in which this new technology will be integrated in a multicenter clinical research environment.

133

Quantitative Theranostics in Nuclear Medicine

M. Lassmann[1]
[1] Department of Nuclear Medicine, University of Würzburg, Germany

Purpose: In 2005, the word "theranostics" was used for the first time for describing the use of imaging for therapy planning in radiation oncology. It is defined as the use of individual patient-level biological information in choosing the optimal therapy for that individual [1]. In Nuclear Medicine this term describes the use of short-lived tracers for predicting the absorbed doses in molecular radiotherapy and, thus, safety and efficacy of a treatment.
Materials/Methods: For pre-therapeutic dosimetry for the purpose of dose-planning or for post-therapeutic dose verification, quantitative imaging of the biokinetics of the administered radiolabelled substance is necessary followed by the calculation of the absorbed doses with potential inclusion of biological effects. This comprises the following three steps:

a) *Quantitative Imaging*
The established method for quantitative imaging for dosimetry relies on the measurement of the biokinetics by serial PET/CT, SPECT/CT or whole body scan. For

quantification the proper attenuation, scatter and partial volume corrections need to be applied. If organ or lesion dosimetry is performed, precise determination of organ/lesion volumes is necessary. Care has to be taken for an appropriate calibration of the imaging system.

b) Biokinetics
This requires the determination of a correct temporal sampling and the use of *ad hoc* procedures to integrate the activity within time to obtain the total number of decays occurring in the source organs and thus the time-integrated activity coefficients (TIACs).

c) Absorbed dose Calculation
If the TIACs of the relevant structures are known, a calculation of the absorbed doses can be performed by applying, in most cases, the "MIRD formalism":

$$D = \tilde{A} * S$$

D: the mean absorbed dose to a voxel or a target region from the cumulated activity in a source region.
Ã: the cumulated activity (i.e. the integral of the time-activity curve)
S: S factor (= mean absorbed dose per unit cumulated activity in the voxel or the target region).

Different dose calculation approaches exist: These may either be based on tabulated S factors (with mass correction) of anthropomorphic phantoms, on convolution kernels or on Monte-Carlo simulations.

Results: The most successful pairs of isotopes for theranostics are I-123/I-124/I-131 [2] and Ga-68/Lu-177/Y-90 [3]. In addition, Y-90 PET/CT provides a good estimate of the absorbed doses in selective internal radiotherapy for loco-regional liver treatment [4].

Conclusion: Although many new radiopharmaceuticals are available for imaging and molecular radiotherapy it is still a challenge to establish reliable dose-response relationships.

Keywords: Molecular radiotherapy, quantitative imaging, absorbed dose calculation

References:
[1] Bentzen SM. Lancet Oncol. 2005;6:112–7.
[2] Luster et al. EJNMMI. 2008;35:1941-59
[3] Bodei et al. EJNMMI. 2013;40:800-16
[4] Lhommel et al. EJNMMI. 2009;36:1696

134

Single-cell *S*-value calculations for Auger-electron emitting radionuclides

B.Q. Lee[1], N. Falzone[2,3], J.M. Fernández-Varea[4], K.A. Vallis[2], A.E. Stuchbery[1], T. Kibédi[1]
[1] (Australian National University, Canberra, Australia)
[2] (University of Oxford, Oxford, United Kingdom)
[3] (Tshwane University of Technology, Pretoria, South Africa)
[4] (Universitat de Barcelona, Barcelona, Spain)

Purpose: Auger-electron (AE) emitting radionuclides could be exploited for therapeutic purposes due to the high local energy deposition by low-energy Auger electrons or may deliver an unintentional mean absorbed dose burden when used as medical imaging agents. The aim of this study is to provide *S*-values for selected 14 AE emitting radionuclides based on the latest radiation spectra.

Methods: The Monte Carlo code PENELOPE [1] was used to transport the complete radiation spectra of ^{67}Ga, ^{80m}Br, ^{89}Zr, ^{90}Nb, ^{99m}Tc, ^{111}In, ^{117m}Sn, ^{119}Sb, ^{123}I, ^{124}I, ^{125}I, ^{135}La, ^{195m}Pt and ^{201}Tl using the methodology described in Ref. [2]. Radiation spectra was based on the unabridged nuclear decay data from MIRD RADTABS program [3] and the radiation spectra generated using the BrIccEmis code [4]. Taking the nucleus as the target, simulations were run assuming uniformly distributed activity in the nucleus (N←N), in the cytoplasm (N←Cy) or on the cell surface (N←CS).

Results: A comparison of calculated Auger yields for all 14 radionuclides is shown in the table below. Auger yields from MIRD are consistently higher than the values calculated using the BrIccEmis code. The methodology used to produce data in MIRD did not account for variations in binding energies during atomic relaxation thus overestimated the intensity of low-energy electrons.

Radionuclide	BrIccEmis	MIRD	Radionuclide	BrIccEmis	MIRD
^{67}Ga	4.84	4.96	^{119}Sb	14.29	23.68
^{80m}Br	8.96	9.6	^{123}I	12.31	13.71
^{89}Zr	6.88	9.45	^{124}I	8.38	9.17
^{90}Nb	7.2	8.77	^{125}I	20.0	23.0
^{99m}Tc	4.39	4.41	^{135}La	10.9	N/A
^{111}In	7.17	7.43	^{195m}Pt	25.9	36.6
^{117m}Sn	5.72	14.2	^{201}Tl	18.8	20.9

BrIccEmiss determined *S*-values were generally lower compared with MIRD *S*-values with the greatest differences noted when the source is far from the target region, i.e. for the N←Cy and N←CS configurations.

Conclusions: Realistic modelling of atomic relaxation following nuclear decay is essential for producing the radiation spectra needed for the calculations of *S*-values.

Keywords Auger-electron emitter; Monte Carlo simulation; *S*-values; Nuclear medicine;

References:
[1] F Salvat, PENELOPE-2011; NEA 6416
[2] N Falzone J Nucl Med 2015; 56(9): 1441
[3] KF Eckerman and A Endo, MIRD Radionuclide Data and Decay Schemes 2008
[4] B Lee et al. Comp Math Meth Med 2012; 651475

135

Range Verification with Ionoacoustics: simulations and measurements at a clinical proton synchro-cyclotron

S. Lehrack W. Assmann[1], A. Maaß[1], K. Baumann[1], G. Dedes[1], S. Reinhardt[1], P. Thirolf[1], G. Dollinger[2], F. Vander Stappen[3], J. Van de Walle[3], S. Henrotin[3], B. Reynders[3], D. Bertrand[3], D. Prieels[3], K. Parodi[1]
[1] Department for Medical Physics, Ludwig-Maximilians-Universität München, Am Coulombwall 1, 85748 Garching b. München, Germany
[2] Institute for Applied Physics and Instrumentation, Universität der Bundeswehr, Werner-Heisenberg-Weg 39, 85577 Neubiberg, Germany
[3] IBA, 3 chemin du Cyclotron, 1348 Louvain-la-Neuve, Belgium

Purpose: The local temperature increase induced by ion energy deposition in tissue creates an "ionoacoustic" ultrasound signal, particularly at the dose maximum (Bragg peak)[1-3]. This signal may be used for range verification in ion beam therapy in the future, which is still an important challenge for this irradiation modality. This approach has recently been revisited by several groups in simulations [4, 5], and by our group in simulations and also in proof-of-principle experiments with pulsed 20 MeV proton beams [6]. Here we present new simulations and first measurements of the ionoacoustic signal produced in water by proton beams accelerated up to energies of 227 MeV at a clinical synchro-cyclotron.

Material and Methods: In preparation of ionoacoustic experiments at clinically relevant energies, we extended our simulations from previously 20 MeV to beam energies of 120-230 MeV. The propagation of ultrasound waves was simulated by the MATLAB toolbox k-Wave using Geant4 for calculations of the initial dose deposition. The corresponding experimental setup to measure the ionoacoustic signal consisted of a broadband hydrophone (500 Hz - 250 kHz) placed in a water phantom with protons entering through the water surface. We measured the transit time of the ionoacoustic signal from the Bragg peak to the hydrophone and varied this distance either by using different energies (227, 226 and 145 MeV) or by changing the detector position while using the maximum energy.

Result: The simulations showed a distinct frequency shift of the ionoacoustic signal spectrum from a few MHz at 20 MeV from our previous experiments to about 100 kHz and below at proton beam energies above 120 MeV. At the new IBA synchro-cyclotron, we were able to measure ionoacoustic

signals from a pulsed proton beam (about 5 pC/pulse, 6 µs FWHM) and detector shifts down to 2 mm. The measured relative shifts of the Bragg peak position of 2.3 mm for 1 MeV energy change and 173.25 mm for 82 MeV are in perfect agreement with Geant4 predictions. However, the low signal amplitude below 1 mV required an averaging with 1024 acquisitions.
Conclusion: Measuring the ionoacoustic signal at the IBA synchro-cyclotron, the detectability of 2 mm range shifts could be demonstrated. Experimental upgrades will be discussed, from which we reasonably assume to improve the resolution to 1 mm and below. In order to determine an absolute ion range in water in future ionoacoustic experiments, a method using an additional ultrasound transducer to measure the distance of the hydrophone to the water surface was developed. Remaining challenges on signal detectability for clinical dose rates as well as perspectives of future setup improvements will be discussed.
Acknowledgment: Supported by DFG (Excellence Cluster MAP). We thank Stephan Kellnberger and Vasilis Ntziachristos for the fruitful discussion and support in previous experiments.

Keywords: Ionoacoustics, Range Verification, Ultrasound

References:
[1] Hayakawa, Y., et al., Acoustic pulse generated in a patient during treatment by pulsed proton radiation beam. Radiation Oncology Investigations, 1995. 3(1): p. 42-45.
[2] Sulak, L., et al., Experimental Studies of the Acoustic Signature of Proton-Beams Traversing Fluid Media. Nuclear Instruments & Methods, 1979. 161(2): p. 203-217.
[3] Albul, V.I., et al., Acoustic field generated by a beam of protons stopping in a water medium. Acoustical Physics, 2005. 51(1): p. 33-37.
[4] Alsanea, F., V. Moskvin, and K.M. Stantz, Feasibility of RACT for 3D dose measurement and range verification in a water phantom. Med Phys, 2015. 42(2): p. 937-46.
[5] Jones, K.C., et al., Proton beam characterization by proton-induced acoustic emission: simulation studies. Phys Med Biol, 2014. 59(21): p. 6549-63.
[6] Assmann, W., et al., Ionoacoustic characterization of the proton Bragg peak with submillimeter accuracy. Med Phys, 2015. 42(2): p. 567-74.

136
Monte Carlo simulation of prompt-γ emission in proton therapy using a track length estimator
J. M. Létang[1], W. El Kanawati[1], D. Dauvergne[2], M. Pinto[2,3], D. Sarrut[1], É. Testa[2], N. Freud[1]
[1] CREATIS, Université de Lyon; CNRS UMR5220; INSERM U1044; INSA-Lyon;
Université Lyon 1; Centre Léon Bérard, Lyon, France
[2] IPNL, Université de Lyon; CNRS/IN2P3 UMR5822; Université Lyon 1 Lyon, France
[3] now with Ludwig Maximilians University, Munich, Germany

Purpose: Online in vivo control of the ion range in a patient during proton therapy is a major challenge for quality assurance of treatments. After measurements showed that prompt-γ emission is correlated to the ion range (Min *et al* 2006, Testa *et al* 2008), prompt-γ imaging emerged as a promising method (Verburg *et al* 2013). Fast methods are required to compute accurate prompt-γ emission maps to design and predict the camera response from treatment plans. An analytic computation method based on the structure of the dose calculation engines in treatment planning system has recently been proposed (Sterpin *et al* 2015). An alternative technique based on variance reduction in Monte Carlo (MC) calculations is developed here for computing prompt-γ emission maps in proton therapy.
Materials/Methods: The track length estimator (TLE) method is a standard variance reduction technique in voxel-based dose computation in the kerma approximation (Williamson 1987), and similar approaches have also been developed for positron emitter distributions in proton therapy (Parodi *et al* 2007). A specific track length estimator has been developed here to design a continuous process along the proton track that locally deposits the expected value of the prompt-γ emission (induced by proton inelastic scattering) that would have occurred if a large number of protons with the same incident energy had followed the same step (i.e. track element). First an elemental database of prompt-γ emission spectra is established in the clinical energy range of incident protons for all elements in the composition of human tissues. This database of the prompt-γ spectra is built offline with high statistics. Regarding the implementation of the prompt-γ TLE MC tally, each proton deposits along its track the expectation of the prompt-γ spectra from the database according to the proton kinetic energy and the local material density and composition. All software developments have been carried out with the Gate/Geant4 toolkit.
Results: A detailed statistical analysis is reported to characterize the dependency of the variance reduction on the geometrical (track length distribution) and physical (linear prompt-γ spectrum database) parameters. Benchmarking of the proposed technique with respect to an analogous MC technique is carried out. A large relative efficiency gain is reported, ca. 10^5. Such an efficiency gain could reduce the MC computing time of a full treatment from some weeks to less than one hour. Implementation issues are also addressed.
Conclusions: This MC-based technique makes it possible to deal with complex situations such as heterogeneities for which proton straggling and secondary protons may have a decisive contribution. When considering translation to clinic, measurements for the prompt-γ spectrum database, or at least a sound calibration protocol of the simulated prompt-γ spectra, will have to be carried out.

Keywords: prompt-γ imaging, Monte Carlo simulation, variance reduction

References:
[1] Min *et al* (2006) App Phys Lett 89 183517
[2] Parodi *et al* (2007) Phys Med Biol 52 778–86
[3] Sterpin *et al* (2015) Phys Med Biol 60 4915
[4] Testa *et al* (2008) App Phys Lett 93 093506
[5] Verburg *et al* (2013) Phys Med Biol 58 L37-49
[6]Williamson (1987) Med Phys 14 567-76

137
Preclinical imaging and radiotherapy of prostate cancer using the theranostic twins(^{68}Ga/^{177}Lu)-radiolabeled peptides
J. C. Lim, E. H. Cho, S. Y. Lee, S. H. Dho, S. Y. Kim, S. H. Jung
Korea Atomic Energy Research Institute

Since the gastrin-releasing peptide receptor(GRPR) has been shown to be overexpressed in prostate cancer, bombesin which is the ligand of GRPR has been investigated to be a successful candidate for the peptide receptor radiotherapy(PRRT)[1]. The present study describes the imaging and therapeutic efficacy of the theranostic twins(^{68}Ga/^{177}Lu)-labeled bombesin derivatives for the PRRT of GRPR-overexpressing prostate tumors.
A series of DOTA-conjugated bombesin derivatives were synthesized using a solid-phase synthesis. Competitive binding studies were performed for selecting a GRPR-targeting peptide with high affinity. The selected peptide was labeled with ^{68}Ga using the NaCl method for imaging[2], and labeled with ^{177}Lu which was produced by the HANARO research reactor (thermal neutron flux of 1.8×10^{14} $n \cdot cm^{-2} \cdot s^{-1}$) for therapy. The labeling yield was evaluated by iTLC-SG, and the PET/CT imaging and therapeutic efficacy of the radiolabeled peptides were evaluated using nude mice bearing PC-3 human prostate carcinoma xenograft.
Hydrophilic-modified bombesin derivative showed a nanomolar binding affinity for GRPR. The peptide was labeled with the both radionuclides in high incorporation yields(>98%). ^{68}Ga-labeled peptide was quickly cleared from the blood and clearly visualized in PC-3 tumors at 1 hr p.i. ^{177}Lu-labeled peptide were also rapidly accumulated in a PC-3 tumor, and the % ID/g of the tumor was 12.42 ± 2.15 1 hr p.i. The radio-peptide significantly inhibited the tumor growth

(P<0.05), and treatment-related toxicity was not observed in the pancreas and kidneys while slight glomerulopathy was detected.
The pharmacokinetic, imaging, and therapy studies suggest that the theranostic twins(^{68}Ga/^{177}Lu)-labeled bombesin derivatives have promising characteristics for application in nuclear medicine, namely, for the diagnosis and treatment of GRPR-overexpressing prostate tumors.

Keywords: Theranosis, Prostate cancer, Bombesin, Radionuclide

References:
[1] Cescato, R., et al., Bombesin receptor antagonists may be preferable to agonists for tumor targeting. J Nucl Med, 2008. 49(2): p. 318-26.
[2] Mueller, D., et al., Simplified NaCl based (68)Ga concentration and labeling procedure for rapid synthesis of (68)Ga radiopharmaceuticals in high radiochemical purity. Bioconjug Chem, 2012. 23(8): p. 1712-7.

138
The role of adipose stromal cells for reversal of radiation fibrosis
X. Zhao[1,3], P. Psarianos[3], J.H. Lee, L[3]. Ailles, K. Yip[4], F.F. Liu[4]
[1] Institute of Medical Sciences
[2] Department of Radiation Oncology
[3] Department of Otolaryngology - Head and Neck Surgery
[4] Princess Margaret Cancer Centre, University Health Network

Hypothesis: Radiation fibrosis (RF) effects up to 70% of patients who have undergone radiotherapy. It is characterized by irreversible scarring of normal tissue resulting in functional morbidity and increased risk of surgical complications. Adipose-derived stromal cells (ADSCs) are a subcategory of mesenchymal stromal cell. Much of the therapeutic benefit of ADSCs has been attributed to secretion of cytokines and growth factors involved in immunomodulation, cell survival, and metabolism. We hypothesize that ADSCs may be therapeutically effective for RF through reversal of metabolic aberrations.
Methods: A mouse model of RF was developed and ADSC isolation was confirmed by surface marker expression and by differentiation capacity down the mesenchymal lineage. GFP and luciferase labelled ADSCs were used to assess biodistribution and cell survival after transplantation. To determine the therapeutic effect of ADSC transplantation for RF, we assessed functional changes to tissue elasticity using a leg contracture measurement tool and to collagen deposition using trichrome blue staining. To determine the mechanism of ADSC-mediated fibrosis reversal, we assessed transcriptomic changes to RF tissue.
Results: A RF model was created by radiating the hind limb of C3H mice. This model showed a dose dependent leg contracture and histological findings of fibrosis. We confirmed the immunophenotype of isolated ADSC and their ability to differentiate into adipogenic, chondrogenic, and osteogenic lineages. ADSC transplantation showed a statistically significant trend towards improved leg contracture (2-way ANOVA, p<0.05) and reduced collagen deposition. Biodistribution studies confirmed the presence of ADSCs in the subdermis of RF tissue with persistence for at least 18 days post-transplantation. Preliminary RNA-seq over-representation pathway analysis showed that lipid metabolism and PPARG signaling were among the top pathways down regulated in radiation fibrosis and was partially reversed with ADSC treatment. ADSCs directly reversed alterations to lipid metabolism in radiated fibroblasts through indirect co-culture.
Conclusions: ADSC transplantation may be an effective treatment for the reversal of radiation fibrosis through metabolic reprogramming. As cancer survivorship increases, the prevalence of radiation fibrosis will rise and necessitate increased focus on effective treatment strategies for this condition.

Keywords: Adipose Derived Stromal Cells, Radiation Fibrosis, Cancer Survivorship

139
Characterization and test beam results of a $LaBr_3$ Compton Telescope for treatment monitoring.
G. Llosá[1], J. Barrio[1], A. Etxebeste[1], C. Lacasta[1], J.F. Oliver[1], P.G. Ortega[1,2], C. Solaz[1], P. Solevi[1].
[1] Instituto de Física Corpuscular (CSIC/UVEG), Parque Científico. C/. Catedrático Beltrán, 2. E-46980 Paterna, Spain.
[2] CERN (European Organization for Nuclear Research), CH-1211 Geneva, Switzerland

Purpose: The detection of gamma rays for monitoring purposes can overcome some of the limitations of PET, since they are more abundant than positron emitters and are produced within nanoseconds after irradiations. However, their continuous emission spectrum up to high energies (more than 10 MeV) make their detection challenging [1]. Collimated systems and Compton cameras are being developed for this application.
The IRIS group of the Instituto de Fisica Corpuscular (IFIC-CSIC/UVEG, Valencia) has developed a three-layer Compton telescope based on $LaBr_3$ scintillator crystals for hadron therapy monitoring within the ENVISION project.
Materials and Methods: The telescope consists of three planes of $LaBr_3$ crystals, which provide high energy resolution and fast response, coupled to silicon photomultiplier arrays. A custom made data acquisition system has been developed to read out the detectors and operate them in time coincidence, employing the VATA64HDR16 ASIC[2]. The system aims at combining two- and three-layer events in order to profit from the high efficiency of the former and the high precision of the latter. The functionality of the device has been tested in the laboratory with radioactive sources, and also in beam tests. A dedicated image reconstruction ML-EM code has also been developed for both types of events.
Results: The system has been characterized in the laboratory acquiring data with radioactive sources of different energies. The detector response in terms of linearity, uniformity and spatial, energy and timing resolution has been obtained for the three layers, improving the results of the first tests. In addition, images of a point-like Na-22 source have been reconstructed with two and three-layer systems. The preliminary spatial resolution obtained is 7.3 mm FWHM with the two-layer system and 8.6 mm FWHM with the three-layer system.
The two-layer system has also been tested in a proton beam at KVI-CART, Groningen. Data were taken with a 150 MeV proton beam with an intensity of about 10^8 protons/s and a lateral beam spread of 5.3 mm impinging on a PMMA phantom. The PMMA target was placed in two different positions along the beam separated by 10 mm. The data analysis and image reconstruction of the data have shown a difference in the reconstructed profile consistent with the phantom position [3].
Conclusions: The laboratory tests carried out assess the correct functioning of the device. In-beam results show the capability of detecting range shifts. Current work is focused on performance improvement of the system and on simultaneous operation of two and three detector layers. Further tests in beam are planned at HZDR Dresden for December 2015.

Keywords: Compton Telescope, Hadron therapy, treatment monitoring.

References:
[1] Roellinghoff, F. et al. Design of a compton camera for 3d prompt-imaging during ion beam therapy. Nuclear Instruments and Methods A 648, S20–S23.
[2] Trovato, M., Solevi, P., Torres-Espallardo, I., Gillam, J., Lacasta, C., Rafecas, M., et al. A three layer compton telescope for dose monitoring in hadron therapy. 2014 IEEE NSS MIC.

[3] Solevi, P. et al. First on-beam test of a Compton Telescope for Ion-Beam Therapy Monitoring. Submitted to Phys. Med. Biol. 2015.

140

Recent Improvements and Applications of the FLUKA Monte Carlo code in Hadrontherapy

A. Mairani [1,2] on behalf of the FLUKA collaboration
[1] Medical Physics Unit, CNAO Foundation Pavia, Italy
[2] Heidelberg Ion Beam Therapy Center, Heidelberg, Germany

Purpose: Monte Carlo (MC) codes are widely used in the hadrontherapy community due to their detailed description of radiation transport and interaction with matter. In this work, we present the latest developments and applications of the FLUKA Monte Carlo code [1,2].
Material/methods: MC methods are being utilized at several institutions for a wide range of activities spanning from beam characterization to quality assurance and dosimetric/radiobiological studies. The suitability of a MC code for application to hadrontherapy demands accurate and reliable physical models for the description of the transport and the interaction of all components of the expected radiation field. This becomes extremely important to correctly perform not only physical but also biological dose calculations. In addition, accurate prediction of emerging secondary radiation is of utmost importance in emerging areas of research aiming at *in-vivo* treatment verification.
Results: Validations and applications at several experimental sites as well as proton/ion therapy facilities with active beam delivery systems will be presented:

- Physical database generation: laterally integrated depth-dose profiles, lateral-dose distributions at different depths, secondary fragment yields and fragment energy spectra at different depths.
- Forward MC re-calculations of physical/RBE-weighted dose distributions of proton and carbon ion treatment plans.
- MC-based treatment planning for proton and heavy ions beam therapy.
- Studies for introducing *new* ions (^{4}He and ^{16}O) in the clinical practice.

Conclusions: FLUKA's flexibility and the satisfactory agreements with several dosimetric data and nuclear fragment yields demonstrate that the code is a valuable and powerful support for the hadrontherapy community.

Keywords:
Particle therapy, Monte Carlo code, dosimetry

References:
[1] Böhlen, T. T., Cerutti, F., Chin, M. P. W., Fassò, A., Ferrari, A., Ortega, P. G., Mairani, A., Sala, P. R.,Smirnov, G., Vlachoudis, V. (2014). The FLUKA Code: Developments and challenges for high energy and medical applications. Nuclear Data Sheets
[2] Ferrari, A., Sala, P. R., Fasso, A., & Ranft, J. (2005). FLUKA: A Multi-Particle Transport Code. SLAC, 773(October), 406

141

Investigation of the use of inhomogeneous fractional dose distributions in IMPT to improve the therapeutic index

L. Manganaro[1,2], G. Russo[3], F. Dalmasso[1,2], F.M. Milian[4], F. Bourhaleb[3], R. Cirio[1,2], A. Attili[2]
[1] Università degli Studi di Torino, Torino, Italy
[2] INFN (Istituto Nazionale di Fisica Nucleare), Torino, Italy
[3] I-SEE (Internet-Simulation Evaluation Envision), Torino, Italy
[4] Universidade Estadual de Santa Cruz, Salobrinho, Ilhéus, Brazil

Purpose: Conventionally, intensity modulated particle therapy (IMPT) fields are optimized independently of the fractionation scheme. Following some precursory works [1—3], this study aims at investigating whether the application of spatial and temporal modulations in fractionation patterns, which involve the delivery of daily inhomogeneous fractional dose (IFD) distributions, may increase the therapeutic gain.
Materials/Methods: We simulated the irradiation of different clinical cases with different ions (^{1}H, ^{4}He, ^{12}C) and we carried out a comparison between two types of treatment plans. These were: (1) a conventional plan with a standard fractionation scheme in which each beam irradiates the whole planning target volume (PTV) delivering a uniform dose of 2 Gy per fraction; (2) an alternative plan that implies IFD distributions, delivering homogeneous dose to distinct regions of the PTV in different fractions. Each field was weighted to minimize its contribution to the proximal region of the PTV, so to limit the dose excursion in the surrounding normal tissues and obtain different local fractionation schemes in the volumes of interest. The comparison was based on the evaluation of the tumor complication probability (TCP) and normal tissue complication probability (NTCP). We evaluated these quantities following the approach proposed by Kallman *et al.* [4], based on the Linear-Quadratic-Poisson model. We considered a variable relative biological effectiveness (RBE) and the impact of the variable linear energy transfer (LET) distributions on the sensitivity to the time structure of the irradiation.
Results: For the considered cases, the comparison showed that the IFD-based approach leads to an improvement of the therapeutic index with respect to the standard approach (+6-10%). The extent of the gain is dependent, among other factors, on the sensitivity of the tissues to the employed ion radiation. Some critical issues were identified related to the choice of weights and spatial configurations of the fields.
Conclusions: This work investigates the possibility to improve the therapeutic index by delivering temporally and spatially heterogeneous dose distributions in the PTV, following the IFD paradigm. A methodology has been found which has proven to be successful in the considered clinical cases.

Keywords: Inhomogeneous fractionation, intensity modulated particle therapy, therapeutic index

References:
[1] J.Unkelbach and C.Zeng, *Medical Physics* 40, 091702 (2013)
[2] C.Zeng, D.Giantsoudi, C.Grassberg, S.Goldberg, A.Niemjerko, H.Paganetti, J.A.Efstathiou and A.Trofimov, *Medical Physics* 40, 051708 (2013)
[3] J.Unkelbach and D.Papp, *Medical Physics* 42, 2234-2241 (2015)
[4] P.Kallman, A.Agren and A.Brahme, *International Journal of Radiation Biology* 62, 249-262 (1992)

142

MONDO: a neutron tracker for particle therapy secondary emission fluxes measurements

M. Marafini [1,2], V. Patera [1,2,4], D. Pinci 1, A. Sarti [2,3,4], A. Sciubba [1,2,4], E. Spiriti [3]
[1] INFN Sezione di Roma, Roma, Italy
[2] Museo Storico della Fisica e Centro Studi e Ricerche "E.Fermi", Roma, Italy
[3] Laboratori Nazionali di Frascati dell'INFN, Frascati, Italy
[4] Dipartimento di Scienze di Base e Applicate per Ingegneria, Sapienza Università di Roma, Roma, Italy

In Particle Therapy, cancer treatments are performed using accelerated charged particles whose high irradiation precision and conformity allows the tumor destruction while sparing the surrounding healthy tissues. Dose release monitoring devices using photons and charged particles produced by the beam interaction with the patient body have already been proposed, but no attempt based on the detection of the abundant secondary radiation neutron component has been made yet. The reduced attenuation length of neutrons yields a secondary particle sample that is larger in number when compared to photons and charged particles. Furthermore, neutrons allow for a backtracking of the emission point that is not affected by multiple scattering. Since neutrons can release a significant dose far away from the tumor region, a precise measurement of their flux, production energy and angle distributions is eagerly needed

in order to improve the Treatment Planning Systems (TPS) software, so to properly take into account not only the normal tissue toxicity in the target region, but also the risk of late complications in the whole body [1,2]. All the aforementioned issues underline the importance for an experimental effort devoted to the precise characterization of the neutron production gaining experimental access both to the emission point and production energy.
The technical challenges posed by a neutron detector aiming for high detection efficiency and good backtracking precision will be addressed within the MONDO (MOnitor for Neutron Dose in hadrOntherapy) project. The MONDO main goal is to develop a tracking detector targeting fast and ultrafast secondary neutrons.
The main interaction mechanism of fast and ultrafast neutrons in plastic scintillators is the elastic scattering with hydrogen nuclei. In case of double elastic scattering events, if both protons recoil are measured, the neutron energy and direction can be reconstructed. The tracking and energy resolution achievable on the two recoiling protons drive the neutron energy and angular resolutions. The tracker is than composed by matrix (10 x 10 x 20 cm^3) of squared scintillating fiber of 0.250 mm). The fibers are used at the same time as target for the elastic n-p scattering of the impinging neutrons and as active detector for the recoiling protons. The light produced and collected in the fibers will be amplified using a triple GEM [3] and acquired using CMOS Single Photon Avalanche Diode arrays [4].

The neutron tracker will measure the neutron production yields, as a function of production angle and energy, using different therapeutical beams (protons, 12C ions and possibly 4He and 16O ions).
The MONDO project and the preliminary test of the different components will be presented.

Keywords: Tracking detector, Neutrons, Particle Therapy

References:
[1] M.Durante, W.D.Newhauser, *Review:Assessing the risk of second malignancies after modern radiotherapy*, Nature Reviews Cancer 11 (2011) 438-448. http://dx.doi.org/10.1038/nrc3069
[2] Hultqvist, Gudowska, *Importance of nuclear fragmentations in light ion therapy Monte Carlo simulations of secondary doses to the patient*, Phys. Med. Biol. 55.
[3] M.Marafini *et al.*, *High granularity tracker based on a Triple-GEM optically read by a CMOS-based camera*, arXiv:1508.07143 (submitted to JINST).
[4] L.Braga et al., *A fully digital 8 x 16 sipm array for pet applications with per-pixel tdcs and real-time energy output*, Solid-State Circuits, IEEE Journal of 49 (1) (2014) 301-314. http://dx.doi.org/10.1109/JSSC.2013.2284351

143
Modeling the effect of symmetrical division of cancer stem cells on tumour response to radiation
L.G. Marcu[1,2], D. Marcu[1]
[1] Faculty of Science, University of Oradea, Romania
[2] School of Physical Sciences, The University of Adelaide, SA 5005, Australia

Purpose: A growing body of evidence on cancer stem cells (CSC) relates their presence in tumours to poor treatment outcome. Symmetrical division of CSC during therapy is a key factor that contributes to repopulation and treatment failure. However, the literature lacks quantification of the CSC fraction and their division pattern. Head and neck cancers (HNC) are challenging due to high hypoxic content and repopulation ability by CSCs. The aim of this work was to quantify the symmetrical division of CSC in a hypoxic HNC model treated with hyperfractionated radiotherapy and assess tumour response as a function of the interplay between CSC and the hypoxic fraction.
Methods: A Monte Carlo technique was employed to grow a HNC consisting of CSC, differentiated and quiescent cells. For a biologically realistic growth, the initial symmetrical division probability of CSC was 1.9%, leading to a pre-treatment CSC population of 5.9%. The model considers various hypoxia levels as a function of the mean partial oxygen tension, from 3mmHg to 10mmHg. CSC radioresistance was established according to literature [1] and adapted for HNC.
Results: Initial CSC fraction changes during treatment due to repopulation, radioresistance and hypoxia. Figure 1 shows the variation of CSC fraction during therapy for three hypoxic scenarios. The figure shows that in mildly hypoxic tumours (9 mmHg) the fraction of CSCs during treatment overtakes the fraction of CSC in severely hypoxic ones (3 mmHg). It nearly appears that hypoxia keeps the CSC subpopulation under control. This behaviour is due to the fact that in well-oxygenated tumors CSCs are the most resistant subpopulation and they outlive non-stem cells, while in hypoxic tumors there are hypoxic resistant subpopulations as well as CSCs, thus the hypoxic content and CSC fraction are intertwined.

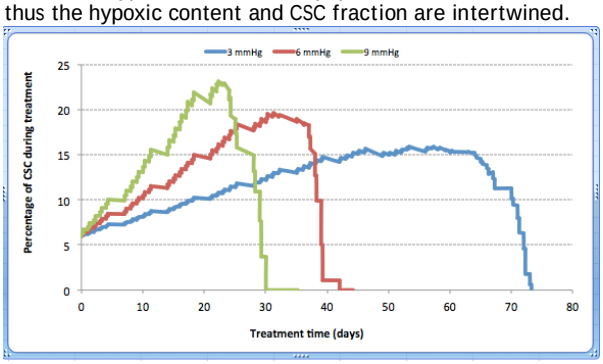

While hyperfractionation (1.2Gy in 70 fractions) is likely to be the most optimal radiotherapy schedule for advanced HNC [2] the model shows that if repopulation occurs via symmetrical division of CSCs with a probability greater than 5%, radiotherapy as a sole agent is not efficient for hypoxic HNC (table 1). However, oxic HNC benefit from hyperfractionation even for larger probabilities of symmetrical division, thus an overall dose of 84Gy in two 1.2Gy daily fractions is effective to overcome repopulation.
Conclusions: Quantitative evaluation of CSCs and hypoxia are crucial for designing successful treatment regimens for resistant subpopulations.

	Probability of CSC symmetrical division	1.9%	5%	10%	20%	30%
Number of 1.2Gy fractions for complete tumour eradication	*Oxic HNC*	48	49	52	58	70
	Mildly hypoxic HNC	52	53	56	65	81
	Moderately hypoxic HNC	74	78	86	117	210
	Severely hypoxic HNC	131	154	199	> 250*	

* The shaded areas correspond to clinically unfeasible situations

Keywords: cancer stem cell; hypoxia; hyperfractionated radiotherapy

References:
[1] Phillips TM, McBride WH, Pajonk F. *J Natl Cancer Inst* 98:1777, 2006.
[2] Beitler JJ, Zhang Q, Fu KK, et al. *Int J Radiat Oncol Biol Phys* 89:13, 2014.

144
Hadron minibeam radiation therapy: feasibility study at the Heidelberg Ion-Beam Therapy Center (HIT)
I. Martínez-Rovira[1,2], S. Brons[3] and Y. Prezado[1]
[1] Laboratoire d'Imagerie et Modélisation en Neurobiologie et Cancérologie, Centre National de la Recherche Scientifique, CNRS, Orsay, France
[2] Departament de Física, Universitat Autònoma de Barcelona, Bellaterra, Spain
[3] Heidelberg Ion Beam Therapy Center, Heidelberg University Clinic, Heidelberg, Germany

Purpose: Despite recent advancements in radiotherapy and radiosurgery, significant limitations remain. Hadrontherapy, which has been in clinical use for more than 15 years, has shown remarkable effectiveness. However, it still could benefit from a lower impact on non-targeted tissues to allow its administration at higher doses. This is the reason why we propose a new approached called hadron minibeam radiation

therapy (hadron MBRT). The technique is based on the well established tissue-sparing effect of arrays of parallel, thin or small beams, observed in studies performed with synchrotron radiation [1-2]. In parallel, significant tumor growth delay was observed in highly aggressive tumors by using interlaced irradiations [1-3]. Hadron MBRT combines the advantages of MBRT with the high dose conformability and the remarkable biological effectiveness of hadrontherapy. This novel strategy might guarantee tissue recovery and reduce the side effects of radiation in healthy tissues. The main goal of this study was to explore this new approach from a dosimetric point of view and to verify its technical feasibility at a clinical center (HIT, Germany). In particular, carbon and oxygen minibeams were studied.
Materials/methods: Carbon and oxygen minibeams were generated through a tungsten multislit collimator with line apertures of 700 µm separated by 3500 µm. Scanned 12C and 16O pencil beams were used to cover a given irradiation field size (1x1 cm2) and a spread out Bragg peak (SOBP) region of 5 cm at 8 cm-depth in water. Radiochromic films (EBT3) were placed at several depths in a solid-water slab phantom to evaluate dose distributions. Quenching effects of these films were also assessed and results were accordingly corrected.
As a figure of merit, the ratio between the central dose of one minibeam (peak dose) and the dose in the middle of two consecutive beams (valley dose) was evaluated. This magnitude, named peak-to-valley dose ratio (PVDR), is a very relevant magnitude in such spatially fractionated techniques [4].
Results: The measured lateral dose profiles in carbon and oxygen MBRT consisted in a pattern of peaks and valleys, which prove the technical feasibility of this approach. This first dosimetric study showed PVDR values around 10-20 in the first centimeters of the phantom. PVDR values progressively decrease up to around 5 at 8-cm-depth. These PVDR values are in the order of the ones obtained in x-rays MBRT, for which biological effectiveness has already been proven.
Conclusions: This is the first exploratory study that experimentally proves the technical feasibility of hadron MBRT at a clinical center. The PVDR values obtained showed the potential of this radiotherapy approach, which might allow reducing side effects in the healthy tissues. Animal experiments are warranted.

Keywords: minibeam radiation therapy, hadron therapy, experimental dosimetry

References:
[1] Dilmanian, Proc. Natl. Acad. Sci. USA 103 (2006).
[2] Deman, Int. J. Radiat. Oncol. Biol. Phys. 82 (2012).
[3] Prezado, J. Synchrotron Radiat. 19 (2012).
[4] Dilmanian, Neuro. Oncol. 4 (2002).

145
Infrared study of the biochemical effects in glioma cells induced by x-rays and Gd nanoparticles: first studies at SESAME synchrotron (Jordan)
I. Yousef[1,2], O. Seksek[3], J. Sulé-Suso[4], S. Gil[5], Y. Prezado[3] and I. Martínez-Rovira[3,6]
[1] SESAME Synchrotron-light for Experimental Science & Applications in the Middle East, Amman, Jordan
[2] ALBA Synchrotron, Cerdanyola del Vallès, Spain
[3] Laboratoire d'Imagerie et Modélisation en Neurobiologie et Cancérologie, Centre National de la Recherche Scientifique, CNRS, Orsay, France
[4] Institute for Science and Technology in Medicine, Keele University, Keele, UK
[5] Hospital Parc Taulí, Sabadell, Spain
[6] Departament de Física, Universitat Autònoma de Barcelona, Bellaterra, Spain

Purpose: One strategy to improve the clinical outcome in radiotherapy (RT) is to increase the dose effects in the tumor. This can be achieved by using specific nanoparticles (NP). Numerous studies have shown an enhanced effectiveness of tumor cell killing when NP were associated to irradiation [1-3]. However, the mechanisms of action are not yet clear. In addition to the damage due to a possible local dose enhancement, the interaction of NP with essential biological macromolecules could lead to changes in the cellular function, such as cell arrest at radiosensitive phases [4]. These effects, which could be amplified with a subsequent irradiation, might increase their anticancer effectiveness. Along this line, in this study we used F98 glioma rat cells as an *in vitro* model to evaluate the intracellular biochemical changes induced by x-ray irradiations in combination with Gadolinium NP by using Fourier transform infrared microspectroscopy (FTIR). FTIR allows *in situ* chemical structure determination of intracellular biomolecules. In addition, this technique has significantly contributed to study apoptosis, as well as cell cycle and cell death modes.
Materials/methods**:** FTIR measurements were performed using the internal source of infrared radiation at SESAME synchrotron (Jordan). Principal Component Analysis (PCA) was performed to show the variances between the different sets of spectra.
Results: Noticeable spectra alterations in the presence or absence of NP were detected in the proteins, DNA and lipids regions, indicating changes in the cellular function (even in the absence of radiation). In particular, biochemical changes related to apoptosis were detected. These include a shift toward the low wavenumbers in the amide I and II bands, relative amplitude changes in the CH2 and CH3 stretching modes, along with DNA chromatin condensation indications [5]. The figure below shows an example of PCA analysis in the DNA region of the infrared spectral range in the presence and absence of NP for a dose deposition of 10 Gy.

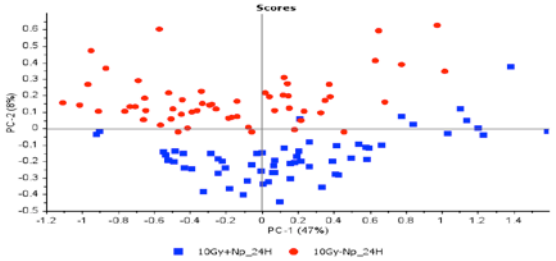

Conclusion: This is one of the first research studies performed at the Emira laboratory of the SESAME Synchrotron (Jordan). This infared work provides new insights on the biochemical effects induced by the combination of radiotherapy and nanoparticles, for which the full mechanisms of interaction are not well known up to now. Results will be discussed in relation to cell viability studies.

Keywords: Fourier Transform Infrared Microspectroscopy, radiotherapy and nanoparticles, F98 glioma cells.

References:
[1] J.F. Hainfield et al. *Phys. Med. Biol.* 49 309 [2004];
[2] S. Jain et al. *Br. J. Radiol.* 85 101 [2009];
[3] L. Sancey et al. *Br. J. Radiol.* 87 20140134 [2014];
[4] X.P. Choudhury et al. Nano*scale* 5 4476 [2013];
[5] H.N. Holman *Biopolym. Biospectrosc.* 57 329 [2000].

146
Construction and first tests of a PET-like detector for hadrontherapy beam ballistic control
R. Chadelas[1], C. Insa[1], D. Lambert[1], L. Lestand[1], M. Magne[1], F. Martin[1], G.Montarou[1], A. Rozes[1]
[1] Laboratoire de Physique Corpusculaire, Université Blaise Pascal, IN2P3-CNRS

We present the first results obtained with a detector, called Large Area Pixelized Detector (LAPD), dedicated to the beam ballistic control in the context of hadrontherapy.
The purpose is to control the ballistics of the beam delivered to the patient by in-beam and real time detection of secondary particles, emitted during its irradiation. These particles could be high energy photons (γ prompt), or charged particles like protons, or 511 keV γ from the annihilation of a

positron issued from the β^+ emitters induced in the patient tissues along the beam path. These methods require being able to detect with a huge efficiency, and with a minimum dead time, these secondary particles emitted when the beam hits the patient.
The LAPD is similar to a conventional Positron Emission Tomography camera. The 511 keV γ are detected and the reconstructed line of responses allow to measure the β^+ activity distribution. Nevertheless, when trying to use γ from positron annihilations for the ballistic control in hadrontherapy, the large γ prompt background should be taken into account and properly rejected.
This detector is made of two half-rings of 120 channels each (figure 1).

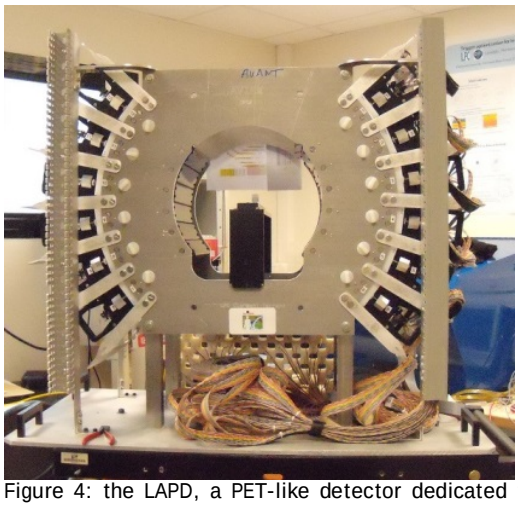

Figure 4: the LAPD, a PET-like detector dedicated to beam ballistic control in hadrontherapy.

Each channel consists of a 13*13*15 mm^3 LYSO crystal glued to a PMT. The PMT signal is sent to an Analog Sampling Module (ASM board). This VME 6U board is based on the DRS4 chip technology (Switch Capacitor Array) from the Paul Sherrer Institute and was specially designed for the LAPD detector. This board receives up to 24 differential analog input signals, with maximum amplitude of 600 mV, digitized by 12 bits - 33 MHz ADC. The sampling rate varies between 1 and 5 GHz, for a maximum buffer size of 1024 samples.
The first part of the talk is devoted to the description of the detector and its electronics. Then, we describe the various trigger strategy, and the on-going upgrade of the VME-based acquisition system to a µTCA-based technology. The selection of the coincident 511 keV γ is also discussed, and the reconstruction using an iterative MLEM algorithm is presented. In the last part of the talk, few results from an experiment with one third of the detector, using proton and carbon ion beams at the Heidelberg Ion-Beam Therapy Center in 2014, are also described, and the Coincidence Resolution Time and energy resolution are given. First reconstruction results, obtained with a phantom filled with a high intensity FDG source at the cancer research center of Clermont-Ferrand in 2015 are also shown.
This detector is now characterized, and will be installed at the Lacassagne hadrontherapy center (Nice, France), on the 65 MeV line (Medicyc) in December 2015 first, and on the future 230 MeV line (S2C2 from IBA) in 2016. The capability of this detector and its associated electronics to measure the ballistic of the proton beam in real clinical conditions with a sufficient precision will be evaluated.

Keywords: hadrontherapy, PET, beam ballistic control

References:
[1] https://indico.cern.ch/event/396441/contribution/27

147
Visualization of target inhomogeneities in carbon ion radiotherapy using nuclear fragments

M. Martišíková*[1,2], M.Reinhart[2], T. Gaa[2], J. Jakubek[3], B. Hartmann[1,2],
P. Soukup[3], and O. Jäkel[1,2]
[1] Heidelberg University Hospital,Im Neuenheimer Feld 400, D-69120 Heidelberg, Germany
[2] German Cancer Research Center, Im Neuenheimer Feld 280, D-69120
[3] Heidelberg, Germany 3-Czech Technical University in Prague, Horská 3a/22, 12800 Prague, Czech Republic

Purpose: Ion beams are used for highly precise radiotherapy, making an accurate dose deposition in tissue crucial. However, this accuracy can be compromised by unpredictable changes of the patient. Therefore an online monitoring of the beam within the patient is of large interest. The main challenge is given by stopping of the entire beam inside of the patient. Our group investigates the possibility to collect and reconstruct the information about the beam extension in the patient by detecting light ions emitted from the irradiated object, suggested in [1]. Exploiting the directions of secondary ions measured, a method for visualization and quantification of the carbon ion beam profile in a homogeneous phantom was published in [2]. In this contribution, the capability of the method to detect inhomogeneities in otherwise homogeneous phantoms is presented.
Materials & methods: The experiments were performed at the Heidelberg Ion Beam Therapy Center (HIT) in Germany. Narrow carbon ion beams of therapy-relevant energies, were directed onto homogneneous plastic phantoms with a typical head size. Secondary ions emerging from the phantom during the irradiation, were detected by a Timepix detector [3] developed by the Medipix Collaboration at CERN. A multilayered detector, consisting of 3 parallel Timepix detectors, was used to measure their tracks in 3D. The track distributions acquired with a full phantom were compared with cases when parts of the phantom were missing at several positions, simulating cavities in the body.
Results: It was found that exploiting the information carried by secondary ions enables to visualize cavities in the irradiated volume at different positions of the Bragg curve. The method was found to be sensitive also to cavities situated behind the Bragg peak (in the fragment tail). Moreover, a three-dimensional image reconstruction based on maximum likelihood expectation maximization (MLEM) exploiting the measured secondary particle tracks was developed. In the resulting images, air cavities and inhomogeneities with density differences down to 0.3 g cm^{-3} to the surrounding material are clearly visualized for the first time.
Conclusions: Our experimental results demonstrate that this novel imaging modality enables clear visualization of down to 1 cm-sized air cavities in head-sized phantoms, under clinical irradiation conditions. Therefore we conclude that secondary ions, being a by-product of the irradiation, are an attractive source of information on the actual beam extension in the irradiated body.
Keywords: carbon ion radiotherpy, in-vivo beam monitoring, secondary charged particles

Acknowledgements: We thank the German Cancer Aid for financial support of parts of this project. This work was performed within the Medipix Collaboration.

References:
[1] Amaldi et al., Nucl. Instrum. Meth. A 617 (2010)
[2] Gwosch et al., Physics in Medicine and Biology 58 (2013)
[3] Llopart et al.: Nucl. Instrum. Meth A 581 (2007)

148
The effect of fractionated administration of thalidomide at γ-ray irradiation on tumor response and lung metastasis

S. Masunaga[1], K. Tano[1], Y. Sanada[1], Y. Sakurai[2], H. Tanaka[2], M. Suzuki[3], N. Kondo[3], M. Narabayashi[3], T. Watanabe[3], Y. Nakagawa[3], A. Maruhashi[2], and K. Ono[3]
[1] Particle Radiation Biology
[2] Radiation Medical Physics

[3] Particle Radiation Oncology
Department of Radiation Life and Medical Science, Research Reactor Institute, Kyoto University, 2-1010, Asashiro-nishi, Kumatori-cho, Sennan-gun, Osaka 590-0494, Japan

Purpose: To evaluate the significance of fractionated administration of thalidomide combined with γ-ray irradiation in terms of local tumor response and lung metastatic potential, referring to the response of intratumor quiescent (Q) cells.
Materials/methods: B16-BL6 melanoma tumor-bearing C57BL/6 mice were continuously given 5-bromo-2'-deoxyuridine (BrdU) to label all proliferating (P) cells. The tumor-bearing mice then received γ-ray irradiation after thalidomide treatment through a single or 2 consecutive daily intraperitoneal administrations up to a total dose of 400 mg/kg in combination with an acute hypoxia-releasing agent (nicotinamide, 1,000 mg/kg, intraperitoneally administered) or mild temperature hyperthermia (MTH, 40 centigrade for 60 minutes). Immediately after the irradiation, cells from some tumors were isolated and incubated with a cytokinesis blocker. The responses of the Q and total (= P + Q) cell populations were assessed based on the frequency of micronuclei using immunofluorescence staining for BrdU. In other tumor-bearing mice, 17 days after irradiation, macroscopic lung metastases were enumerated.
Results: Thalidomide raised the sensitivity of the total cell population more remarkably than Q cells in both single and daily administrations. Daily administration of thalidomide elevated the sensitivity of both the total and Q cell populations, but especially the total cell population, compared with single administration. Daily administration, especially combined with MTH, decreased the number of lung metastases.
Conclusions: Daily fractionated administration of thalidomide in combination with γ-ray irradiation was thought to be more promising than single administration because of its potential to enhance local tumor response and repress lung metastatic potential.

Keywords: Quiescent cell: Lung metastasis: Thalidomide

149
The Malthus Project - updated predictions of national radiotherapy demand to 2030
T.Mee[1], N.F.Kirkby[1], K.J.Kirkby[1], R.Jena[2]
[1] Institute of Cancer Sciences, University of Manchester
[2] Department of Oncology, University of Cambridge

Purpose: The Malthus model is an evidence based simulation of radiotherapy demand in England, which was designed to estimate radiotherapy utilisation at local and national level, in order to assist in planning of radiotherapy services. The model utilised cancer registration data from the national cancer registration service, together with predictions of population growth from the Office of National Statistics, and cancer incidence projections. We present the results of an updated model that utilises the latest population projection estimates, and cancer incidence data.
Materials and Methods: Base data on cancer registration was provided by the National Cancer Intelligence Network, broken down by disease site, local Clinical Commissioning Groups (CCGs), age and sex. Equivalent population data was sourced from the Office for National Statistics. These two datasets were combined with data from 2,000 evidence-based clinical decisions, covering 22 different cancer sites. Clinical practice was peer-reviewed by over 100 British oncologists and at a national forum. An updated cancer incidence projection model and population projection model were also used to enable annual demand predictions up to 2035.
Results: The Malthus model estimates that the access rate for radiotherapy in England in 2015 should be 40.5% with a fraction burden of approximately 47,500 fractions per million population. To highlight how different regions within a country can be, Table 1 displays two regions and the England average for comparison. The predicted demand for radiotherapy is also increasing for England. Over the next few year the predicted fractions per million will increase by 0.9% per year, this will increase to 1% per year in 2020 and is expected to hit 1.1% per year by 2026.

	# per Million				
Region	All Sites	Breast	Lung	Prostate	H&N
England	47500	12500	5900	13100	4200
Dorset	65900	17000	6300	22600	5300
Tower Hamlets	19400	4000	3400	4000	3000

Table 1. Fractions per Million for the 'Big 4' for England and two different regions.

Conclusions: The Malthus model with updated cancer incidence data suggests a radiotherapy utilisation rate of 40.5%, with a predicted annual increase of fractions per million of around 1% per year. Whilst the observed rates of radiotherapy utilisation still lag behind the model's predictions, the observed activity increases in England (from the Radiotherapy Data Set) over the last 3 years exceed the rate of rise in predicted demand. Customised simulations for individual regions, such as what Malthus can do, allows local cancer profiles to be taken into account for more accurate current and future demand predictions. The customisability also allows for simulations looking at the impact of new technology, such as MRI Linac and Proton therapy, and data from other countries can be incorporated as well.
Keywords: Health Service Research, Demand Prediction

150
Progress with MRI-linac image-guided radiation dose imaging
P. Metcalfe[1], S. Alnaghy[1], M. Gargett[1], M. Lerch[1], M. Patesecca[1], A. Rosenfeld[1], L. Holloway[2], B. Oborn[3], G. Liney[4]
[1] CMRP, UOW, Australia
[2] Liverpool and Macarthur Cancer Therapy Centre
[3] Ingham Institute for Applied Medical Research, Australia
[4] Ingham Institute for Applied Medical Research, Australia

Purpose: MRI-linacs will enable 4D image-guided radiotherapy and require accurate MR visible and compatible dosimeter systems for verification.
Methods: Motion-tracking utilising a MagicPlate (M512) silicon array dosimeter capable of high resolution dosimetry (Petasecca, 2015) (figure 1a,b)has been modified for purpose of MR imaging during dynamic detector-tracking (i.e. so named 'MR guided dynamic dosimaging'). The detector was tested for MRI-safety and functionality without irradiation in a 1T fringe field of 3T Siemens Skyra MRI. As solid water can not be visualized on MRI a tissue-equivalent, gel-water phantom (CIRS® Computerized Imaging Reference Systems Inc. VA, USA), providing signal for detector and fiducial visualisation, was utilised to enable MR imaging (fast spin echo sequence).
Results: MR images of a non-powered detector system demonstrated detector visualization (see figure 1c). Detector movements approximating breathing were also acquired during dynamic MRI acquisition (fast gradient echo), showing that fiducial markers could be visualised when placed on a passive device and tracked. The detector functioned at the 1T bore entry position to simulate the magnetic field of our impending MR linac whilst a water phantom was imaged simultaneously at the mid-bore 3T position, with noise (see figure 1d) seen due to detector RF interference being reduced by aluminium foil shielding of the device and cables (figure 1e).
Conclusions: The current MRI-guided dynamic dosimaging set-up has been demonstrated to be successful in detector visualisation and tracking with a non-powered detector. Noise reduction has been achieved with the detector in operational mode. A MRI-compatible motion platform will be paired with M512. These measurements will be compared to acquisition in MRI-linac magnetic fields on the MRI-linac device being installed at the Ingham Institute in Australia.

Keywords: Radiotherapy, MRI-linac, dosimetry

References:
Petasecca, M. et al (2015), *Med Phys*, 42(6):2992-3004.

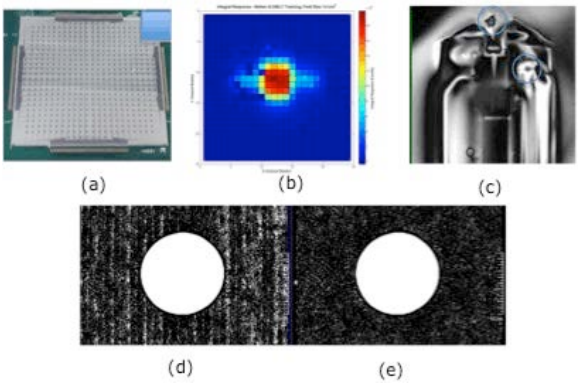

Figure 1: (a) M512 array, (b) M512 dosimetry acquisition of 1x1cm^2 field, (c) Passive M512 MR imaged at 3T, blue circles indicate fiducials (d) MR image of water phantom imaged without dosimeter noise suppression, (e) MR image of water phantom imaged with dosimeter noise suppression.

151

Plerixafor Improves Local Control and Reduces Metastases in Cervical Cancer Treated with Radiotherapy and Chemotherapy

N. Chaudary[1], M. Pintilie[2], R.P. Hill[1,4,5], M. Milosevic[3,4]
[1] Ontario Cancer Institute, Toronto, Canada
[2] Department of Biostatistics, Princess Margaret Cancer Centre, Toronto, Canada
[3] Radiation Medicine Program, Princess Margaret Cancer Centre, Toronto, Canada
[4] Department of Radiation Oncology, University of Toronto, Toronto, Canada
[5] Department of Medical Biophysics, University of Toronto, Toronto, Canada

Purpose: There is an important need to improve the effectiveness of radio-chemotherapy (RTCT) for cervical cancer. These tumors recruit myeloid cells from the bone marrow via the CXCL12/CXCR4 pathway, which in turn influence vascular function and radiotherapy response. The objective of this study was to explore combined treatment with Plerixafor (a CXCL12/CXCR4 inhibitor) and standard RTCT on primary tumor control and the development of metastases, using orthotopic primary xenografts derived directly from patients with cervical cancer.
Materials/Methods: Two primary cervix xenografts (OCICx13 and OCICx20) were grown in the cervices of immune deficient mice. These tumor models have been shown to mirror the clinical and biological behavior of cervical cancer in patients. To simulate clinical treatment, image-guided radiotherapy (30 Gy in 15 daily fractions) and concurrent weekly cisplatin (4 mg/kg) were administered, with or without Plerixafor (5 mg/kg/day). The primary endpoints were tumor growth delay, the frequency of lymph node metastases and animal survival. Chemokine expression and neutrophil recruitment were evaluated by immunohistochemistry. Acute gut toxicity was assessed using the crypt cell assay. Blood and normal organs were examined for late toxicity.
Results: The combination of RTCT and Plerixafor produced substantial tumor growth delay, reduced metastases and improved survival compared to standard RTCT alone in patient-derived xenograft models. There was a reduction in chemokine signaling (CXCL12/CXCR4) and myeloid cell infiltration (GCSF, CD11b) with combination treatment compared to RTCT alone. There was no effect of Plerixafor on acute GI toxicity, nor were there changes in blood counts or organ morphology to indicate increased late hematological or normal tissue toxicity.
Conclusion: This preclinical study demonstrates that the addition of Plerixafor to standard RTCT for cervical cancer improves local tumor control and reduced metastases with no increase in toxicity. Plerixafor is commercially available for other indications, which will facilitate translation of these findings to phase I/II clinical studies.

Keywords: Cervical cancer, radiotherapy, Plerixafor, CXCL12, myeloid cells

152

Optimizing prostate cancer irradiation: from technology to fractionation

R. Miralbell
Service de Radio-Oncologie, Hôpitaux Universitaires de Genève;
Institut Oncològic Teknon, Barcelona.

Curative 3D standard external beam radiotherapy (EBRT) for prostate cancer has been able to improve disease control with dose escalation during the last 15 years though against the token of significant toxicity. Exploring changes in fractionation, doses-distribution optimization with modulated RT, and reducing CTV-PTV safety margins due to off- or on-line imaging before or during irradiation, may be alternatives worth to be implemented in order to reach the highest possible toxicity-free cure rates.
Accurate imaging helping to better define the irradiation target/s (e.g., multiparametric MRI, PET-CT/MRI, SPECT); modulated EBRT optimizing the dose distribution; and image guided RT (e.g., kV imaging, CBCT, fiducial markers, transponders, endorectal balloons, recto-prostatic spacers) controlling for patient repositioning and organ motion are presently available allowing the implementation of high precision treatment techniques.
Biomathematical modeling has helped to better understand the very special dose-response relationships of EBRT on prostate cancer concerning fractionation sensitivity (low α/β value), overall treatment time (tumor cell repopulation kinetics), and fraction delivery time (potential biological effective dose modifier). All these factors are rather suggestive that prostate cancer patients, especially those with low- or intermediate-risk disease, can be better treated with "more" dose/fraction, "less" number of fractions, and a "shorter" time protraction and delivery time per fraction. Two opposed modalities conceived to deliver large doses in few fractions are either stereotactic body RT (SBRT) or high-dose rate brachytherapy (HDR-BT) given alone or as a boost. The latter procedure may be limited by dose inhomogeneities and geographical misses. Even a small underdosage of the target or a heterogeneous dose-rate delivery may have a negative influence on outcome. This seems to be especially determinant for tumors with very low α/β values as it is the case for prostate cancer. Thus, SBRT may be theoretically more advantageous because the radiobiological reliability of a homogeneous dose distribution compared to HDR-BT, besides being less invasive and probably less costly.

153

Evaluation of the DNA damage induced by 60 MeV proton irradiation by cytogenetic and molecular methods

J. Miszczyk[1], K. Rawojć[1,2], A. Panek[1], P.G.S. Prasanna[3], M.M. Ahmed[3], A. Gałaś[4], J. Swakoń[5], L. Malinowski[5], W.M. Kwiatek[1]
[1] Department of Experimental Physics of Complex Systems, The H. Niewodniczański Institute of Nuclear Physics Polish Academy of Sciences, Krakow, Poland
[2] Marian Smoluchowski Institute of Physics, Jagiellonian University, Krakow, Poland
[3] Radiation Research Program, National Cancer Institute, National Institutes of Health, Bethesda, Maryland, USA
[4] Department of Epidemiology, Chair of Epidemiology and Preventive Medicine, Jagiellonian University – Medical College, Krakow, Poland
[5] Cyclotron Center Bronowice, Proton Radiotherapy Group, The H. Niewodniczański Institute of Nuclear Physics Polish Academy of Sciences, Krakow, Poland

Proton radiotherapy provides a promising and emerging treatment approach for cancer patients. However, understanding of the differences in terms of DNA damage and cell proliferation post-proton irradiation is relatively poor. The purpose of this study was to evaluate DNA damage induced by proton beams using various cytogenetic and molecular methods.

The response of human peripheral blood lymphocytes (HPBL) was characterized using: the cytokinesis-blocked micronucleus (CBMN) assay, premature chromosome condensation (PCC) assay, FITC-Annexin V labeling procedure, chip-based DNA ladder assay, and the comet assay. The samples of whole blood or isolated lymphocytes collected from 10 different healthy donors were irradiated *in vitro* with 60 MeV protons or 250 kV X-rays, in the dose range of 0.3 Gy – 4.0 Gy. The HPBL were located in Eppendorf vessels located in especially prepared PMMA (Poly(methyl methacrylate)) phantom and irradiated with protons in the fully modulated Spread Out Bragg Peak (SOBP) mode. Dosimetry was performed in accordance to the recommendations of the IAEA TRS-398 protocol.
Peripheral blood lymphocytes showed decreased ability to proliferate after irradiation that reduced with increasing radiation doses of either radiation types as evident by the reduced nuclear division index seen in the cytokinesis-block micronucleus (CBMN) assay. Proton irradiation resulted in a relatively higher incidence of cell death compared to those irradiated with X-rays. Cell death was due to both apoptosis and necrosis. Chip-based DNA ladder assay showed different degrees of fragmentation of the genomic DNA after proton irradiation indicating peripheral blood lymphocytes, which are prone to undergo an apoptotic mode of cell death, predominantly undergo a necrotic mode of cell death after proton irradiation. Differences in DNA damages following irradiation with protons and X-rays were apparent also at the intracellular distribution of cytogenetic damages as visualized by the PCC and CBMN assays. Alkaline comet assay showed a linear dose-response relationship for the DNA damage immediately after irradiation. Dose response relationship for the DNA damage indicated higher efficiency of protons in inducing DNA strand breaks presented as the ratio of the two α coefficients (1.37).
Our results, contribute to a better understanding of the differences in the response of human peripheral blood lymphocytes to proton and X-ray irradiation. These studies may eventually help determine the suitability of patients with cancer for treatment with a given radiation type based on their normal tissue response and ability to predict treatment related adverse effects.

Keywords: Proton beam, Human lymphocytes, DNA damage

Note: These investigations were carried out as a part of an extended examination of the 60 MeV proton beam at IFJ PAN by cytogenetic and molecular methods and were supported by the Grant DEC-2013/09/D/NZ7/00324 from the National Science Centre, Poland and by the Malopolska Regional Operational Program Measure 5.1 Krakow Metropolitan Area as an important hub of the European Research Area for 2007-2013. The special acknowledge is placed for DIAGNOSTYKA Sp. z o. o. in Krakow, Poland for help in blood samples collection.

154
Biological issues and their clinical implications in proton therapy
R. Mohan
MD Anderson Cancer Center, Houston, TX, USA

In the clinical practice of proton therapy, the biologic effectiveness of protons relative to photons (i.e., the "relative biologic effectiveness" or RBE) has simplistically been assumed to have a generic fixed value of 1.1. This value is based on an average of results of numerous in-vitro and in-vivo experiments conducted under limited conditions – most commonly, at high doses per fraction (e.g., 6–8 Gy) and in the middle of the spread-out Bragg peak where the RBE is relatively constant and close to the average value of 1.1. Furthermore, the RBE data have been acquired for only a limited number of cell lines, tissues, and endpoints. To justify the assumption of RBE of 1.1, it is argued that, clinically, no adverse responses have been reported with its use. However, large uncertainties in the treatment processes may have obscured the variability of the RBE.
In reality, the RBE is a function of multiple variables including dose per fraction, linear energy transfer (LET), cell and tissue type, endpoint, etc. It has been shown to vary from values lower than 1.1, perhaps lower than even 1, to as much as 4. Emerging clinical evidence, still somewhat anecdotal, is showing that neglecting RBE variability may lead to unforeseen toxicities and recurrences. However, establishing an unequivocal connection between unforeseen events and the use of RBE of 1.1 is challenging since there are numerous confounding factors. These include uncertainty in the particle therapy dose actually delivered and patient-specific factors.
As a consequence, there is a continuing debate about the validity of the assumption of RBE=1.1. At the same time, efforts to obtain more precise and accurate RBE information are accelerating. High-precision in-vitro and in-vivo experiments are being designed and conducted to obtain the large amounts of data required. Attempts are also being made to extract clinically-relevant RBE from treatment response data, particularly from PET and MR image biomarkers. Such RBE data need to be incorporated into predictive models of RBE, which can be used to explain treatment response more reliably and to design treatment plans. The improved knowledge of variable RBE is expected to not only help explain unforeseen events but, more importantly, to lead to improvements in treatment planning, which in turn may enhance the effectiveness of proton therapy. This could, for instance, be achieved by incorporating variable RBE in the optimization of IMPT in such a way as to confine high RBE protons to within the target volume and away from critical normal tissues.
This presentation will focus on proton therapy. For particles heavier than protons, the RBE is generally not assumed to have a fixed generic value. Nevertheless, considerable uncertainties exist in RBE for all particles, which can have a significant impact on outcomes.

Keywords: Proton Therapy, Relative Biological Effectiveness, Intensity-Modulated Proton Therapy

155
Induction of NSCs Quiescence and Neurogenesis Preservation in Mouse Adult Brain after FLASH Whole Brain Irradiation
P-G. Montay-Gruel[1,3], B. Petit[1], V. Favaudon[2], J. Bourhis[1], M-C. Vozenin[1].
[1]Radio-Oncologie/Radiothérapie, Centre Hospitalier Universitaire Vaudois, 1011 Lausanne, Switzerland
[2] INSERM U612, 91405 Orsay, France
[3]Université Paris-Sud XI, 91405 Orsay, France. Fellow of Ecole Normale supérieure de Cachan and Fond National Suisse

Most of adult stem cells are maintained in a quiescent state considered as a survival mechanism responding to DNA damages induced by ionizing radiation. Stem cells then are able to rapidly proliferate and are essential for restoration of tissue function. In the brain, Neural Stem Cells (NSCs) are known to be responsible for adult neurogenesis participating to cognition and Whole Brain Radiotherapy (WBRT) induces memory loss due to impaired neurogenesis. Here we compared the effect of FLASH versus conventional-RT on NSCs after WBRT and especially investigated quiescence and neurogenesis potential.
WBRT at FLASH and conventional dose rate was performed using LINAC prototypes. Mice received single doses RT at 50GyFLASH (>50Gy/s), 10GyCONV (0.04Gy/s) and sham-RT. Two months post-IR, before the sacrifice, cognitive tests were performed to evaluate memorization impairments. Two hours before the sacrifice animals received BrdU injection. Brains were collected for immunohistochemical analysis of NSCs quiescence using FoxO3-Sox2 (Renault et al. 2009).
We showed that 50GyFLASH-RT does not induce any macroscopic toxicity whereas 10GyCONV is the maximum tolerated dose (Acharya et al. 2009). We observed a memorization loss after 10GyCONV-RT whereas cognition is not affected at 50GyFLASH two months post-IR. At the same time point, SGZ BrdU+ clusters are maintained at doses up to 20GyFLASH whereas 10GyCONV totally impairs the

neurogenesis. Concerning quiescence, more Sox2+NSCs express FoxO3 after 30GyFLASH-RT than in CONV-RT groups. Nevertheless, the number of Sox2+FoxO3+NSCs decreases at higher doses probably due to the RT-induced cell death.
Altogether these results suggest that FLASH-WBRT induces different responses in the NSCs compared to CONV-RT. Indeed, FLASH-RT does not induce cognitive impairment two months post-IR compared to CONV-RT. This observation correlates with a preservation of neurogenesis in the SGZ. Moreover, after FLASH-RT, SVZ NSCs show a quiescent status which could explain their preservation after irradiation and their ability to re-induce neurogenesis.

Keywords: Neural Stem Cells ; Whole Brain Irradiation ; FLASH-RT

156

J-PET: a novel TOF-PET scanner based on plastic scintillators

P. Moskal[1*], D. Alfs[1], T. Bednarski[1], P. Białas[1], E. Czerwiński[1], A. Gajos[1], M. Gorgol[2], B. Jasińska[2], D. Kamińska[1], Ł. Kapłon[1,3], W. Krzemień[4], G. Korcyl[1], P. Kowalski[5], T. Kozik[1], E. Kubicz[1], M. Mohammed[1], Sz. Niedźwiecki[1], M. Pałka[1], M. Pawlik-Niedźwiecka, L. Raczyński[5], Z. Rudy[1], O. Rundel[1], N. G. Sharma[1],M. Silarski[1], A. Słomski[1], A. Strzelecki[1], A. Wieczorek[1,3], W. Wiślicki[5], B. Zgardzińska[2], M. Zieliński[1]
[1]Faculty of Physics, Astronomy and Applied Computer Science, Jagiellonian University, S. Łojasiewicza 11, 30-348 Kraków, Poland
[2]Department of Nuclear Methods, Institute of Physics, Maria Curie Sklodowska University, Pl. M. Curie-Sklodowskiej 1, 20 031 Lublin, Poland
[3]Institute of Metallurgy and Materials Science of Polish Academy of Sciences,
W. Reymonta 25, 30-059 Kraków, Poland
[4]High Energy Physics Division, National Centre for Nuclear Research, A. Soltana 7, 05-400 Otwock-Świerk, Poland
[5]Świerk Computing Centre, National Centre for Nuclear Research, A. Soltana 7, 05-400 Otwock-Świerk, Poland
* e-mail: p.moskal@uj.edu.pl ufmoskal@gmail.com

Purpose: The purpose of the reported research is the elaboration of the method for construction of the cost-effective whole-body single-bed positron emission tomography scanner enabling simultaneous PET/CT and PET/MRI imaging.
Material and methods**:** The Jagiellonian Positron Emission Tomography scanner (J-PET) is built out of axially arranged plastic scintillator strips, forming a cylinder [1]. The light signals produced in scintillators are converted to electrical pulses by photomultipliers placed at opposite ends of each strip [2]. The pulses are probed in the voltage domain by a newly developed electronics [1,3], and are collected by the novel trigger-less and reconfigurable data acquisition system [1,4]. The hit-position and hit-time of gamma quanta are reconstructed based on the time of arrival of light signals to the ends of the scintillator strips. The reconstruction procedures make use of the compressing sensing theory [5,6] and the library of synchronized model signals [1,7]. Moreover, for the image reconstruction novel algorithms are being developed and adopted for fast iterations on the graphics processing units [8].
For estimation of the J-PET characteristics the computer simulations were performed [9] using GATE package [10]. Simulations were conducted taking into account known physical and instrumental effects as e.g. photon emission spectrum, time distribution of emitted photons, losses and time spread of photons due to their propagation through the scintillator, as well as quantum efficiency and transit time spread of photomultipliers.
Results: In autumn 2015 a construction of the full scale J-PET prototype was completed. J-PET consists of 192 strips arranged axially in three layers forming a cylindrical diagnostic chamber with the diameter of 85 cm and axial field-of-view (AFOV) of 50 cm, and it is characterized by 300 ps coincidence resolving time.
The performance characteristics, simulated according to standards defined by the National Electrical Manufacturers Association (NEMA-NU-2)**,** indicate a comparable performance of the J-PET with respect to current TOF-PET modalities as regards e.g. accidental coincidences [9], sensitivity, scatter fraction and point spread function.
Conclusions: An axial arrangement of long strips of plastic scintillators, and their small light attenuation allows us to make a TOF-PET scanner with a longAFOV.
The estimated coincidence resolving time changes from 230 ps to 430 ps when extending AFOV from 16 cm to 100 cm.
This result opens perspectives for construction of the cost effective TOF-PET scanner with significantly improved TOF resolution and larger AFOV with respect to the current TOF-PET modalities [11,12].
The talk will include presentation of the J-PET scanner along with the description of its characteristics estimated according to NEMA-NU-2 standards, and presentation of perspectives of combining J-PET with CT and MRI.

Keywords: Time-of-Flight Positron Emission Tomography, Plastic Scintillators, PET/MRI

References:
[1] Patents granted: EP2454612B1, WO2011008119, EP2454611B1, WO2011008118 and further 14 International Patent Applications available at http://koza.if.uj.edu.pl/patents/ and at http://worldwide.espacenet.com/
[2] P. Moskal et al., Nucl. Inst. and Meth. A 764 (2014) 317.
[3] M. Pałka et al., Bio Algorithms and Med-Systems 10 (2014) 41.
[4] G. Korcyl et al., Bio-Algorithms and Med-Systems 10 (2014) 37.
[5] L. Raczynski et al., Nucl. Inst. and Meth. A 764 (2014) 186.
[6] L. Raczynski et al., Nucl. Instr. Meth. A 786 (2015) 105.
[7] P. Moskal et al., Nucl. Inst. and Meth. A 775 (2015) 54.
[8] P. Białas et al., Acta Phys. Polon. A 127 (2015) 1500.
[9] P. Kowalski et al., Acta Phys. Polon. A 127 (2015) 1505.
[10] S. Jan et al., Phys. Med. Biol. 49, 4543 (2004).
[11] Conti M, Eur. J. Nucl. Med. Mol. Imaging 38 (2011) 1147.
[12] Bettinardi V et al., Medical Physics 38 (2011) 5394.

157

Targeted Radionuclide Therapy with ^{161}Tb: Investigation of Anti-Tumor Effects and Undesired Side Effects

C. Müller[1], S. Haller[1], C. Vermeulen[1], U. Köster[2], G. Pellegrini[3], R. Schibli[1,4], N.P. van der Meulen[1,5]
[1] Center for Radiopharmaceutical Sciences ETH-PSI-USZ, Paul Scherrer Institute, Villigen-PSI, Switzerland
[2] Institut Laue-Langevin, Grenoble, France
[3] Laboratory for Animal Model Pathology (LAMP), Institute of Veterinary Pathology, Vetsuisse Faculty, University of Zurich, Zurich, Switzerland
[4] Department of Chemistry and Applied Biosciences, ETH Zurich, Zurich, Switzerland
[5] Laboratory of Radiochemistry and Environmental Chemistry, Paul Scherrer Institute, Villigen-PSI, Switzerland

Purpose: The radiolanthanide ^{161}Tb ($T_{1/2}$ = 6.89 d) emits ß$^-$-particles ($E_{ß^-}$ = 154 keV) similar to ^{177}Lu ($T_{1/2}$ = 6.64 d, $E_{ß^-}$ = 34 KeV), but also a significant number of Auger electrons (~12e$^-$/decay). This radiation profile may result in more efficient tumor cell killing, in particular, if the radioconjugate targets the cellular nucleus where DNA is damaged by the short-ranged Auger electrons. Herein, we investigated ^{161}Tb in combination with folate and somatostatin analogs in vitro and in vivo and compared the results to those obtained with the ^{177}Lu-labeled pendants.
Materials/methods: ^{161}Tb was produced via irradiation of a Gd target at the reactor at ILL and separated from the target material by ion exchange chromatography at PSI. A DOTA-folate conjugate (cm10, [1]) was labeled with ^{161}Tb and ^{177}Lu and investigated in mice. The KB tumor sizes were measured and undesired side effects were monitored by determination of body weights and blood plasma parameters (BUN, creatinine), as well as histological investigation, as previously reported [2]. DOTATOC and its analog DOTATOC-NLS, which contains a nuclear localizing signal (NLS), were labeled with

^{161}Tb (30 MBq/nmol) and investigated in vitro using somatostatin receptor-positive AR42J rat tumor cells. Viability and survival assays were performed in vitro.
Results: In vivo application of ^{161}Tb-folate (10 MBq) resulted in a reduced KB tumor growth and, as a consequence, in an increased survival time (54 d) of mice compared to those treated with ^{177}Lu-folate (10 MBq, 35 d) [3]. Based on BUN and creatinine plasma values and histological investigations of renal tissues, ^{161}Tb-folate did not result in more severe damage to the kidneys than ^{177}Lu-folate, however. In vitro investigations with ^{161}Tb-DOTATOC and ^{161}Tb-DOTATOC-NLS revealed comparable uptake into AR42J cells, but externalization of ^{161}Tb-DOTATOC-NLS was lower (~25%) than for ^{161}Tb-DOTATOC (~55%) after 6 h. After 2 h of incubation the fraction of internalized ^{161}Tb-DOTATOC-NLS, which was localized in the nucleus (~3%), was significantly higher than the fraction of ^{161}Tb-DOTATOC (<0.5%). AR42J cell killing after application of ^{161}Tb-DOTATOC-NLS was more effective (IC50 ~1.5 MBq/mL) than after treatment with ^{161}Tb-DOTATOC (IC50 ~8 MBq/mL).
Conclusion: Due to additional Auger electron emission, ^{161}Tb appears to be more effective for tumor treatment than ^{177}Lu. The effect caused by Auger electrons was found to be more powerful if the radioconjugate targets the cellular nucleus by means of a NLS. Interestingly, kidney damage was not enhanced after therapy with ^{161}Tb compared to the treatment with ^{177}Lu. Based on these findings, ^{161}Tb has a great potential to be used in future clinical practice as it may kill single cancer cells and cell clusters more efficiently than ^{177}Lu without causing additional side effects.

Keywords: ^{161}Tb, Auger electron, nuclear localizing signal

References:
[1] Müller et al. 2013 J Nucl Med 1:124-131.
[2] Haller et al. 2015 Nucl Med Biol 42:770-779
[3] Müller et al. 2014 Eur J Nucl Med Mol Imaging 41:476-485.

158
The GEMPIX detector for energy deposition measurements in Hadrontherapy
F. Murtas[1,2], M. Ciocca[3], S.P.George[1], A.Mirandola[3], A. Rimoldi[4], M. Silari[1], A. Tamborini[4]
[1] CERN
[2] LNF-INFN
[3] Centro Nazionale di Adroterapia Oncologica
[4] University of Pavia & INFN

A triple GEM detector with a 55 μm pitch pixelated ASIC for the readout has been used at CNAO in Pavia for a detailed measurements of energy deposition inside a water phantom. The detector was operated with a gas mixture of Ar CO_2 CF_4 at a moderate gain and the measurements were performed with a beam of 120 MeV protons and 330 MeV/u Carbon ions. The energy deposition was measured at different positions in depth allowing a 3D reconstruction of the beam inside the phantom as shown in the figure. A small number of single event upsets in the pixel readout appear only in the Bragg peak and the DAQ can recover them for each acquisition. A detailed simulation was performed with GEANT4 and it was found in good agreement with the experimental data.
The future uses and upgrade of this device, including its potential application in microdosimetry, are discussed.

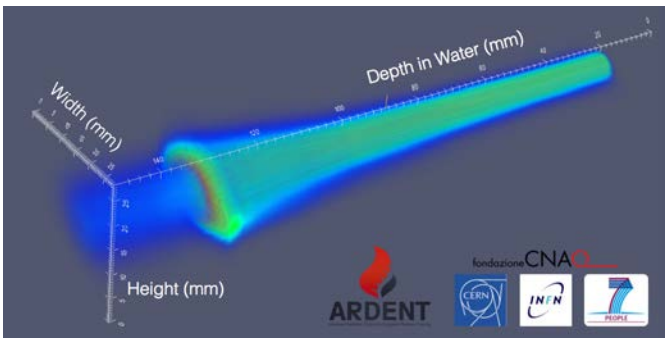

Keywords: GEM Detector, Timepix readout, Hadrontherapy

References:
[1] F.Murtas, Applications of triple GEM detectors beyond particle and nuclear physics, 2014 JINST 9 C01058
[2] S. P. George et al., Particle Tracking with a Timepix Based Triple GEM Detector, 2015 JINST_024P_0615
[3] P. Piersimoni et al., Optimization of a general-purpose, actively scanned proton beamline for ocular treatments: Geant4 simulations, Journal of applied clinical medical physics, volume 16, number 2, 2015

159
OPEN-MED: LEIR Based biomedical infrastructure @ CERN
M. Baumann[1,2,3,4], P. Lambin[5], S. Myers[6], G. Roy[6], M. Waligorski[7,8]
[1] OncoRay – National Center for Radiation Research in Oncology, Faculty of Medicine and University Hospital Carl Gustav Carus, Technische Universität Dresden, Helmholtz-Zentrum Dresden – Rossendorf, Dresden, Germany
[2] Department of Radiation Oncology, Faculty of Medicine and University Hospital Carl Gustav Carus, Technische Universität Dresden, Dresden, Germany
[3] Helmholtz-Zentrum Dresden - Rossendorf, Institute of Radiooncology, Dresden, Germany
[4] German Cancer Consortium (DKTK), Dresden and German Cancer Research Center (DKFZ), Heidelberg, Germany
[5] Maastro Clinic, Maastricht, The Netherlands
[6] CERN
[7] Institute of Nuclear Physics PAN, Radzikowskiego 152, 31-342 Krakow Poland
[8] Centre of Oncology (COOK), Garncarska 11, 31-115 Krakow Poland

The need for an open-access biomedical research facility was first raised by the scientific community at the 2010 Physics for Health workshop, where CERN was asked to take the lead on this initiative.
In 2012, a brainstorming meeting evaluated the possibility of modifying the existing CERN Low Energy Ion Ring (LEIR) accelerator to establish such an infrastructure. The medical and radiobiological communities united in broad agreement on the need for such a dedicated research facility.
The Biomedical facility at CERN (OPEN-MED) would create an open collaborative biomedical research infrastructure. By sharing the facility internationally, more rapid progress can be made by:

- Complementary collaboration with leading universities, research facilities and industry
- Comprehensively investigate complex physical and biological parameters that control radiation cell killing efficiency under highly controlled conditions.
- Provide accurate data for the modelling of radiation effects for proton and ion beam clinical applications
- Study comparative beam ballistics and dosimetry in phantoms and so improve predicted physical dose distributions.
- Provide a range of beams and infrastructure for developing new instrumentation for detection and imaging.
- Provide adequate beam time

It is essential that we develop a better understanding of how radiation interacts with cells at the cellular and molecular level, both to understand the nature of radiation-induced cancers resulting from radio-therapy and to devise more effective treatments, especially combining radiation therapy with other treatment modalities. Key to this is a more complete understanding of the underpinning radiobiology. OPEN-MED would aim to provide a coherent homogeneous database which is now necessary to take advantage of the recent rapid advances in cellular and molecular biology, using a wide range of human derived cells and eventually tissues. This requires advanced computational infrastructure which is also available at CERN.
Therefore it is proposed to convert the existing accelerator LEIR at CERN, which is used typically for a few months each year for pre-accelerating heavy ions (mostly lead) for the Large Hadron Collider, by adding a new set of ion sources (protons, light ions such as lithium, boron and carbon and perhaps heavier ions like oxygen and neon), a new extracted beam line and a radiobiology facility dedicated to radiobiology experiments for at least eight months of each year.
Unique features of the facility would be:

- A range of ions from proton to oxygen at the first stage, but using higher energies and other ions relevant for space radiobiology in a later second phase
- Versatile energy, charge, mass, beam switching and pulsed capabilities
- Versatile biological end station for optimal sample configuration and analysis
- Beam time availability for 8 months each year
- Internationally shared expertise

The facility would enhance research training standards with benefits to medical physics, radiation biology, radiation oncology and radioprotection. The data acquired would lead to an improved understanding of the technical requirements for the design of future accelerators and associated technology for cancer therapy. This strategy would provide the capability for a systematic assay of radiobiological properties, and be complementary to the clinical research in hospitals and other places, where in vivo and specific trials translating this work into clinical use can be performed.

Keywords: Radiobiology, ions, biomedical research, beam time, dosimetry, beam ballistics

References:
[1] M Dosanjh, B Jones, S Myers. A Possible Biomedical Facility at CERN. Brit J Radiology. May;86(1025-9), 2013.
[2] M. Holzscheiter, N Bassler, M Dosanjh, B. Singers-Sørensen, J. Overgaard. A community call for a dedicated radiobiological research facility to support particle beam cancer therapy

160
MRI Guided Proton Therapy: pencil beam scanning in an MRI fringe field
B. M. Oborn[1,2], S. Dowdell[2], P. E. Metcalfe[2,4], S. Crozier[5], S Guatelli[2], A. B. Rosenfeld[2], R. Mohan[6], P. J. Keall[7,4]
[1] Illawarra Cancer Care Centre, Wollongong, NSW 2500, Australia.
[2] Centre for Medical Radiation Physics, University of Wollongong, NSW 2500, Australia
[3] Shoalhaven Cancer Care Centre, Nowra, NSW 2541, Australia
[4] Ingham Institute for Applied Medical Research, Liverpool, NSW 2170, Australia
[5] School of Information Technology and Electric Engineering, University of Queensland, St Lucia, Qld 4072, Australia
[6] Department of Radiation Oncology, MD Anderson, Houston, Texas 77030.
[7] School of Medicine, University of Sydney, Sydney, NSW 2006, Australia

Purpose: To present novel modeling results showing the feasibility of proton pencil beam scanning (PBS) in the presence of an MRI scanner. This is a key requirement of potential future MRI Guide Proton Therapy systems [1].
Materials and Methods: Magnetic and Monte Carlo modelling of a 1 T split-bore MRI system[2] coupled with a proton pencil beam scanning assembly (Universal Head, IBA, Belgium) were performed (figure 1a). The impact of an active scanning PBS assembly on the MRI imaging potential was assessed as well as the impact of the MRI fringe field on performance of the PBS system.
Results: With the PBS assembly present the MR imaging field non-uniformity increased from 7 parts per million (ppm) to 55 ppm which is correctable via conventional shimming. With full scanning currents (active mode) the non-uniformity was 55+/-2.5 ppm. Thus MR image quality is expected to be maintained with dynamic scanning. Monte Carlo modelling further predicts that the MRI fringe field does not perturb the inherent magnetic deflection process of the PBS assembly. However once scanned, the pencil beams undergo an energy dependent and complex 3D deflection as they pass through the MRI fringe field[1]. Therefore a detailed calibration process is required to correct for each pencil beam so that PBS can be performed accurately. This correction process will be integrated in the plan optimization process to account for the magnetic field within a patient[3,4]. As an example, the path of a 170 MeV pencil beam is shown in a water phantom, and then what is required to obtain the same Bragg-peak with the fringe field (figure 1b and 1c). Both energy and direction changes are required.

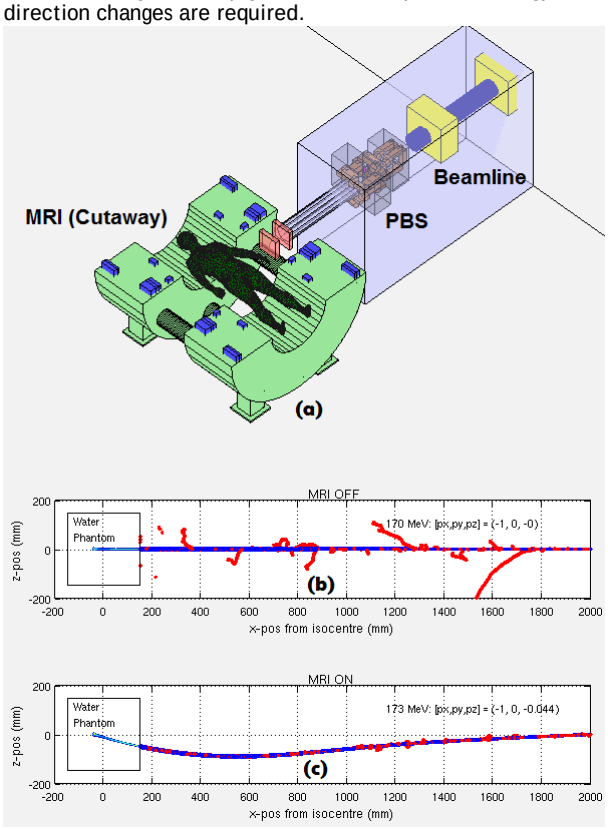

Figure1. (a) Layout of the MRI Guided Proton Therapy system showing the MRI scanner, patient location, and PBS assembly. (b) Path of a 170 MeV proton pencil beam (blue) with no MRI fringe field entering a water phantom. (c) Path of a steered 173 MeV pencil beam passing through the fringe field. Both of these beams have a Bragg-peak at 190 mm depth on the beam central axis. Secondary electrons are shown in red.

Conclusions: PBS in MRI-guided proton therapy appears feasible with current methods. Calibration of the inherent fringe field deflections of proton beams will be an essential part of the commissioning process. Future work will include modeling of the expected performance of beam monitoring devices in the presence of MRI fringe fields.

Keywords: MRI, proton therapy

References:
[1] "Proton beam deflection in MRI fields: Implications for MRI-guided proton
Therapy". Oborn, B. M. and Dowdell, S. and Metcalfe, P. E. and Crozier, S. and Mohan, R. and Keall, P. J., Medical Physics, 42, 2113-2124 (2015), DOI:http://dx.doi.org/10.1118/1.4916661
[2] Agilent Technologies, Oxford UK. This split-bore magnet design will be employed in the Australian MRI-linac Program.
[3] "Dosimetric feasibility of real-time MRI-guided proton therapy". Moteabbed, M. and Schuemann, J. and Paganetti, H., Medical Physics, 41, 111713 (2014), DOI:http://dx.doi.org/10.1118/1.4897570
[4] **"**Dosimetric feasibility of intensity modulated proton therapy in a transverse magnetic field of 1.5 T.**".** Hartman J, Kontaxis C, Bol GH, Frank SJ, Lagendijk JJ, van Vulpen M, Raaymakers BW. Phys Med Biol. 2015 Aug 7;60(15):5955-69. doi: 10.1088/0031-9155/60/15/5955.

161

Monte Carlo study of a high resolution monolithic silicon diode array for MRI-linac applications

M. Gargett[1], B. M. Oborn[2,1], S. Alnaghy[1], M. Petasecca[1], A. Rosenfeld[1], P. Metcalfe[1,3]
[1] Centre for Medical Radiation Physics, University of Wollongong, NSW 2500, Australia
[2] Illawarra Cancer Care Centre, Wollongong Hospital, NSW 2500, Australia
[3] Ingham Institute for Applied Medical Research, Liverpool, NSW 2170, Australia

Purpose: We undertake a preliminary Monte Carlo study to assess the suitability (in terms of radiation dose response) of a novel monolithic silicon detectoras a possible array detector for use in MRI-linac facilities.
Methods: The detector, named MagicPlate512 (M512), is a thin (470 μm) monolithic silicon with 512 diodes spaced 2 mm apart across a maximum detection area of 46 x 46 mm^2. The array has been designed specifically for small-field measurements [1]. Using the GEANT4 toolkit (v9.6.p02), the M512's geometry was simulated at 1.5 cm depth in a 30 x 30 x 30 cm^3 water phantom at 100 cm SSD. Phase space files based on the spectrum of a 6MV linac [2] were used as the particle source. Field sizes ranging from 0.5 x 0.5 cm^2 to 3 x 3 cm^2 were used. Uniform magnetic fields of strength 1 T and 3 T were applied, in both the in-line and perpendicular magnetic-field-to-photon-beam orientations. Simulations were run until the average of 100 runs gave 0.5% error along the central axis, which generally involved recycling particles 780 times (approx. 96 CPUh).
Results: In the in-line orientation, the M512 responds to within 3% of the water equivalent response, which is comparable to the zero-field case (see Figure 1 parts (a) and (b)). In the perpendicular orientation we see an over- and under- response in opposing penumbral regions respectively (along the Lorentz force vector running from left to right, see Figure 1 part (c)). The behavior in penumbral regions is similar to that of the silicon array detector previously investigated [3] by this group.
We also observed the consequences of a 2 mm air gap above the detector's sensitive volumes for the perpendicular field orientation; it caused a drop in output of (22.0 ± 0.5)% and (57.0 ± 0.5)% for 1 T and 3 T field strengths respectively, relative to the 0 T case.

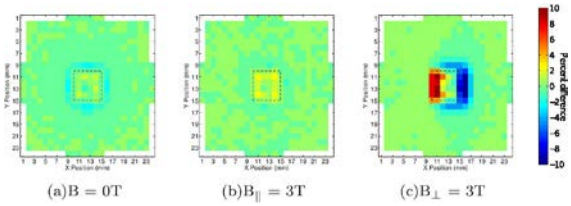

Figure 1: Dose-difference maps of the M512 compared to the water-equivalent case, for zero magnetic field (part (a)), a 3 T in-line magnetic field (part (b)) and a 3 T perpendicular magnetic field (part (c)). The dotted line represents the photon field edge (1 x 1 cm^2). Adjacent pixels are spaced 2 mm apart.

Conclusions: The M512 is expected to be a valuable tool for 2D dose-mapping in MRI-linac facilities, especially considering its closely pitched diodes for detecting changes to beam profiles in a magnetic field. Future work includes experimental validation of simulation results using a custom designed permanent magnet system.

Keywords: MRI-linac, silicon array detector, dosimetry

References:
[1] Aldosari, A. et al (2014), Med. Phys. 41(9) 091707
[2] Oborn, B. et al (2014), J. Phys.: Conference Series 489(1), 012020
[3] Gargett, M. et al (2015), Med. Phys. 42(2), 856

162

Application of biophysical modelling for normal tissue response with immunological aspects in radiotherapy

M. Oita[1], H. Aoyama[2], M. Sasaki[3], M. Tominaga[4], H. Honda[5], Y. Uto[6]
[1] Okayama University Graduate School of Health Sciences, Graduate School of Health Sciences, Okayama, Japan.
[2] Okayama University Hospital, Radiology, Okayama, Japan.
[3] Tokushima University Hospital, Radiology, Tokushima, Japan.
[4] The Tokushima University, Department of Radiological Technology- Institute of Health Biosciences, Tokushima, Japan.
[5] Ehime University Hospital, Radiology, Toon, Japan.
[6] The Tokushima University, Department of Life System-Institute of Technology and Science, Tokushima, Japan.

Purpose: Recent advances of immunotherapy make possible to combine with radiotherapy. Applying a radiobiological model for radiotherapy is one of the methods to optimize treatment plans and regimens, biologically. The aim of this study was to assess the NTCP model with immunological aspects[1,2)] including stochastic distribution as intercellular uncertainties.
Material/Methods: In the clinical 3D radiotherapy treatment planning system (Eclipse ver.11.0, Varian medical systems, US), biological parameters[3)] such as α/ß, n, m, TD_{50} including repair parameters (repair half-life) can be set as any given values to calculate the NTCP of normal tissues such as the rectum and bladder. Using a prostate cancer patient data with VMAT commissioned as a 6 MV photon beam of Novalis-Tx (BrainLab, US) in clinical use, the dose fraction protocols in this analysis were set as 70-78Gy/35-39fr, 72-81Gy/40-45fr, 52.5-66Gy/16-22fr, 35-40Gy/5fr of 5-7 fractions in a week. By use of stochastic biological model applying for Gaussian distribution, the effects of the NTCP variation of repair parameters of the immune system as well as the intercellular uncertainty of normal tissues have been evaluated.
Results: As respect to the difference of the α/ß, the changes of the NTCP between fraction schedules were increased especially in hypo-fraction regimens. The difference of the n, m affects the variation of the NTCP with the fraction schedules, independently. The elongation of repair half-time (long) increased the NTCP twice or much higher in case of hypo-fraction scheme. The effects of stochastic distributions of the α/ß affects the increase of the NTCP, however the distributions of the m affects decrease of the NTCP in case of hypo-fraction schemes.
Conclusion: We have shown the variety and difference of the α/ß, n, m, TD_{50} including repair parameters (repair half-life) of normal tissues compared to default fixed value, which have highly affected by probability of cell death and cure. Hypo-fractionation schemes seemed to have advantages for the variations of the m, while disadvantages for the variations of the α/ß. The possibility of an increase of the

α/β or TD_{50} in normal tissue by immunological aspects was expected to improve normal tissue response in radiotherapy. For more precise prediction of such optimal protocols, treatment planning systems should be incorporated the biological optimization in clinical practice.

Keywords: Immuno-radiotherapy, normal tissue response, NTCP

References:
[1] S.C. Formenti, S. Demaria. Combining radiotherapy and cancer immunotherapy: a paradigm shift. J Natl Cancer Inst. 105(4):256-65, 2013.
[2] P.G. Prasanna, H.B. Stone, R.S. Wong et al. Normal tissue protection for improving radiotherapy: Where are the Gaps? Transl Cancer Res. 1(1):35-48, 2012.
[3] R. G. Dale, B Jones. Radiobiological Modelling in Radiation Oncology. British Inst of Radiology, 2007.

163
Current Status of particle therapy at CNAO
R. Orecchia[1,2], M. Bonora[1], E. Ciurlia[1], M. R. Fiore[1], A. Facoetti[1], P. Fossati[1, 2], A. Iannalfi[1], B. Vischioni[1], V. Vitolo[1], M. Ciocca[1], E. Mastella[1], A. Mirandola[1], S. Molinelli[1], S. Russo[1], F. Valvo[1]
[1] Fondazione CNAO, Pavia, Italy.
[2] European Institute of Oncology, Milano , Italy

The Italian Center for Oncologic Hadrontherapy is up to date in the fifth year of its clinical activity. The total number of patients treated is 685 (up to November 2015). The treatments with carbon ions are about three times those with protons. An important part of treatments with carbon ions is directed on sarcomas, bones and soft tissue sarcomas, salivary glands tumours. In the table, treated patients are listed according to the clinical trials approved by the Italian Ministry of Health.
Another substantial part of treatments regards re-irradiation of several pathologies, especially head and neck re-treatments of several tumours.
An important goal reached in the last year is the treatment of moving targets. Pancreatic adenocarcinomas, hepatocellar carcinomas and pathologies located in moving sites are treated through the vertical beam line with gating and rescanning technology.
Treated volumes' issue has been discussed. Many pelvic sarcomas and chordomas cases refer to hadrontherapy treatment when already reached remarkable volumes. These cases are subject of discussion amongst radiation oncologists and medical physicists. The parameters taken in consideration are PTV (Planning Treatment Volume) and GTV (Gross Tumour Volume). They are statistically evaluated to elaborate the best treatment strategy in term of dose and planning option. This issue has also economic implications. The treatment of major tumour volumes using mostly more than one field occupies the treatment room for a period of time equal, when not superior, to two or more patients. The next challenge is to improve all steps to give such treatments in less time.
Most of the patients treated at CNAO are referred from Italian Cancer institutes but an increasing number of EU patients comes to Pavia through international agreements.
In the coming period CNAO is expected to receive the authorization to treat all the clinical case worth to receive hadrontherapy treatment.

Clinical study description	Particle	Total number of patients treated
Proton radiation therapy for chordomas and chondrosarcomas of the skull base	Protons	52
Proton therapy of spine chordoma and chondrosarcoma (amended)	Protons	16
Proton therapy of intracranial meningioma	Protons	24
Proton therapy of brain tumors	Protons	11
Proton therapy of recurrent cervico-cephalic area tumors	Protons	21
Proton boost for locally advanced cervico-cephalic area tumors	Protons	28
Proton therapy of glioblastoma	Protons	1
Proton re-irradiation of recurrent spine chordoma and	Protons	6
Carbon ion therapy of adenoid cystic carcinoma of salivary glands	Carbon ions	106
Carbon ion re-irradiation of recurrent pleomorphic adenomas	Carbon ions	19
Carbon ion re-irradiation of recurrent rectal cancer	Carbon ions	8
Carbon ion radiotherapy for bone and soft tissue sarcoma of cervico-cephalic area	Carbon ions	94
Carbon ion radiotherapy for bone and soft tissue sarcoma of trunk	Carbon ions	119
Carbon ion therapy of recurrent cervico-cephalic area tumors	Carbon ions	90
Carbon ion therapy of malignant melanoma of the mucous of the upper aerodigestive tract	Carbon ions	14
Carbon ion therapy for high risk prostate cancer	Carbon ions	9
Carbon ion therapy of primary and secondary orbital tumors	Carbon ions	13
Carbon ion therapy for pancreatic cancers	Carbon ions	11
Carbon ions therapy of primary malignant tumors of the liver	Carbon ions	4
Carbon ion re-irradiation of recurrent spinal chordoma and	Carbon ions	7
Protons and/or carbon ion integrated radiotherapy for poor prognosis in patients with inoperable sinonasal tumor	Protons/ Carbon ions	4
Other	-	28
		685

Keywords: carbon ions, gating, volumes.

References:
[1] Giordanengo S, Garella MA, Marchetto F, et al. The CNAO dose delivery system for modulated scanning ion beam radiotherapy. Med Phys. 2015 Jan;42(1:263-75.
[2] Via R, Fassi A, Fattori G, et al. Optical eye tracking system for real-time noninvasive tumor localization in external beam radiotherapy. Med Phys. 2015 May;42(5):2194.

164
Molecular imaging for theranostics
W.J.G. Oyen
The Institute of Cancer Research & The Royal Marsden Hospital, London, U.K.

Molecular imaging provides unique information on the tumor phenotype (i.e. tumor cells and tumor microenvironment), influencing treatment decisions and adaptation of therapy by early prediction of treatment outcome. With the increasing importance of systemic targeted therapies and of high precision external beam radiotherapy, interrogating tumor characteristics before and during therapy becomes increasingly important.
Key features like tumor metabolism, proliferation and protein synthesis can be depicted by the well-known radiopharmaceuticals FDG, FLT and e.g. FAZA, respectively. Furthermore, imaging receptor expression on tumor cells with e.g. radiolabeled antibodies and peptides can provide information on the presence, heterogeneity, accessibility, and modulation of these receptors for targeted therapies. Thirdly, small molecules like TKI may radiolabeled providing similar insight in tumor pathophysiology allowing better selection of patients likely to respond to treatment. A distinct form of theranostics utilizes targeting molecules, radiolabeled with an gamma or positron emission for imaging selecting patients for treatment with the same molecule, now radiolabeled with a beta-emitter.
In conclusion, various applications of theranostics provide crucial insight in tumor biology, the choice and adaptation of treatment, allowing better selection of treatment to achieve better outcomes for cancer patients.

Keywords: molecular imaging, theranostics, radiopharmaceuticals

165
Comparative evaluation of the in vitro the comet assay for the detection of genotoxic effects of 60 MeV protons and X-ray radiation

A. Panek [1], J. Miszczyk [1], K. Rawojć [2], J. Swakoń[3], T. Horwacik[3], L. Malinowski[3].
[1] Department of Experimental Physics of Complex Systems, The H. Niewodniczański Institute of Nuclear Physics Polish Academy of Sciences, Krakow, Poland
[2] Marian Smoluchowski Institute of Physics, Jagiellonian University, Krakow, Poland
[3] Cyclotron Center Bronowice, Proton Radiotherapy Group, The H. Niewodniczański Institute of Nuclear Physics Polish Academy of Sciences, Krakow, Poland

The aim of the study was to investigate the biological effects in human lymphocytes irradiated with the 60 MeV proton beam in the Bronowice Cyclotron Center IFJ PAN. The relative biological effectiveness (RBE) of the proton beam in comparison to X-ray's was estimated by the comet method.
Whole blood samples were collected from 5 healthy donors. For dose-response studies lymphocytes were used submerged in agarose on microscopic slides, set in a specially designed PMMA phantom located at the isocenter. Cells were irradiated in Eppendorf vessels located in the mead of Spread-Out Bragg Peak (SOBP) in the fully modulated proton beam with range of 29 mm.
For reference, the lymphocytes were exposed to the 250 kV X-rays. For both sources of radiations, dose-effect curves at a dose range (0-4Gy) were estimated. The level of DNA damage was assessed using the alkaline version of comet assay, also called the DNA single cell gel electrophoresis (SCGE).
The obtained dose-response relationships for the level of DNA damage showed linear character for both sources of radiation (R^2 = 0.994 for protons and R^2 = 0.995 for X-rays). The efficiency of protons in inducing DNA strand breaks for the dose range from 0.3 to 4 Gy calculated as the ratio of the two α coefficients was 1.37. The average RBE calculated from the proton and X-ray dose required for the iso-effective TDNA comet assay parameter was 1.51 + / - 0.05 (range 1.45-1.66).
This observation suggests that the standard alkaline comet assay is reliable technique for estimation of DNA damage caused by proton and X-ray radiation *in vitro*.

Keywords: Proton beam, Human lymphocytes, DNA damage

Note: These investigations were partially supported by grant DEC-2013/09/D/NZ7/00324 from the National Science Centre, Poland.

166
The project of radio-isotope complex RIC-80 at PNPI
V.N. Panteleev, A.E. Barzakh, L.Kh. Batist, D.V. Fedorov, V.S. Ivanov, S.A. Krotov, F.V. Moroz, P.L. Molkanov, S.Yu. Orlov, Yu. M.
NRC "Kurchatov Institute" PNPI, 188300, Gatchina,, Russia

Presently for production of medical radionuclides the cyclotrons are widely used which are very safe and reliable installations. At PNPI a high current cyclotron C-80 with the energy of extracted proton beam of 40-80 MeV and the current up to 200 μA has been constructed. One of the main goals of C-80 is production of a wide spectrum of medical radio-nuclides for diagnostics and therapy. At the beam of C-80 the project of radioisotope complex RIC-80 (Radio Isotopes at the cyclotron C-80) has been worked out. In the presented submission the project of RIC-80 complex is discussed, which includes three target stations for production of radio-nuclides for medicine. The peculiarity of the proposed radio-isotope facility is the use of the mass-separator with the target-ion source device as one of the target stations for on-line, or semi on-line production of a high purity separated radio-nuclides. The results on the target development for production of radio-isotope generator for PET diagnostics ^{82}Sr are presented.

Keywords: Radioisotopes for medicine, mass-separator, targets for radioisotope production

167
Fused Toes Homolog (FTS) regulates EGF-induced epithelial–mesenchymal transition (EMT) and migration of cervical cancer cells
W. Park[1], S. Muthusami[1], D.S. Prabakaran[1]and J. Yu[2]
[1]Department of Radiation Oncology, Chungbuk National University College of Medicine, Cheongju, 361-763, Republic of Korea
[2]Department of Environmental and Tropical Medicine, Konkuk University College of Medicine, Chungju, 380-701, Republic of Korea

Purpose: Epithelial–mesenchymal transition (EMT) allows tumor cells to acquire the capacity to infiltrate surrounding tissue and to ultimately metastasize to distant sites. Limited information is available on the regulation of EMT in cervical cancer. Epidermal growth factor (EGF) has beenreported as a potent stimulator of cervical cancer invasiveness. Upregulation of epidermal growth factor receptor (EGFR) expression is reported in the recurrent cervical cancer. Fused Toes Homolog (FTS) has been reported as a general regulator of AKT activity in the control of differentiation, proliferation, and apoptosis in many cell types. Importantly, studies from our laboratory have shown overexpression of FTS in cervical cancer specimens and the expression of this protein increases with advancement of the disease. Hence, we studied the role of FTS in EGF-induced EMT in cervical cancer cells.
Materials and Methods: A human cervical carcinoma cell line ME180 was used. Gene silencing was obtained using siRNA. Protein expression was studied by Western blot and immunofluorescence. Cell migration and invasion was assessed by wound healing and matrigel migration assay.
Results: EGF treatment induced the change of EMT markers and increased cell migration. EGF treatment also increased phosphorylated EGFR and ERK and nuclear level of ATF-2. The binding of ATF-2 to the promoter region of FTS was evidenced after EGF treatment. Pretreatment with PD98059 and gefitinib prevented EGF-induced FTS expression. FTS-silencing reduced EMT and cell migration by EGF treatment.
Conclusions: These results suggest that upregulation of FTS by EGF is mediated via EGF/EGFR/ERK/ATF-2 and this facilitates EGF-mediated EMT process in cervical cancer cells. FTS can be a potential target to circumvent cervical cancer progression driven by EGF.

Keywords: Fused Toes Homolog (FTS), Cervix cancer, Epithelial–mesenchymal transition (EMT)

168
Tuning of a 4D ML reconstruction strategy for treatment verification in ion beam radiotherapy
E. De Bernardi[1], K. Parodi[2], R. Ricotti[3], M. Riboldi[4], G. Baroni[4], C. Gianoli[2,5]
[1] Medicine and Surgery Department – Tecnomed Foundation, University of Milano-Bicocca, Milan, Italy
[2] Department of Experimental Physics - Medical Physics and Department of Radiation Oncology, Ludwig Maximilian University of Munich, Germany
[3] Department of Radiation Oncology, European Institute of Oncology, Milano, Italy
[4] Dipartimento di Elettronica, Informazione e Bioingegneria (DEIB), Politecnico di Milano, Italy
[5] Department of Radiation Oncology, Ludwig Maximilian University of Munich, Germany

Purpose: In PET-based treatment verification the low counting statistics PET data acquired during/after the treatment (Measured PET) must be compared to a Monte Carlo estimate of the β+ distribution induced by the treatment (Expected PET) based on the planning Computed Tomography (CT) images [1]. Given the extremely low quality of Measured PET images and the consequent difficulties in mismatch estimation, we proposed to use a 4D Maximum Likelihood (ML) reconstruction strategy considering Expected PET and Measured PET as two frames of a 4D dataset and providing an estimate of the motion field mapping one frame to the other [2].
The aim of this work is to optimize the strategy on a

simulated dataset mimicking real data characteristics, but provided with a ground truth for performance assessment.
Materials/methods: Three possible implementations of the 4D ML reconstruction strategies are considered and schematically represented in Fig. 1. Briefly, Method 1 (original version [2]) reconstructs the ß+ distribution in a virtual reference frame and estimates the motion fields mapping it to the Expected and to the Measured PET frames. Method 2 reconstructs it in the Expected PET frame and estimates the motion field mapping Expected PET to Measured PET. Method 3, conversely, reconstructs in the Measured PET frame and estimates the motion field taking Measured PET to Expected PET.
To initialize the reconstruction process a uniform activity distribution in the Filed Of View was considered. The three methods were validated on an analytical dataset simulating the ß+ distribution induced by two orthogonal beams on an inhomogeneous tissue on a 200x200x50 voxel grid with voxel size 2mm. Poisson statistics, 66% washout and Gaussian mismatch between Expected and Measured PET were considered.
Results were assessed after 30 iterations, by comparing: 1) the reconstructed Enhanced Measured PET with its ground truth, in terms of Normalized Mutual Information (NMI), Cross Correlation (CC) and Root Mean Square Error (RMSE); 2) the estimated motion field mapping Expected to Measured PET with its ground truth in terms of RMSE (RMSE_mot).
Results: Results are presented in Table.

	NMI	CC	RMSE	RMSE_mot
Method 1	1,55	0,93	0,06	2,30
Method 2	1,61	0,98	0,03	2,19
Method 3	1,59	0,98	0,02	2,22

Method 1 performs worst than the others since the number of motion unknown variables to be estimated is double. Method 2 and method 3 perform similarly. Reconstructions were all initialized with a uniform activity distribution. The possible improvements of method 2 achievable with an initialization corresponding to Expected PET have still to be assessed.
Conclusions: Three possible implementations of an innovative 4D ML reconstruction strategy for PET-based treatment verification have been compared on a simulated phantom mimicking real data. The two methods halving the number of motion variables showed better performances.

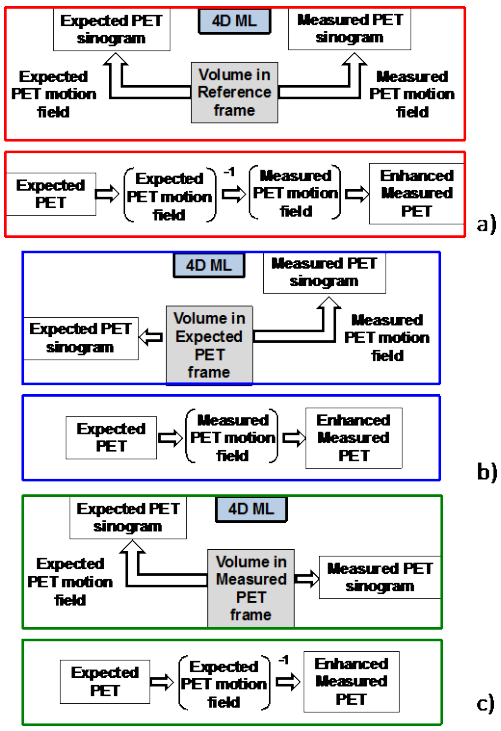

Figure1: The three compared methods are illustrated: a) Method 1, b) Method 2 c) Method 3.

Keywords: Treatment verification, 4D ML reconstruction, ion beam radiotherapy

References:
[1] K. Parodi, "PET monitoring of hadrontherapy" Nuclear Medicine Review, vol. 15(C), pp. 37-42, 2012.
[2] De Bernardi E et al, "4D ML Reconstruction as a tool for volumetric PET-based Treatment Verification in Ion Beam Radiotherapy", under review in *Medical Physics*

169
FRED: a fast MC tool for treatment planning and dose verification in proton therapy
G.Battistoni[1], M.Ciocca[2], G.Magro[2], A. Mairani[2], S.Molinelli[2], V.Patera[3], S. Pioli[4], A. Schiavi[3], M. Senzacqua[3]
[1] Istituto Nazionale di Fisica Nucleare, Sezione di Milano, Italy
[2] CNAO, Centro Nazionale di Adroterapia Oncologica, Pavia, Italy
[3] Universita' di Roma "La Sapienza", Rome, Italy
[4] Istituto Nazionale di Fisica Nucleare, Laboratori Nazionali di Frascati, Italy

Purpose: Particle therapy is an approach to tumor treatment which uses ion beams (in particular protons and carbon ions). The peculiar dose-depth relation of charged particles, that release most of their energy at the end of their range, enhances the dose conformity and the possibility to spare the healthy tissues. To exploit these features, the charged beam parameters needs to be carefully optimized by the Treatment Planning Systems (TPS).
Commercial TPS are based on analytic representation in water (WEPL approach) of the patient and produce results in time of the order of hour(s). On the other hand Monte Carlo (MC) simulations can accurately take into account beam particle interactions, patient tissue morphology and elemental composition. Their application in the clinical routine is prevented by the huge amount of CPU needed to simulate the evolution of the beam in the patient.
We developed a software (FRED) for MC dose calculation and Treatment Planning optimization for proton therapy that runs both on CPU and on GPU (Graphics Processing Units). FRED has been tailored on the CNAO delivery system in view of applications such as an independent dosimetric verification of TPS dose distributions and a fast recalculation of the TPS taking into account daily residual positioning uncertainties.
Materials/Methods: FRED transports the protons in a voxelized geometry of the patient, retrieved from the DICOM information of the CT. The voxel HU of the CT is converted in elemental composition following the method by Schneider[1]. The stopping power is computed using conversion factors from the PSTAR tabulated values in water. Different models (single Gaussian, double Gaussian, Rutherford) can be used to reproduce Multiple Coulomb Scattering, while secondary protons and deuterons are produced in the beam nuclear interaction following the multiplicity, energy and angular distributions provided by ICRU63, and interpolated for other materials. Alpha and heavier fragments produced are treated as local dose deposition and (in this version) neutral particles are not produced. The RBE value of the proton is kept constant, but FRED could be easily interfaced with a library of RBE values. The FRED MC dose matrix can be processed by an optimizer based on a least-squares optimization algorithm as in [2]. All the output/input system has been adapted to the CNAO environment.
Results: The agreement between the CNAO clinical depth-dose database and the FRED results is within 1%.

In Figure 1, as an example of the clinical-like capabilities of FRED, a satisfactorily comparison between the DVH obtained by FRED and by MCTPS [3] and a TPS commercial software is shown.

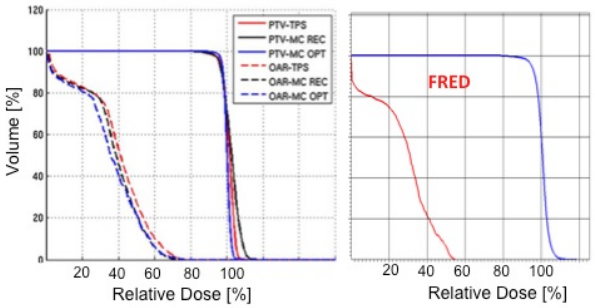

Figure 5 Comparison between the DVH from Fred and ref [3]

The time needed to trace the protons and optimize the dose is 20 s on 4x GPU NVIDA GTX 980 machine. The MC speed is 0.33 μs/primary.

Conclusions: The satisfactorily dosimetric agreement between FRED predictions and TPS/dosimetric data supports its future use at CNAO as fast dose recalculation tool *based on in room patient geometry* and as an independent patient plans verification platform.

Keywords: Proton therapy, MC, GPU

References:

[1] Schneider et al.1996 Phys. Med. Biol. 41 111
[2] Lomax et al 1999 Phys. Med. Bio. 44 185-205
[3] Mairani et al., 2013 Phys Med Bio . 58, 2471-2490

170

Radiolabeled Acridine Orange (AO) Derivatives as DNA-Targeted Probes for Auger Therapy

E. Pereira[1], L. Quental[1], M.C. Oliveira[1], P. Raposinho[1], A. Belchior[1], S. Di Maria[1], I. Correia[2], J. Lavrado[3], F. Mendes[1], P. Vaz[1], Isabel Santos[1], A. Paulo[1]
[1] Centro de Ciências e Tecnologias Nucleares, IST, Universidade de Lisboa, Estrada Nacional 10, 2695-066 Bobadela LRS, Portugal.
[2] Centro de Química Estrutural, IST, Universidade de Lisboa, Av. Rovisco Pais 1, 1049-001 Lisboa, Portugal
[3] iMed.ULisboa, Faculdade de Farmácia, Universidade de Lisboa, Av. Prof. Gama Pinto, 1649-003 Lisboa, Portugal

In recent years, some Auger-emitting radionuclides clinically used for imaging/diagnostics started to be envisaged also for selective and targeted radiotherapy. Among the Auger-emitting radionuclides, ^{125}I is of particular interest, as it emits about 20 electrons per decay, as opposed to 4 electrons per decay emitted by ^{99m}Tc. Nevertheless, ^{99m}Tc still is the most used radionuclide in diagnostic Nuclear Medicine; therefore, the possibility of Auger therapy with ^{99m}Tc should open new avenues in cancer theranostics. Auger electrons travel a short distance within human tissues (about 1-10 nm) and, thus, the Auger-emitting radionuclide must be transported to the cell nucleus to elicit DNA damage.
Following previous encouraging results,[1] we have designed and evaluated ^{99m}Tc(I)/Re(I) tricarbonyl complexes and $^{125/127}$I heteroaromatic compounds that contain an AO group for enhanced nuclear uptake and strong DNA intercalation. To have an insight on the relevance of these radiolabeled compounds for DNA-targeted Auger therapy we have investigated: i) their ability to cause DNA chain breaks; ii) the influence of the two different radionuclides in DNA damage; iii) the effect of the distance between the AO intercalating unit and the radioactive atom (^{99m}Tc or ^{125}I). To address these issues several studies were carried out: i) evaluation of DNA binding and DNA damage; ii) cellular and nuclear internalization experiments; iii) □-H$_2$AX assays; iv) molecular docking and v) nanodosimetric calculations.
Both classes of compounds are able to induce DNA double strand breaks (dsb) (either in plasmids or in tumor cells) but the extent of DNA damage (e.g. dsb yield) and the role of direct effects are strongly dependent on the linker used to attach the Auger emitting radionuclide (^{125}I or ^{99m}Tc) to the AO moiety. Experimental data were corroborated by the docking and nanodosimetric studies; furthermore, most of the tested compounds presented a moderate to high uptake in tumor cells, with a significant accumulation in the cell nucleus. Altogether, these results give impetus to pursue with the pre-clinical evaluation of these radiolabeled AO derivatives as new radioactive probes for anticancer Auger therapy.

Acknowledgements: This work was funded by FCT: projects EXCL/QEQ-MED/0233/2012 and UID/Multi/04349/2013, and FCT Investigator Grants to I Correia and F Mendes.

References:

[1] Esteves, F. Marques, A. Paulo, J. Rino, P. Nanda, C. J. Smith, I. Santos, Nuclear targeting with cell-specific multifunctional tricarbonyl M(I) (M is Re, ^{99m}Tc) complexes: synthesis, characterization, and cell studies, J. Biol. Inorg. Chem. 16 (2011) 1141–1153.

171

The efficacy of IMRT, VMAT and IMPT to deliver highly conformal FET-PET guided boost in gliomas

J.B.B. Petersen[1], A.I.S. Holm[1], K. Seiersen[1], P. Borghammer[2], S. Lukacova[3]
[1]Department of Medical Physics, Aarhus University Hospital, Aarhus, Denmark
[2]Department of Nuclear Medicine & PET Centre, Aarhus University Hospital, Aarhus, Denmark
[3]Department of Oncology, Aarhus University Hospital, Aarhus, Denmark

Purpose: Radiotherapy plays an important role in treatment of gliomas even though the clinical outcome is relatively poor, mainly due to local failure. A higher uniform tumour dose may however increase the risk of adverse effects, especially for lager target volumes.
A selective boost to the ^{18}F-fluoro-ethyl-tyrosine (FET)-PET active volume, might prolong time to progression without increasing the risk of adverse effects. The present treatment planning study investigate and compare the ability of three techniques, VMAT, IMRT and IMPT to deliver a high conformal high dose boost to the BTV in patients with gliomas.
Material/methods: Seven patients with a pre therapeutic FET-PET/CT and MRI were used in the study.
For each patient a standard IMRT treatment plan giving 60 Gy in 30 fractions to the BTV and 46 Gy to the CTV(46 Gy) was calculated as a benchmark. A CTV(46 Gy) was defined as tumor and/or tumor cavity added a 2 cm margin. The BTV was defined from the FET PET and covered a tumor-to-brain cut-off ratio of FET uptake ≥ 1.6 (pre-surgery) and ≥ 2.1 (post-surgery). Both BTV and CTV(46 Gy) were modified to respect anatomic barriers. Planning target volumes (PTV), PTV(boost) and PTV(46 Gy) were generated by uniformly expanding the BTV and CTV(46 Gy), respectively with 3mm. The standard IMRT plans were used to define the base level of dose to the organs at risk (OAR) and PTV(46 Gy) homogeneity. To evaluate the dose to the OAR the mean dose was used. The PTV(46 Gy) homogeneity was defined as the volume of PTV(46 Gy) subtracted PTV boost which received more than 107% of the prescribed 46 Gy. The IMRT, VMAT and IMPT dose escalating treatment plans were optimized in order to get the highest achievable mean PTV boost dose, without increasing the mean dose to critical OAR and without decreasing the PTV(46 Gy) homogeneity. For all plans the dose boost was given as the integrated boost over 30 fractions. All treatment plans were carried out using the Eclipse treatment planning system (Varian Medical systems, Palo Alto, CA, USA).
Results: A standard IMRT plans were calculated for all patients and the base level for PTV(46 Gy) homogeneity was found to range between 65 % to 86 %, with a median value of 77%. Dose escalating, while maintaining this homogeneity, was found feasible using all three techniques. The mean doses to PTV(boost) were 77.1Gy, 79,2Gy and 85.1Gy for

IMRT, VMAT and IMPT respectively and the maximum doses were 82.5Gy, 87.4Gy and 89.9Gy. On top of the significant increase in mean and maximum PTV boost dose obtained for IMPT, the PTV(46 Gy) homogeneity can be improved to a median value of 30.4%.
Conclusion: Dose escalating a FET PET based target volume to above 77 Gy in 30 fractions by IMRT, VMAT, and IMPT without increasing both the PTV(46 Gy) homogeneity and the mean dose to the OAR was found feasible. For IMPT the PTV(46 Gy) homogeneity was substantially improved, implicating a reduction of the risk of morbidity.

Keywords: Treatment technique comparison, biological guided treatment planning, Particle therapy

172
Dosimetry of ultra high dose rate irradiation for studies on the biological effect induced in normal brain and GBM
K. Petersson[1]* M. Jaccard[1]*, MC. Vozenin[2,3], P. Montay-Gruel[2,3], F. Trompier[4], T. Buchillier[1], JF. Germond[1], F. Bochud[1], J. Bourhis[2], C. Bailat[1]
[1] Institute of Radiation Physics (IRA), Lausanne University Hospital, Lausanne, Switzerland
[2] Department of Radiation Oncology, Lausanne University Hospital, Lausanne, Switzerland
[3] Radio-oncology laboratory, Lausanne University Hospital, Lausanne, Switzerland
[4] IRSN, Fontenay aux roses, France
* Equal contribution to the work

Purpose: Published studies concerning radiotherapy at ultra high dose rate (Flash) show a possible increase in the differential response between normal and tumour tissue compared to conventional radiotherapy [1-2]. Since we have access to a prototype linac capable of pulsed electron irradiation at those dose rates, we have setup a research program to investigate the biological effects of Flash irradiation on normal tissues and tumours. Irradiations at ultra high dose rates means short (< 1 s) beam-on times with a very intense beam. This makes the dosimetric precision needed for pre-clinical studies rather challenging. The overall purpose of our project is to address all technical and dosimetric questions related to irradiation at ultra high dose rates, along with pre-clinical studies.
Material and methods: The first step of the program was to investigate if the standard types of dosimeters can still be used for electron absolute dosimetry in these radiation intense conditions, especially for ionization chambers which are known to saturate. Hence, dose rate dependence was investigated for a wide variety of dosimeters used in radiotherapy by studying their response at various dose rates. The second step was to investigate the relative biological effect. Normal tissue toxicity and GBM response was studied in vitro and in mice after whole brain irradiation with Flash and at conventional dose rate.
Results: Four of the tested dosimeters (Radiochromic film (Gafchromic EBT3), TLD, Alanine pellets, and a chemical dosimeter based on Methyl Viologen) showed no dose rate dependence. The response of the Advanced Markus ionization chamber (PTW-Freiburg) was measured to depend only on the dose-per-pulse and unlike most ion-chambers did not saturate completely in our beam. Consequently, the chamber can still be used after correction from ion collection efficiency (Figure). With the use of these dosimeters we then have the precision in dose delivery (uncertainty ≈ 5%) needed to perform pre-clinical radiobiological studies. Studies were conducted on Neural Stem Cells (NSCs) and showed that the neurogenesis was preserved at doses up to 20 Gy with FLASH, whereas 10 Gy was sufficient at conventional dose rate to totally impair the neurogenesis, at the same time point. The preservation of neurogenesis was associated with preserved cognitive skills. Studies on GBM response are ongoing.

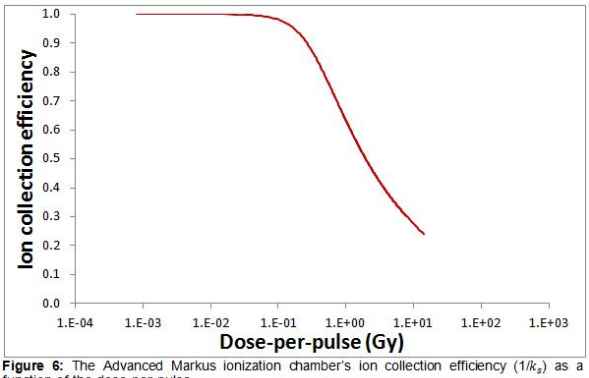

Figure 6: The Advanced Markus ionization chamber's ion collection efficiency ($1/k_s$) as a function of the dose-per-pulse.

Conclusions: Radiotherapy treatment at ultra high dose rate is almost instantaneous (< 1 s) and it could be the next major treatment improvement in medical radiation oncology. Our dosimetric measurements show that a variety of standard dosimeters can still be used for accurate dose determination at these dose rates and our first pre-clinical studies show that FLASH irradiation induces different responses in the brain NSCs compared to irradiation at conventional dose rate.

$$\frac{1}{k_s} = \frac{1}{\left(1+\left(\frac{0.3}{Dose-per-pulse}\right)^{-2}\right)^{a}} \Leftrightarrow k_s = \left(1+\left(\frac{Dose-per-pulse}{0.3}\right)^{2}\right)^{a}$$

Keywords: Flash irradiation, Dosimetry

References:
[1] Favaudon V, Caplier L, Monceau V, Pouzoulet F, Sayarath M, Fouillade C, Poupon M F, Brito I, Hupe P, Bourhis J, Hall J, Fontaine J J and Vozenin M C. 2014. Ultrahigh dose-rate FLASH irradiation increases the differential response between normal and tumor tissue in mice. Science translational medicine. 6 245ra93.
[2] Favaudon V, Fouillade C and Vozenin M C. 2015. Ultrahigh dose-rate, "flash" irradiation minimizes the side-effects of radiotherapy. Cancer radiotherapie : journal de la Societe francaise de radiotherapie oncologique. 19 526-31.

173
Extremely high-granularity digital tracking calorimeter for the estimation of proton energy in proton Computed Tomography
H. Pettersen[1], D. Röhrich[2], E. Rocco[3], T. Peitzmann[3], O. H. Odland[1]
[1] Haukeland University Hospital
[2] University of Bergen
[3] Utrecht University

A compact, high-granularity digital calorimeter detector is a candidate for a high-speed Bragg Peak detector, for use in proton Computed Tomography. Applications range from dose plan validation before particle therapy to proton Stopping Power Ratio estimates prior to dose planning. Due to the large number of pixels the device will be able to cope with large particle multiplicities, thus providing a breakthrough in rate capabilities.
The development of this device profits from R&D performed for high-energy physics experiments. In this context, a small prototype, a silicon/tungsten sandwich calorimeter (4 cm x 4 cm x 10 cm total volume) with 24 layers of Monolithic Active Pixels Sensors (30 µm x 30 µm pixel size) has been constructed [2]. As a proof of principle for its application in therapy, the prototype has been irradiated with therapeutic proton beams ranging in energy from 122 MeV to 190 MeV, where the protons are stopped in the detector. A similar setup is reproduced in the Monte Carlo code GATE/Geant4 [3] for validation and optimization.
Detector performance from these tests will be presented. Of importance is the conversion of an energy signal into a charge diffused binary signal, which leads to an

approximation of the energy deposited by each individual proton in each layer.
A tracking algorithm is able to find the water equivalent path length of each individual proton. When this information is combined with the approximated energy deposition on each layer, an estimate of the incoming proton energy is obtained by locating the high energy deposit of the Bragg Peak.
Results from this analysis, as well as the capabilities of alternative setups will be presented, to show the feasibility of using such a calorimeter for proton Computed Tomography.

This project is supported by Helse Vest PhD grant 911933.

Keywords: Calorimeter, Hadron Therapy, Pixel Sensors

References:
[1] T. Peitzmann, *Prototype studies for a forward EM calorimeter in ALICE, Proceedings of CHEF2013*, preprint arXiv:1308.2585.
[2] D. Fehlker *et al*. *Electronics for a highly segmented electromagnetic Calorimeter prototype.* TWEPP 2012; 2012-09-17 - 2012-09-21.
[3] S. Jan *et al*., *GATE: a simulation toolkit for PET and SPECT*. Phys. Med. Biol. 49 4543 (2004).

174
Proton Minibeam Radiation Therapy (pMBRT): implementation at a clinical center
C. Peucelle[1], C. Nauraye[2], A. Patriarca[2], L. de Marzi[2], E. Hierso[2], N. Fournier-Bidoz[2],
I. Martínez-Rovira[1] and Y. Prezado[1]
[1] IMNC – UMR 8165, IN2P3-CNRS, Université Paris 7, Université Paris 11, Orsay, France
[2] Institut Curie – Centre de Protonthérapie d'Orsay (ICPO), Orsay, France

Purpose: The more selective energy deposition of protons in depth is advantageous compared to photons to preserve normal tissues. Nevertheless, an even better tissue sparing might be possible in proton therapy if combined with the well-established tissue preservation of spatially fractionated submillimetric beams. This sparing effect has been observed in studies performed with synchrotron minibeam radiotherapy (MBRT) [1,2].
The innovative approach proposed here, called proton minbeam radiation therapy (pMBRT), was shown to lead to favorable dose distributions in Monte Carlo (MC) studies [3]. The dose profiles in normal tissue consist in peaks and valleys, while the tumour receives a (quasi)-homogenous dose distribution [3]. The goal of this study was to implement this promising approach at a clinical center, as well as to gather a complete set of dosimetric data that will serve to guide the ongoing biological experiments [4].
Material and Methods: The implementation of pMBRT was carried out at the Proton Therapy Center in Orsay (ICPO). 100 MeV-proton minibeams (400 and 700 µm-width) were generated by means of a multislit collimator. The dose distributions (depth dose curves, lateral profiles, peak-to-valley dose ratios (PVDR) [6], beam widths and output factors) were measured by means of Gafchromic EBT3 films and the new PTW microDiamond detector [5].
In parallel, a very first MC-based calculation engine for pMBRT is under development using Gate v7.0.
Results: The experimental data confirm that a spatial fractionation of the dose is maintained in normal tissues (PVDR up to 7) while a quasi-homogeneous dose distribution is reached at the Bragg peak location, in agreement with theoretical predictions [3]. The reduced penumbras (600-1100 µm) in healthy tissue make pMBRT a good candidate for radiosurgery applications.
Similar results were obtained using either EBT3 films or the PTW microDiamond detector. The preliminary MC calculations were consistent with experimental dose distributions.
Conclusion: This is the first work providing both a complete set of dosimetric data in such small proton field sizes and a practical implementation of this promising approach using a clinical set-up and beam energy. The dose distributions showed the potential of this technique, which might lead to a reduction of the normal tissue complication probability. Animal irradiation experiments are ongoing to confirm the normal tissue sparing capability of pMBRT.

Keywords: Proton Minibeam Radiation Therapy (pMBRT), small field dosimetry, novel approaches

References:
[1] P. *Deman et al.*, Int. J. Radiat. Oncol. Biol. Phys., 82 (2012)
[2] *Y. Prezado et al.*, Rad. Research 2015
[3] *Y. Prezado et al.*, Med. Phys. 40 (3) (2013).
[4] *C. Peucelle et al.*, *submitted, Med. Phys.*
[5] PTW website (www.ptw.de), microDiamond – Synthetic Diamond Detector Specifications
[6] *F. A. Dilmanian et al., J. Neuro-Oncol. 4, (2002).*

175
Contribution of direct and bystander effects to therapeutic efficacy of alpha-RIT using ^{212}Pb-labeled mAbs
R. Ladjohounlou[1,2,3,4], A. Pichard[1,2,3,4], V. Boudousq[1,2,3,4], S. Paillas[1,2,3,4], M. Le Blay[1,2,3,4], C. Lozza[1,2,3,4], S. Marcatili[5], M. Bardiès[5], J. Torgue[7], I. Navarro-Teulon[1,2,3,4] and J-P Pouget[1,2,3,4]
[1] IRCM, Institut de Recherche en Cancérologie de Montpellier, Montpellier, F-34298, France
[2] INSERM, U1194, Montpellier, F-34298, France
[3] Université de Montpellier, Montpellier, F-34090, France
[4] Institut régional du Cancer de Montpellier, Montpellier, F-34298, France
[5] UMR 1037 INSERM/UPS, Centre de Recherche en Cancérologie de Toulouse, Toulouse F-31062, France
[7] AREVA Med, 4800 Hampden lane, Bethesda, MD 20814, USA

Purpose: We assessed *in vitro* and *in vivo* the relative contribution of direct and bystander effects in the therapeutic efficacy of RIT using ^{212}Pb-labeled mAbs for treating cancer cells.
Materials and Methods: A-431 cells were *in vitro* exposed to increasing activities (0–0.5 MBq/mL; 37 MBq/mg) of either 35A7 (anti-CEA), Trastuzumab (anti-HER2) or PX (non-specific) ^{212}Pb-labeled mAbs. The relative contribution of direct and bystander effects was determined using standard medium transfer protocol. Biological end points included clonogenic survival and DNA double strand breaks (using 53BP1 and gamma-H2AX immunofluorescence detection) measured both in donor (direct effect) and in recipient cells (bystander effects). *In vivo*, nude mice with intraperitoneal (i.p.) 2-3 mm A-431 tumour cells xenografts were i.p. injected with increasing activities (370–1480 kBq; 37 MBq/mg) of the above mentioned anti-CEA, anti-HER2 or non-specific ^{212}Pb-mAbs. Tumour growth was determined and the distribution of radioactivity at the tissue level was assessed using digital micro-autoradiography (DAR) followed by voxel dosimetry. Biological markers including 53BP1 and Ki67 proteins together with abnormal mitosis were also determined on tumour sections.
Results: *In vitro* we showed in donor cells the strong efficacy of ^{212}Pb-35A7 and ^{212}Pb-trastuzumab mAbs and also to a lower extent of ^{212}Pb-PX mAb. Significant bystander cytotoxicity was measured in all recipient cells with the three radiolabeled mAbs. The complexity of DNA damage (53BP1 foci) observed in donor cells confirmed the high LET cytotoxic effects of ^{212}Pb-mAbs while less complex damage were observed in recipient cells.
In vivo DAR and voxel dosimetry indicated the strong heterogeneity in anti-CEA ^{212}Pb-mAbs distribution in tumours. Conversely, distribution of anti-HER2 ^{212}Pb-mAbs was much more homogeneous. These data could explain the lower therapeutic efficacy of the latter mAbs compared with anti-HER2 ^{212}Pb-mAbs (median survival of 94 days for anti-CEA ^{212}Pb-mAbs versus 20 days for control, not reached for anti-HER2 ^{212}Pb-mAbs). Moreover, voxel dosimetry indicated that about 30% of the tumours of mice treated with anti-CEA ^{212}Pb-mAbs received 0Gy. However, we also observed in the same tumours, homogeneous formation of DNA damage

independently of absorbed doses distribution, together with abnormal mitosis. The latter results indicate that bystander effects could also be involved. However, at this stage, we may assume that they do not fully counterbalance the lack of efficacy due to heterogeneous distribution of anti-CEA ^{212}Pb-mAbs, possibly because lesions are not as complex as those produced by high LET radiation.
Conclusions: Our results showed *in vitro* and *in vivo* that, besides the strong direct effect of ^{212}Pb-labeled mAbs in killing tumour cells, bystander effects have also to be considered.

Keywords: Radionuclide therapy, Radiobiology, Bystander effects

176
Predictive Biomarkers for Improving Radiation Therapy
P. Prasanna
Radiation Research Program
National Cancer Institute, National Institute of Health, Bethesda, MD, USA.
Pat.Prasanna@nih.gov

Radiotherapy is an important treatment modality for millions of patients with cancer worldwide. Current treatment decisions do not take into account individual patients' or cohorts of patients' sensitivities to this treatment modality. As such, patients treated with radiation therapy experience a large variation in normal tissue toxicity that results in dose-limiting acute and irreversible progressive side effects. Important examples of these adverse effects include mucositis, pneumonitis, and cognitive damage, respectively representing acute, intermediate, and late effects. Stratification of patients based on radiation sensitivities will allow delivery of suitable alternative treatments to high-risk patients and dose escalation to tumors in less sensitive patients. Current focus on radiation biomarkers/biodosimeters appears to be primarily to assess radiation doses after catastrophic accidental radiation exposure. Recent advances have brought together several cross-disciplinary areas such as biological assays, analytical platforms, and algorithms to rapidly assess dose to individuals. These technologies are at different maturation levels. This immense progress is also an opportunity to use them to predict heterogeneity of radiation sensitivities among cancer patients to improve radiation therapy outcome and their quality of life. This talk will emphasize the need for discovery, development, and validation of predictive biomarkers, provide some examples of biomarkers, and discuss the translational challenges involved in leveraging advances in radiation-specific biomarker research to radiotherapy, which for the foreseeable future likely to remain a cornerstone of cancer treatment.

Disclaimer: Author declares no conflict of interest. Views expressed here are the personal views of the author and does not represent the views of NCI.

177
Prompt gamma imaging of passively shaped proton fields with a knife-edge slit camera
M. Priegnitz*[1], S. Barczyk*[2,3], I. Keitz[2], S. Mein[2], F. V. Stappen[6], G. Janssens[6], L. Hotoiu[6], J. Smeets[6], F. Fiedler[1], D. Prieels[6], W. Enghardt[2-5], G. Pausch[2], C. Richter[2-5]
[1] Helmholtz-Zentrum Dresden – Rossendorf, Institute of Radiation Physics, Bautzner Straße 400, 01328 Dresden, Germany
[2] OncoRay – National Center for Radiation Research in Oncology, Faculty of Medicine and University Hospital Carl Gustav Carus, Technische Universität Dresden, Helmholtz-Zentrum Dresden-Rossendorf, Dresden, Germany
[3] Department of Radiation Oncology, University Hospital Carl Gustav Carus, Technische Universität Dresden, Dresden, Germany
[4] Helmholtz-Zentrum Dresden – Rossendorf, Institute of Radiooncology, Bautzner Straße 400, 01328 Dresden, Germany
[5] German Cancer Consortium (DKTK), Dresden, Germany and German Cancer Research Center (DKFZ), Heidelberg, Germany
[6] Ion Beam Applications SA, Chemin du Cyclotron 3, 1348 Louvain-la-Neuve, Belgium
* Both authors contributed equally to this work

Purpose: Range verification in proton therapy is highly desirable to fully exploit the advantageous properties of proton beams for tumor therapy. In this context, prompt gamma imaging (PGI) is of growing interest and different technical concepts for realization are currently under investigation. The feasibility of range shift detection with a slit camera has previously been shown for different targets irradiated with protons in pencil beam scanning mode [1-3]. In preparation of the clinical application of the slit camera within a patient study, we report on the first application of the slit camera to passively shaped proton beams.
Materials / Methods: Targets with increasing complexity have been irradiated with passively shaped proton beams (double scattering mode). For artificial range shift induction, the energy of the protons was varied. Prompt gamma emission was monitored by means of a knife-edge shaped slit camera.
Prompt gamma rays emitted during the irradiation are projected through a slit aperture onto a segmented detector. Thus, a one-dimensional depth distribution of detected prompt gamma rays is obtained.
In double scattering mode, a high neutron induced background hampers direct range shift evaluation from these detected gamma distributions. In order to quantify this background, measurements have been repeated with a closed slit aperture of the camera. This facilitates a subtraction of the background from the measurements with open slit.
Time resolved analysis of the measurements allows for a mapping of single prompt gamma profiles to different steps of the range modulator wheel, and, thus, to different iso-energy layers.
Results: Global range shifts of several millimeters in homogeneous as well as inhomogeneous targets were detected with the slit camera measurement during proton irradiation with passive field formation. Figure 1 shows the experimental setup with a head target (left) and detected prompt gamma profiles for different proton energies, i.e. different requested proton ranges (right). Separation of different prompt gamma profiles related to single steps of the range modulator wheel was possible.

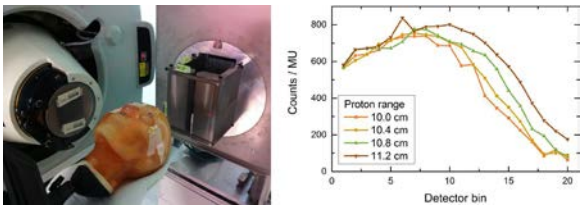

Figure 1: Left: Experimental setup of a prompt gamma slit camera measurement during irradiation of a head phantom with a passively shaped proton beam. Right: Measured prompt gamma depth profiles, normalized to the applied monitor units (MU) for different requested proton ranges, i.e. different proton energies.

Conclusions: In preparation of the application of the slit camera to patient treatment, we investigated the detectability of range shifts in double scattering proton irradiation. Global range shifts of a few millimeters were detected from measurements with the slit camera. Time resolved analysis allows for separation of prompt gamma profiles correlated to protons of different iso-energy layers. This might provide additional information on potential sources of range deviations.

Keywords: prompt gamma imaging, slit camera, proton range verification

References:

[1] Smeets, J.; Roellinghoff, F.; Prieels, D.; Stichelbaut, F.; Benilov, A.; Busca, P.; Fiorini, C.; Peloso, R.; Basilavecchia, M.; Frizzi, T.; Dehaes, J. & Dubus, A.: Prompt gamma imaging with a slit camera for real-time range control in proton therapy. Phys. Med. Biol., 2012, 57, 3371-3405
[2] Perali, I.; Celani, A.; Bombelli, L.; Fiorini, C.; Camera, F.; Clementel, E.; Henrotin, S.; Janssens, G.; Prieels, D.; Roellinghoff, F.; Smeets, J.; Stichelbaut, F. & Stappen, F. V.: Prompt gamma imaging of proton pencil beams at clinical dose rate. Phys. Med. Biol., 2014, 59, 5849-5871
[3] Priegnitz, M.; Helmbrecht, S.; Janssens, G.; Perali, I.; Smeets, J.; Stappen, F. V.; Sterpin, E. & Fiedler, F.: Measurement of prompt gamma profiles in inhomogeneous targets with a knife-edge slit camera during proton irradiation. Phys. Med. Biol., 2015, 60, 4849-4871

178

MEDICIS-PROMED: MEDICIS-Produced Radioisotope Beams for Medicine an Innovative Training Network

D. Viertl[1,2], F. Buchegger[2], J. O. Prior[2], Ph. Morel[1], O. Ratib[1], L. Bühler[1], Th. Stora[3], CERN-MEDICIS collaboration[4]
[1]Hôpitaux Universitaires de Genève, Gabrielle-Perret-Gentil 4, 1205 Genève
[2]Lausanne University Hospital, Rue du Bugnon 46, 1011 Lausanne
[3]Organisation Européenne pour la recherche nucléaire (CERN), Route de Meyrin 385, 1217 Meyrin
[4]C2TN (Centro de Ciências e Tecnologias Nucleares, Lisbonne), CERN (Meyrin), CHUV (Lausanne), HUG (Genève), ISOLDE (Meyrin), ISREC-EPFL (Ecublens), KUL (Katholieke Universiteit Leuven), SINP (Saha Institute of Nuclear Physics India), Nuclear Medicine Sofia (Bulgaria).

MEDICIS-PROMED aims to develop a network of academic, medical and industrial partners providing an extensive doctoral program to 15 young scientists in the field of new personalized treatments using radioisotope beams, notably for treatment of ovarian cancer.
This field is expected to expand rapidly and provide new types of treatments combining imaging and personalized treatment with the same radiopharmaceutical and different types of isotopes, emitting positron or gamma light for imaging on one side, and Auger electron, beta and alpha radiation for treatment on the other side, known as theranostics pairs [1]. In addition, positron emitting isotopes such as ^{11}Carbon can personalize hadron therapy treatments by imaging the dose distribution of the implanted ions [2,3].
In this scheme, CERN, the European Organization for Nuclear Research is the coordinating partner, and collaborates with local hospitals which are able to exploit short-lived isotopes produced in the newly constructed CERN-MEDICIS facility. It also fits within an extended network of high-technology companies and leading academic research institutes, which will design new components for the development or tests of innovative radiopharmaceuticals and imaging agents for personalized treatment. It brings world-class researchers together in the field of lasers and isotope mass separation, accelerators, material science, oncology, entrepreneurial radiopharmaceutical production, and imaging, to propose new solutions to the second deadliest cancer for women.
The program will develop along three R&D work packages integrating multidisciplinary intersectorial training teams:
• Development of new radioisotopes and techniques using isotope mass separation for medicine and based on CERN-MEDICIS.
• Development and test of ^{11}Carbon PET-aided hadron therapy.
• Synthesis & tests of radiopharmaceuticals to diagnose and treat ovarian cancer.
Because of the unique capability of CERN-MEDICIS to produce medical batches of innovative isotopes, such as ^{149}Terbium [4] and thanks and to the new generation of young scientists that will be trained in the relevant fields the MEDICIS-PROMED innovative training network will significantly advance the use of radioisotopes for personalized medicine in Europe and go beyond the present common practices.

Keywords: Radiopharmaceuticals, Nuclear Medicine, Pre-Clinical and Clinical Strategies

References:
[1]LE Kandalaft, DJPowell, N Singh, G Coukos Immunotherapy for ovarian cancer: what's next? *J Clin Oncol* 29:925. (2011)
[2] U. Amaldi et al, Accelerators for hadron therapy: From Lawrence cyclotrons to linacs, *Nuclear Instruments and Methods in Physics Research* A620 563–577 (2010).
[3] T. Mendonca et al., Intense post-accelerated ^{11}Carbon beams for hadron therapy: Treatment and at the same time 3D dose mapping by PET imaging, CERN-ACC-NOTE-2014, in the press. http://cds.cern.ch/
[4] R. Augusto et al. CERN-MEDICIS (MEDical Isotopes Collected from ISOLDE): A new facility, CERN-ACC-NOTE-2014-0019, http://cds.cern.ch/

179

Investigating the impact of a variable RBE on proton dose fractionation across an actively scanned spread-out Bragg peak.

K. M. Prise[1], T.I. Marshall[1], P. Chaudhary[1], A. Michaelidesová[2,3,4], J. Vachelová[2], M. Davídková[2], V. Vondráček[3] and G. Schettino[5],
[1] Centre for Cancer Research and Cell Biology, Queen's University Belfast, UK
[2] Dept of Radiation Dosimetry, Nuclear Physics Institute CAS, Praha 8, CZ
[3] Proton Therapy Center Czech, Budínova 2437/1a, Praha 8, CZ
[4] Department of Dosimetry and Application of Ionizing Radiation, Czech Technical University in Prague, Prague 1, Czech Republic
[5] Radiation Dosimetry, National Physical Laboratory, Teddington, TW11 0LW, UK

Purpose: Experimental data for the impact of fractionated proton beam exposures is limited. Using acute exposures, the current clinical adoption of a generic, constant cell killing RBE has been shown to underestimate the effect of the sharp increase in Linear Energy Transfer (LET) in the distal regions of the spread-out Bragg peak (SOBP). Here we aim to investigate the clinical implications of a variable Relative Biological Effectiveness (RBE) on proton dose fractionation.
Methods and Materials: Human fibroblasts (AG01522) were irradiated with 219.65 MeV protons at four depth positions along a clinical SOBP. These were delivered as fractionated regimes with an inter-fraction period of 24 hours at the Prague Proton Therapy Centre. Cell killing RBE variations were measured using standard clonogenic assays and were further validated using Monte Carlo simulations and parameterized using a Linear-Quadratic formalism.
Results: Consistent with previous studies of a single fraction response for both survival and DNA damage (DSB foci) (1,2), significant variations in the cell killing RBE for fractionated exposures along the proton dose profile were observed. The RBE increased sharply towards the distal position, corresponding to a reduction in the cell sparing effectiveness of fractionated proton exposures at lower energies and higher LET. The effect is more pronounced at smaller doses per fraction. Experimental survival fractions were adequately predicted using a Linear Quadratic formalism assuming full repair between fractions. The data were also used to validate a parameterized variable RBE model based on linear alpha parameter response with LET that showed considerable deviations from clinically predicted isoeffective fractionation regimes.
Conclusions: The biologically effective dose calculated using the clinically adopted generic RBE of 1.1 significantly underestimates the biological effective dose from variable RBE for single and fractionated regimes with low doses per fraction. Coupled with an increase in effective range in fractionated exposures, the study indicates the needs for the optimization of proton therapy particularly in the move towards hypofractionation.

Keywords:
RBE protons fractionation

References:
[1] Chaudhary et al., *Int J. Radiation Oncol Biol Phys,* 2014 **90**:27-35
[2] Chaudhary et al., *Int J. Radiation Oncol Biol Phys,* 2015 Jul 29. pii: S0360-3016(15)03070-9. doi: 10.1016/j.ijrobp.2015.07.2279.

180

Quantum dots imaging tests on SPAD for nanodosimetric applications

L. Pancheri[1,2], A. Quaranta[1,2], G. F. Dalla Betta[1,2], A. Ficorella[1], M. Dalla Palma[1,3]
[1] University of Trento, Department of Industrial Engineering, via Sommarive 9, I-38123 Povo, Trento, Italy.
[2] INFN, TIFPA, via Sommarive 14, I-38123 Povo, Trento, Italy.
[3] INFN, Laboratori Nazionali di Legnaro, Viale dell'Università, 2, I-35020 Legnaro (Padova), Italy.

Purpose of this work: Nowadays it is well assessed that the particle track structure plays a key role in the damage of living cells[1]. Therefore, the quantification of the dose within nanometric volumes is of paramount importance for characterizing the effectiveness of cancer treatments with ion beams. There are currently several facilities suitable for the detailed on-line analysis of the number of ionizations left by an impinging ions into nanometer equivalent gas volumes.[2,3] Nonetheless, the realization of a portable system for nanodosimetry quantification would be extremely useful for the dose control in treatment plants. In this work we propose the use of Single Photon Avalanche Diode (SPAD) arrays for the luminescence imaging of quantum dots (QDs) structures.[4] In particular, the analysis of QD layers will be performed before and after ion irradiation in order to study how the released dose affects the optical properties of the system.
Materials and methods: The luminescence of CdSe/ZnS QD layers is excited with a pulsed LED (475 nm central wavelength and 20 ns pulse width).[5] The luminescence light is collected with a high-numerical aperture optics and delivered to the detector through an optical filter to eliminate the residual scattered excitation light (Figure 1a). A SPAD pixel array[6] is placed in the focal plane to collect the fluorescence map of the sample under analysis. The light signal is collected in time-gated mode in order to measure the QD lifetime before and after irradiation (Figure 1b). Moreover, time-gated detection can be used as a time-domain excitation filtering technique, thus simplifying the design of a portable and compact nanodosimeter.
Results: The luminescence intensity and lifetime of QD irradiated with different fluencies of 2.0 MeV protons and X-rays will be studied and compared with non-irradiated samples. The changes in light yield and lifetime will be correlated to the damage released by the impinging radiation through Monte Carlo calculations.
Conclusions: Although SPAD arrays have already been employed in the past for the sensing of QD luminescence, this is the first time that QD lifetime measurements is proposed as a probing tool applied to nanodosimetry. This preliminary study will give an experimental confirmation on the validity of the idea.

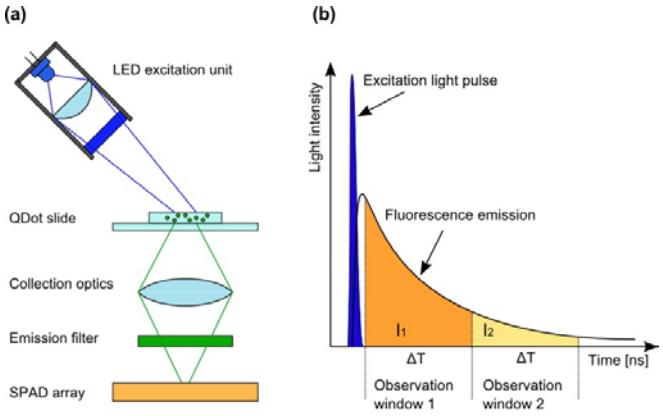

Figure 1. (a) Simplified system diagram (b) Illustration of time gated detection principle

Keywords: nanodosimetry, Quantum Dots, SPAD

References:
[1] H. Rabus, H. Nettelbeck, "Nanodosimetry: bridging the gap to radiation biophysics", Radiation Measurements, Vol. 46, pp. 1522-1528, 2011
[2] V. Conte et al. "Track structure of light ions: experiments and simulations", New Journal of Physics, Vol. 14, pp. 1-38, 2012
[3] V. Conte et al., "Track nanodosimetry of 20-MeV protons at 20 nm", Radiation Protection Dosimetry, Vol. 143, pp. 455-458, 2011.
[4] L. Pancheri, et al., "SPAD image sensor with analog counting pixel for time-resolved fluorescence detection", IEEE Transactions on Electron Devices, Vol.60, No.10, pp. 3442 - 3449, 2013.
[5] L. Pancheri, et al., "Protein detection system based on 32x32 SPAD pixel array", Proc. SPIE 8439, 843913 (2012).

181

Evaluation of the usefulness of dose calculation algorithms in radiotherapy planning

B. Kiełtyka[1], K. Rawojć[1], K. Kisielewicz[3], I. Markiewicz[2]
[1] Marian Smoluchowski Institute of Physics, Jagiellonian University, Cracow, Poland
[2] Maria Sklodowska-Curie Memorial Cancer Centre and Institute of Oncology, Warsaw, Poland
[3] Maria Sklodowska-Curie Memorial Cancer Centre and Institute of Oncology Krakow Branch, Cracow, Poland

Purpose: One of the main goals of radiotherapy is to achieve tumor control and minimize probability of normal–tissue complications. For this reason radiation oncology requires high accuracy, which implies no more than 2 – 3% uncertainty levels in the treatment planning calculations [1]. That is challenging, when heterogeneous tissues such as lungs and bones are involved [2,3]. To verify the accuracy of the dose calculation algorithms numerous approaches might be performed. The most common are point dose, one-dimensional profile and two-dimensional isodose line comparison with experimental measurements [3].
Materials/Methods: In presented study, results of transport modeling and the deposited spatial distribution of the dose, obtained by Anisotropic Analytical Algorithm (AAA) and Pencil Beam Convolution algorithm (PBC), were compared to measurements recorded during the experiment. To achieve meaningful conclusions, three parameters: dose difference (DD), distance to agreement (DTA) and gamma parameter (γ) were taken into consideration and examined. The irradiation was performed using CIRS anthropomorphic phantom. For dose detection gafchromic EBT films were used and scanned after exposure using Epson Scanner. Measured and planned dose distributions were analyzed via FilmQA software.
Results and Conclusions: Preliminary results showed that the AAA, with its complex accounting of heterogeneities, provides more accurate dose calculation within an area of a high density gradient, than PBC does. The level of the data

accuracy derived from the experiment was: DD (5%) – 83.4% and 68% pixels passing, DTA (3mm) – 99.0% and 96,7%, gamma parameter (for DD (3%), DTA (3mm)) – 90% and 75,5% respectively for AAA and PBC algorithms. The comparison between studied parameters DD, DTA and γ for both algorithms implicated AAA as an appropriate approach in radiotherapy treatment planning.

Keywords: Radiotherapy planning algorithms, radiology, medical physics.

References:
[1] – Gagné I M, Zavgorodni S, *Evaluation of the analytical anisotropic algorithm in an extreme water–lung interface phantom using Monte Carlo dose calculations*, Journal Of Applied Clinical Medical Physics, Vol. 7, 2007.
[2] – International Commission on Radiation Units and Measurements (ICRU). *Determination of absorbed dose in a patient irradiated by beams of X or gamma rays in radiotherapy procedures*. ICRU Report 24, Washington (DC): ICRU,1976.
[3] – Van Escha A, Namur E, Tillikainen L, Pyykkonen J, Tenhunen M, Helminen H, Siljamäki S, Alakuijala J, Paiusco M, Iori M, Huyskens D P, *Testing of the analytical anisotropic algorithm for photon dose calculation,* American Association of Physicists in Medicine (AAPM), 2006.

182
Nuclear fragmentation in protontherapy
P. Rebello Teles[1], M. Hussein[2]
[1] Centro Brasileiro de Pesquisas Fisicas, Rio de Janeiro, Brazil
[2] Instituto de Física, Universidade de São Paulo, São Paulo, Brazil

The effect of nuclear fragmentation in the passage of 180MeV protons through the human body tissue is discussed. Prostate cancer protontherapy with these intermediate-energy protons is discussed in light of model calculation.

Keywords: Nuclear fragmentation, protontherapy, prostate cancer

References:
[1] G. Kraft, Tumor therapy with heavy charged particles, Progress in Particle and Nuclear Physics, 2000
[2] A.J. Kreiner and A.A. Burlon, Novel Applications of Particle Accelerators to Radiotherapy, Heavy Ion Physics 16, 243 (2002)
[3] B.V. Carlson, R.C. Mastroleo and M.S. Hussein, Phys. Rev.C46, R3 (1992);
[4]B.V. Carlson, Phys. Rev. C51, 25 (1995)
[5] A.S. Goldhaber, Phys. Lett. B 53, 306 (1974)

183
Internalization of iron nanoparticles by macrophages for the improvement of glioma treatment
S. Reymond[1,2,3,4], P. Gimenez[1,2,3,4,9], R. Serduc[1,3], J. Arnaud[5], J.-P. Kleman[6], V. Djonov[7], W. Graber[7], J.A. Laissue[7], J.-K. Kim[8], S.-J. Seo[8], J.-L. Ravanat[4, 9,10], H. Elleaume[1,2,3,4]
[1] INSERM, U836, Grenoble, France;
[2] Université Joseph Fourier, Grenoble Institut des Neurosciences, UMR-S836, Grenoble, France;
[3] European Synchrotron Radiation Facility, Grenoble, France;
[4] LabEx PRIMES Lyon, France;
[5] CHU Grenoble, France;
[6] IBS Grenoble, France;
[7] University of Berne, Bern, Switzerland;
[8] Catholic University of Daegu, Daegu City, Korea;
[9] INAC/SCIB LAN CEA-Grenoble, France;
[10] Université de Grenoble, France

Rationale: An alternative approach for the improvement of radiotherapy consists in increasing differentially the radiation dose between tumors and healthy tissues using nanoparticles (NPs) that have been beforehand internalized into the tumor. These high-Z NPs can be photo-activated by monochromatic synchrotron X-rays, leading to a local dose enhancement delivered to the neighboring tumor cells[1]. This enhancement is due to secondary and Auger electrons expelled from the NPs by the radiations. In order to carry the NPs into the tumor center, macrophages are currently under study for their phagocytosis and diapedesis abilities[2] (*cf.* Figure adapted from [3] and [4]). In this study we characterized J774A.1 macrophages' internalization kinetics and subcellular distribution of iron NPs and compared them to the internalization abilities of the F98 glioblastoma cell line.
Materials and Methods: Three aspects of internalization were examined: first, the *location of internalized NPs* in J774A.1 macrophages and F98 glioblastoma cells following a 24h incubation with iron NPs (0.3 mg/mL in the cell culture medium) was determined by optical microscopy after cell slicing. Subsequently, the *iron intake* after a 24h incubation with NPs (0.3 mg/mL and 0.06 mg/mL in the cell culture medium) was characterized for the two types of cells using ICP-MS. Finally, the *internalization dynamics* were studied by live phase-contrast microscopy imagining for 11 hours and by absorbance measurements for 24 hours using a plate reader.
Results: F98 tumor cells and J774A.1 macrophages are both able to endocytose NPs: we measured ~61±10 pg of internalized iron per macrophage compared with ~33±5 pg per F98 cell (initial iron concentration: 0.3 mg/mL in culture medium). F98 internalizing NPs for 10 hours showed stress signs during the first minutes after the NPs injection, but behaved like F98 control cells during the rest of the experiment. Finally, we determined that the internalization kinetics for J774A.1 had a typical saturation time of one hour.
Conclusion: Macrophages seem to be promising vectors for NPs, being able to endocytose and retain in their cytoplasm larger quantities of NPs than tumor cells. Our following studies will attempt to shed light on their other potential abilities as "Trojan Horses".

Keywords: radiotherapy; nanoparticles; cell-carriers

References:
[1] F. Taupin *et al.*, Phys Med Biol 60 (2015).
[2] J. Choi *et al.*, Biomaterials 33 (2012).
[3] R. Weissleder *et al.*, Nature Materials 13 (2014).
[4] M.R. Choi *et al.*, Nano Letters 7 (2007).

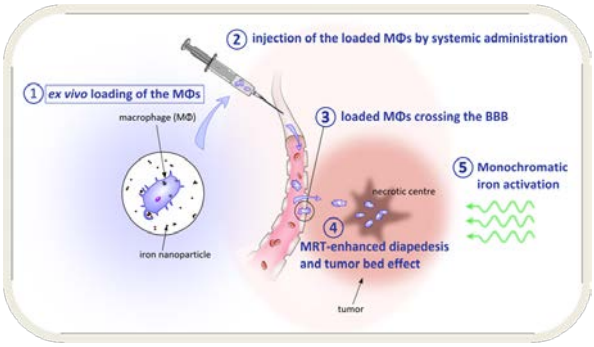

184
First clinical application of a prompt gamma based *in vivo* proton range verification using a knife-edge slit camera
C. Richter[1-4], G. Pausch[1-3], S. Barczyk[1,2], M. Priegnitz[3], I. Keitz[1], J. Thiele[2], J. Smeets[5], F. Vander Stappen[5], L. Bombelli[6], C. Fiorini[7], L. Hotoiu[5], I. Perali[7], D. Prieels[5], W. Enghardt[1-4], M. Baumann[1-4]
[1] OncoRay – National Center for Radiation Research in Oncology, Faculty of Medicine and University Hospital Carl Gustav Carus, Technische Universität Dresden, Helmholtz-Zentrum Dresden - Rossendorf, Dresden, Germany
[2] Department of Radiation Oncology, University Hospital Carl Gustav Carus, Technische Universität Dresden, Dresden, Germany
[3] Helmholtz-Zentrum Dresden – Rossendorf, Dresden, Germany

[4] German Cancer Consortium (DKTK), Dresden, Germany and German Cancer Research Center (DKFZ), Heidelberg, Germany
[5] Ion Beam Applications SA, Louvain-la-Neuve, Belgium
[6] XGLab S.R.L., Milano, Italy
[7] Politecnico di Milano, Dipartimento di Elettronica, Informazione e Bioingegneria, Milano, Italy

Purpose: To improve precision of particle therapy, in vivo range verification is highly desirable. Methods based on prompt gamma rays emitted during treatment seem promising but have not yet been applied clinically. Here we report on the worldwide first clinical application of prompt gamma imaging (PGI) based range verification.
Material / Methods: A prototype of a knife-edge shaped slit camera [1,2] was used to measure the prompt gamma ray depth distribution during a proton treatment of a head and neck tumor for seven consecutive fractions and one of three fields. The treatment was delivered with passively double scattered proton therapy (DS), although the slit camera was originally developed for pencil beam scanning. Before clinical application, the feasibility of the DS applicability was shown in a separate work [3], e.g. by introducing subtraction of the neutron-induced background. Inter-fractional variations of the prompt gamma profile were evaluated for the time integrated prompt gamma profile (sum profile) as well as for prompt gamma profiles corresponding to different steps of the modulator wheel (iso-energy layer resolved profile). For three fractions in-room control CTs were acquired and evaluated for dose relevant changes.
Results: The measurement of PGI profiles during proton treatment was successful. Based on the PGI information of the sum profiles, inter-fractional global range variations, determined with automated shift detection, were in the range of ±2 mm for all evaluated fractions. This is within the uncertainty of the PGI system, as already the position accuracy of the PGI slit camera was determined with 1.1 mm (2σ). The detected range variations are in agreement with the control CT evaluation showing negligible range variations of about 1.5 mm. Also the evaluation of the iso-energy layer resolved prompt gamma profiles was in consistence with the analysis of the sum profiles and provided additional information.

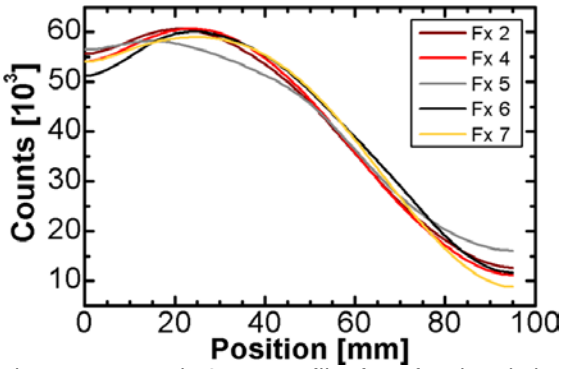

Figure 1: Detected PGI sum profiles for 5 fractions (Fx) after application of a Gaussian filter (FWHM=20 mm). The region between 20k-50k counts was used for automated shift detection. Please note that for two fractions no data were available - one was used for a background measurement with closed slit (Fx 3), and for another one (Fx 1) a deficient background subtraction disturbed the sum profile.
Conclusions: For the first time, range verification based on prompt gamma imaging was applied for a clinical proton treatment. Further plans include the continuation of the clinical study to perform systematic evaluations based on an appropriate patient number. With the translation from basic physics experiments into clinical operation, the authors are confident that a prompt gamma ray based technology is capable of range verification and can be used in the near future for online quality assurance as well as in midterm for potential margin reduction.

Keywords: prompt gamma imaging; range verification; slit camera

References:
[1] Smeets, Roellinghoff, Prieels, Stichelbaut, Benilov, Busca, Fiorini, Peloso, Basilavecchia, Frizzi, Dehaes, Dubus: Prompt gamma imaging with a slit camera for real-time range control in proton therapy. Phys. Med. Biol., 2012, 57, 3371-3405
[2] Perali, Celani, Bombelli, Fiorini, Camera, Clementel, Henrotin, Janssens, Prieels, Roellinghoff, Smeets, Stichelbaut, Vander Stappen: Prompt gamma imaging of proton pencil beams at clinical dose rate. Phys. Med. Biol., 2014, 59, 5849-5871
[3] Priegnitz, Barczyk, Keitz, Mein, Vander Stappen, Janssens, Hotoiu, Smeets, Fiedler, Prieels, Enghardt, Pausch, Richter: Prompt gamma imaging of passively shaped proton fields with a knife-edge slit camera. Abstract submitted for ICTR-PHE 2016

185
Clinical applicability of the Compton camera for Prompt γ-ray Imaging during proton therapy

H. Rohling[1], M. Priegnitz[1], S. Schoene[1], A. Schumann[1], W. Enghardt[2,3,4,5], C. Golnik[2] , F. Hueso-González[3], T. Kormoll[2], G. Pausch[2], J. Petzoldt[2], K. Römer[1], F. Fiedler[1]
[1]Helmholtz-Zentrum Dresden – Rossendorf, Institute of Radiation Physics, Bautzner Landstr. 400, 01328 Dresden, Germany
[2]OncoRay - National Center for Radiation Research in Oncology, Faculty of Medicine and University Hospital Carl Gustav Carus, Technische Universität Dresden, Helmholtz-Zentrum Dresden – Rossendorf, Fetscherstr. 74, PF 41, 01307 Dresden, Germany
[3]Helmholtz-Zentrum Dresden – Rossendorf, Institute of Radiooncology, Bautzner Landstr. 400, 01328 Dresden, Germany
[4]Department of Radiation Oncology, Faculty of Medicine and University Hospital Carl Gustav Carus, Technische Universität Dresden, Fetscherstr. 74, 01307 Dresden, Germany
[5]German Cancer Consortium (DKTK), Dresden, Germany

Purpose: In order to guarantee the best outcome of a therapeutic irradiation with protons and other light ions a non-invasive in-vivo range verification is desired. One approach in this field is Prompt γ-ray Imaging (PGI). A possible detection system for the prompt γ-rays is the Compton camera. Several groups have been working on the construction of Compton camera prototypes [1-5]. Up to now, Compton cameras have not been used in clinical practice for the monitoring of particle therapy. By means of Geant4 simulations, we performed an end-to-end test to evaluate the clinical applicability of a Compton camera detection system and to determine the requirements regarding hardware and image reconstruction.
Materials/methods: First, a treatment plan for a therapeutic proton irradiation for the head-neck region was prepared using XiO (Electa AB, Sweden). Based on this treatment plan, the γ-ray emissions from the patient's tissue were simulated with Geant4. As a next step, the detector response was modelled, also with Geant4, for two large Compton cameras arranged around the patient in an angle of 90 degrees. Large-area detectors were already recommended [6]. Each camera was built up from a scatter layer (CZT) of dimension 10 × 10 × 0.5 cm^3 and an absorber layer (LSO) of size 20 × 20 × 2 cm^3. In practice, these cameras would be replaced by several smaller camera modules. For the simulation of the detector response a total number of previously simulated γ-ray emissions were used as input corresponding to an applied dose of 1 Gy, i.e. a common dose of one field of one treatment session. After extracting the resulting coincident events, the image was reconstructed using a 3D MLEM algorithm [7]. The impact of the number of events, filters, as well as background on the image quality was also studied.

Results: Figure 1 shows the images for the planned dose, the distribution of the γ-ray emissions and the reconstructed image obtained with 128 iterations of the MLEM algorithm. For the considered number of events and the chosen voxels

of 5 mm^3 the runtime of the reconstruction was about two days on a cluster.

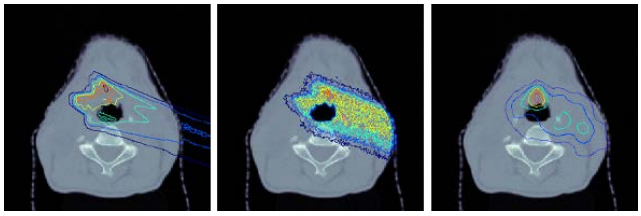

Figure 1: Dose (left), γ-ray emissions (center), and reconstructed image (right) for the simulated patient case.

Conclusions: By means of Geant4, an end-to-end test was performed which models clinical conditions. The impact of various parameters on the applicability of the Compton camera was evaluated. The reconstruction algorithm still has potential for improvements with respect to performance. Furthermore, in practice, the costs and the complexity of a Compton camera system could lead to the preference of simpler methods of PGI.

Keywords: Compton camera, Geant4 simulations, image reconstruction

References:

[1] Kormoll T, Fiedler F, Schoene S, Wüstemann J, Zuber K and Enghardt W 2011 A Compton imager for in-vivo dosimetry of proton beams - A design study. Nucl. Instrum. Methods Phys. Res. A 626-627 114-119
[2] Llosá G, Cabello J, Callier S, Gillam JE, Lacasta C, Rafecas M, Raux L, Solaz C, Stankova V, Taille CL, Trovato M, Barrio J 2013 First Compton telescope prototype based on continuous LaBr3-SiPM detectors Nucl. Instrum. Meth. Phys. Res. Sec. A 718 130 – 133
[3] Thirolf PG, Lang C, Aldawood S, v.d. Kolff HG, Maier L, Schaart DR and
Parodi K 2014 Development of a Compton Camera for Online Range Monitoring of Laser-Accelerated Proton Beams via Prompt-Gamma Detection. EPJ Web of Conferences 66(11036)
[4] Hueso-González F, Golnik C, Berthel M, Dreyer A, Enghardt W, Fiedler F, Heidel K, Kormoll T, Rohling H, Schoene S, Schwengner R, Wagner A and Pausch G 2014 Test of Compton camera components for prompt gamma imaging at the ELBE bremsstrahlung beam. J. Instrum. 9 P05002
[5] Polf JC, Avery S, Mackin D and Beddar S 2015 Imaging of prompt gamma rays emitted during delivery of clinical proton beams with a Compton camera: feasibility studies for range verification. Phys Med Biol. 60(18) 7085-7099
[6] McCleskey M, Kaye W, Mackin DS, Beddar S, He Z and Polf JC 2015 Evaluation of a multistage CdZnTe Compton camera for prompt imaging for proton therapy. Nucl. Instrum. Methods Phys. Res. A 785 163-169
[7] Schoene S, Enghardt W, Fiedler F, Golnik C, Pausch G, Rohling H and Kormoll T 2015 An Evaluation System for Compton Camera Imaging for In-vivo Dosimetry of Therapeutic Ion Beams. Submitted to Trans. Nucl. Sci.

186

Design of electronic data processing system for radiotherapy study: lessons learned from VoxTox

M. Romanchikova[1], K. Harrison[2], S.J. Thomas[1], A. Bates[3], M.P. Sutcliffe[4], M.A. Parker[2], N.G. Burnet[4]
[1] Medical Physics and Clinical Engineering, Cambridge University Hospitals NHS Foundation Trust, United Kingdom
[2] Cavendish Laboratory, University of Cambridge, United Kingdom
[3] Cambridge Cancer Trials Centre, Cambridge University Hospitals NHS Foundation Trust, United Kingdom
[4] Department of Engineering, University of Cambridge, United Kingdom
[5] Department of Oncology, University of Cambridge, United Kingdom

Radiotherapy (RT) research studies operate with vast amounts of imaging and planning data. A purpose-built electronic data processing system helps to eliminate errors, prevent data losses and achieve high data quality. This work presents methods and tools used in data processing pipeline for the VoxTox study.
The study will include over 1000 patient data sets comprised of TomoTherapy® imaging and planning data. Data is collected at hospital site, anonymised, tested and transferred to Cavendish Laboratory for processing and storage.
A pseudo-anonymisation system was designed, in which each patient identifier was substituted by a token that can be decrypted at the hospital site to re-identify the patient. A token is auto-generated upon adding patient details to the study master file and saved in a dedicated database.
Patient imaging and planning data are extracted and converted to Digital Imaging and Communications in Medicine (DICOM) format by in-house developed software. The software tokenises data on-the-fly and makes use of DICOM private tags to add auxiliary data.
Testing is performed before and after transfer between sites using MD5 hashes and file lists. As the time gap between RT completion and data collection is small, missing data are identified early and can be recovered.
Daily doses are calculated using a modification of CheckTomo application distributed on a computer cluster with 228 job slots via GANGA job management tool originally developed for ATLAS project.
The images are outlined using purpose-built Matlab software based on Chan-Vese segmentation algorithm. Both tools are user-interface (UI) free and configurable via text input files that can be auto-generated. Root framework is used for data analysis and visualisation.
Toxicity data is collected in the clinic using MOSAIQ® oncology information system and collated with the patient reported outcomes in KeyPoint® software. The electronic-only data acquisition guarantees consistency of format and freedom from transcription errors.
On average, VoxTox toolkit outperforms conventional tools used in the clinic by factor 6 (Table 1). Data retrieval is conventionally done via UI on TomoTherapy planning station. There is no tool to obtain TomoTherapy daily doses. Conventional contouring is performed by an experienced oncologist. Toxicity questionnaires are usually entered on paper forms and transcribed to electronic documents. Conventional data testing is a manual check of all files and folders in patient data set.

Method	Data Processing Step				
	Data retrieval	Daily dose calculation	Contouring	Toxicity questionnaire	Data testing
VoxTox	2	60	74	30	2
Existing tools	60	N/A	550	45	15

Table 1: Time in minutes required to complete a single task for one patient data set using tools existing in the clinic and using VoxTox software. VoxTox toolkit processing times are given for a single computer with 2GHz CPU and 8GB of RAM.

We created a system that is modular, robust and efficient. All processing tools can run on a single computer or be deployed in a job management system on a cluster. Utilization of existing tools and staff skills minimizes project costs and accelerates the development. Key design elements such as pseudo-anonymisation, text-based inputs, batch processing and electronic data entry can be applied to any RT study.

Keywords: DICOM, automated processing, TomoTherapy

187

A model for the relative biological effectiveness of protons based on the linear energy transfer spectrum

E. Rørvik[1], K.S. Ytre-Hauge[1]
[1] Department of Physics and Technology, University of Bergen, Norway

Purpose: In proton therapy a generic relative biological effectiveness (RBE) of 1.1 has traditionally been clinically applied, implying that protons are slightly more effective than photons. However, there exist large amounts of data, mainly from in vitro studies, demonstrating that the RBE is variable and dependent on a set of factors, including the radiation quality of the beam. Most of the phenomenological models made for estimating the RBE use the dose average Linear Energy Transfer (LET_d) as a parameter for the radiation quality. However, such a simplified description of the quality might lead to inaccurate RBE. In this work a new RBE model for proton therapy has been developed, utilizing the dose weighted LET spectrum (d(L)) to describe the radiation quality.
Materials/methods: A new formalism for RBE calculation is introduced, based on the concept of RBE_{max} and the usage of biological weighting functions. RBE_{max} is found by weighting the LET spectrum by $r_{max}(L)$, a smooth continuous function for the full LET range of protons (0-83 keV/µm). We assumed that $r_{max}(L)$ is nonlinear and symmetric around a turnover point (LET_u). A quantitative description of $r_{max}(L)$ was found by making a regression fit to the α/α_x of 96 data points, where the α and α_x are coefficients of the linear-quadratic model, for proton and photon irradiation respectively. These points were extracted from experiments with semi-monoenergetic proton beams found in literature. In our model we have assumed that $\beta = \beta_x$ and thus $RBE_{min} = 1$. A Fluka Monte Carlo simulation was done to check the new calculation method was benchmarked against a constant RBE of 1.1 and an existing LET_d based model for variable RBE (McNamara et al., 2015).
Results: By fitting $r_{max}(L)$ to the data, we found a peak at LET_u=34.5 keV/µm. The fit had a R^2 value of 0.634. In the simulated example, the new model estimated a RBE of 1.00-1.02 in the entrance region. The RBE rises from 1.05 to 1.6 along the SOBP. This indicates that a constant RBE of 1.1 leads to an overestimate of the dose to the normal tissue, as well to the proximal part of the tumour. Compared to the LET_d based model, the RBE is approximately 9-11% lower at all depths.
Conclusions: A dose and tissue dependent RBE model, based on the LET spectrum has been developed for application in proton therapy. Compared to LET_d-based model, this approach might give a better estimation of the biological dose in a mixed radiation field. The model could be further optimized, by adjusting the definition of $r_{max}(L)$ and introducing a term for $r_{min}(L)$, taking into account a variable LET dependent β parameter.

Keywords: RBE, dose average LET, LET spectrum

References:
[1] A.L. McNamara et al, Phys. Med. Biol. 60, 8399. (2015)

188
DoPET: an in-treatment monitoring system for particle therapy
V.Rosso[1*],G. Battistoni[2], N. Belcari[1], N. Camarlinghi[1], G.A.P. Cirrone[3], F. Collini[4], G. Cuttone[3], M.Ciocca[5], A. Del Guerra[1], A. Ferrari[6], S. Ferretti[1], A.C. Kraan[1], A. Mairani[5], M. Pullia[5], S. Molinelli[5], F. Romano[3], P. Sala[6], G. Sportelli[1], E. Zaccaro[1]
[1] Department of Physics, University of Pisa and INFN, Pisa, Italy.
[2] INFN Milano, Milano, Italy
[3] INFN - Laboratori Nazionali del Sud, Catania, Italy
[4] Department of Physical Sciences, Earth and Environment, University of Siena and INFN, Pisa, Italy
[5] CNAO Foundation, Pavia, Italy
[6] CERN, Geneva, Switzerland

Purpose: The growing interest in charged particle therapy has led to the development of dedicated systems able to monitor the dose delivered to the patient. Positron Emission Tomography (PET) is a non-invasive way for in-vivo verification of the dose delivery. In fact, during particle irradiation, various β^+-emitting isotopes (^{15}O, ^{11}C etc.) are generated in the patient and this activity distribution can be related to the delivered dose.
Materials/methods: A compact PET system was developed to be installed close to the patient. The PET system, DoPET, is based on two planar heads. Over the years the dimension of the heads was increased, from 5cm x 5cm, to 10cm x10cm and finally to the dimension of 15cm x 15cm per head. The heads result from the assembly of several detecting modules: in the present prototype there are 9 modules (3x3) per head. Each detecting module, (5cm x 5cm) consists of a segmented LYSO crystal matrix (2 mm pitch) coupled to a PSPMT. The readout is performed by custom electronics, and the data acquisition was designed to cope with the high fluxes present during the treatment plan (TP) delivery. The data reconstruction of the measured 3-D β^+-activity distribution, based on a MLEM-OSEM 3D algorithm takes less than one minute.
The system was mostly characterized for proton therapy applications: at CATANA, a cyclotron-based center(LNS-INFN Catania, Italy), and at CNAO a synchrotron-based center (Pavia, Italy). Preliminary characterization for carbon irradiations were also performed.
Results: The DoPET spatial resolution guarantees the reconstruction of the distal fall activity profile with a sensibility of 1 mm, operating in-treatment [1, 2]. The in-treatment data were useful. In fact, DoPET provided information on a whole protonTP and on its very early phases [3]. A study was done delivering only the proton TP Highest Energy Layer: thanks to the sharp shape of the mono-energetic activity fall- off profile, the shift due to the presence of a small air cavity was evident.
The experimental β^+-activity profiles were also compared to calculated data obtained with FLUKA Monte Carlo, with very satisfactory agreement [3].
Conclusions: DoPET represents a reliable and fast in-treatment monitoring system that could act as an image guidance in the case of hypo-fractionation scheme. The present head dimension allows studies with anthropomorphic phantoms that will be done before moving onto patients.

Keywords: Particle therapy monitoring, on-line PET
References:
[1] N. Camarlinghi et al. An In-beam PET System For Monitoring Ion-beam Therapy: Test On Phantoms Using Clinical 62 MeV Protons; JINST 9 C04005 (2014) 1-12
[2] G. Sportelli et al. First full-beam PET acquisitions in proton therapy with a modular dual-head dedicated system; Phys. Med. Biol. 59 (2014) 43–60;
[3] A.C. Kraan et al. First tests for an on line treatment monitoring system with in-beam PET for proton therapy; JINST, 10, C01010 (2015) 1-11

Left: one head of the DoPET prototype. Center: the prototype ready for the data taking with an antropomorphic phantom at CNAO, Pavia, Italy. Right: a slice of the reconstructed activity after a 2Gy proton treatment plan

189
Design of an innovative beam monitor for particle therapy for the simultaneous measurement of beam fluence and energy
R. Sacchi[1,2], N.Cartiglia[1], F. Cenna[1], L. Fanola[1,2], M. Ferrero[2], S. Giordanengo[1], F. Marchetto[1], V. Monaco[1,2], A. Vignati[1], M. Varasteh Anvar[1,2], R. Cirio[1,2]
[1] Istituto Nazionale di Fisica Nucleare (INFN), division of Torino, Torino, Italy
[2] Department of Physics, University of Torino, Torino, Italy

Purpose: Monitoring the prescribed dose in particle therapy with the raster-scan method is equivalent to monitoring the correct delivery of the number of ions and the sequence of beam positions for every energy of the primary beam. The first task is typically carried out by using parallel plate ionization chambers working in transmission mode, where the number of particles is derived from the collected ionization charge with an accuracy in the order of 1%. The use of gas detectors has several drawbacks: they need to be calibrated daily against standard dosimeters and their dependence on beam quality factors need to be fully characterized and controlled with high accuracy. A detector capable of single particle counting is proposed which would overcome all these limitations. Combined with a gas ionization chamber, it will allow determining the average particle stopping power, thus providing an effective method for the online verification of the selected particle energy and range of the beam during the irradiation of the patient.
Materials and methods: Low-Gain Avalanche Detectors (LGADs) are innovative n-in-p silicon sensors with moderate internal charge multiplication occurring in the strong field generated by an additional p+ doping layer implanted at a depth of a few μm in the bulk of the sensor.

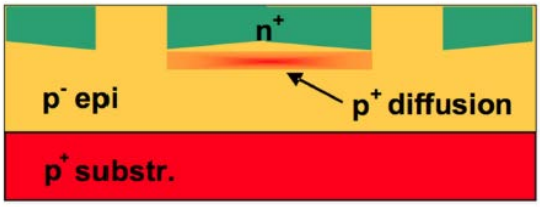

The increased signal-to-noise ratio allows designing very thin, few tens of micron, segmented LGADs, called Ultra Fast Silicon Detectors (UFSD) that, due to their large and very fast signal collection time, would be suitable for charged particle counting at high rates in particle therapy applications. We have finished the design of a sensor prototype, with a matrix of 100 pixels which will provide first indications on the particle rate capability and count accuracy. The sensors are expected in early spring 2016.
Results: Different LGAD diodes have been characterized both in laboratory and beam tests, and the results compared both with those obtained with similar diodes without the gain layer and with a program simulating the signal in the sensors. The signal is found to be enhanced in LGADs, while the leakage current and the noise is not affected by the gain. Additional results, as the information on the doping profiles, extracted from the study of CV curves and radiation tolerance studies, are also shown. Possible alternative designs and implementations are also presented and discussed.
Conclusions: Thanks to their excellent counting capabilities, UFSD detectors are a promising technology for future beam monitor devices in hadron-therapy applications. Studies are ongoing to better understand their properties and optimize the design in view of this application.

Keywords: Particle Therapy, Beam Monitoring, Silicon Detectors

190
Variance Reduction of Monte Carlo Simulation in Nuclear Medicine
P. Saidi
Nuclear Engineering Dept., Science and Research Branch, Islamic Azad University, Tehran, Iran

Purpose: A method, which has had a great impact in many different fields of computational science,is called "Monte Carlo".The range of Monte Carlo application is enormous, from the Nuclear medicine, Radiation therapy, Reactor design, Quantum chromo dynamicsto Traffic flow and econometrics.One of the difficulties associated with Monte Carlo simulations is the amount of computer time required to obtain results with high precision. To shorten the calculation time and also improve the efficiency, there comes the idea to use the variance reduction techniques.
Method: There are many ways in which a user can improve the precision of a Monte Carlo simulation. In this study several of the more widely used variance reduction techniques such as: Splitting/ Russian Roulette, Energy cut off, Time cut off, Weight window, Implicit capture, Forced collision and Exponential transformation are presented. Application of variance reduction and guideline for these techniques in simulation are described.
Results: In Splitting/ Russian roulette technique each region is classified as important and unimportant. If the selected region is unimportant the Russian roulette has been used and in contrary if the important region is selected Splitting is used.
The energy cutoff and time cutoff are similar but more caution is needed in energy cut off because low energy particles can produce high energy particles.
The weight window technique is space energy dependent and can control weight fluctuation by define upper and lower energy bounds. Weight window technique is used to avoid following very low weight particles which causes reasonable computer timer during the simulation.
The main advantage of implicit capture is that a particle always survives a collision. It means when a particle reaches near the tally region would not be absorbed just before a score is made.
The exponential transformation is designed to enhance efficiency for deep penetration problems, but it should be noted that due to the large weight fluctuation that can be produced by this technique, it should be used accompanied by weight controls.
Conclusion: Variance Reduction techniques are used to produce more accurate and precise estimation in Monte Carlo simulations. There is a problem that these techniques may lead to results not being analyzed correctly but it should be noted that experience will lead the users to find the tricks for using these techniques to obtain the more accurate results.

Key words: Variance reduction, Monte Carlo, Simulation

191
Simulation of cell survival for proton broad and minibeam radiotherapy with hexagonal and square minibeam alignment
M. Sammer[1,*], S. Girst[1], C. Greubel[1], J. Reindl[1], C. Siebenwirth[2,1], J.J. Wilkens[2], T.E. Schmid[2], G. Dollinger[1]
[1] Universitaet der Bundeswehr Muenchen, Neubiberg, Germany;
[2] Klinikum rechts der Isar, Technische Universitaet Muenchen, Germany;
*Corresponding author: matthias.sammer@unibw.de

Purpose: Proton radiotherapy using so-called minibeams of sub-millimeter dimensions allows to additionally enhance the advantages of proton therapy by spatial fractionation. This leads to a lower fraction of cells suffering from direct radiation damage and thus to reduced side effects compared to conventional proton therapy, which has been shown in a human skin and a mouse ear model [1,2]. Tumor control is maintained via homogeneous irradiation of the tumor due to minibeam widening with increasing depth. The minibeam distances need to be maximized for improved tissue sparing while generating a homogeneous tumor dose. Here, the required distances for quadratic vs. hexagonal minibeam arrangement are analyzed (see Figure 1). The resulting dose distributions are simulated in a water phantom with clinically relevant energies leading to different cell survival fractions and side effects.
Figure 1: *Minibeam arrangement on a quadratic lattice (left) and on a hexagonal lattice (right).*

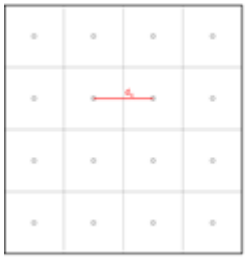
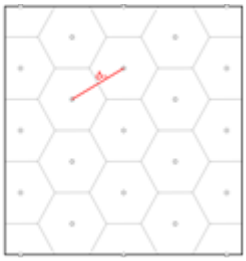

Materials/methods: The different lattice constants d_q for quadratic and d_h hexagonal minibeam arrangement are calculated under the constraint of a homogeneous dose distribution ($0.95<D/D_{tumor}<1.07$ [3]) in the same treatment volume using equal initial beam sizes.
For a fictitious tumor in 10-15 cm depth, both minibeam scenarios (initial beam size σ=200μm) are simulated and normalized to the SOBP depth dose profile of the corresponding broad beam irradiation. The resulting depth and spatial dose distributions are used to approximate the mean cell survival at a tumor dose of 60 Gy for comparison of the two minibeam modes and the homogeneous irradiation.
Results: While homogeneous irradiation leads to significant mean cell death, minibeam irradiation spares up to ~85% of the healthy tissue, especially in the superficial tissues.
For a hexagonal alignment, the lattice constants d_h can be increased by a factor of 1.144 in comparison to the quadratic lattice constant d_q. This improves tissue sparing additionally by a few percent compared to the square arrangement.
Conclusion: These results confirm again that proton minibeam radiotherapy reduces side effects compared to conventional broad beam irradiation. A small additional positive effect can be achieved by a hexagonal alignment of the minibeams instead of the previously used quadratic lattice. Nevertheless, both arrangements make minibeam radiotherapy an attractive new approach for clinical proton and/or heavy ion therapy.

Supported by the DFG Cluster of Excellence: Munich-Centre for Advanced Photonics.

References:
[1] Zlobinskaya O, Girst S, Greubel C et al., Radiat. Environ. Biophys 2013; 52, 123-133.
[2] Girst et al., Proton minibeam radiotherapy reduces side effects in an in-vivo mouse ear model, Int. J. Radiat. Oncol. Biol. Phys. 2015 (in press)
[3] ICRU report 50

192
Study of the radiation produced by therapeutic He, C and O ion beams impinging on a PMMA target

G. Battistoni[7], F. Collamati[1,2], E. De Lucia[3], R. Faccini[1,2], P. M. Frallicciardi[5], C. Mancini[1,2], M. Marafini[2,5], I. Mattei[7], S. Muraro[7], R. Paramatti[2], V. Patera[2,4,5], L. Piersanti[3,4], D. Pinci[2], A. Rucinski[2,4], A. Russomando[1,2,6], A. Sarti[3,4,5], A. Sciubba[2,4,5], E. Solfaroli Camillocci[1], M. Toppi[3], G. Traini[1,2], C. Voena[2]
[1] Dipartimento di Fisica, Sapienza Università di Roma, Roma, Italy
[2] INFN Sezione di Roma, Roma, Italy
[3] Laboratori Nazionali di Frascati dell'INFN, Frascati, Italy
[4] Dipartimento di Scienze di Base e Applicate per l'Ingegneria, Sapienza Università di Roma, Roma, Italy
[5] Centro "E. Fermi", Roma, Italy
[6] Center for Life Nano Science@Sapienza, IIT, Roma, Italy
[7] INFN Sezione di Milano, Milano, Italy

Charged Particle Therapy (CPT) is an effective tool for cancer treatment that exploits the high localization of the charged ions incoming radiation dose deposition to increase the cancer cell death induction while sparing the surrounding Organs At Risk. Besides protons, currently the most common ion beam type in clinical centers, there has been recently a growing interest in heavier ions beams (He, C, O) due to their increased Radio Biological Effectiveness, reduced multiple scattering and Oxygen Enhancement Ratio, in spite of the presence of nuclear fragmentation. Online monitoring of the deposited dose range, currently missing in clinical practice, would substantially improve the CPT Quality Control: the high dose deposition conformity requires an improved control of the beam settings to avoid any potential harm resulting from patient mis-positioning and biological / anatomical changes occurred between the CT scan acquisition and the treatment. Dose Monitoring in CPT [1] is performed using the secondary radiation produced by the interaction of the beam inside the patient body. The study and precise characterization of such radiation (beta+, prompt gamma, charged fragments) is the cornerstone of any R&D activity aiming for online monitoring development. In this contribution we present the measurements of the secondary radiation generated by He, C and O beams of therapeutic energies, impinging on a beam stopping PMMA target collected at the Heidelberg Ion-beam Therapy center (HIT).
The experimental setup, as well as the analysis strategies will be reviewed. The detected particle fluxes, as a function of the emission angle with respect to the beam direction, and the spatial emission distributions will be presented and compared to other available measurements [2,3,4,5,6].
The implications for dose monitoring applications will be discussed, in the context of the current (or planned) state-of-the-art detector solutions.

Keywords: Dose range monitoring concepts and apparatus; Instrumentation for hadron therapy

References:
[1] R. Faccini and V. Patera, *Dose monitoring in particle therapy*, *Mod. Phys. Lett.* A 30 (2015) 1540023.
[2] L. Piersanti et al., *Measurement of charged particle yields from PMMA irradiated by a* 220 *MeV/u* 12*C beam*, *Phys. Med. Biol.* 59 (2014) 1857.
[3] E. Testa et al., *Monitoring the Bragg peak location of* 73 *MeV/u carbon ions by means of prompt* γ*-ray measurements*, *Appl. Phys. Lett.* 93 (2008) 093506
[4] E. Testa et al., *Dose profile monitoring with carbon ions by means of prompt-gamma measurements*, *Nucl. Instrum. Meth.* B 267 (2009) 993.
[5] C. Agodi et al., *Precise measurement of prompt photon emission for carbon ion therapy*, 2012 *JINST* 7 P03001 [*Erratum ibid.* 8 (2013) E11002]. [6] M. Pinto et al., *Absolute prompt-gamma yield measurements for ion beam therapy monitoring*, *Phys. Med. Biol.* 60 (2015) 565.

193
New Results with Monolithic Scintillators for Time-of-Flight PE

G. Borghi,[1] V. Tabacchini,[1] B.J. Peet,[1] and D.R. Schaart[1]
[1] Delft University of Technology, Mekelweg 15, Delft, The Netherlands

Purpose: Reducing PET scanning times and radiation exposure while improving image quality and quantitative accuracy requires detectors with better detection efficiency, spatial resolution, and time resolution. Digital photon counter (DPC) arrays are fully digital, solid-state single-photon sensors. DPC arrays are almost transparent to 511 keV gamma quanta, opening up new degrees of freedom in PET detector design.
This work compares the detector performance of monolithic LYSO:Ce crystals read out with DPC arrays in so-called dual-sided readout (DSR) configuration and conventional back-side readout (BSR). Moreover, first imaging results are presented with BSR monolithic scintillators in a setup representative of a 70 cm diameter clinical TOF-PET scanner.
Materials and Methods: DPC arrays consisting of 8 x 8 DPC pixels and having a total area of 32 mm x 32 mm were optically coupled to commercially available, standard-grade LYSO:Ce crystals having dimensions of 32 mm x 32 mm x 22 mm. Either a single DPC array was coupled to the 32 mm x 32 mm back surface of the crystal (BSR configuration) or DPC

arrays were coupled to both the front- and back-surfaces of the crystal (DSR configuration). The spatial-, time- and energy-resolutions of both configurations were measured.
Furthermore, two detector modules containing 4 BSR monolithic scintillator detectors each were mounted in a "table-top gantry" setup allowing the emulation of a full PET ring of arbitrary diameter using only 2 detectors in a step-and-shoot acquisition approach. Three-dimensional (3D) phantom images were acquired with both of the BSR detectors rotating at a radius of 35 cm from the center of the field-of-view.
Results: In conventional BSR configuration, a detector spatial resolution of ~1.7 mm FWHM and a DOI resolution of ~3.7 mm FWHM was obtained, averaged over the entire detector area. In DSR configuration, a spatial resolution of ~1.1 mm FWHM was achieved in combination with a depth-of-interaction (DOI) resolution of ~2.4 mm FWHM. The energy resolution was ~10% in both detectors. The coincidence resolving time (CRT) in BSR and DSR configurations were ~215 ps FWHM and ~147 ps FWHM, respectively.
Conclusions: Monolithic scintillator detectors based on dSiPMs are promising for PET applications in which high spatial resolution, TOF resolution, and detection efficiency are required, all at the same time. Compared to BSR, the DSR configuration significantly improves the time-, spatial- and DOI resolutions of the detector. At the conference, first images obtained with BSR detectors in a TOF-PET setup representative of a 70 cm diameter clinical scanner will be presented.

Keywords: Time-of-Flight Positron Emission Tomography (PET), Digital Silicon Photomultiplier (dSiPM), Monolithic Scintillator Detector

Acknowledgements: This work was supported in part by EU FP7 project SUBLIMA, Grant Agreement No 241711 (www.sublima-pet-mr.eu).

194
Reduced side effects by proton minibeam radiotherapy in a mouse ear model
T. E. Schmid[1,2], S. Girst[3], C. Greubel[3], J. Reindl[3], C. Siebenwirth[1,3], K. Ilicic[1], D.W.M. Walsh[1,3], G. Dollinger[3], J. Wilkens[1,2], G. Multoff[1,2], S.E. Combs[1,2]
[1] Klinikum rechts der Isar, Technische Universitaet München, Germany
[2] Institute of Innovative Radiotherapy (iRT), Department of Radiation Sciences, Helmholtz Zentrum München, Germany
[3] Universität der Bundeswehr München, Neubiberg, Germany

Purpose: Proton minibeam radiotherapy aims to minimize normal tissue damage in the entrance channel while keeping tumor control through a homogeneous tumor dose due to channel widening with increasing track length. Side effects of proton minibeam irradiation were examined in an in-vivo mouse model to account for immune system, vasculature and higher complexity. Here, we report on our comparative study of minibeam and broad beam irradiation in the ear of Balb/c mice, to prove this hypothesis of reduced adverse effects in normal tissue.
Methods: At the ion microprobe SNAKE, 20 MeV protons were administered to the right ear of 2-3 months old, female Balb/c mice, using an average dose of 60 Gy in a field of 7.2 x 7.2 mm2 in the central part of the ear, in two irradiation modes, homogeneous and minibeams. The 4 x 4 minibeams of 180 x 180 µm2 size were set in a distance of 1.8 mm, resulting in a dose of 6000 Gy in the channels, but with negligible dose in between. Inflammatory response, i.e. ear swelling and skin reactions were monitored for 90 days following irradiation, as well as genetic damage and release of inflammatory proteins.
Results: No ear swelling or other skin reaction was detected after the minibeam irradiations, while significant ear swelling (up to 4-fold), erythema and desquamation (crust formation) developed in homogeneously irradiated ears 3-4 weeks after irradiation. Loss of hair follicles was only detected in the homogeneously irradiated fields after 4-5 weeks.
Conclusion: Our results prove that proton minibeam radiotherapy leads to reduced side effects compared to conventional broad beam irradiation and could become an option in clinical proton and/or heavy ion therapy.
Supported by the DFG Cluster of Excellence: Munich-Centre for Advanced Photonics.

Keywords: proton, minibeam radiotherapy, mouse

195
The relevance of DNA damage clustering on the nanometer and micrometer scale for the quantitative prediction of radiation effects
T. Friedrich[1], F. Tommasino[1,2], L. Herr[1], U. Scholz[1], A. Hufnagl[1], M. Durante[1,2], M. Scholz[1]
[1] GSI Helmholtzzentrum für Schwerionenforschung, Darmstadt
[2] TIFPA Trento Institute for Fundamental Physics and Applications, Trento

Purpose: The Local Effect Model (LEM)[1,2] and the Giant-Loop Binary-Lesion (GLOBLE) model[3] both are based on the analysis of DSB distribution within the cell nucleus and particularly focus on DNA lesion clustering properties with respect to the nanometer level as well as higher-order chromatin structure. According to this concept, radiation effects are uniquely determined by the number and microscopic spatial distribution of DSB. Here we demonstrate that this universal concept allows quantitative prediction of a wide variety of biological endpoints for different radiation qualities.
Methods: Clustering on the nanometer level is considered on the level of SSB and leads to an increased yield of DSB as a consequence of interaction of two SSB induced in the DNA within a short distance. Clustering at the micrometer level is taken into account by the distinction of two DSB classes, depending on the number of DSB induced within chromatin loops of about 2 Mbp size: isolated DSB (iDSB) corresponding to exactly one DSB/loop, and clustered DSB (cDSB) corresponding to more than one DSB/loop. Predictions of biological effects are solely based on the yields of iDSB and cDSB, respectively.
Results: For high-LET radiation, the concept allows predicting the observed increased relative biological effectiveness (RBE) and its dependence on the ion species, LET, dose and cell type[1,2] based on the knowledge of the corresponding photon dose response curves. Furthermore, the two classes of iDSB and cDSB can be identified with the two components leading to biphasic rejoining kinetics, and the model is able to correctly predict the fractions of fast and slow rejoining over a wide spectrum of different radiation qualities[4].
For high energetic photon radiation, the concept allows explaining the linear quadratic shape of the photon dose response curve and predicts a transition to a more linear shape at high doses[3]. The model also correctly reproduces dose rate effects after photon irradiation[5]. Furthermore the increased effectiveness of ultrasoft x-rays is predicted by the model as a consequence of the increased DSB yield[6].
Finally, based on the cell cycle dependent replication of chromatin loops the cell cycle dependent variation of radiosensitivity is reproduced. Based on the model parameters derived from normal cells, the different cell cycle dependent sensitivity of NHEJ-deficient and HR-deficient cells is predicted by the model[7].
Conclusion: Using the LEM and the GLOBLE model it could be shown that the knowledge of the initial spatial DSB distribution pattern induced by low- and high-LET radiation allows accurate quantitative prediction of radiation effects for a wide variety of different radiation qualities and biological endpoints. The consistent and simultaneous applicability of the model framework to widespread radiobiologic phenomena is a strong support for the underlying assumptions.

Keywords:
Biophysical Modelling, RBE, chromatin loop, DSB

References:
[1] Elsässer T. et al., *Int. J. Radiat. Oncol. Biol. Phys.*, 78:1177-1183 (2010)

[2] Friedrich, T. et al. *Int. J. Radiat. Biol*. 88, 103-107 (2012)
[3] Friedrich, T. et al., *Radiat. Res.* 178, 385-394 (2012)
[4] Herr L. et al, PLoS One, 9, e83923 (2014)
[5] Tommasino, F. et al., *Radiat. Res.* 180, 524-538 (2013)
[6] Friedrich T. et al., *Radiat. Res.,* 181, 485-94 (2014)
[7] Hufnagl A. et al., DNA Repair 27 :28-39 (2015)XXX

196

Helium and Oxygen beam models in TRiP98: implementation, treatment planning tests and experimental verification

E. Scifoni[1], O. Sokol[1], R. Grün[1], T. Friedrich[1], M. Scholz[1], W. Tinganelli[1], S. Brons[2], C. Schuy[1], M. Rovituso[1], M. Durante[1] and M. Krämer[1]
[1] Biophysics Dept., GSI Helmholtzzentrum für Schwerionenforschung, Darmstadt (D)
[2] Heidelberger Ionenstrahl-Therapiezentrum (HIT), Heidelberg (D)

Since some of the most modern ion therapy facilities are offering or considering the irradiation with alternative ion beams, beyond proton and carbon, it has raised new attention the need for a proper description of these beams, in order to exploit their use for specific applications. In particular, helium and oxygen beams are presently available in the research cave of the Heidelberg Ion therapy facility (HIT).
We developed and integrated in TRiP98, our research treatment planning system, specific beam models for these ions, which have been validated experimentally on different levels.
For the Helium beam a semiempirical model for dose deposition and fragmentation was implemented, by modification of algorithms conventionally used in space radiation transport studies, translated to the typical therapeutic range of energies [1].
For Oxygen beam, the standard transport model of TRiP98 was tuned on recent attenuation experiments and the fragmentation cascade has been improved using the latest beam models of the low-lying ions.
Several treatment planning tests have been performed, showing no universal indications but rather selective advantages of the different beams, and revealing for example a considerable convenience of using Helium beams in specific configurations [2], or proposing combination of different ions [3].
Experimental verification has been performed for both ion beams at the experimental room of HIT, analyzing different endpoints: basics physics data, delivered 3D physical dose distribution and biological effect. Monoenergetic and extended target irradiations of different extensions with single and double opposed fields have been verified. In the case of oxygen beams, considering that its main importance is related to a possible indication for partially hypoxic tumors, the biological verification was extended beyond the RBE weighted dose effect, but also including the OER effect. As previously obtained with carbon ions [4], the kill-painting method, allowing to restore an homogeneous survival level on a differently oxygenated target, was verified with oxygen beams. It is found that with the latter ion beams, for a partially hypoxic target an inversion of the relative profile occurs, as compared to a normoxic case, with a slightly reduced normal tissue damage for same cell killing in the target than with the carbon irradiation.

Keywords: Particle Therapy, Adaptive Treatment Planning, Helium beams, Oxygen beams, Hypoxia

References:
[1] M. Krämer, E. Scifoni, C. Schuy, M. Rovituso, W. Tinganelli, A. Maier, R. Kaderka, W. Kraft-Weyrather, S. Brons, T. Tessonnier, K. Parodi and M. Durante, subm. to Med Phys. (2015)
[2] R. Grün, T. Friedrich, M. Krämer, K. Zink, M. Durante, R. Engenhart-Cabillic and M.Scholz, Med Phys 42, 1037 (2015)
[3] M. Krämer, E. Scifoni, F. Schmitz, O. Sokol and M. Durante, Eur Phys J D 68, 306 (2014)
[4] W. Tinganelli, M. Durante, R. Hirayama, M. Krämer, A. Maier, W. Kraft-Weyrather, Y. Furusawa, T. Friedrich and E. Scifoni, Sci Rep. (2015) in print

197

Medical isotope production at TRIUMF and future collaboration with MEDICIS-PROMED

Y. Seimbille[1]
[1] TRIUMF, Division of Life Sciences, 4004 Wesbrook Mall, Vancouver, Canada

The demand for personalized medicine is increasing, and considering that the population suffering from chronic diseases (i.e. cancer, Alzeihmer) is continuously growing it is expected that the consumption of molecular diagnostic products and radiotherapeutics will continue to increase. In this scenario, TRIUMF and its fleet of proton accelerators ranging from 13 to 500 MeV is offering a unique environment for scientists to enable the production of isotopes with potential applications in molecular imaging or radiotherapy. A multidisciplinary program involving target design, isotope production and radiopharmaceutical chemistry has emerged in the Division of Life Sciences to facilitate and accelerate the translation from bench-to-bedside.
A brief overview of the recent efforts related to the production and applications of medical isotopes at TRIUMF will be presented. Comprehensive studies have been conducted to improve the production of conventional PET isotopes by a better understanding of the physical phenomenon occurring inside the target during beam irradiation. Feasibility of the production, from liquid targets, of radiometals (i.e. ^{44}Sc, ^{68}Ga, ^{86}Y and ^{89}Zr) used in medical imaging has also been demonstrated. The results of the ITAP project, led by TRIUMF and including a consortium of institutions, on accelerator-based production of ^{99m}Tc will be discussed. It has been shown that a reliable commercial scale (TBq) production of ^{99m}Tc is achievable by using ^{100}Mo coated tantalum targets at energies up to 24 MeV. Investigations on the production and isolation of the therapeutic isotope ^{211}At and its imaging companion ^{209}At will be mentioned.
Novel radiolabeling strategies and technologies have recently emerged to prepare radiopharmaceuticals and will be discussed. Isotopic exchange reactions are getting popular to rapidly and efficiently synthesize PET imaging probes. Click chemistry is also representing an attractive approach to radiolabel molecules because of its simple process, short reaction times and clean product synthesis. Microfluidic devices bear great promises in the field of radiochemistry as it is expected that they will allow faster reaction rate, exquisite reaction selectivity, reduced reagent consumption, and possibly revisit the hot-lab concept. An overview of the tracer development performed at TRIUMF (e.g. cysteine transporter, angiogenesis) will be presented.
Finally, within the framework of the MEDICIS-PROMED consortium, a collaboration between TRIUMF and the Institute of Translational Molecular Imaging (ITMI) at the University Hospital of Geneva and the Laboratory of Bioorganic Chemistry and Molecular Imaging at EPFL will soon take place. This presentation will conclude with a short summary of our ambitious project on the development of dual modality molecular probes for ovarian cancer and their preclinical validations in animal models.

Keywords: medical isotope, radiochemistry, radiopharmaceuticals

198

Size dependence of GNPs dose enhancement effects in cancer treatment – Geant4 and MCNP code

M.Sharabiani[1], M.Vaez-zadeh[1], S.Asadi[1]
[1] Department of Physics, K.N.Toosi University of Technology, Tehran, Iran

Purpose: The main purpose of the present work is to evaluate the effects of gold nanoparticles (GNPs) in different sizes and concentrations on cancer cells which undergo treatment with photon therapy.

Material and Method: This work was carried out with MCNP and Geant4 codes. The 10x10x10 cm3 cubic water phantom and a tumor region with a size of 1x1x1 cm3 were simulated. Factors such as different concentrations and GNP sizes were implemented into the simulation, so as to obtain the optimum results, specifying the maximum absorbed dose within the tumor while sparing healthy tissue. In a certain concentration, different sizes of GNPs including 30, 50, 70 and 100 nm were defined within the tumor and the absorbed dose by the GNPs-loaded tumor were calculated for different sizes. Similarly, the absorbed dose was calculated for different concentrations of 7, 10, 18 and 30 (mg Au/ gram of tumor) in a certain size of GNPs. The dose enhancement factor which is defined as the ratio of the absorbed dose by the tumor in the presence of nanoparticles to the absorbed dose by the same organ in the absence of nanoparticles was estimated for different concentrations and sizes of GNPs.
Results and Conclusion: The calculations show results for different sizes and concentrations and a comparison is made between the two Monte Carlo codes (MCNP and Geant4). In a certain diameter of GNPs the higher concentration made more increase in absorbed does by the tumor. In a certain concentration, higher size of GNPs made higher absorbed dose by the tumor. Given the fact that therapeutic applications of GNPs in acquiring the proper DEF have demanded much attention in recent years, defining the proper size and concentration would be considered extremely vital for pre-treatment plans.

Keywords: Geant4, Size and Dimension, GNPs, Radiotherapy

199

Therapeutical Dose to Thyroid Remnants Determination for Low-risk Thyroid Carcinoma Patient Treated with rhTSH and 1.1 GBq 131I

P. Solný[1,2], T. Kráčmerová[1,2], L. Jonášová[2], P. Vlcek[2]
[1] Department of Dosimetry and Application of Ionizing Radiation Faculty of Nuclear Sciences and Physical Engineering, Czech Technical University in Prague
[2] Department of Nuclear Medicine and Endocrinology 2nd Faculty of Medicine, Charles University in Prague and Motol University Hospital

Purpose: Aim of this study was to investigate, practically prove contribution, and verify dosimetry possibilities for low-risk patients (rhTSH stimulation and 1.1 GBq 131I administration) undergoing first Radioiodine therapy (RAIT). Furthermore, it was intended to verify whether the administered activity deliver sufficient dose to thyroid remnants so it can be called "thyreo-ablative".
Materials and methods: Siemens Symbia S gamma camera was used for quantitative imaging of 131I accumulation in remnants of patients thyroid and 131I accumulating nods. Vials with known activity of 131I were used to calibrate the system. Verification of activity determination was done by measuring the vial together with patient for comparison, if necessary. All of the patient-volunteers were around 3 months after thyreoablation due to thyroid carcinoma. As a low-risk indicated patients, they were prepared by injections of rhTSH during two days before therapy. Weight of the accumulating remnants or nods was established using ultrasound, if visible or roughly estimated using phantom measurements causing serious uncertainties.
17 patients (15 women, 2 men) participating the study undergone up to 6 quantitative imaging by the gamma camera during 70 hours after administration. Minimum of the gamma camera examination was 4. General time schedule of examination was 5, 24, 30, 48, 70 hours after administration.

Results: Absorbed doses within remnants or nodes vary from tens of Gy up to several hundred Gy with uncertainty from 25% up to 100% depending mainly on mass of the remnants estimation. For 5 of the patient the administered therapeutic activity caused absorbed dose which was considered to be rather insufficient in terms of thyreo-elimination (at least for one of accumulating remnants). For 4 patients the absorbed dose was considered to be particularly thyreo-eliminative. Measurements for 5 patients confirmed thyreo-eliminative dose and in case of 3 patients no accumulation was detected. Consequent follow-up for all patients is being done.
Conclusions: Though in nearly 30% of all patients absorbed dose did not reach 300 Gy in thyroid remnants and 80 Gy in nods, due to low-risk staging it is probable that the treatment was successful. However, it is necessary to do consequent follow up and include all data for annual treatment evaluation. Based on the results appropriate grant for further investigation will be seek out.

Keywords: dosimetry, iodine therapy, 1.1 GBq

200

Augmented reality supporting innovation and accuracy in advanced radiation therapy facilities

S. Spoto[1], F. Bourhaleb[1], G. Petrone[2]
[1] Internet Simulation Evaluation Envision (I-See)
[2] Department of Computer Science, University of Turin, Italy

Purpose: Particle therapy cancer treatments require a work flow that involve several professional figures, working with a complex hardware and software set up. Each professional role needs access to a considerable set of information in the everyday clinical practice. In particular quality assurance protocols demand checking a sensible amount of data.
The drawback is that often required information are physically accessible outside the treatment room, being distributed on several computer in different places.
Integrate and display needed information in an organic and easily accessible way can speed up the clinical practice, reducing potential time loss and providing a better continuous quality control.
Methods: We propose an innovative tool based on Augmented Reality (AR). In AR a view of the physical world is augmented with computer generated elements. Our AR tool could be installed on a modern mobile device, a tablet or a cellphone. Users gets information in real-time about any equipment in the *treatment room* simply pointing the device at it.
The AR client recognizes medical equipment using the device camera, then gathers corresponding information from a cloud server, where all data stored.
The access to the data server is secured with different level of privileges: a user can visualize and use only predetermined kind of relevant information, according to his role. Moreover, all information related to the patient and the medical environment are hosted in a private cloud, not accessible without proper authentication.
Results: We present a prototype of AR application for particle therapy centre that improves and speeds up the whole work flow, making the access to information easier and more centralized.
Here we present a three different use cases that illustrate the use of our AR application: medical doctor, medical physicists and technical engineer.
Conclusion: Augmented Reality is the perfect candidate to help healthcare organizations make their existing processes more precise and efficient. Using AR tools, useful information can be provided and related in real-time to the specific need of the different systematic tasks that are daily checked accurately in an advance radiation therapy facility.

Keywords: e-heathcare, augmented reality, particle therapy

201

Manufacturing and Nuclear Medicine Applications of the Novel Isotope Sn-117m

N. Stevenson
R-NAV, LLC

Sn-117m has unique characteristics that make it ideal for a variety of nuclear medicine applications. The $t_{1/2}$=14d isotope emits a primary 159 keV imaging photon (86%) that is easily detectable with any SPECT camera system. The accompanying mono-energetic conversion electrons (~140 keV; 110%) have a therapeutic effect limited to a range of ~300 µm which also minimizes any shipping and handling issues. Together these characteristics make this theranostic

isotope a prime candidate for several personalized nuclear medicine applications.
This isotope can be produced in large quantities as a low specific activity (up to 800 GBq/g) product in reactors via the Sn-116(n,γ) or Sn-117(n,n'γ) reactions. A carrier-free, high specific activity (up to 800 TBq/g) isotope can be manufactured with ~50 MeV cyclotrons employing either Sb(p,x) or Cd-116(α,3n). Methods for extracting and purifying the Sn-117m from Sb or Cd have been developed.
Sn-117m has been used to label a wide variety of targets including proteins, anti-bodies and small molecules. In recent animal and human Phase I/II cardiovascular trials to detect and treat vulnerable plaque, the Sn-117m was chelated to aminobenzyl DOTA before being conjugated to annexin V. Results demonstrated the ability of this molecule to both target and image the plaques. Additionally, a remarkable therapeutic effect was observed at very low doses (~10 cGy).
In oncology, Sn-117m (chelated to DTPA) has been successfully used in over 120 humans for bone pain palliation in a Phase I/II trial. Labeling of neuroendocrine cancer targeting molecules has also been demonstrated. The isotope, in low specific activity form, has been electroplated onto stents and implanted into several animal models to demonstrate the efficacy and finite range of the conversion electrons. Human and veterinary applications are under development.
Rheumatological applications include a homogeneous Sn-117m colloid that is being used to treat (radiosynoviorthesis) canine osteoarthritis (OA). Future veterinary applications include treating equine OA and human rheumatoid arthritis (RA). Labeled compounds are also being developed to image and treat RA systemically.
Additional future applications being explored take advantage of the limited irradiation of normal tissue in immune and inflammatory CNS conditions that could provide new therapeutic advantages to this immunologically privileged system. In conclusion, the novel isotope Sn-117m is successfully finding application in several aspects of human nuclear medicine and is now also creating new opportunities in the emerging field of veterinary nuclear medicine.

Keywords: Sn-117m, manufacturing, nuclear medicine applications

202
A comprehensive omics approach for development of prognostic or predictive biomarkers in squamous cell carcinoma of the head and neck treated with radiation
M.D. Story[1], T-H. Hwang[2], L-h. Ding[1], H. Tang[2] and N. K. Karanam[1]
The University of Texas Southwestern Medical Center, 2201 Inwood Rd. Dallas, TX 75390
Departments of [1]Radiation Oncology and [2]Clinical Sciences

Purpose: We have taken a comprehensive approach to develop biomarkers of potential therapeutic radioresponse. This approach includes gene, miRNA, and protein expression, as well as methylation and mutation analysis. Methods: Specimens from 102 HNSCC patients identified by surgical and pathologic criteria considered high risk for local recurrence (LR) or distant metastasis (DM) after post-operative radiotherapy as well as 22 specimens from adjacent normal tissue were used. We have strived to avoid the pitfalls of biomarker discovery such as inadequate clinical phenotyping, the use of specimens of convenience, poorly annotated specimens, heterogeneous specimens and underpowered sample sets amongst others.
Results: While a 46 gene signature was able to stratify patients based upon risk for overall survival, no gene signature was able to segregate specimens specific to LR or DM. This 46 gene signature, however, was able to stratify patients by overall survival in this data set, 5 independent HNSCC data sets as well as the TCGA data set. However, using a 36 miRNA signature PORT outcomes (LR or DM could be predicted. Unfortunately, when applied to the TCGA data set 13 miRNA were unavailable limiting the external validation to survival only. DNA methylation analysis, which is still ongoing, has identified DM and LR and includes genes in pathways associated with EMT and DNA repair, respectively. We have also taken the approach that biomarkers should have a biological basis and we have examined a set of 49 HNSCC cells lines for gene and miRNA expression, and methylation. Furthermore, full radiation survival curves were generated. Filtering through miRNA target databases and examining negative correlations of miRNA and gene expression led to the isolation of several miRNA for further analysis. For example, miR-125a was under-represented in the LR cohort. miR-125a is a negative prognostic indicator in gastric cancer, targeting ERBB2. ERBB2 gene expression is anti-correlated with miR-125a expression in tumor specimens and in our 49 HNSCC cell lines. Furthermore, up-regulation of miR-125a in HN5 cells led to radiosensitization while down-regulation of miR-125a led to radioresistance. Within the DM group, miR-551a and 551b-3p are over-represented. These miRNA drive cell proliferation, migration and invasion. A target of these miRNA is GLIPR2. The GLIPR2 protein binds BCLN1 and sequesters it within the golgi. Release of BCLN1 allows cells to enter into autophagy and by modulating miRs 551a and 551b-3p, we can drive cells into autophagy, enhance invasiveness and increase radioresistance.
Conclusions: The expression of miRs 551a and 551b-3p as well as GLIPR2 gene expression can stratify patient outcome in our patient cohort, other HNSCC cohorts as well as other invasive cancers. Their expression is also highly associated with late stage HNSCC. Lastly, we are now integrating data sets to take a panomics approach to biomarker development.

Keywords: head and neck cancer, omics, radiation therapy, biomarkers

203
Development of a High Resolution Module for PET scanners
G. Stringhini [1,2], M.Pizzichemi[2], T. Niknejad[3], S. Tavernier [3], J. Varela [3], P. Lecoq [1], M. Paganoni[2], E. Auffray[1]
[1] CERN, Geneve, Switzerland
[2] University of Milano-Bicocca, Italy
[3] Laboratorio de Instrumentacao e Fisica Experimental de Particulas, Portugal

Purpose: PET ("Positron Emission Tomography") scanners have to guarantee high performances in term of spatial resolution and sensitivity allowing to detect cancer mass while it is still sufficiently small and has not had time to spread to other parts of the body. in this frame we focused on the development of the scintillator module that can reach high performance as compared to the current scanners and at the same time that keeps low costs and not complex design. To guarantee high performance in term of spatial resolution, the Depth of Interaction (DOI) information has to be reached. Instead of using the usual approach, with a double side readout, to have DOI capability we have developed a new PET module that can provide the DOI information using just a single side readout.
Materials and Method: The module presented is based on a 64 LYSO ("Lutetium-yttrium oxyorthosilicate") crystals matrix and on an MPPC ("Multi Pixels Photon Counter") as detector that guarantee a 4 to 1 coupling between the crystals and the detector and a single side readout. The lateral surfaces of the crystals are optically processed. Different configuration with light guide between the MPPC and the crystals matrix The readout of the signal is performed by a digitizer that record for each trigger event the charge collected by each MPPC after the integration of the signal. The digitizer is connected to a custom designed acquisition card that provides at the same time bias voltage to all the MPPC channels. The matrix is fixed to the board using a PVC custom made holder that also keep all the parts of the module in place. To characterize the module a ^{22}Na radioactive source is placed 2 cm above the matrix exciting the scintillators. To test the DOI capability of the module a LYSO crystal is placed on the opposite side of the source allowing to illuminate a given vertical portion of the crystals and to permit to scan the vertical length of the module.
Results: Combinations of the collected charge can be used to

identify in which crystal the scintillation event takes place but also can provide information about the depth of interaction of the gamma along the vertical length of the crystal. In the module the light output of the crystals is related to the vertical position of the interaction point and it is proved that the DOI can be reach using a single side readout. The different configurations are tested and compared to obtain the best DOI resolution.
Conclusions: A innovative PET module is developed and tested and shows high performances according with a spatial resolution less then 1.5 mm and a DOI resolution of about 4 mm FWHM obtained using a single side readout.

Keywords: Positron Emission Tomography, Depth of Interaction, high resolution module

204
Fast Beam Profile Monitors for Microbeam Radiation Therapy
E. Alagoz[1], E. Brauer-Krisch[2], A. Bravin[2], I. Cornelius[3], P. Fournier[3], T-E. Hansen[4], A. Kok[4], M. Lerch[3], E. Monakhov[5], J. Morse[2], N. Pacifico[1], M. Petasecca[3], M.Povoli[5], H. Requardt[2], D. Roehrich[1], A.B. Rosenfeld[3], H. Sandaker[1], M.Salomé[2], B. Stugu[1]. (3DMiMic collaboration)
[1] Department of Physics and Technology, University of Bergen, Norway
[2] ESRF, European Synchrotron Radiation Facility, Grenoble, France.
[3] Centre for Medical Radiation Physics, University of Wollongong, Australia
[4] SINTEF MiNaLab, Deptartment of Microsystems and Nanotechnology, Norway
[5] Centre for Material Sciences and Nanotechnology, University of Oslo, Norway.

Microbeam Radiation Therapy (MRT) is a novel, promising technique for X-ray therapy [1]. The proposed treatment consists of intense, highly collimated, parallel arrays of X-ray beams of widths between 20 and 100 μm and separations between 100 and 400 μm generated by synchrotron radiation and suitable microslit collimators. Due to extremely high dose rate (up to 20 kGy/sec), a fast and reliable monitoring system is essential, but extremely challenging to construct, as it must cope with the high intensity, as well as very steep intensity gradients within the microscopic dimensions of the beams.
In order to meet the requirements, the 3DMiMic collaboration has designed and fabricated 10 μm thick silicon strip beam monitors. Several strip layouts have been produced for simultaneous monitoring of the full array of microbeams.
Tests using both single channel and multichannel readout at the ESRF biomedical beam-line ID17 demonstrate that the detector and readout system work well and constitutes a viable system for coping with the challenge [2].
In this presentation we will give details of the sensor design and results obtained from the tests at the ID17 beam-line. 2D response scans and time evolution studies of the sensor performed with an X-ray microprobe at the ID21 beam-line will also be presented.

Keywords: Micro-beams, Silicon sensors, X-rays.

References:
[1] A. Bravin,P. Olko,E. Schültcke, J.Wilkens (Editors) "Radiation Therapy with Synchrotron Radiation: Achievements and Challenges": European Journal of Medical Physics 31 (2015) 561-646.
[2] M. Povoli et al.: "Thin silicon strip detectors for beam monitoring in Micro-beam Radiation Therapy" ArXiv:1509.08714, submitted to JINST.

205
Improved proton stopping power ratio estimation for a deformable 3D dosimeter using Dual Energy CT
V. T. Taasti[1], Ellen Marie Høye[1], David Christoffer Hansen[1], Ludvig Paul Muren[1], Jesper Thygesen[2], Peter Sandegaard Skyt[1], Peter Balling[3], Niels Bassler[3], Cai Grau[4], Gabriela Mierzwińska[5], Marzena Rydygier[5], Jan Swakoń[5], Pawel Olko[5], Jørgen Breede Baltzer Petersen[1]
[1] Department of Medical Physics, Aarhus University / Aarhus University Hospital, Aarhus, Denmark.
[2] Dept. of Clinical Engineering and Dept. of Radiology, Aarhus University / Aarhus University Hospital
[3] Department of Physics and Astronomy, Aarhus University, Aarhus, Denmark.
[4] Department of Oncology, Aarhus University / Aarhus University Hospital, Aarhus, Denmark.
[5] Institute of Nuclear Physics PAN, ul. Radzikowskiego 152, 31-342 Krakow, Poland.

Purpose: The highly localized dose distribution in proton therapy (PT) makes this treatment modality sensitive to organ motion and deformations. E.g. in proton pencil beam scanning interplay effects may be significant, resulting in dose degradations. Due to the complexity of PT dose delivery, investigations of the consequences of motion and of motion mitigation strategies may benefit from use of 3D dosimetry. A new family of silicone-based 3D dosimeters is currently being developed. These dosimeters can be moulded into anthropomorphic shapes and can be deformed during beam delivery, which allows for simulation of organ motion and deformation.
Treatment planning with protons is based on CT scans of the patient anatomy and a conversion of the HU for the tissue to a stopping power ratio (SPR) relative to water. To ensure that the same procedure can be performed for the dosimeter it must be verified that its SPR is estimated correctly from its HU. The aim of this study was therefore to investigate if the use of Dual Energy (DE) CT and dedicated DE calibrations can improve the calculation of the SPR for the dosimeter compared to use of Single Energy (SE) CT together with the stoichiometric calibration method.
Method: The dosimeter was CT scanned with a Dual Source CT scanner (Siemens Somaton Definition Flash). First a CT scan was obtained in SE mode with a tube voltage of 120 kVp, and this scan was used in the stoichiometric calibration. Next a set of CT scans was obtained in DE mode with a tube voltage pair of 80/140Sn kVp (Sn: 0.4 mm extra tin filtration); this CT image set was used for SPR calculation with two published DE calibrations. The $CTDI_{vol}$ of the two scanning modes was set to be the same (~20 mGy).
A thin slab of the dosimeter material was placed in a water tank and irradiated with a 60 MeV proton beam. The range of the protons was measured with and without the dosimeter intersecting the beam to determine the range difference. The SPR of the dosimeter was calculated from its thickness and the range difference.
Results: The two DE calibration methods both gave an estimate of SPR_{est} = 1.01, whereas the SE stoichiometric calibration estimate was SPR_{est} = 1.10. From the range measurements, the SPR of the dosimeter was calculated to be SPR_{meas} = 0.97. The measured SPR did not fall on the stoichiometric calibration curve of the reference tissues (Figure; the high content of silicon makes the dosimeter not tissue equivalent). The dosimeter was found to have a HU corresponding to bone (CT number = 135 HU) but a SPR corresponding to fat.

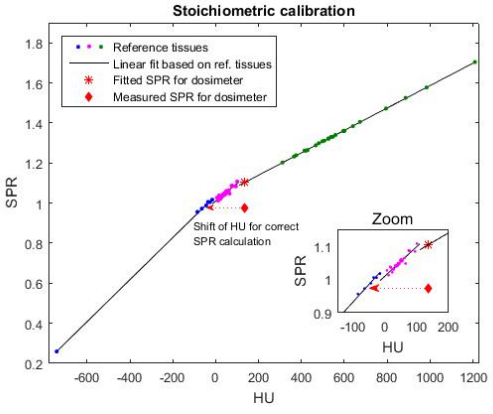

Figure: Stoichiometric calibration curve. The HU shift for the dosimeter needed for a correct SPR estimation based on the curve is indicated with a red arrow.
Conclusion: The stoichiometric method overestimates the measured SPR by 13%. Using DE this error is reduced, to an overestimation of 3%. If the stoichiometric method is used for the 3D dosimeter its HU must be corrected in the treatment planning system.

Keywords: Stoichiometric calibration method, Dual Energy CT, 3D dosimetry

References:
[1] E. M. Høye, P. S. Skyt, E. S. Yates, L. P. Muren, J. B. B. Petersen and P. Balling, "A new dosimeter formulation for deformable 3D dose verification", Journal of Physics: Conference Series 573, 012067 (2015).
[2] Y. De Deene, R. Hill, P. S. Skyt and J. Booth, "Flexydos3D: A new deformable anthropomorphic 3D dosimeter readout with optical CT scanning", Journal of Physics: Conference Series 573, 012025 (2015).
[3] U. Schneider, E. Pedroni and A. Lomax, "The calibration of CT Hounsfield units for radiotherapy treatment planning", Phys. Med. Biol. 41, 111-124 (1996).
[4] N. Hünemohr, B. Krauss, C. Tremmel, B. Ackermann, O. Jäkel and S. Greilich, "Experimental verification of ion stopping power prediction from dual energy CT data in tissue surrogates", Med. Phys. 59, 83-96 (2014).
[5] D. C. Hansen, J. Seco, T. S. Sørensen, J. B. B. Petersen, J. E. Wildberger, F. Verhaegen and G. Landry, "Beyond the stoichiometric method: A comparison of dual energy CT and proton CT for stopping power estimation", submitted to Med. Phys. (2014).

206
Organizational response of the hypothalamus and pituitary to external beam radiation
N. Taku[1], M. Romanchikova[2], S.J. Thomas[2], A.M. Bates[1], R. Jena[1], N.G. Burnet[1]
[1] Department of Oncology, University of Cambridge, Addenbrooke's Hospital, Cambridge, UK
[2] Department of Medical Physics and Clinical Engineering, Addenbrooke's Hospital, Cambridge, UK

Purpose: Hypothalamic-pituitary axis (HPA) dysfunction is a dose-dependent sequela of brain irradiation. Meta-analysis of studies on non-pituitary central nervous system tumours performed by Appelman-Dijkstra et al. [*The Journal of Clinical Endocrinology & Metabolism*, 8, 2330 (2011)] found estimated doses of 25-97 Gy to the HPA and 0.54 prevalence of pituitary deficiency. However, no included study reported the site-specific doses to the hypothalamus or pituitary. As the hypothalamus is thought to be more radiosensitive than the pituitary, greater understanding of the structural organization and normal tissue tolerances of these two structures is necessary to better describe the relationship between HPA radiation dose and secondary insufficiency. The purpose of this study is to characterize the radiation dose to the HPA in adults treated for non-pituitary brain tumours.
Materials/Methods: Twelve patients, 3 males and 9 females, have been enrolled in our prospective VoxTox study that will continue to recruit until 2017. Primary diagnoses included meningioma (7), pineal tumor (3), and glioma (2). Patients were treated with TomoTherapy® and received 50-60 Gy to the tumour bed in 30 fractions. Digital Imaging and Communications in Medicine radiotherapy data, including dose cubes, contours and planning imaging, were retrieved from TomoTherapy® archives using an in-house software and imported into ProSoma virtual simulation software. Quality assurance of hypothalamus and pituitary contours was performed. Parametrisation of dosimetric data from planning computed tomography scans was used to determine mean radiation doses to the hypothalamus and pituitary separately. Dose volume histogram data were exported to Matlab®. Equivalent uniform doses (EUDs) for a parallel structure (a=1) and serial structure (a=20) were calculated utilizing a freely available program and normal tissue tolerance parameters for the lung and spinal cord, respectively.
Results: The mean radiation doses to the hypothalamus and pituitary were 35 Gy and 34 Gy, respectively. Serial and parallel EUDs for each patient are presented in Figure 1. The mean EUDs for a=1 and a=20 were 30 Gy (range 14-52) and 33 Gy (range 19-52), respectively, for the hypothalamus and 29 (range 8-46) and 31 Gy (range 8-46), respectively, for the pituitary. The mean difference between serial and parallel EUD values was 3 Gy for both the hypothalamus and the pituitary.
Conclusions: The organization of the hypothalamus and pituitary into serial or parallel structures may not be predictive of HPA response to radiation. Future studies are necessary to isolate the dose-volume effects of these two organs.

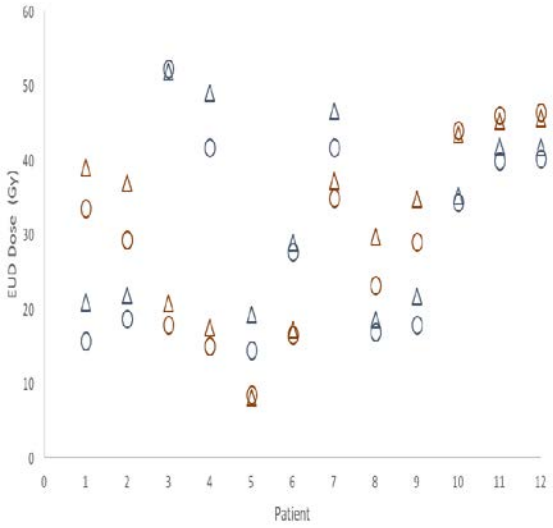

Figure 1. EUD doses to the hypothalamus (blue) and pituitary (red) are presented for parallel (circle) and serial (triangle) structures for each patient.

Keywords: brain tumours; pituitary; hypothalamus

207
Response-based Bayesian Network Approaches for Adaptive Radiotherapy of Non-Small Cell Lung Cancer (NSCLC)
Y. Luo[1], I. El Naqa[1], D.L. McShan[1], I. Lohse[1], M.M. Matuszak[1], M. Schipper[1], S. Jolly[1], F.M. Kong[2], R.K. Ten Haken[1]
[1] Department of Radiation Oncology, The University of Michigan, Ann Arbor, MI, USA
[2] Department of Radiation Oncology, Georgia Regents University, Augusta, GA, USA

Purpose: In NSCLC radiotherapy, personalized radiation treatment is intended to deliver an appropriate amount of dose to control the tumor while reducing radiation-induced toxicities such as radiation pneumonitis, esophagitis, carditis. The outcomes of radiation treatment may depend on radiation dose and patients' physical, clinical, biological and genomic characteristics before and during the course of radiotherapy. We intend to find hierarchical biophysical relationships influencing the observed outcomes from retrospective data and develop practical Bayesian Networks (BN) for adaptive radiotherapy of the NSCLC.
Materials/methods: Our study includes 79 NSCLC patients treated on prospective protocols under IRB approval. In addition to dosimetric information, each patient had 179 features from five categories including clinical factors (10) (e.g., age, KPS), cytokines before (30) and during (30) the treatment course, microRNAs (49), and single-nucleotide polymorphisms (SNPs) (60). A large-scale Markov blanket based on the HITON algorithm is employed for selecting relevant biophysical predictors of outcomes. The corresponding BN structure is obtained using the hill-climbing algorithm implemented in the R programming environment.

The BN is guarded against overfitting using k-fold cross validation.
Results: BNs representing the biophysical relationships before and during the course of radiotherapy behind the radiation outcomes are identified and designated as "biophysical BNs''. They can be adjusted to "practical BNs" for adaptive therapy purposes, with a possibility of minor compromise of estimated prediction power. Given a patient's pretreatment data, an appropriate treatment plan can be chosen from a practical BN to control the tumor and keep the radiation toxicities under a certain level. When the patient's during treatment information is available, the planned dose can be adjusted in the BN according to his/her responses, to better control tumor without increasing the chance of the complication. Cross validation is employed to measure the prediction power of the BNs. For example, while the performance of a pretreatment BN to predict radiation pneumonitis ≥G2 is 0.80 with 95% CI: 0.69-0.90 based on 2000 stratified bootstrap replicates, the AUC of the BN with patients' responses during radiotherapy can reach 0.84 (95% CI: 0.78-0.92).
Conclusions: We developed clinically practical systems to predict the radiation outcomes in NSCLC patients before and during the course of radiation treatment based on retrospective data. The prediction performance of the BN improves by incorporating during treatment information. Our approach can handle high dimensional predictors and can be an important component of decision support for personalized adaptive radiation treatment. However, it still needs to be validated in external independent data.

Keywords: Adaptive Radiotherapy, Radiation Outcomes Prediction, Bayesian Networks

208

Experimental dosimetric comparisons of protons, helium, carbon and oxygen ion beams

T. Tessonnier [1,4], A. Mairani [2,3], S. Brons[2], T. Haberer[2], J. Debus[1,2], K. Parodi[2,4]
[1] Department of Radiation Oncology, University Hospital Heidelberg, Germany
[2] Heidelberg Ion Beam Therapy Center, Heidelberg, Germany
[3] Medical Physics Unit, CNAO Foundation Pavia, Italy
[4] Department of Medical Physics, Ludwig-Maximilians University Munich, Germany

Purpose: The interest in particle therapy is growing worldwide with clinical applications focused on protons and carbon ion beams. Moreover, at the Heidelberg Ion Beam Therapy Center, helium and oxygen ions are available for research purposes with an active scanning beam delivery system. While most of the planning studies comparing these four ions are based on non-experimentally validated calculations, this work is focused on the basic experimental dosimetric characterizations and comparisons of these ions at the same facility.
Material/methods: Laterally integrated depth-dose distributions of pencil-like beams, for 10 different energies in the therapeutic range have been experimentally studied, with a range in water similar for every ion. Several parameters were evaluated, as the range, the entrance-to-peak ratio, the width of the Bragg peak, the distal fall-off and the tail-to-peak ratio, and this with and without ripple filter (used to broaden the pristine peaks). The measurements were performed using a water column, by delivering quasi-monoenergetic pencil-like beams on the central axis.
The lateral dose profiles of these ions, at low, middle and high beam energy, were investigated at different depths in water (without ripple filter). Along with the acquisition of these data, a double-Gaussian parametrization was performed and the evolution of its components along the depth in water was examined. The measurements have been done in a water tank coupled with 24 motor-driven PinPoint ionization chambers by delivering a vertically scanned beam.
Results: For the depth-dose characterization, the evolution of the investigated parameters presents a different behavior depending on the energy, the ion and the presence or not of ripple filter. Helium ions present interesting intermediate characteristics with a distal fall-off smaller than protons and a reduce fragmentation tail compare to heavier ions. These characteristics suggest different advantages and/or drawbacks for the ions depending on the situation, and a compromise among them has to be found for later treatment planning.
The lateral profiles and their double Gaussian parametrizations present net advantages of the heavy ions compared to protons with intermediate results for helium ions.
Conclusions: Our experimental results indicate that helium ions could be a good candidate for further particle therapy improvements, with intermediate properties between the clinically used proton and carbon ions. The main features are the favorable physical characteristics, especially a smaller lateral scattering than protons and a very low tail-to-peak ratio compared to carbon ions. This study was used to create the first helium ions database, allowing biological experiments needed to ensure proper treatment planning and future fair comparisons for planning studies between the ions.
We acknowledge funding from DFG (KFO Schwerionentherapie 214).

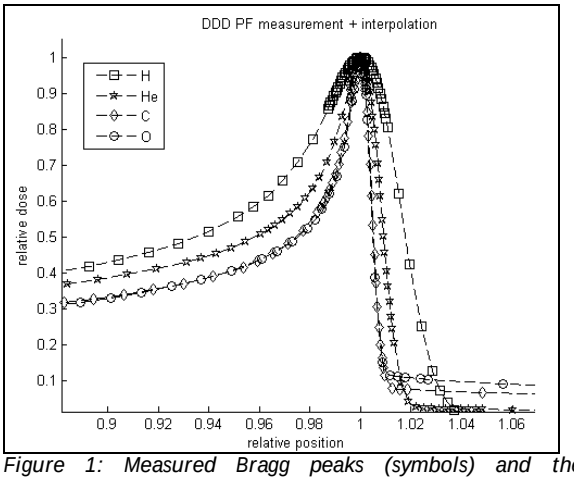

Figure 1: Measured Bragg peaks (symbols) and their interpolation (lines), normalized to maximum and to the peak position, for a range in water of ~15cm.

Keywords: Particle therapy, Experimental dosimetry, Ions comparison

209

Orthotopic tumor models for glioma and NSCLC

J. Theys, S. van Hoof, V. Sosa Iglesias, L. Schijns, L. Barbeau, N. Lieuwes; L. Dubois; F. Verhaegen; M. Vooijs.
Department of Radiation Oncology /GROW School for Oncology, University of Maastricht, Maastricht, The Netherlands

Over the last decades, survival rates for most cancer patients have only marginally increased. One reason for the limited decline in this death rate is the lack of effective treatment strategies especially in advanced cancers. In oncology research, drug development processes have proven to be very inefficient and this has been partly attributed to the lack of adequate preclinical testing modalities. Research in our lab is specifically focused on lung and brain cancer, both amongst the most malignant and difficult to treat neoplasms with very poor overall 5-year survival rates. In advanced disease most patients receive chemo- and radiotherapy (CRT), but response to treatment is generally poor with only minimal effects on survival while decreasing the patients' quality of life. Tumors almost invariably recur or are intrinsically resistant to chemotherapy. Improvement of tumor control at primary and distant locations is compulsory. The goal of our research is to identify novel treatment combinations that will result in improved outcome for patients with advanced lung or brain malignancies.

We have established reliable 3D MCTS system and used it to show proof-of-principle for identification of more efficacious promising treatment [1]. In order to test these strategies, clinically relevant tumor models are essential. In our lab we have set up orthotopic glioma [2] and NSCLC models in mice. Injection of tumor cells into the organ of origin allows for organotypical interaction between the tumor cells and the surrounding stroma. Such models replicate human disease with high fidelity and are highly suitable for evaluation of therapy response.
Tumors were monitored using cone beam computed tomography (microCBCT) imaging using a small animal micro-irradiator (SmART) and microCBCT was correlated with bioluminescence (BLI), to detect the tumor as early as possible and follow-up tumor growth. In addition to tumor growth monitoring, data on the implementation and of a small animal irradiation treatment planning software (SmART-Plan) in these orthotopic models will be presented.

Keywords: orthotopic, lung cancer, glioma, microCT, bioluminescence

References:
[1] Yahyanejad S, van Hoof SJ, Theys J, Barbeau LM, Granton PV, Paesmans K, Verhaegen F Vooijs M. An image guided small animal radiation therapy platform (SmART) to monitor glioblastoma progression and therapy response. Radiotherapy and oncology : journal of the European Society for Therapeutic Radiology and Oncology 2015;116:467-472.
[2] Yahyanejad S, Granton PV, Lieuwes NG, Gilmour L, Dubois L, Theys J, Chalmers AJ, Verhaegen F Vooijs M. Complementary use of bioluminescence imaging and contrast-enhanced micro-computed tomography in an orthotopic brain tumor model. Molecular imaging 2014;13:1-8.

210
Monte Carlo validation of the microPET FOCUS PET scanner using FLUKA
Y. Toufique[1], A Ferrari[2], O. Bouhali[1], PG Ortega[2], R. Santos Augusto[1,3], V. Vlachoudis[2]
[1]Texas A&M University at Qatar.
[2]European Laboratory for Particle Physics (CERN), CH-1211 Geneva 23, Switzerland
[3]LMU, Munich, Germany

Monte Carlo simulations play a key role in research and development of positron emission tomography devices as it provides a flexible method to evaluate alternative prototypes and scenarios, minimizing both the development cost and time.
In this work we present a new PET-dedicated Monte Carlo tool based on FLUKA [1, 2]. This latter is a multi-purpose particle physics code for calculations of particle transport and interaction with matter. It is used in a wide range of applications in high energy experimental physics and engineering including accelerator driven systems, shielding, detector or target design, neutrino physics, dosimetry, activation and medical physics etc.
The new tool has been implemented on FLAIR [3, 4] the GUI of FLUKA which makes it is an easy-to-use application allowing comprehensive simulations of PET systems within FLUKA.
The developed tools include a PET scanner geometry builder and a dedicated scoring routine for coincident event determination. The geometry builder allows efficient construction of PET scanners with nearly arbitrary parameters. We also present recent medically-oriented developments for FLAIR, which allows to import DICOM files and convert them into FLUKA voxel geometry or into a density map of radioactive isotopes, which could be employed as a source in a convenient way. The coincidence events from the scoring can be saved in standard output formats, including list mode and binary sinograms. Such coincidence events can be further 2D- or 3D-reconstructed using Filtered back-projection (FBP) or Maximum Likelihood Expectation Maximization (MLEM) algorithms [5]. In the MLEM method, the user can specify the size of the voxel as well as the size of the reconstructed image. Another source of flexibility is the possibility of adding new functionalities: a user can write a Python, C++ and FORTRAN routine and add it to FLAIR.
The objective of this work is to validate the FLUKA simulations of a Preclinical PET Focus 220 scanner [6]. FLUKA results are compared to experimental data obtained according to the National Electrical Manufacturers Association (NEMA) NU2-2008 standards [7]. A detailed implementation of the geometrical and functional models of the scanners and the NEMA phantoms was conducted, allowing the evaluation of the simulated absolute sensitivity, spatial resolution and count rates. In order to evaluate the image quality, a cylindrical phantom with four 1 cm diameter inserts was used to measure the contrast recovering. Good agreement was found between the simulated results and the measured data. This validation study represents an important step towards the use of FLUKA as an aid for the optimization of the current acquisition protocols and the validation of reconstruction and data correction techniques.

Keywords: Monte Carlo codes, FLUKA, Preclinical PET.

References:
[1] T. T. Boehlen, F. Cerutti, M.P.W. Chin, A. Fassò, A. Ferrari, P. G. Ortega, A. Mairani, P. R. Sala, G. Smirnov, V. Vlachoudis, "The FLUKA Code: Developments and Challenges for High Energy and Medical Applications", Nuclear Data Sheets, vol. 120, p. 211-214 (2014).
[2] G. Battistoni, S. Muraro, P. R. Sala, F. Cerutti, A. Ferrari, S. Roesler, A. Fasso, and J. Ranft,. "The FLUKA code: Description and benchmarking," M. Albrow and R. Raja, Eds. Proceed. of the Hadronic Shower Simulation Workshop 2006, 2007, AIP Conference Proceed. 896 (2007) 31-49.
[3] V.Vlachoudis et al., "Flair: A powerful but user friendly graphical interface for fluka," in Proc. Int. Conf. on Mathematics, Computational Methods & Reactor Physics (M&C 2009), Saratoga Springs, New York, 2009.
[4] FLAIR User's Guide http://www.fluka.org/flair/doc.html.
[5] Saha GB. Basics of PET Imaging: Physics, Chemistry, and Regulations. Springer Science+Business Media, Inc. 2005.
[6] Y.-C. Tai, A. Ruangma, D. Rowland, S. Siegel, D. F. Newport, P. L. Chow, and R. Laforest., "Performance evaluation of the microPET focus: A third-generation microPET scanner dedicated to animal imaging," J. Nucl. Med., vol. 46, pp. 455–463, 2005.
[7] National Electrical Manufacturers Association. NEMA Standard Publication NU 4-2008: Performance Measurements of Small Animal Positron Emission Tomographs (Rosslyn, VA: National Electrical Manufacturers Association; 2008).

211
4D dose calculations: Tetrahedral meshes versus voxel-based structures
Y. Touileb[1], H. Ladjal[12], J. Aznecot[1], M. Beuve[2], B. Shariat[1]
[1] Claude Bernard University Lyon 1, LIRIS, UMR 5205 F-69622, France
[2] Claude Bernard University Lyon 1, IPNL, UMR 5822 F-69622, France

Purpose: The estimation of the distribution patterns of energy and dose in respiratory-induced organ motion represents a technical challenge for hadron therapy treatment planning, notably in the case of lung cancer in which many difficulties arose, like tissue densities variation and the tumor position shifting during breathing. This study focuses on the comparison between deformable tetrahedral meshes and voxel-based structures used as computational phantoms in four-dimensional dose calculations. The former use a continuous representation of tissue densities by respecting mass conservation principle, while the latter is a discrete grid of density values (CT-scan).
Methods: The movement used to simulate breathing is generated with deformable image registration (DIR) of CT images (Castillo, 2010) (Klein, 2010) (Shamonin, 2013). Tissue tracking for tetrahedral model is implicitly performed by the fact that the meshes maintain their topology during

deformations. The dose distribution is calculated using the time-dependent tetrahedral density map issued from 4D-CT scans (Petru Manescu, 2014). Unlike image-based methods, the deposited energy is accumulated inside each deforming tetrahedron of the meshes. An implementation of this dose computation method on a deformable anatomy in the case of a passive scattering beam line is demonstrated using the Geant4 code (Agostinelli, 2003). Besides, energy values in voxel-based structures are calculated for each time step and accumulated using the transformations provided by the registration. Then, values are accumulated back onto the reference image and divided by the mass to obtain the 4D dose map. Figure 1 illustrates the process used to accumulate dose in respiratory-induced simulations.

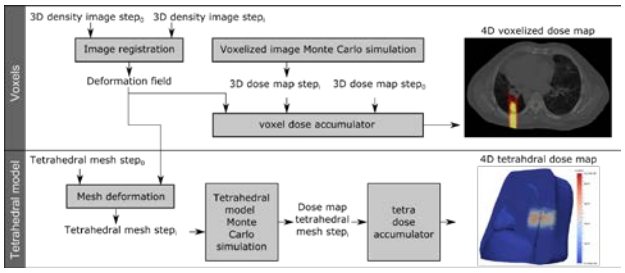

Figure 1. Flow chart of 4D dose accumulation in respiratory motion-induced simulation

Results: The tetrahedral mesh dose distribution was compared to the conventional voxel-based structure using a thoracic 4D-CT data of a patient case. Preliminary results show that dose distributions for both representations are in a good agreement (figure 2), and dose homogeneity is about the same (table1). However, motion-induced dose accumulations are more intuitive using a tetrahedral model since they do not introduce additional uncertainties with image resampling and interpolation methods, and also for the fact that they respect mass conservation principle.

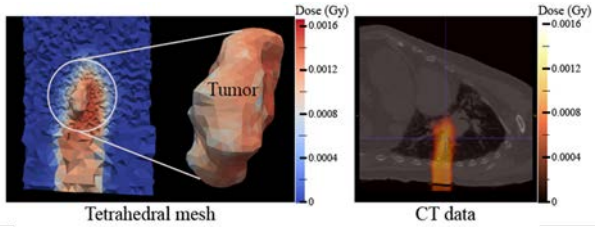

		Dose ($\times 10^{-4}$Gray)			HI
		D_{min}	D_{max}	D_{mean}	
No motion	Voxels	0.64	1.77	1.41	1.30
	Tetras	0.40	1.97	1.41	1.30
With motion	Voxels	6.82	15.09	12.72	1.60
	Tetras	3.45	15.50	12.93	1.47

Figure.2: 4D Dose distributions. Left: accumulated dose in tetrahedral mesh. Right: accumulated dose in CT data for all phases. Table 1: Evaluation of dose distribution on tumor volume. D_{min}, D_{max}, D_{mean} are respectively the minimum, the maximum and the mean dose deposited. Hi (Homogeneity index).

Conclusion: We have developed a 4D tetrahedral model for Monte Carlo dose calculations alongside its implementation on the Geant4 platform. Results of comparison with conventional methods based on voxels have shown that dose distributions are in good agreement. This novel structure can be of a great aid for treatment planning of moving targets. An experimental validation based on 4D anthropomorphic phantom (e.g. LuCa phantom developed in paul scherrer institute) (Neihart, 2013) would draw a clear conclusion regarding the performance of the presented method in comparison with the classical methods. Nevertheless, the main advantage of this method is that, coupled with a patient-specific biomechanical model, it could be used in the future to correct motion artefacts in treatment planning.

Keywords: Dosimetry, Tetrahedral mesh, 4D-CT.

References:

[1] Agostinelli, S. et al. (2003). GEANT4—a simulation toolkit. *Nuclear instruments and methods in physics research section A: Accelerators, Spectrometers, Detectors and Associated Equipment* , 250-303.
[2] Castillo, E. et al. (2010). Four-dimensional deformable image registration using trajectory modeling. *Physics in medicine and biology*, 305.
[3] Klein, S. a. (2010). Elastix: a toolbox for intensity-based medical image registration. *Medical Imaging, IEEE Transactions on*, 196--205.
[4] Manescu, P. et al. (2014). Four-dimensional radiotherapeutic dose calculation using biomechanical respiratory motion description. *International journal of computer assisted radiology and surgery*, 449-457.
[5] Shamonin, D. P. (2013). Fast parallel image registration on CPU and GPU for diagnostic classification of Alzheimer's disease. *Frontiers in neuroinformatics*.
[6] Neihart, J.L. (2013) Development and implementation of a dynamic heterogeneous proton equivalent anthropomorphic thorax phantom for the assessment of scanned proton beam therapy.

212

Realization of an innovative Dose Profiler for online range monitoring in particle therapy treatments

G. Battistoni[7], F. Collamati[1,2], E. De Lucia[3], R. Faccini[1,2], M. Marafini[2,5], I. Mattei[7], S. Muraro[7], R. Paramatti[2], V. Patera[2,4,5], D. Pinci[2], A. Rucinski[2,4], A. Russomando[1,2,6], A. Sarti[3,4,5], A. Sciubba[2,4,5], E. Solfaroli Camillocci[1], M. Toppi[3], G. Traini[1,2], C. Voena[2]
[1] Dipartimento di Fisica, Sapienza Università di Roma, Roma, Italy
[2] INFN Sezione di Roma, Roma, Italy
[3] Laboratori Nazionali di Frascati dell'INFN, Frascati, Italy
[4] Dipartimento di Scienze di Base e Applicate per l'Ingegneria, Sapienza Università di Roma, Roma, Italy
[5] Centro "E. Fermi", Roma, Italy
[6] Center for Life Nano Science@Sapienza, IIT, Roma, Italy
[7] INFN Sezione di Milano, Milano, Italy

Particle Therapy (PT) exploits accelerated charged ions, typically protons or carbon ions, for cancer treatments. In PT a better dose release accuracy is achieved with respect to the conventional radiotherapy, as a consequence of the nature of energy deposition processes of charged ions, that lose most of their energy near the end of their range, in the Bragg Peak (BP) region, preserving healthy tissues and Organ At Risk (OAR) around tumor. The high cancer cells killing power of this technique requires a precise control of the ion beam delivery, and hence target voxel, to take into account a possible patient mis-positioning or biological or anatomical changes. The development of an on-line dose conformity monitoring device is of paramount importance to assure an high quality control accuracy in PT treatments.
In this contribution we propose a novel detector named "Dose Profiler" (DP) tailored for dose range monitoring applications in PT. The beam range inside the patient will be monitored detecting secondary fragments, whose emission is correlated to dose release, at large angles with respect to the beam direction. The DP is being developed in the framework of the INSIDE (Innovative Solutions for In-beam Dosimetry in Hadrontherapy) project, and will be tested at CNAO (Centro Nazionale Adroterapia Oncologica), Pavia (IT). The detector layout foresee a tracker followed by a calorimeter (as shown in Figure 1). Six layers of square scintillating fibers, whose light is collected by Silicon PhotoMultipliers (SiPMs), provides the x,y particles positions used for the charged particles backtracking, while a matrix of

sixteen pixellated LYSO crystals, coupled to multi-anode PhotoMultiplier, provides the particle energy measurement. The front-end electronics is composed of 4096 channels, and the read-out is performed by 128 ASICs (BASIC32_ADC) specifically designed for SiPMs read-out application [1], while trigger system and data acquisition are implemented with a system of 21 FPGAs.
The detector design and optimization of the detector have been performed using Monte Carlo (MC) simulations based on the results of experimental measurements ([2], [3]). The DP hardware features of DP will be reviewed. The expected performance, as resulting from the MC, will be discussed in the clinical application framework.

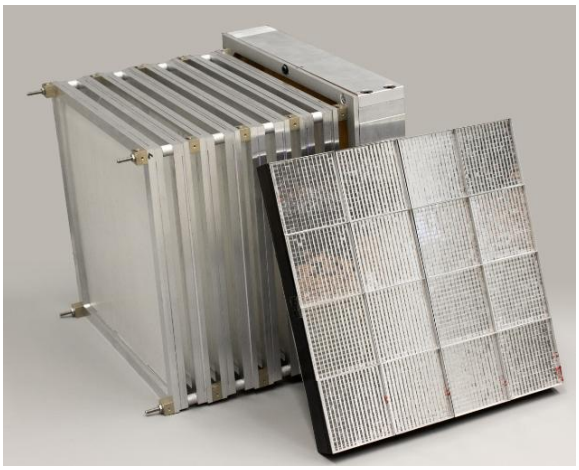

Figure 6: Tracker and calorimeter detectors

Keywords: Dose range monitoring concepts and apparatus; Instrumentation for hadron therapy

References:
[1] F. Ciciriello et al., *BASIC32 ADC a Front-end ASIC fo SiPM Detectors, Nuclear Science Symposium and Medical Imaging Conference (NSS/MIC), IEEE (2013), pp. 1–6.*
[2] L. Piersanti et al., *Measurement of charged particle yields from PMMA irradiated by a* 220 *MeV/u* 12*C beam*, *Phys. Med. Biol.* 59 (2014) 1857.
[3] C. Agodi et al., *Charged particle's flux measurement from PMMA irradiated by 80 MeV/u carbon ion beam*, *Phys. Med. Biol.* 57 (2012) 5667.

213
Small Large Momentum Acceptance Gantries for Proton and Carbon Cancer Therapy
D. Trbojevic, N. Tsoupas, Brett Parker, and H. Witte

We present an isocentric, carbon/proton superconducting and permanent magnet proton gantries, respectively, with a fixed magnetic field but very large momentum acceptance. During a treatment it is possible to do longitudinal and transverse spot scanning for the whole energy range required. The size and cost are dramatically reduced; for example compared to the weight of the Heidelberg 630 tons the weight is estimated to be about one tons. The proton gantry is of a size of the present PSI gantry, but it is made of small permanent Halbach magnets. It can transport very precisely the proton beam within a 30-250 MeV kinetic energy range, under the permanent magnetic field, with variation of the scanning magnets only with an infinite S.A.D.

214
The role of functional imaging for radiation oncology – The whole translational chain from animals to clinics
E.G.C. Troost[1,2,3,4]
[1] Institute of Radiooncology, Helmholtz-Zentrum Dresden-Rossendorf, Dresden, Germany.
[2] Department of Radiation Oncology, Medical Faculty and University Hospital Carl Gustav Carus an der Technischen Universität Dresden, Dresden, Germany.
[3] OncoRay, National Center for Radiation Research in Oncology
[4] Deutsches Konsortium für Translationale Krebsforschung (DKTK), Partnerstandort Dresden und Deutsches Krebsforschungszentrum (DKFZ), Heidelberg

As opposed to surgical disciplines, radiation oncology relies on non-invasive imaging of the target volume (tumor, lymph nodes or metastases). Apart from anatomical imaging for target volume delineation (e.g., CT, MRI), functional imaging (e.g., PET, functional CT and MRI) is increasingly being integrated in modern radiotherapy techniques. Functional imaging is used prior to therapy for guidance, dose-escalation strategies and treatment selection, but also early during irradiation for response monitoring and consequently treatment adaptation. Moreover, functional imaging is incorporated in the radiotherapy chain for identification of patients at increased risk of normal tissue complications (e.g., SPECT and CT for prediction of radiation pneumonitis). This presentation will present the current status of functional imaging for radiation oncology prior to and during treatment, both for the target volume and normal tissues.

Keywords: CT, MRI, PET, target volume, normal tissues, adaptation

215
Clinical trials for carbon-ion radiotherapy in Japan
H. Tsujii[1], T. Kamada[1]
[1]Research Center for Charged Particle Therapy, National Institute of Radiological Sciences, Chiba, Japan

As compared to photon beams, charged particle therapy such as both proton beam therapy (PBT) and carbon-ion radiotherapy (CIRT) offers improved dose distribution, localizing sufficient dose within a target volume while minimizing the dose to the surrounding normal tissues. In addition, carbon-ions being heavier than protons provide a higher radiobiological effectiveness (RBE), which increases with depth reaching the maximum at the end of the beam's range. This theoretically is an ideal property from the standpoint of cancer radiotherapy.
In Japan, PBT and CIRT were both initiated at NIRS in 1979 and 1983, respectively. Since then, various types of tumors have been prospectively treated. As of December 2015, there are a total of 13 charged particle therapy facilities in operation including 9 for PBT and 4 for CIRT. Several other facilities are under construction or being planned for either PBT or CIRT. In 2003, we established JCPT (Japan Clinical Study Group of Particle Therapy) for the purpose of changing information and improving therapeutic techniques for charged particle therapy, as well as collecting clinical data from existing facilities in Japan. According to the survey of JCPT, a total of 30,850 patients were treated in Japan from 1979 to 2014, including 17,858 patients (58%) with PBT and 12,922 patients (42%) with CIRT. Male/female was 73%/27%. The age of the patients ranging <51, 51-60, 61-70, 71-80, >80 was 12%, 17%, 34%, 29%, and 8%, respectively. As with the tumor types, the major tumors for PBT were prostate (30%), liver (19%), H&N (13%), lung (12%), GI (6%) and pancreas (4%), and those for CIRT were prostate (24%), H&N (14%), B&S (11%), lung (11%), liver (10%) and rectum/pancreas (5% each).
Among 4 facilities for CIRT, the largest numbers of patients were treated at NIRS, starting CIRT in 1994 using HIMAC (Heavy-ion medical accelerator in Chiba). More than 9,000 patients have been so far treated based on > 70 protocols, by which the benefit of CIRT over other modalities has been demonstrated in locally, advanced tumors and non-squamous cell types of tumors. Based on their unique biophysical characteristics, a significant reduction in overall time and fraction has been achieved with minor toxicities. This included a single-fraction RT for early-stage NSCLC, one or two-fraction RT for liver cancer and 12-fraction RT for prostate cancer. Even for other tumors, CIRT with 16 or

smaller fractions have been safely performed. This means that the facility can be operated more efficiently in CIRT, permitting treatment for a larger number of patients than is possible with other modalities over the same period of time. In 2010, a new treatment facility with three rooms was completed with the beam lines being extended from the existing accelerators, in which CIRT with a pencil beam scanning became available. Recently, we have successfully begun treatment of moving organs using respiratory-gated irradiation with a pencil beam scanning. At the new facility a compact rotating gantry was constructed with its commissioning to be finished in the spring of 2016.
In order to exchange information and perform a prospective study for CIRT, we have recently established J-CROS (Japan Carbon-ion Radiation Oncology Study Group). Under the framework of J-CROS, we will conduct multi-institutional studies on such tumors as head and neck tumors, NSCLC (mainly T2 tumors), hepatoma, pancreas cancer, post-operative recurrence of rectal cancer, and bone & soft tissue sarcoma. These tumors are chosen based on the recognition that therapeutic techniques have not yet been fully established and treatment outcome should be further improved, as well as that reproducibility of NIRS clinical results should be evaluated by other groups. The J-CROS study will also include the study producing benchmark results in selected tumors, as well as a randomized study comparing CIRT with PBT or photon therapy.

Keywords: Carbon-ion, Proton, Hypofractionation, RBE, Dose distribution

References:
[1] Tsujii H, Kamada T, Shirai T, et al (eds): Carbon-Ion Radiotherapy; Principles, Practices and Treatment Planning. Springer Japan, 2014.
[2] Tsujii H, Kamada T.: A review of update clinical results of carbon-ion radiotherapy. Jpn J Clin Oncol 2012; 42(8): 670–685.
[3] Schulz -Ertner D, Tsujii H.: Particle radiation therapy using proton and heavier ion beams. J Clin Oncol 2007; 25(8): 953-964.
[4] Kamda T, Tsujii H, Debus J, et al: Carbon ion radiotherapy in Japan: an assessment of 20 years of clinical experience. Lancet Oncol 2015; 16(2): e93-e100.
[5] Tsujii H, Kamada T, Baba M, et al.: Clinical advantages of carbon-ion radiotherapy. New J Phys. 2008; 10:1367–2630.

216
Ocular Brachytherapy Dosimetry for^{103}Pd and^{125}I in The Presence of Gold Nanoparticles: Monte Carlo Study
S.Asadi[1], M.Vaez-zadeh[1], M.Vahidian[1], M.Marghchouei[1], S.Farhad Masoudi[1]
[1] Department of Physics, K.N. Toosi University of Technology, Tehran, Iran.

Purpose: The aim of the present Monte Carlo study is to evaluate the variation of energy deposition in healthy tissues in the human eye which is irradiated by brachytherapy sources in comparison with the resultant dose increase in the gold nanoparticle (GNP)-loaded choroidal melanoma.
Material and method: The effects of these nanoparticles on normal tissues are compared between ^{103} Pd and ^{125}I as two ophthalmic brachytherapy sources. Dose distribution in the tumor and healthy tissues has been taken into account for both mentioned brachytherapy sources. Also, in certain points of the eye, the ratio of the absorbed dose by the normal tissue in the presence of GNPs to the absorbed dose by the same point in the absence of GNPs has been calculated. In addition, differences of the absorbed dose in the tumor observed in the comparison of simple water phantom and actual simulated human eye in presence of GNPs are also a matter of interest that have been considered in the present work.
Result and conclusion: The difference between the eye globe and the water phantom is more obvious for ^{125}I than that of the ^{103} Pd when the ophthalmic dosimetry is done in the presence of GNPs. Whenever these nanoparticles are utilized in enhancing the absorbed dose by the tumor, the use of ^{125}I brachytherapy source will greatly amplify the amount of dose enhancement factor (DEF) in the tumor site without inflicting much damage to healthy organs, when compared to the ^{103} Pd source. Furthermore in Monte-Carlo studies of eye brachytherapy, more precise definition of the eye phantom instead of a water phantom will become increasingly important when we use ^{125}I as opposed to when ^{103} Pd is considered.

Keywords: Brachytherapy, Gold nanoparticles, ^{103}Pd and ^{125}I

Refrences:
[1] M. J. Rivard, B. M. Coursey, L. A. Dewerd et al. Update of AAPM Task Group No.43 Report: A revised AAPM protocol for brachytherapy dose calculations. Med. Phys. (2004) ; 31:633-674.
[2] R. E. P. Taylor et al. Benchmarking BrachyDose: voxel-based EGSnrc Monte Carlo calculations of TG--43 dosimetry parameters. Med. Phys. (2007) ; 34:445-457.
[3] S. Asadi, M. Vaez-zadeh, S. Farhad Masoudi, et al. Gold nanoparticle-based brachytherapy enhancement in choroidal melanoma using a full Monte Carlo model of the human eye. Jornal of applied clinical medical physics. (2015) ; 16(5):1-13.

217
GEANT4 versus MCNP5: Monte-Carlo ophthalmic brachytherapy dosimetry in the presence of gold nanoparticles for ^{125}I and ^{103}Pd
Sh.Vahidian Qazvini[1], M.Vahidian[1], S.Asadi[1], M.Vaez-zadeh[1]
[1] Department of Physics, K.N. Toosi University of Technology, Tehran, Iran.

Purpose: The emphasis of the present work is to compare the effects of gold nanoparticles (AuNPs) on healthy human ocular tissues in ophthalmic brachytherapy dosimetry, between water and eye phantoms by utilization of the two most noteworthy Monte-Carlo codes of GEANT4 and MCNP5.
Material and method: The intended study was based upon a simulated model of the human eye consisting different parts such as Lens, Cornea, retina, Choroid, Sclera, skull bone, Anterior Chamber and a melanoma tumor which was latticed to house AuNPs required for the dosimetry comparisons of two uniquely defined radionuclides of ^{125}I and ^{103}Pd. The effects of the presence of AuNPs on the absorbed dose by the tumor have been taken into account using both Monte-Carlo codes mentioned above; furthermore, the aberrations in dose calculations of the simple eye phantom and the realistic eye model were also an element of consideration. The importance of such evaluations on various compositions that are most common in Monte Carlo studies could prove to be rewarding, especially in presence of external anomalies such as AuNPs.
Result and Conclusion: With respect to the numerous distinctions between codes themselves, it is always fruitful to compare multiple of these programs with one another; hence, a rigorous inspection of the results has been executed, and dissimilarities have been highlighted for better understanding of the advantages and deficiencies of both codes. All in all, it is best stated that interdisciplinary methods of combining diverse therapeutic applications have gained much ground in our current era, and serve to significantly increase efficiency of cures worldwide.

Keywords: GEANT4, Gold nanoparticles, ophthalmic dosimetry brachytherapy

218
A novel method to predict *a priori* the toxicity reduction of a prostate-rectum spacer: Virtual Rectum Spacer
S. van der Meer[1], B.G.L. Vanneste[1], D. Herfs[1], W. van Elmpt[1], C. Schubert[2], M. Pinkawa[2], P. Lambin[1]
[1] Department of Radiation Oncology, MAASTRO clinic, GROW - School for Oncology and Developmental Biology, Maastricht University Medical Center, Maastricht, The Netherlands
[2] Department of Radiation Oncology, University Hospital RWTH Aachen, Aachen, Germany.

Purpose: A method to decrease the risk of rectal toxicity during prostate radiotherapy treatments consists of an implantation of a rectum spacer (RS). Nevertheless the implantation of a RS is expensive and invasive. Therefore a decision support system to identify a priori whether a specific patient would benefit from a RS would be very beneficial.
We have developed a novel method to predict the CT images with a 'virtual' RS based on a CT scan without RS. Predictions of the gain of dose, and consequently of toxicity reduction can be obtained through a validated multifactorial nomogram.
Materials/methods: A patient dataset consisting of 16 prostate cancer patients with CT imaging prior and after a gel RS implantation (SpaceOAR™ System, Augmenix Inc.) was used. The median inserted gel volume was 10.5 cc. Gel contours of the first 8 patients were used as a training set to derive the spatial deformation model of the RS.
A deformation model of the RS was build, based on overlapping volumes of RS's of different patients with a probability of >3 contour corresponded with a volume of 10 cc. From this model, a deformation field was calculated that mimics the expansion of the RS between the prostate and the rectum. The CT images of the remaining 8 patients were used to validate the virtual RS model, for this the distance between the rectum and the prostate was compared for the virtual RS and the actual RS. For one patient the dose was planned on all 3 CT's (no, real and virtual spacer) according to our clinical practice (70 Gy: 28 x 2.5 Gy). We used a validated multifactorial nomogram developed for predicting acute and late radio-induced rectal toxicities.
Results: The average minimum distances between the prostate and rectum of all 8 patients in the validation set increased with 3.7±2.4 (1SD) mm when the virtual RS was applied. For the real RS the average increase in minimum distance was 5.4±2.7 mm. The mean distances between the prostate and rectum without RS was 15.8±3.2 mm, with the virtual RS this was 19.5±3.3 mm comparable to the real RS 22.0±4.3 mm.
For one patient the planned dose on all 3 CT's is shown in the table and figure.
The virtual spacer revealed a large decrease in volume receiving more than 65 Gy, which however correlated in no significant difference of predicted late toxicity.

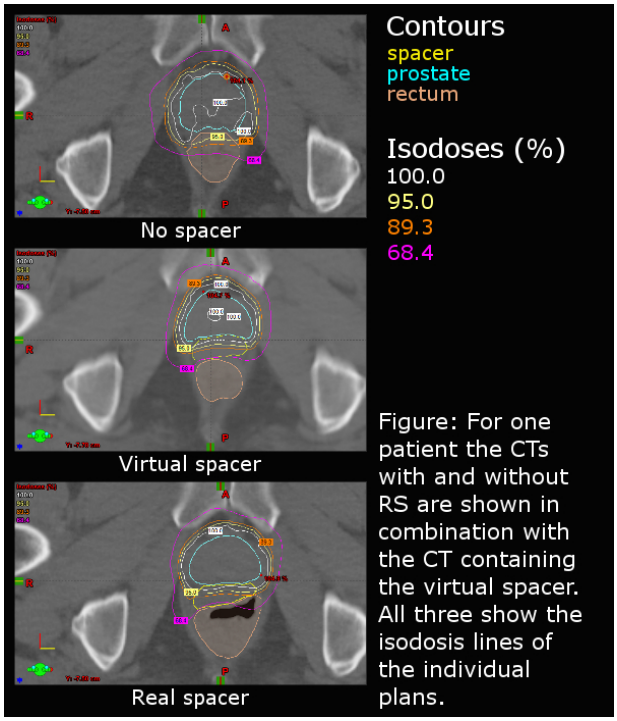

Figure: For one patient the CTs with and without RS are shown in combination with the CT containing the virtual spacer. All three show the isodosis lines of the individual plans.

Table: Planned Target Volume (PTV) coverage and dose in the organ at risk (anorectum).

	No spacer	Virtual spacer	Real spacer
PTV coverage	99.3 %	99.0 %	99.5 %
Anorectum			
V_{65}	4.3 %	1.0 %	3.3 %
D_{max}	69.1 Gy	69.7 Gy	70.5 Gy

Conclusions: We have developed a novel method to simulate a prostate-rectum spacer that is a useful tool to identify patients with a potential dose and outcome benefit of a RS implantation. The volume of the virtual RS can be estimated through the use of different deformation fields. For the presented patient the RS would not give a clinical benefit, so this patient should not get a RS. We envision that in the future this virtual spacer-based decision support system will be used to quantify a priori the potential benefit of such approach, more particularly before extremely hypofractionated schedules.

Keywords: Prostate Cancer – Rectum Spacer – Virtual Spacer – Predicted Gain

219

The use of ^{149}Tb and ^{152}Tb in preclinical investigations: an update on its mass separation and subsequent application for imaging and therapy

N. P. van der Meulen[1,2], C. Vermeulen[1], U. Köster[3], K. Johnston[4], S. Haller[1], R. Schibli[1,5], A. Türler[2,6], C. Müller[1]
[1] Center for Radiopharmaceutical Sciences ETH-PSI-USZ, Paul Scherrer Institute, Villigen-PSI, Switzerland
[2] Laboratory of Radiochemistry and Environmental Chemistry, Paul Scherrer Institute, Villigen-PSI, Switzerland
[3] Institut Laue-Langevin, Grenoble, France
[4] ISOLDE-CERN
[5] Department of Chemistry and Applied Biosciences, ETH Zurich, Zurich, Switzerland
[6] Department of Chemistry and Biochemistry, University of Bern, Bern, Switzerland

Purpose: Terbium is a unique element as it provides a quadruplet of radionuclides suited for diagnostics and therapy in nuclear medicine [1]. As part of the PSI-ISOLDE collaboration, we concentrated on the collection and purification of ^{149}Tb (α-emitter, $T_{1/2}$ = 4.1 h – for potential therapy) and ^{152}Tb (β^+-emitter, $T_{1/2}$ = 17.5 h – for use in PET imaging), for significant imaging and therapy investigations.
Materials/methods: Mass-separated beams of ^{149}Tb and ^{152}Tb, respectively, were implanted at ISOLDE-CERN into Zn-coated Au foils. With 1.5 hours of collection and 2 hours decay of co-implanted activities, up to 200 MBq ^{149}Tb could be transported to PSI. Collections of ^{152}Tb lasted 4 to 6 hours and up to 2 GBq ^{152}Tb could be shipped to PSI.
The Tb radionuclides were extracted from the Zn foils by dissolving them in HNO_3/NH_4NO_3, loaded on to a macroporous strongly acidic cation exchange resin and the Tb radionuclides eluted using dilute α-hydroxyisobutyric acid (α-HIBA). The product eluent was used directly for the radiolabeling process.
Complementing previous therapy studies with ^{149}Tb-folate and ^{161}Tb-folate [2, 3], we focused on the possible side effects of such a treatment. Healthy mice, without tumors, were injected with increasing activity levels to investigate kidney damage after α-therapy with ^{149}Tb-folate and compare it with the damage caused by ^{161}Tb-folate-based ß-therapy. These mice are monitored with regard to potential undesired side effects. DOTANOC and DOTA-RGD were also labelled with ^{152}Tb, a radionuclide which can potentially be used for PET imaging. They were injected into AR42J and U87MG tumor-bearing mice, which were imaged using a benchtop small animal PET/CT scanner (Genisys8, Sofie Biosciences).
Results: The ^{149}Tb and ^{152}Tb were effectively separated from Ce, Pr, Ba and La, yielding a radionuclidically pure product. The product in question was successfully labelled to DOTANOC and DOTA-RGD at high specific activity of up to 10 MBq/nmol and radiochemical purity of >95%. The ^{149}Tb-folate dose escalation study was conducted with six mice injected

with 5 MBq/mouse and three untreated controls which were injected with α-HIBA only. No impairment of animal kidney function was observed to date.
Tumor visualization was readily achieved with both ^{152}Tb-labeled peptides and, due to the high sensitivity of this scanner, it was possible to also image the tumors at late time points after injection of the mice.
Conclusion: The latest run of experiments in the PSI/ISOLDE collaboration proved to be the most successful to date, with reproducible harvesting of ^{149}Tb and ^{152}Tb and its subsequent chemical separation from impurities. The product was successfully labelled to peptides and folate and injected into mice for imaging and long-term studies to determine kidney damage, in the case of ^{149}Tb. Following these encouraging results, more ambitious studies are planned in future.

References:
[1] C. Müller et al., J. Nucl. Med. 53, 1951 (2012).
[2] C. Müller et al., J. Nucl. Med. 54, 124 (2013).
[3] C. Müller et al., Nucl. Med. Biol. 41, e58 (2014).

220
Is dual energy CT the next standard imaging modality for radiotherapy?
W. van Elmpt
Department of Radiation Oncology (MAASTRO), GROW – School for Oncology and Developmental Biology, Maastricht University Medical Centre, Maastricht, The Netherlands.

Over the past years, dual energy CT (DECT) scanners have been installed in many radiology departments. Recently, also possibilities are under investigation to use this equipment for radiotherapy purposes. Several strategies using DECT imaging may allow optimization of radiation treatment in a variety of fields: e.g. tumour detection and characterization, improved dose calculation accuracy, objective normal tissue function quantification. DECT allows a robust way of material characterization that easily can quantify the electron density and effective atomic number. These approaches improve radiotherapy dose calculation accuracy. Especially in brachytherapy and proton therapy this is necessary due to the larger uncertainties in dose calculation compared to high energy photon treatments. Other possible applications involve advanced metal artifact reduction techniques. The use of iodinated contrast material allows an objective quantification for quantitative assessment of perfusion of tumours and normal tissues. Future perspectives for DECT for radiotherapy will be discussed together with the next steps for implementation in clinical practice.

221
Can we replace high quality simulation CT by simple kV-cone-beam CT images to extract an externally validated radiomics signature?
J.E. van Timmeren[1], R.T.H. Leijenaar[1], W. van Elmpt [1], P. Lambin[1]
[1]Department of Radiation Oncology (MAASTRO), GROW – School for Oncology and Developmental Biology, Maastricht University Medical Centre (MUMC), Maastricht, the Netherlands

Objective: A validated CT-based radiomic signature showed to have prognostic information for lung cancer patients[1,2]. The prognostic value of radiomic image features derived from cone-beam CT (CBCT) images has not yet been described. Furthermore, due to the fact that a CBCT image is acquired prior to each fraction it has the potential to monitor response to treatment. The goal of this study was to investigate the stability and correlation between features of the radiomic signature derived from planning CT vs. kV-CBCT and between CBCTs of different fractions.
Material/Methods: A total of 26 stage II-III NSCLC patients who received radiation therapy were included in this study. The planning CT (CT1), the CBCT prior to the first (CBCT-FX1) and second fraction (CBCT-FX2) were used in this study (see Figure). CBCT images were registered to CT1 using an automatic rigid registration prior to feature extraction. The prognostic radiomic signature[1] consists of four features: I) tumor intensity: 'Energy', II) texture: 'Grey Level Nonuniformity, III) wavelet: 'Grey Level Nonuniformity HLH' and IV) shape: 'Compactness'. Since a rigid registration was used without redelineation, the fourth feature 'Compactness' was not analyzed since no changes were performed to the shape. For the remaining three features, the correlation between feature values derived from (1) CT1 and CBCT-FX1 and (2) CBCT-FX1 and CBCT-FX2 were analyzed. Correlations were calculated using an intraclass correlation coefficient ICC(2,1).

A B

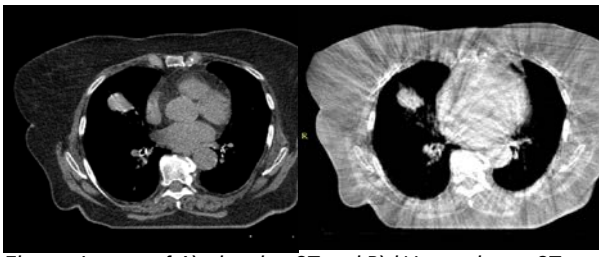

Figure: Images of A) planning CT and B) kV-cone-beam CT

Results: All three features of the radiomic signature I) 'Energy', II) 'Grey Level Nonuniformity and III) 'Grey Level Nonuniformity HLH' showed correlation of ICC>0.8 between CT1 and CBCT-FX1 (ICC = 0.98, 0.88 and 0.81 respectively) and between CBCT-FX1 and CBCT-FX2 (ICC = 0.89, 0.83 and 0.95 respectively).
Conclusion: Three features that previously showed to have prognostic performance in lung and head & neck cancer patients for CT images show a correlation above 0.8 between CT1 and CBCT-FX1. The features also show an ICC>0.8 for CBCT-FX1 vs. CBCT-FX2, which suggests stability of those features using CBCT imaging. These results show the potential of CBCT imaging in monitoring treatment and acquiring prognostic and predictive information. In the future, radiomic features derived from CBCT images will be investigated to monitor changes of CBCT features over the course of treatment (the so-called "Delta-radiomics" approach) and to evaluate its prognostic significance.

Keywords: radiomics, cone-beam computed tomography

References:
[1]*Aerts, H. J. W. L. et al. Decoding tumour phenotype by noninvasive imaging using a quantitative radiomics approach. Nat. Commun. 5:4006 doi: 10.1038/ncomms5006 (2014)*
[2]*Leijenaar RT, Carvalho S, Hoebers FJ, Aerts HJ, van Elmpt WJ, Huang SH, Chan B, Waldron JN, O'sullivan B, Lambin P. External validation of a prognostic CT-based radiomic signature in oropharyngeal squamous cell carcinoma. Acta Oncol. 2015 Oct;54(9):1423-9.*

222
PET-ToF system with highly integrated SiPM readout
T. Niknejad[1], R. Bugalho[2], J. Carlos Rasteiro Da Silva[1,2], A. Di Francesco[1], L. Ferramacho[2] , C. Leong[2], M. Rolo[1,4], R. Silva[1] , M. Silveira[2], S. Tavernier[2,3], J. Varela[1,2]
[1] LIP, Lisbon, Portugal
[2] PETsys Electronics, Oeiras, Portugal
[3] Vrije Universiteit Brussel, Belgium
[4] INFN, Turin, Italy

SiPMs allow a dramatic improvement of PET performance. The good timing performance of SiPMs will result in better Time Of Flight time resolution, and therefore in better effective sensitivity. The small and independent photodetector pixels allow using one-to-one coupling between a SiPM pixels and a LYSO crystals. This will result in significant improvement of the spatial resolution compared to PMT base systems. To take advantage of SiPMs in PET applications, it is mandatory to have highly integrated electronics readout.
The present work expands the research in SiPM-based PET-ToF pursued by the authors since several years, in particular developing the TOFPET readout ASIC, a 64 channel mixed-

mode chip designed in 130 nm CMOS technology [1]. We present results of a PET-ToF demonstrator scanner based on this ASIC and featuring a highly integrated readout and DAQ system.
The Detector Module is composed of 8 matrices of 4x4 LYSO scintillating crystals, each with a size of 3.1 x 3.1 x 15 mm3. These matrices are optically coupled to 8 arrays of Hamamatsu TSV-MPPCs. The crystal matrices and associated MPPCs plug directly in the Frontend Boards forming a compact detecting unit with active area 59x29 mm2. The present results were obtained with a partially assembled ring (16 Modules) corresponding to 2048 SiPM readout channels.
The Frontend board integrates two ASICs allowing the readout and digitization of 128 MPPC pixels. On-chip TDCs produce two time measurements allowing the determination of the event time and of the time-over-threshold. A Concentrator board reads the data from eight Frontend boards (1024 channels) and transmits assembled data frames through a serial link to the PCIe based DAQ board in the data acquisition PC.
At present the PET-ToF demonstrator is fully assembled and in operation (Figure 1). We will report on the detector performance, including energy resolution, spatial resolution, time resolution and rate performance of the system. Images with phantoms will also be presented.

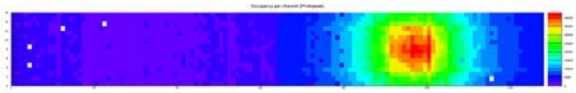

Figure 1 - Flood histogram of the full scanner obtained with a Na22 point source.

References:
[1] M.D. Rolo, R. Bugalho, F. Goncalves, G. Mazza, A. Rivetti, J.C. Silva, R. Silva, and J. Varela. TOFPET ASIC for PET applications. Journal of Instrumentation, 8(02):C02050, 2013.

223

Novel anti-tumour agents targeting the cell membrane

M. Verheij[1], A. van Hell[2]
[1]The Netherlands Cancer Institute, Amsterdam, The Netherlands
[2] Memorial Sloan Kettering Cancer Center, New York, USA

The cell membrane not only functions as a physical barrier between the intracellular and extracellular space, it harbors critical components involved in receptor-ligand interactions, signal transduction and drug uptake. Targeting the cell membrane represents a novel strategy to improve anti-cancer therapy. Our work focuses on two different approaches. The first involves lipid rafts. These are dynamic, cholesterol/sphingolipid-enriched microdomains within biological membranes, and play a crucial role in the induction of (apoptotic) cell death by radiation, pro-apoptotic receptor agonists and synthetic alkyl-phospholipids.
The second approach addresses insufficient drug delivery into tumor cells, which represents a major limitation of cytostatic therapy. We found that co-formulation and co-administration of liposome-encapsulated chemotherapy and synthetic short-chain sphingolipids (SCS) improves drug availability by enhancing intracellular drug uptake. Specific biophysical requirements of both the SCS (chain length and polarity) and chemotherapeutic agent (amphiphilicity) determine the optimal conditions for improved drug delivery. Doxorubicine and mitoxantrone are two frequently prescribed chemotherapeutic agents that benefit from this cell membrane-targeting approach. In vitro and in vivo studies demonstrate higher drug efficacy and/or lower toxicity in relevant tumor model systems. Mechanistic analyses demonstrate that SCS preferentially insert into tumor cell membranes enhancing the intrinsic capacity to translocate amphiphilic drugs.

Keywords: cell membrane, sphingolipids, liposomes

References:
[1] Van Hell AJ, Melo MN, van Blitterswijk WJ, Gueth DM, Braumuller TM, Pedrosa LR, Song JY, Marrink SJ, Koning GA, Jonkers J, Verheij M. Defined lipid analogues induce transient channels to facilitate drug-membrane traversal and circumvent cancer therapy resistance. Sci Rep. 2013;3:1949.

224

Assessment of MicroDiamond PTW 60019 detector and its use in small radiosurgery fields of Leksell Gamma Knife

T. Veselsky[1,2,3] , J. Novotny Jr.[1,2,3] , V. Pastykova[1,2] , J. Pipek[1]
[1] Czech Technical University in Prague, Faculty of Nuclear Sciences and Physical Engineering, Department of Dosimetry and Application of Ionising Radiation, Prague, Czech Republic
[2] Na Homolce Hospital, Prague, Czech Republic
[3] University Hospital in Motol, Prague, Czech Republic

Purpose: Modern radiotherapy is based on using small radiation fields and their segments. For clinical use they need to be verified by measurement. But measurement of small radiosurgery fields is very problematic task because of dosimetry challenges, such as loss of charged particle equilibrium, accurate positioning of detector and its small size. Purpose of this study is to assess new synthetic single crystal MicroDiamond PTW 60019 detector. Its dosimetry characteristics from the manufacturer and especially small size of its sensitive volume (0.004 mm^3) make the detector promising tool for this task.
Materials and Method: In this study basic dosimetry characteristics of MicroDiamond detector were verified in clinical linear accelerator photon and electron beams. Measurements involved short time stability and detector response dependence on dose rate, beam energy, temperature and angular dependence. In addition, measurement of relative output factors for Leksell Gamma Knife Perfexion was performed in order to test dosimeter performance for small fields. Collimator sizes 4 mm, 8 mm and 16 mm were used. Results obtained by this detector were compared with ELEKTA reference values and independent Monte Carlo Geant4 simulation.
Results: Stabilization of detector response was always performed before starting measurement. For this purpose 40 minutes irradiation in reference conditions was necessary (corresponding delivered dose was about 100 Gy). After this time the response was relatively stable with difference between maximum and minimum value 0.25% and standard deviation of all measurements 0.07% within an hour (normalized for this and all subsequent measurements to mean value of response). Dose rate dependence was measured for 6 different dose rates. Difference between maximum and minimum value was 0.24%. Energy dependence of detector was performed for 2 photon energies (6 and 18 MV) and 5 electron energies (6-20 MeV). Difference between maximum and minimum photon beam values was 0.12%, for electron beams this difference was 4.54% with standard deviation of response values 1.62%. Results for temperature and angular dependence are not finalized yet. Finally, results of comparative measurement for relative output factors of the Leksell Gamma Knife for 4 and 8 mm collimators were 0.831 and 0.900, respectively. These values are in a good agreement with vendor values (0.814 and 0.900) and Monte Carlo simulation.
Conclusion: New MicroDiamond PTW 60019 detector appears to be a promising detector for relative output factor measurements in small radiosurgery fields. Verified dosimetric properties of the detector are in limits set by manufacturer. However, relatively long pre-irradiation process is necessary prior to measurement before the detector can produce reliable data. Further measurements will follow. This work was supported by CTU grant no. SGS15/217/OHK4/3T/14.

Keywords: MicroDiamond, small field dosimetry

References:
http://www.ptw.de/2732.html

225

ENTERVISION biological dosimetric phantom. Proof of concept and results

T.V.M. Lima[1,2,3], F. Marchetto[4], A. Ferrari[3], A. Mairani[5], K. Ricketts[2], G Royle[2], M. Dosanjh[3]
[1] KSA
[2] UCL
[3] CERN
[4] INFN
[5] CNAO

Development of clinical treatment protocols for radiation therapy is dependent on the availability of information on the biological efficacy of radiation doses. In order to gain robust data, multiple cell irradiation experiments must be performed at different dose points, using a range of cell lines. Therefore, it is important to be able to verify the biological effects of complex dose distributions in homeomorphic phantoms, alongside
measurements of physical dose. One of the ENTERVISION projects focuses on the development of a biological dosimetric phantom. Firstly, the phantom and desired set-ups were evaluated then its suitability for radiobiology studies were accessed during a set of cell irradiations. Status: The phantom was irradiated mimicking the patients' pathway starting with the CT scan, followed by treatment planning and being irradiated. For the irradiation, an uniform dose distribution was delivered with a proton beam and the process was repeated using a carbon ion beam. The dose was measured from pinpoint ionisation chambers readings and the uniformity was assessed with radiochromic films. The experimental results were compared with the TPS and Monte Carlo calculations. Using MC simulations it was also investigated how the simulation of a more detailed geometry would affect the obtained results. From the radiobiology studies the cell survival by analyzing its proliferation was studied. Results: The calculated mean deviation was below 2% for both beams used. This brings the result within the acceptance threshold as desired by CNAO QA procedures. Conclusion: The experimental results obtained showed good agreement with both TPS and Monte Carlo simulations. And the radiobiological results showed the possibility of multi-variable analysis (LET and Dose) that is available to be done with the ENTERVISION Phantom.

Keywords: LET, RBE, Radiobiology,

226

Evaluation of Patients Dose in PET Studies from CT Contrast Agents

T.V.M. Lima[1,2,3], J. Binder[1], I. Oezden[1], K. Strobel[4], S. Matijasevic[4], A. Bopp[5], E. Nitzsche[5], G. Lutters[1]
[1] Fachstelle Strahlenschutz, Kantonsspital Aarau AG, Aarau, Switzerland
[2] Life Science Section, CERN - European Organization for Nuclear Research, Geneva, Switzerland
[3] Division of Surgery and Interventional Science, University College London, London, UK
[4]Nuklearmedizin, Luzerner Kantonsspital, Luzern, Switzerland
[5] Nuklearmedizin, Kantonsspital Aarau AG, Aarau, Switzerland

Introduction: The increased availability of PET-CT devices in addition to the interchange of people and technology between nuclear medicine and radiology explains the increased use of CT techniques like enhanced contrast CT in nuclear medicine. The benefits of the use of contrast agents, especially in terms of the increased accuracy, for enhancing different image modalities are understood and well discussed in the literature. On the other hand, in terms of evaluating the different side effects from the use of these contrast agents only the visible and short-term reactions have been discussed. In respect to studying for a possible increase in dose exposure from the interaction of the radiopharmaceutical radiation with the contrast agent in a contrast enhanced PET-CT study and its effect in the patient radiation exposure is yet to be investigated.
Materials and Methods: This study is aimed to investigate the dose deposition differences with respect to the nuclear medicine isotope radiation interaction with the high density and atomic number of the contrast agent due to increased absorption and scatter of the internal radiation in the patients' tissue. This has been performed with the use of Monte Carlo simulations of 10 patient studies where contrast agent had been used.
Results: Preliminary results show an increase in the dose deposition in the regions enhanced by contrast and its surroundings.
Conclusion: Further quantification of this increased dose deposition in different organs at risk and its estimated effect will be presented.

Keywords: PET-CT, Nuclear Medicine, Patient dose

227

Proton radiotherapy at PTC Czech in Prague

M. Andrlik[1], K. Badraoui-Cuprova, O. Sevela[1], P. Morichau-Beauchant[2], J. Vilimovsky[1], A. Michaelidesova[1], J. Stokucova[1], D. Trojkova[1], Z. Poulova[1], V. Dziedzicova[1], P. Holanova[1], P. Maca[1], M. Navratil[1], L. Zamecnik[1], J. Podolinsky[1], D. Sindelar[1], V. Vondracek[1]
[1] PTC Czech Prague
[2] École Polytechnique Université Paris-Saclay

Purpose: In the last two decades, particle therapy is slowly spreading from complementary programs of research institutions to dedicated healthcare facilities. Together with this evolution, particle therapy is refocusing from passive modes to the active pencil beam scanning mode (PBS). Higher degree of freedom, in sense of treatment conformity in PBS, is followed by more extensive demands in patient geometry determination. PTC Czech in Prague launched in December 2012 in PBS and it is the only mode of proton beam delivery currently used for patient treatment. The use of PBS technique raised new challenges such as plan robustness during the treatment course and mitigation of breathing motion influence on PBS treatment field delivery. The purpose of this poster is to demonstrate some of motion management studies conducted in the course of preparation for lung/breast lesions treatment.
Materials and Methods: A study with "MartiXX phantom" simulating breathing movement was conducted in order to examine the use of the repainting technique combined with respiratory gating. The goal was to evaluate the benefit of this combination for dose distribution delivery robustness against prolonged treatment time in the case of repainting itself. In another study, four Hodgkin's lymphoma patients, where respiratory gating system (Dyn'R) was applied, were examined. The inter-fractional movement of diaphragm on their setup X-ray images was evaluated. For the evaluation a script for edge detection using ITKsnap library was created. The error of this method was 1 mm.
Results: The evaluation of the "MartiXX phantom" experiment demonstrated significant mitigation of breathing motion when respiratory gating was applied. In this case, the treatment time was increased by 98 %. The use of gating combined with 5 times repainting demonstrated only mild improvement in movement mitigation compared to gating only case at cost of 233 % time increase. The degree of the dose distribution delivery improvement was evaluated through gamma analysis of dose planes acquired with MartiXX detector for dynamic and static case.
The evaluation of the diaphragm movement showed for 3 patients the difference trespassing the 5 mm threshold in 2-3 setups out of 7-11 of total, while in the case of the fourth patient all deviations were beneath 4 mm.
Conclusions: The selected studies for this poster suggest a strong benefit of respiratory gating. Additional mitigation technique like repainting might improve the outcome of dose delivery, but at a high treatment time cost. Nevertheless, the choice of the mitigation strategy should be always verified with a PET-QA in order to adopt the strategy if needed. Further, the evaluation of diaphragm position reproducibility gives some encouraging results although there are some papers [6] claiming low correlation of tumor lesion and diaphragm position.

Keywords: Motion management

References:
[1] S M Zenklusen, E Pedroni and D Meer, A study on repainting strategies for treating moderately moving targets with proton pencil beam scanning at the new Gantry 2 at PSI, 2010 Phys. Med. Biol. 55 5103
[2] Eike Rietzel, Christoph Bert, Respiratory motion management in particle therapy, Med. Phys. 37, February 2010
[3] Christoph Bert, Sven O Grözinger and Eike Rietzel, Quantification of interplay effects of scanned particle beams and moving targets, Phys. Med. Biol. 53 (2008) 2253–2265
[4] Joao Seco, Daniel Robertson, Alexei Trofimov and Harald Paganetti, Breathing interplay effects during proton beam scanning: simulation and statistical analysis, Phys. Med. Biol. 54 (2009) N283–N294
[5] A.Schätti, M. Zakova, D. Meer and A.J. Lomax, Experimental verification of motion mitigation of discrete proton spot scanning by re-scanning, Phys. Med. Biol. 58 (2013) 8555–8572
[6] Laura I Cerviño, Alvin K Y Chao, Ajay Sandhu and Steve B Jiang , The diaphragm as an anatomic surrogate for lung tumor motion, Phys. Med. Biol. 54 (2009) (3529-3542)

228
Targeting NOTCH pathway in Glioblastoma

S. Yahyanejad[1], H. King[2], V. S. Iglesias[1], P. V. Granton[3], L. M.O. Barbeau[1], S. J. van Hoof[1], A. J. Groot[1], R. Habets[1], J. Prickaerts[4], A. J. Chalmers[5], S. C Short[2], F. Verhaegen[1], J. Theys[1], M. Vooijs[1]
[1] Department of Radiotherapy (MAASTRO)/GROW – School for Developmental Biology & Oncology, Maastricht University, Maastricht, The Netherlands
[2] Radiation Biology and Therapy group, Leeds Institute of Cancer and Pathology, St James's University Hospital, Leeds, England
[3] Department of Oncology, London Health Sciences Center, London, Ontario, Canada [4]Department of Psychiatry and Neuropsychology, Maastricht University, Maastricht, The Netherlands [5]Translational Radiation Biology, Institute of Cancer Sciences, Wolfson Wohl Cancer Research Centre, University of Glasgow, Glasgow, Scotland

Glioblastoma multiforme (GBM) is the most common malignant brain tumor in adults. The current standard of care includes surgery followed by radiotherapy (RT) and chemotherapy with temozolomide (TMZ). Treatment often fails due to the radiation and TMZ resistance of a small percentage of cells with stem cell-like behavior (CSC). The Notch signaling pathway is expressed and active in human glioblastoma and Notch inhibitors attenuate tumor growth *in vivo* in xenograft models. Here I will discuss the results of studies investigating combination treatments of RT Temozolomide and NOTCH inhibitors in an orthotopic model of Glioblastoma. Small Animal image guided preciscion Radiotherapy (SmART) treatment planning and delivery was used to achieve highly accurate dose prescriptions and treatment monitoring. Studies will be presented that investigate the role for NOTCH signaling in treatment response in different 2D and 3D culture systems.

Keywords: notch, glioblastoma, stem cell, radiotherapy, temozolomide, image guided radiotherapy, bioluminescence, resistance

References:
[1] Yahyanejad, S., van Hoof, S. J., Theys, J., Barbeau, L. M., Granton, P. V., Paesmans, K., Verhaegen, F., and Vooijs, M. (2015) An image guided small animal radiation therapy platform (SmART) to monitor glioblastoma progression and therapy response. *Radiother Oncol* 116, 467-472
[2] Yahyanejad, S., Granton, P. V., Lieuwes, N. G., Gilmour, L., Dubois, L., Theys, J., Chalmers, A. J., Verhaegen, F., and Vooijs, M. (2014) Complementary use of bioluminescence imaging and contrast-enhanced micro-computed tomography in an orthotopic brain tumor model. *Mol Imaging* 13, 1-8

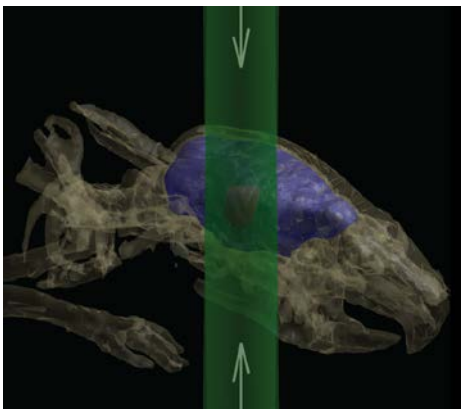

Figure Legend: SmART image-guided treatment plan for orthotopic GBM model. PTV (red), normal brain (blue) and parallel irradiation beams (green)

229
Stroma mediated wound healing signals and cell response to radiation

M-C. Vozenin
CHUV, Lausanne, Switzerland

Stroma mediated wound healing signals induced by radiotherapy have been well characterized in normal tissue response and fibrosis. They are complex and involve the crosstalk between the various cellular type of the tissue including fibroblasts, endothelial, immune, epithelial cells as well as soluble paracrine factors including growth factors and proteases. In addition, recent studies suggest that these wound healing signals may share similarities with the ones produced by tumor's microenvironment. Therefore, their modulation may impact both normal tissue and tumor response to radiation therapy.
This lecture will illustrate the two important aspects of stroma mediated wound healing signals in normal tissue and tumour response to radiotherapy.
In a recent study (1), we investigated the role of macrophages in radiation-induced lung fibrosis, profiled alveolar (AM) and interstitial macrophages (IM) and show that both macrophage subtypes are playing specific and opposite role in fibrogenesis. Acute depletion of AM post-irradiation was shown and associated with cytokine secretion. This acute depletion was followed by a repopulation mediated via the recruitment and proliferation of monocytes/macrophages from the bone marrow. Interestingly, the newly recruited Alveolar macropahages exhibited hybrid polarization (M1/M2), associated with the up-regulation of both Th1 and Th2 cytokines. At delayed times points post-irradiation, interstitial macrophages were M2 polarized and simultaneously, a down-regulation of Th1 cytokines and up-regulation of Th2 cytokines was observed in irradiated lungs. The specific depletion of hybrid AM enhanced the severity of fibrosis whereas anti-fibrotic treatment based upon pravastatin administration decreased M2-IM levels. We also found that M2-IM were able to activate fibroblast into myofibroblasts when co-cultured.
In another study (2), we assessed the crosstalk between primary lung fibroblast and carcinoma cells (TC-1) in response to radiotherapy. We found that fibroblasts were not able to modulate intrinsic radiosensitivity of TC-1 but produce diffusible factors able to modify tumor cell fate. More specifically, RhoB deficient fibroblasts stimulated TC-1 migration through MMPs production whereas WT fibroblasts produce TGF-□.In addition RhoB deficiency stimulated pro-inflammatory signals (IL-6) that would impact on immune recruitment and favor antitumor immune response. In addition, co-irradiation of fibroblasts and TC-1 abrogated the pro-migratory phenotype by repression of TGF-ß and MMP secretion. This last result suggests that conversely to, the current view; irradiated stroma would not enhance

carcinoma migration and could be manipulated to promote anti-tumor immune response. The role of macrophages in this system is currently investigated.

References:
[1] Meziani L, Mondini M, Petit B, Deutsch E and Vozenin MC. Radiation-Induced Lung Fibrosis is Associated with M2-type Interstitial Macrophages and Limited by Hybrid Alveolar Macrophages. Submitted
[2] Arshad A, Deutsch E, Vozenin MC**.** Simultaneous irradiation of fibroblasts and carcinoma cells repress the secretion of soluble factors able to stimulate carcinoma cell migration. Plos One, 2015 Jan 30;10 (1):e0115447.

230

Data from the EORTC Cancer Survivorship Task Force

C. Vrieling[1], L. Moser[2], L. Liu[3], F. Meunier[3] on behalf of the EORTC Survivorship Task Force.
[1] Department of Radiotherapy, Clinique des Grangettes, Geneva, Switzerland
[2] Department of Radiotherapy, Champalimaud Cancer Centre, Lisbon, Portugal
[3] EORTC Headquarters, Brussels, Belgium

During the past decades, important progress has been made in the treatment of cancer. With early detection and more effective treatments, cancer has become a curable disease for many patients, while for others it could now be considered a chronic disease. As a consequence, the number of long-term cancer survivors is rapidly increasing, in particular among patients treated for Hodgkin's lymphoma, testicular, prostate, colo-rectal, breast cancer or children's leukemia.
Most of these patients, however, face immediate (mostly transient) and long term (mostly irreversible) physical and mental side effects: hair loss, changes in body image, fatigue, depression, cognitive dysfunction, as well as increased risk of cardiovascular disease, bone loss, infertility and secondary malignancies. Cancer survivors are also confronted with socio-economical consequences of their disease, including too often exclusion from insurances, mortgages and loss of jobs.
Most of the current knowledge regarding the long-term side effects of cancer and its treatment is based on registry data that is missing important treatment details. Clinical trial databases on the other hand include treatment and outcome data, but often fail to produce very long-term follow-up of outcome and late effects because of the high costs of conducting such long-term follow-up.
The European Organisation for Research and Treatment of Cancer (EORTC) Survivorship Task Force aims to use and, if needed, to complete the impressive EORTC databases accumulated over 50 years of conducting cancer clinical trials. The goal is to document and analyse how long-term outcomes and side effects are associated with cancer treatment. With experience in updates of lymphoma and leukemia trials, early breast cancer trials are now being assessed as well. These studies provide large patient numbers (over 6000 patients for the lymphoma studies and over 10,000 patients for the early breast cancer cohort). For the lymphoma trials, the first results on cardiovascular disease and secondary malignancies (incidence and mortality) have recently been published. The effects of the different treatment components on these endpoints have been quantified. Additional information will be gathered through a number of questionnaires sent to survivors, asking them about the impact of cancer diagnosis and treatment on relationships (social situation, parenthood), education, work and insurance, fatigue, emotional well-being and quality of life. To estimate the relative risks compared to the general population, a linkage with data of registries from several geographic areas is needed. Establishing such a network will enable us to quantify the impact of cancer treatment on late side effects in absolute terms.
The information that the EORTC will gather through this series of projects is expected to help and guide future patients in trading off treatment efficacy and late side effects, seen as important costs in surviving cancer.

Keywords:
Long-term outcome, treatment side-effects, survivorship

References:
[1] Cardiovascular disease after cancer therapy. Aleman BM, Moser EC, Nuver J, Suter TM, Maraldo MV, Specht L, Vrieling C, Darby SC. EJC Suppl. 2014 Jun;12(1):18-28.
[2] Beyond treatment - Psychosocial and behavioural issues in cancer survivorship research and practice. Aaronson NK, Mattioli V, Minton O, Weis J, Johansen C, Dalton SO, Verdonck-de Leeuw IM, Stein KD, Alfano CM, Mehnert A, de Boer A, van de Poll-Franse LV. EJC Suppl. 2014 Jun;12(1):54-64.
[3] Monitoring and optimising cognitive function in cancer patients: Present knowledge and future directions. Schagen SB, Klein M, Reijneveld JC, Brain E, Deprez S, Joly F, Scherwath A, Schrauwen W, Wefel JS. EJC Suppl. 2014 Jun;12(1):29-40.
[4] Current knowledge and future research directions in treatment-related second primary malignancies. Morton LM, Swerdlow AJ, Schaapveld M, Ramadan S, Hodgson DC, Radford J, van Leeuwen FE. EJC Suppl. 2014 Jun;12(1):5-17.
[5] Cancer survivorship: A positive side-effect of more successful cancer treatment. Moser EC, Meunier F. EJC Suppl. 2014 Jun;12(1):1-4.
[6] Cardiovascular disease after treatment for Hodgkin's lymphoma: an analysis of nine collaborative EORTC-LYSA trials. Maraldo MV, Giusti F, Vogelius IR, Lundemann M, van der Kaaij MAE, Ramadan S, Meulemans B, Michel H-A, Aleman BMP, Raemaekers J, Meijnders P, Moser EC, Kluin-Nelemans HC, Feugier P, Casasnovas O, Fortpied C*, Specht L*, on behalf of the European Organisation for Research and Treatment of Cancer (EORTC) Lymphoma Group. Lancet Haematol. 2015 Nov;2:e491-502.

231

RTQA platform of the EORTC

D. C. Weber[1,2,3], A. Branquinho[4], C. Hurkmans[5]
[1] Paul Scherrer Institute, ETH Domain, Villigen, Switzerland
[2] University of Zürich, Zurich, Switzerland
[3] University of Bern, Bern, Switzerland
[4] EORTC HQ, Brussels, Belgium
[5] Department of Radiation Oncology, Catharina Hospital, Eindhoven, The Netherlands.

Radiotherapy (RT) planning and delivery for cancer management has substantially evolved over the last three decades with lately the introduction of intensity modulated RT, image-guided RT and stereotactic ablative RT to name a few techniques. The evaluation of these ehigh precision delivery techniques in routine care and in clinical trials alike requires optimal RT quality (RTQA) assurance programs which aim at defining the range of acceptable variations and importantly developing mechanisms of action for correction and prevention of potential variations[1, 2]. RTQA outside a clinical trial is defined by all processes that ensure consistency of the dose prescription and the safe delivery of that prescription with regard to dose to the target and critical structures, minimization of the exposure of the RT personnel, particularly so the radiation technologists[3]. In the framework of clinical trials assessing the efficacy of RT with or without a combined modality, RTQA is also necessary to avoid the corruption of the study-endpoint[4], as RT variations from study protocol decrease the therapeutic effectiveness and/or increase the likelihood of radiation-induced toxicities[5]. Prospective trials have shown that RTQA variations have a significant impact on the primary study end-point and could bias the analysis of the trial results[6]. Other specific consideration for RTQA in trials includes, but is not limited to, education of the accruing sites in RT-trial guidelines, promotion of consistency between centers and estimation of inter-patient and inter-institutional variations. Additionally, global cooperation is essential in the environment of common and rare cancers alike, in order to be able to create sufficiently large patient data sets within a reasonable recruitment period. This cooperation is not without issues and recently the need to have harmonized

RTQA procedures has been strongly advocated by the Global Harmonisation Group[7].
Ensuring RT compliance with protocol guidelines involves however gradually more resources-intensive procedures which are also labor intensive and are not cost-neutral. This will consequentially have a significant impact on the overall study budget. This financial investment is of paramount importance, as non-adherence to protocol-specified RT requirements in prospective trials is very frequent[8, 9]. The European Organisation for the Research and Treatment of Cancer (EORTC) Radiation Oncology Group started to implement RTQA strategies in the 1980s[10], including on how to write a protocol for RT trials[11, 12], defining RTQA procedures (such as benchmark case, dummy run and complex treatment dosimetry checks)[7], assuring prospective individual case review feasibility and implementing an electronic data-exchange platform[3].

Keywords: Quality assurance, RTQA, prospective trial, patient's outcome, toxicity

References:
[1] Budiharto T, Musat E, Poortmans P, Hurkmans C, Monti A, Bar-Deroma R, et al. Profile of European radiotherapy departments contributing to the EORTC Radiation Oncology Group (ROG) in the 21st century. Radiother Oncol. 2008;88:403-10.
[2] Gondi V, Cui Y, Mehta MP, Manfredi D, Xiao Y, Galvin JM, et al. Real-time pretreatment review limits unacceptable deviations on a cooperative group radiation therapy technique trial: quality assurance results of RTOG 0933. International journal of radiation oncology, biology, physics. 2015;91:564-70.
[3] Fairchild A, Aird E, Fenton PA, Gregoire V, Gulyban A, Lacombe D, et al. EORTC Radiation Oncology Group quality assurance platform: establishment of a digital central review facility. Radiother Oncol. 2012;103:279-86.
[4] Ohri N, Shen X, Dicker AP, Doyle LA, Harrison AS, Showalter TN. Radiotherapy Protocol Deviations and Clinical Outcomes: A Meta-analysis of Cooperative Group Clinical Trials. J Natl Cancer Inst. 2013;105:387-93.
[5] Weber DC, Tomsej M, Melidis C, Hurkmans CW. QA makes a clinical trial stronger: Evidence-based medicine in radiation therapy. Radiother Oncol. 2012;105:4-8
[6] Peters LJ, O'Sullivan B, Giralt J, Fitzgerald TJ, Trotti A, Bernier J, et al. Critical impact of radiotherapy protocol compliance and quality in the treatment of advanced head and neck cancer: results from TROG 02.02. J Clin Oncol. 2010;28:2996-3001.
[7] Melidis C, Bosch WR, Izewska J, Fidarova E, Zubizarreta E, Ulin K, et al. Global harmonization of quality assurance naming conventions in radiation therapy clinical trials. International journal of radiation oncology, biology, physics. 2014;90:1242-9.
[8] Musat E, Roelofs E, Bar-Deroma R, Fenton P, Gulyban A, Collette L, et al. Dummy run and conformity indices in the ongoing EORTC low-grade glioma trial 22033-26033: First evaluation of quality of radiotherapy planning. Radiother Oncol. 2010;95:218-24.
[9] Coskun M, Straube W, Hurkmans CW, Melidis C, de Haan PF, Villa S, et al. Quality assurance of radiotherapy in the ongoing EORTC 22042-26042 trial for atypical and malignant meningioma: results from the dummy runs and prospective individual case Reviews. Radiat Oncol. 2013;8:23.
[10] Weber DC, Poortmans PM, Hurkmans CW, Aird E, Gulyban A, Fairchild A. Quality assurance for prospective EORTC radiation oncology trials: the challenges of advanced technology in a multicenter international setting. Radiother Oncol. 2011;100:150-6.
[11] Fairchild A, Bar-Deroma R, Collette L, Haustermans K, Hurkmans C, Lacombe D, et al. Development of clinical trial protocols involving advanced radiation therapy techniques: the European Organisation for Research and Treatment of Cancer Radiation Oncology Group approach. Eur J Cancer. 2012;48:1048-54.
[12] Bolla M, Bartelink H, Garavaglia G, Gonzalez D, Horiot JC, Johansson KA, et al. EORTC guidelines for writing protocols for clinical trials of radiotherapy. Radiother Oncol. 1995;36:1-8.

232
Yield study and optimization of nuclear isotopes for cancer treatment and diagnostics with ISOLTRAP/CERN

A. Welker[1,8], N.A.S Althubiti[2], D. Atanasov[3], K. Blaum[3], F. Herfurth[4], S. Kreim[3], U. Koester[5], D. Lunney[6], M. Mougeot[6], V. Manea[3], D. Neidherr[4], M. Rosenbusch[7], L. Schweikhard[7], F. Wienholtz[7], R. Wolf[3], K. Zuber[1]
[1] Institut für Kern- und Teilchenphysik, Technische Universität Dresden, Zellescher Weg 19, 01069 Dresden, Germany;
[2] University of Manchester, Manchester, United Kingdom;
[3] Max-Planck-Institut für Kernphysik, Saupfercheckweg 1, 69117 Heidelberg, Germany;
[4] GSI Helmholtzzentrum für Schwerionenforschung GmbH, Planckstr. 1, 64291 Darmstadt, Germany;
[5] Institute-Laue-Langevin, 71 avenue des Martyrs – CS 20156 – 38042 Grenoble Cedex 9;
[6] CSNSM-IN2P3-CNRS, 91405 Orsay Campus, bât. 104, 108, France;
[7] Ernst-Moritz-Arndt-Universität, Institut für Physik, Felix-Hausdorff-Str. 6, 17487 Greifswald, Germany;
[8] CERN, Geneva 23, 1211 Geneva Switzerland

Purpose: The ISOLDE [1] facility at CERN provides a wide choice (>1000 different radioisotopes) of mass-separated ion beams. These serve a variety of disciplines, including radiochemistry, radiobiology and preclinical studies for nuclear medicine. Recently the quadruplet of terbium (Tb) isotopes covering all modalities of nuclear medicine gained considerable interest [2].
Materials/Methods: Neutron-deficient lanthanide isotopes such as 149,152,155Tb are produced at ISOLDE by 1.4 GeV proton induced spallation of tantalum foil targets. The radionuclides diffuse out of the 2000 °C hot target and are surface or laser ionized, accelerated to 30-60 keV and mass separated. Due to the chemical similarity of the lanthanides the separated beam is not mono-isotopic but also contains isobars of the selected mass plus sidebands of oxide ions 16 mass units less. Most of these are radioactive with different half-lives and a wealth of gamma rays which renders difficult a quick on-line assessment of the beam composition by gamma ray spectrometry.
We present a new tool for this purpose, the so called multi-reflection time-of-flight mass spectrometer (MR-TOF MS) [3] which is used at the high-resolution mass spectrometer ISOLTRAP [4]. With the support of the spectrometer it is possible to analyse the composition of the collected beam immediately and vary the production parameters in order to enhance even more the purity of the isotope of interest.
Results: Using ISOLTRAP's MR-TOF MS the yield and purity of the dysprosium beams were successfully optimized on-line. To enhance the usable terbium activity, the dysprosium (Dy) isobars of the isotopes of interest were laser-ionised and collected on a Zn foil, the creation of terbium taking place directly in the sample by beta decay. The foils where shipped after the implantation to PSI where the preparation of the radionuclide pure product took place.
Conclusion: We will present in this contribution the results from terbium collection campaigns taking place in the last three years at ISOLDE. The beam analysis capabilities of ISOLTRAP will be presented, as well as recent results concerning the composition and purity of ISOLDE dysprosium beams.

Keywords: cancer treatment, Tb, CERN

References:
[1] E. Kugler, Hyperfine Interact. 129, 23 (2000).
[2] C. Müller et al., J. Nucl. Med. 53, 1951 (2012).
[3] R.N. Wolf et al. Int. J. Mass Spectrom. 349-350, 123–133 (2013).
[4] S. Kreim et al. Nucl. Instrum. Methods B 317, 492–500 (2013).

233

Sonification as a method to distinguish the isometric force of Attention Deficit Hyperactivity Disorder (ADHD) compared to control participants.

K.A. Neely[1], G.K.R. Williams[1,2], D. Vicinanza[3]
[1] Department of Kinesiology, Pennsylvania State University, University Park, PA, USA
[2] Department of Life Sciences, Anglia Ruskin University, Cambridge, UK
[3] Department of Computing and Technology, Anglia Ruskin University, Cambridge, UK

Purpose: Attention Deficit Hyperactivity Disorder (ADHD) significantly impacts academic, social, and vocational success. Diagnosing ADHD in adulthood can be difficult because childhood reports are not often available. The identification of specific motor deficits that identify ADHD in adults may provide critical information for diagnostic strategies.
The purpose of the present study was to determine if performance in an isometric, visually guided grip force task could discriminate ADHD patients from healthy controls. Sonification was used as a novel method to examine the frequency structure of the isometric force output.
Materials/Methods: 10 individuals participated in the study: 5 with self-reported ADHD and 5 age and sex-matched healthy controls. Participants were required to produce a specific force (25% of their maximal voluntary contraction) with their thumb and index finger in response to visual feedback.
Visual feedback was presented on a 102 cm (40-inch) Samsung television screen with resolution 1920 x 1080 and a 120 Hz refresh rate. Participants were seated upright in a chair (JedMed Straight Back Chair, St. Louis, MO) a horizontal distance of approximately 127 cm from the television screen. Their right forearm rested in a relaxed position at about 100° of flexion on an adjustable non-tilting hospital table. The room was dimly lit to limit glare and reflections on the television screen. Participants held a Bragg-grating fiber-optic precision grip force transducer using precision grip with the dominant hand (Neuroimaging Solutions, Gainesville, FL). The force transducer was calibrated, and had a resolution of 0.025 N.
The amount of visual feedback was varied by changing the gain (i.e., the magnification) of the visual feedback to produce low (0.2), medium (0.6), medium-high (1.6) and high (6.0) gain conditions. Each participant pressed for 4 x 20 s at each gain condition.
Force data was collected for 22 seconds at 125Hz; sonification was performed by resampling the measurement at 4000Hz to generate audible waveforms. Sonograms were then computed using moving Hanning windows for all the sound signals generated by all gain conditions.
Results: This is the first time the isometric force output has been measured across a wider frequency range 0-62.5Hz, compared with the usual 0-20Hz (Mosconi et al., 2015). In Figure 1 it is possible to see that the ADHD sonograms display higher frequency content between 20-62.5Hz compared to the control samples. This characteristic was consistent across all the participants.
In addition, the spectral structure related to ADHD participants showed sensitivity to gain which was not seen in control samples.

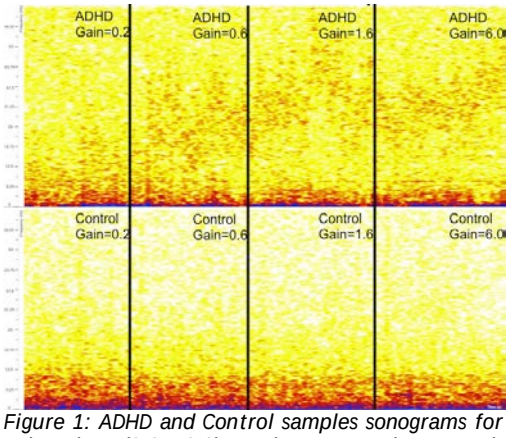

Figure 1: ADHD and Control samples sonograms for different gain values (0.2 – 6.0). In the top row (ADHD patients), it is clearly visible the structured high-frequency content in the 20-62.5Hz band.

Conclusions: The results of sonification enabled us to distinguish between the isometric pinch grip force of adults with ADHD compared to healthy controls based on differences in higher frequency content and structure (20-62.5Hz band). This testing paradigm and analysis method provides a potential inexpensive, portable, non-invasive tool for practitioners diagnosing ADHD in adults, based on differences in psychomotor abilities. Future work aims to explore the use of sonificaton to characterize motor behavior for other health problems.

Keywords: human motor control; grip force ; ADHD; sonification

References:
[1] Mosconi, M.W., Mohanty, S., Greene, R.K., Cook, E.H., Vaillancourt, D.E., and Sweeney, A.J. (2015). Feedforward and Feedback Motor Control Abnormalities Implicate Cerebellar Dysfunctions in Autism Spectrum Disorder, *Journal of Neuroscience, 35(5): 2015-2025*

234

Sonification to investigate gait transition

D. Vicinanza[1], G.K.R. Williams[2]
[1] Department of Computing and Technology, Anglia Ruskin University, Cambridge, UK
[2] Department of Life Sciences, Anglia Ruskin University, Cambridge, UK

Purpose: The purpose of this investigation was to increase our understanding of healthy gait by characterising the complex action using a novel method: sonification. Running involves coordination between all major segments of the body. To simplify the problem, healthy running has been described in terms of lower limb symmetry (Exell et al., 2012), or by principal component analysis into modes of whole body coordination (Daffertshofer et al., 2004; Lamonth et al., 2009). However, in both techniques information about the intricacies of multi segmental movements are lost. Here, we propose sonification as a novel technique to assess multi segment coordination during running. By examining movement in the frequency domain we obtain an individual and situation specific representation of coordination between the major limbs. Since anti-phase frequencies cancel and in-phase frequencies enhance each other, we are able to represent the coordination within the system through the resulting spectrogram. We hope to show the sensitivity of this measure, which does not require data reduction and loss, for identifying and tracking pathological running gait, and use it as a tool to increase our understanding of the adaptability of human motor control. The application of this technique will aid diagnosis and tracking of pathological and perturbed gait, for example highlighting key changes in gait with ageing or leg surgeries. Another project we are working on is exploring the coordination of unilateral lower limb amputees.

Materials/Methods: 1 participant ran on a treadmill that was accelerating between speeds of 0 and 18 Km/h in 2 minutes. CODA automated motion analysis system was used to collect 3D kinematic data from 14 markers placed on the head, shoulders, elbows, wrists, hips, knees, ankles of the participant (sampling frequency 100 Hz, trial length 120 s). Marker position and acceleration data were analysed in the x, y and z directions.
Individual and combined sensor measurements were resampled at 4000Hz to generate audible waveforms. Sonograms were then computed using moving Hanning windows for all the sound signals computed for each marker and combination of markers.
Results: Sonification of individual and combined markers are shown in Figure 1. The transition between the walking and running gaits is clearly visible in all of the sonograms (Figure 1). Sonification of individual markers (Figure 1, top left) shows the frequencies underpinning the marker movement. Combining the markers, sonification shows the cancellation and enhancement of frequencies involved in the gait as a result of coupling the marker waveforms (Figure 1, top right and bottom).

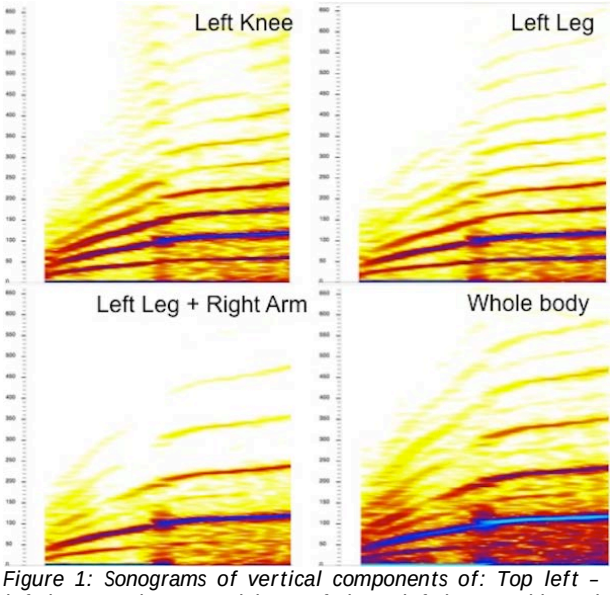

Figure 1: Sonograms of vertical components of: Top left – left knee marker; Top right – Left leg = left knee, ankle and hip markers; Bottom left – Left leg combined with Right arm = right wrist, elbow and shoulder markers; Bottom right – Whole body = combined left leg, right leg, left arm, right arm and head markers

Conclusion: Sonification provides a measure that clearly shows the phase transition between walking and running gaits. Furthermore, this measure is individual specific and situation specific. It is proposed that this method could be a used as a key tool for understanding and identifying and tracking changes in pathological or perturbed gaits; informing health practice.

Keywords: clinical gait analysis, sonification, movement analysis, coordination, biomechanical modeling

References:
[1] Exell, T.A., Irwin, G., Gittoes, M.J.R., and Kerwin, D.G. (2012). Implications of intra-limb variability on asymmetry analysis. *Journal of Sports Sciences,* 30(4), 304-309.
[2] Daffertshofer, A., Lamoth, C.J.C., Meijer, O.G., and Beek, P.J. (2004). PCA in studying coordination and variability: A tutorial. *Clinical Biomechanics,* 19(4), 415-428.
[3] Lamoth, C.J.C., Daffertshofer, A., Huys, R., and Beek, P.J. (2009). Steady and transient coordination structures of walking and running, *Human Movement Science,* 28(3), 371-386.

235
Inhibiting the actions of cathepsin L effects both tumour initiation and metastasis formation.
T.R. Wittenborn[1], P.B. Elming[1], and M.R. Horsman[1]
[1] Department of Experimental Clinical Oncology, Aarhus University Hospital, Aarhus, Denmark.

Purpose: Cathepsin L (CTSL) has been shown to play a role in tumour development and progression through its proteolytic activities. An increased expression and secretion of CTSL from cancerous cells enhances the tumour cell migration, aids in tumour invasion and promotes angiogenesis. In the present study we have investigated the role of the small molecule cathepsin L inhibitor, KGP94, on tumour initiation and metastatic spread in murine tumour models.
Methods: The C3H mammary carcinoma was implanted subcutaneously into the foot of male CDF1 mice. The SCCVII squamous cell carcinoma was either implanted into the foot or intravenously injected into the tail vein of C3H/HeNHsd mice. KGP94 was prepared by dissolving in a mixture of 10% Tween 80 and 90% HEPES-buffer. It was intraperitoneally (i.p.) injected at 0.01ml/g mouse bodyweight. Various doses (1-20mg/kg) were administered starting from the day of tumour implantation/injection. Tumour response was assessed by either determining the tumour growth time for foot tumours or the number of lung metastasis for the injections. Tumour growth time was assessed using a caliper and was the time in days to reach a volume of 500mm^3 (TGT_{500}). Lung metastasis were assessed after 2-3 weeks, where mice were euthanized, lungs were excised, weighed, and stained in Bouin's solution. Results are listed as Mean (± Standard Error). One-way ANOVA comparison of group means was performed, and a $P<0.05$ was considered significant.
Results: The TGT_{500} for control animals was 18.3 days (± 0.4) for the C3H mammary carcinoma and 13.6 days (± 0.7) for the SCCVII carcinoma. Treating the C3H mammary carcinoma with KGP94 significantly increased the TGT_{500} when doses were at 5.0 mg/kg or higher. Similar results were found with the SCCVII-carcinoma, except that a dose of 5.0 mg/kg did not have a significant effect on TGT. At lower doses of KGP94 neither of the tumour models showed significant growth delay. Studies on metastasis formation showed that 50% of animals in the control group developed metastasis within 2-3 weeks. The mean number of metastasis in these mice was 16 (±15). When mice were treated with KGP94 (10mg/kg) on a daily basis only 30% developed metastasis, and the mean number of metastasis in these mice was 5 (±4).
Conclusion: We have shown that inhibiting cathepsin L during the tumour initiation stage significantly delays tumour growth in the C3H and SCCVII murine tumour models. Furthermore, our metastasis study showed decreased metastasis formation in KGP94 treated animals. This suggests that KGP94 treatment can affect both tumour initiation and metastasis formation.

Keywords: Tumour growth inhibition; metastasis formation, cathepsin inhibitor KGP94.

236
New hypoxia probe development based on mass spectrometry
B.G. Wouters[1], L.J. Edgar[2], R.N. Vellanki[1], A.Halupa[2], D. Hedley[1], M. Nitz[2]
[1] Princess Margaret Cancer Centre, Toronto, ON, Canada
[2] University of Toronto, Toronto, ON, Canada

Many human tumors contain substantial regions of low oxygen (hypoxia), which promotes metastasis and resistance to most forms of therapy. Unfortunately, the methods available to assess cellular hypoxia are unable to detect the fluctuating oxygen concentrations that are proposed to be an important source of these cellular phenotypes, and similarly cannot detect changes in hypoxia as a consequence of treatment. We have established a novel method that enables measurement of dynamic changes in hypoxia at the cellular level. We developed a series of small molecule probes with identical chemical structures but containing different isotopes of tellurium that can be independently quantified by mass cytometry (MC) and imaging mass cytometry (IMC). This

technology allows highly multiparameter (up to 34 probes) cytometric or image based quantification of biomarkers on single cells. MC employs inductively coupled plasma mass spectrometric detection in place of the fluorescence optics used in traditional flow and imaging cytometry and circumvents the problems of spectral overlap and compensation required in fluorescence flow cytometry. The key feature of MC that we have exploited is that different mass isotopes of the same heavy metal can be independently quantified and thus used as distinct probes to allow serial measurements over time with the same chemical probe. This has allowed a series of probes that have identical pharmacokinetic profiles to be produced and used to monitor the time dependence of tumor hypoxia in both in vitro and in vivo model systems.

Keywords:
Hypoxia, imaging, mass cytometry

237

HIF-1α plays a key role in the response of HNSCC cancer stem cells to photon and carbon ion exposures

A-S. Wozny[1,2], A. Lauret[1], Y. Saintigny[3], P. Battiston-Montagne[1], M. Beuve[4], G. Alphonse[1,2] C. Rodriguez-Lafrasse[1,2]
[1] Laboratoire de Radiobiologie Cellulaire Moléculaire, EMR3738, Faculté Médecine Lyon-Sud, Université de Lyon, Université Lyon1, 69921 Oullins, France
[2] Hospices Civils de Lyon, Centre Hospitalier Lyon-Sud, 69495 Pierre-Bénite, France
[3] LARIA, CEA, DVS/IRCM au CIMAP/GANIL, 14070 Caen, France
[4] IPNL-LIRIS-CNRS-IN2P3, 69622 Villeurbanne, France

Purpose: Head and neck squamous cells carcinomas (HNSCC) have a poor prognosis due to escapement to anti-cancer therapies which leads to locoregional recurrences. The presence of cancer stem cells (CSCs), resistant to chemo- and radio-therapies, could explain these resistances and recurrences. Hadrontherapy has demonstrated favorable results for many cancers, since carbon ions induced more CSC's cell death than photons. However, for the HNSCC tumor, local control remains low. CSCs are located in a hypoxic microenvironment and hypoxia is well-known for being able to induce the epithelial mesenchymal transition (EMT). The aim of this study is to investigate the response of CSCs to radiotherapy, compared with carbon ions under hypoxic conditions. Many signaling pathways involved in the resistance of CSCs and the invasion/migration process depend on the stabilization of HIF-1α. Reactive Oxygen Species (ROS), which are produced under hypoxia and in response to irradiation, play a key role in this stabilization. However, since few data are available, the mechanisms involving ROS production, HIF-1α stabilization as well as the invasion/migration process that follows, need to be clarified in HNSCC CSCs exposed to carbon or photon radiations in a hypoxic environment.
Material and methods: Two HNSCC cells lines, SQ20B and FaDu, and their CSCs were grown in normoxic and hypoxic (1% O_2) conditions. CSCs were isolated by flow cytometry cell sorting. Cell survival curves were performed in response to photon (250kV) and carbon ion (75MeV/n, GANIL, France) irradiations in order to define the Oxygen Enhancement Ratio (OER). The expression of HIF-1α was followed by Western-Blots. ROS were quantified with a CM-H2DCFDA dye and Migration/Invasion with Boyden chambers.
Results: After photons, HNSCC cells and their CSCs appeared more resistant under hypoxia (OER>1.2) whereas the oxygen effects were cancelled after carbon ions (OER=1). Interestingly, the OER values and the expression of HIF-1α seemed to be linked. HIF-1α was weakly expressed after photon irradiation and fully inhibited after carbon ions. Additionally, under hypoxia, HIF-1α expression appeared earlier in CSCs than in the parental cell lines, confirming their adaptive properties to hypoxia. In CSCs, this expression was correlated with ROS levels. As a consequence, since HIF-1α is known to promote EMT, under normoxia as well as hypoxia, the invasion/migration abilities of CSCs were more important than in non-CSCs. Finally, after carbon ions, either in normoxic or hypoxic conditions, invasion/migration processes were decreased compared with photons.
Conclusion: HIF-1α plays a key role in the radioresistance of CSCs and in their invasiveness abilities. No expression of HIF-1α was found after carbon ion exposure suggesting that carbon ions could be a relevant therapeutic alternative to kill CSCs in their microenvironment.

Keywords: Hypoxia, Cancer stem cells, Carbon ions

238

Magnetic resonance temperature imaging in clinical hyperthermia: past experience and prospects

P. Wust[1], P. Ghadjar[1], V. Budach[1], L. Winter[2], T. Niendorf[2]
[1] Charité Universitätsmedizin Berlin, Clinic for Radiation Oncology
[2] Max-Delbrück Center for Molecular Medicine, Berlin MR Facility

Purpose: Annular phased array systems (APAS) are suitable to heat extremity, pelvic and abdominal tumors and to intensify chemo- or radiotherapy (Issels 2010). In a hybrid approach APAS and 1.5 T MR scanner were combined and clinically validated (Gellermann 2005, 2006). A review is presented regarding available technical solutions, its limitations and the potentials for further developments.
Methods: Dedicated high-frequency (filters, matching) and mechanical solutions are required for a running hybrid system shown in the upper part of the figure. This APA system has an operating frequency of 100 MHz while the MR resonance frequency is at 64 MHz (1.5 T). Gradient-echo sequences are employed to measure phase differences and extracting MR-temperatures (Gellermann 2005a). The key to obtain reliable MR-temperatures is post processing and visualization of MR datasets in a suitable software platform (here Hyperplan). Software modules has been developed for drift correction (via water bolus, calibrating probes, fat tissue), calculation and image processing of 3D MR-temperature distributions. The platform is also used for hyperthermia treatment planning (HTP) in order to compare distributions of pre-planning and online measurements. Simultaneous processing of HTP distributions and registered MR-temperature distributions has been implemented in the hybrid system in Berlin (Weihrauch 2007).
Results: The *hybrid system* was verified in a heterogeneous phantom (MR-temperature vs. direct temperature measurements, Gellermann 2005a) and clinically used for pelvic and extremity tumors under routine conditions (Gellermann 2005b, 2006). With available MR sequences (phase measurements) MR thermography is suitable for extensive fixated tumors such as sarcoma and recurrent rectal carcinoma, but not in the abdomen.
Further developments of temperature sensitive MR sequences (Winter 2016) are strongly desirable in order to correct for tissue heterogeneities (e.g. air, clips) and various forms of motion (pulsation, respiration, peristalsis, different filling in case of bladder etc.). MR thermometry of the liver is already used during thermoablation, but is a challenge for hyperthermia, where errors < 1 °C are requested.
The next technological step is an *integrated system* (lower part of the figure), where multi-antenna applicators have antennas for both heating (i.e. emitting strong phase controlled E-fields) and MR imaging (i.e. transmitting magnetic pulses and receiving the imaging signals). An experimental integrated system (7T, 298 MHz) has been implemented and tested (Winter 2013, 2015). Integrated systems are also conceivable with lower static H-fields and frequencies.
Conclusion: Current hybrid systems should be further developed to integrated multi-channel systems with increased signal-to-noise ratio and the capability of online optimization.

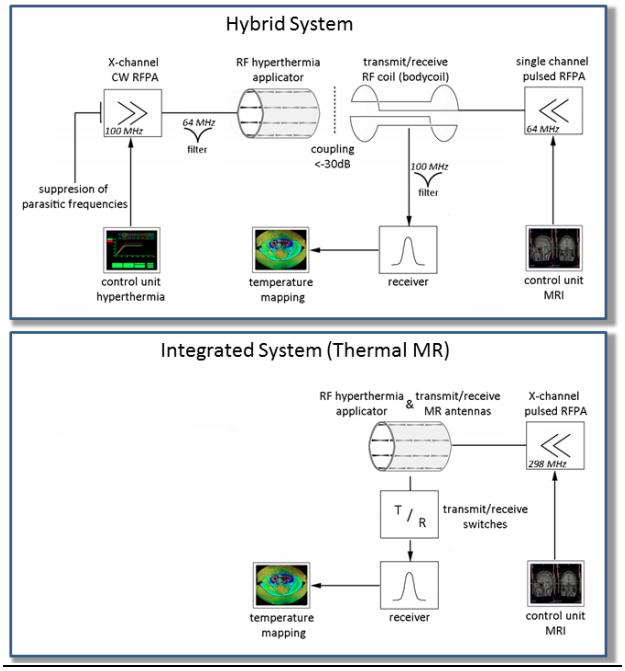

Figure: Scheme of the *hybrid system* (as operated at the Charité Universitätsmedizin Berlin: BSD-2000/3D/MRI in a 1.5T Siemens Symphony) for clinical use (upper part) in contrast to a prototype of an *integrated system* for experimental purposes (developed at the Max-Delbrück Center Berlin: 7T Siemens Magnetom), see Winter 2016.

Keywords: MR thermography, hybrid system, integrated system

References:

[1] Gellermann J, Wlodarczyk W, Ganter H, Nadobny J, Fähling H, Seebass M, Felix R, Wust P.
A practical approach to thermography in a hyperthermia/magnetic resonance hybrid system: validation in a heterogeneous phantom.
Int J Radiat Oncol Biol Phys 2005a; 61(1): 267-77.
[2] Gellermann J, Wlodarczyk W, Hildebrandt B, Ganter H, Nicolau A, Rau B, Tilly W, Fähling H, Nadobny J, Felix R, Wust P.
Noninvasive magnetic resonance thermography of recurrent rectal carcinoma in a 1.5 Tesla hybrid system.
Cancer Res 2005b; 65(13): 5872-80.
[3] Gellermann J, Hildebrandt B, Issels R, Ganter H, Wlodarczyk W, Budach V, Felix R, Tunn PU, Reichardt P, Wust P.
Noninvasive magnetic resonance thermography of soft tissue sarcomas during regional
hyperthermia: correlation with response and direct thermometry.
Cancer 2006; 107(6): 1373-82.
[4] Issels RD, Lindner LH, Verweij J, Wust P, Reichardt P, Schem BC, Abdel-Rahman S, Daugaard S, Salat C, Wendtner CM, Vujaskovic Z, Wessalowski R, Jauch KW, Dürr HR, Ploner F, Baur-Melnyk A, Mansmann U, Hiddemann W, Blay JY, Hohenberger P.
Neo-adjuvant chemotherapy alone or with regional hyperthermia for localised high-risk soft-tissue sarcoma: a randomised phase 3 multicentre study.
Lancet Oncol. 2010;11(6): 561-70.
[5] Weihrauch M, Wust P, Weiser M, Nadobny J, Eisenhardt S, Budach V, Gellermann J.
Adaptation of antenna profiles for control of MR guided hyperthermia (HT) in a hybrid MR-HT system.
Med Phys. 2007; 34(12): 4717-25.
[6] Winter L, Özerdem C, Hoffmann W, Santoro D, Müller A, Waiczies H, Seemann R, Graessl A, Wust P, Niendorf T.
Design and evaluation of a hybrid radiofrequency applicator for magnetic resonance imaging and RF induced hyperthermia: electromagnetic field simulations up to 14.0 Tesla and proof-of-concept at 7.0 Tesla.
PLoS One. 2013; 8(4): e61661.
[7] Winter L, Oberacker E, Paul K, Ji Y, Oezerdem C, Ghadjar P, Thieme A, Budach V, Wust P, Niendorf T.
Magnetic Resonance Thermometry: Methodology, Pitfalls and Practical Solutions
Int J Hyperthermia 2016, in press

239

Measurements and simulations of in-phantom neutron dose from a proton pencil beam

K.S. Ytre-Hauge[1], A. Velure[1], C.H. Stokkevåg[12], O.H. Odland[2] D. Röhrich[1]
[1] Department of Physics and Technology, University of Bergen, Norway
[2] Department of Oncology and Medical Physics, Haukeland University Hospital, Bergen, Norway

Purpose: During proton therapy, patients receive undesired dose from neutrons produced in beam line components or in the patient. The neutron dose is primarily a concern related to long-term consequences such as radiation-induced secondary cancers. The majority of existing experimental data is based on measurements with passive detectors or measurements in air, and most studies have been performed in passive scattering- or uniform scanning beam lines. The aim of this study was to investigate the neutron dose from Pencil Beam Scanning (PBS) proton therapy by in-phantom measurements with a novel active neutron detector.
Materials/Methods: Measurements of the neutron fluence were performed at several positions inside a water phantom irradiated by a 178 MeV proton pencil beam at The Svedberg Laboratory in Uppsala, Sweden. The measurements were conducted with a recently developed neutron detector based on registration of single event upsets in static random access memories (SRAMs). Fluka Monte Carlo simulations were performed and compared to the measurements. The results were also compared to previously published neutron doses measured under similar experimental conditions. Fluence-to-dose conversion factors from ICRP were applied to calculate neutron ambient dose equivalent (H*(10)).
Results: The measurements indicated that the neutron dose at the Bragg peak depth decreased exponentially from 0.17 pSv/proton to 0.03 pSv/proton from 5 cm to 14 cm lateral distance from the beam axis inside the water phantom (Table I). For an extended target volume of 3x3x3 cm^3, this corresponds to neutron doses ranging from approximately 1 mSv/Gy to 0.1 mSv/Gy. The neutron dose varied only to a small degree with depth in the phantom. The measurements and simulations showed similar relative distributions of neutron dose, but the simulations predicted overall lower doses, typically by a factor two. The experimental values were in relatively good agreement with previous results in the literature.
Conclusions: The neutron dose in the water phantom from the proton pencil beam was measured to be on the order 1 mSv/Gy at 5 cm lateral distance from the primary beam axis at the Bragg peak depth, while decreasing to approximately 0.1 mSv at 14 cm lateral distance. Variation in neutron dose as a function of depth in the water phantom was modest. The results demonstrate the feasibility of using the SRAM detector for in-phantom measurements, and can be applied in estimation of secondary cancer risk from PBS proton therapy.

Table I. Neutron ambient dose equivalent as a function of lateral distance from the beam axis at Bragg peak depth

	[pSv/proton]			[mSv/Gy]*		
Distance from beam axis [cm]	Measurements	Schneider et al.	FLUKA	Measurements	Schneider et al.	FLUKA
0			0.30			1.71
3			0.13			0.72
5.2	0.17		0.07	0.96		0.39
6.6		0.14			0.79	
7.3	0.07		0.04	0.39		0.24
9.5	0.06		0.03	0.32		0.15
11.4 (11.6 in Schneider et al.)	0.03	0.02	0.02	0.19	0.11	0.10
13.7	0.03		0.01	0.15		0.07

*Based on a 3x3x3 cm^3 target (5.65×10^9 protons/Gy)

Keywords: Proton therapy, neutron dose, neutron detection

References:

U. Schneider et al., Int J Radiat Oncol Biol Phys. 53, 244-251 (2002)

240
Radiomics in Liquid Biopsies
F. Zenhausern
University of Arizona

In view of the growing trend in personalizing medicine and with the development of sophisticated equipment and algorithms for guiding radiotherapies, more precise doses and/or particle beams can be delivered to the target tumor while minimizing side effects to the surrounding healthy tissue, which opened up access to new delivery modalities and clinical protocols. Although many clinical studies are trying to evaluate the differential effects between different types of radiotherapy on patients' outcomes, the biological response at the cellular level, and the different cellular pathways involved, are yet inadequately be explored. Novel technologies to evaluate genomics or proteomics-based effects in tumor tissue, but also in bodily fluids, have revealed molecular information that will open the doors for new clinical understanding in Oncology. This lecture will discuss these omics applications in the context of the most recent technologies.

241
Small fields dose calculation algorithms in the presence of lung inhomogeneity
I. Zergoug [1,*], A. Mesbahi [2,3]
[1] Radiotherapy Department , EHS Emir Abdelkader, Oran, ALGERIE.
[2] Medical physics department, Institute of Health Sciences, Dokuz Eylul University, Izmir, Turkey.
[3] Radiation Oncology Department, Dokuz Eylul University hospital , Izmir, Turkey.
[*] Corresponding author: zergoug.ismail@gmail.com

In radiotherapy, dose calculation algorithms are used to calculate dose distribution in human body.
Different algorithms are used by several treatment planning and differ in the accuracy of dose calculation.
In this study, a dose calculation accuracy of two commercial treatment planning systems (TPS) were evaluated regarding Monte Carlo method.
The Linac head of Primus Simens was modeled using MCNPX Monte Carlo code based on manufacturer information. Four analytic dose calculation algorithms including PBC, AAA from Eclipse TPS, convolution and superpostion from XiO treatment planning system were evaluated for a small solid tumor in lung. A solid tumor with diameter of 1.8 cm was considered in a thorax phantom and calculations was performed for 1×1, 2×2, 3×3, 4×4 cm^2 field sizes for 6MV and 18 MV energies. The results of TPSs were compared with the results of MC method as a most reliable method.
A dose overestimation of up to 110% inside lung region and 25% for tumor was found for field size of 1×1 cm in the 18 MV photon beam for PBC and convolution methods, comparing to MC results.
For AAA, superposition a close agreement was seen with Monte Carlo simulation in all studied field sizes.
Our results showed that the PBC and convolution methods overestimate the lung dose as well as the solid tumor dose significantly and large errors could arise in treatment plans of lung region and change the outcome of treatment. The Use of MC based methods, AAA and superposition methods are recommended for lung treatments with small fields.

Keywords: Lung dose, Small fields, Treatment planning algorithms, Monte Carlo method

242
The mobile PET insert for simultaneous PET/MRI imaging
M. Zieliński[1@], B. Głowacz[1], D. Alfs[1], T. Bednarski[1], P. Białas[1], E. Czerwiński[1], A. Gajos[1], M. Gorgol[2], B. Jasińska[2], D. Kamińska[1], Ł. Kapłon[1,3], G. Korcyl[1], P. Kowalski[4], T. Kozik[1], W. Krzemień[5], E. Kubicz[1], M. Mohammed[1], M. Pawlik-Niedźwiecka[1], S. Niedźwiecki[1], M. Pałka[1], L. Raczyński[4], Z. Rudy[1], O. Rundel[1], N. G. Sharma[1], M. Silarski[1], A. Słomski[1], A. Strzelecki[1], A. Wieczorek[1,3], W. Wiślicki[4], B. Zgardzińska[2], P. Moskal[1]
[1]Faculty of Physics, Astronomy and Applied Computer Science, Jagiellonian University, S.Łojasiewicza 11, 30-348 Kraków, Poland
[2] Department of Nuclear Methods, Institute of Physics, Maria Curie Sklodowska University, Pl. M. Curie-Sklodowskiej 1, 20 031 Lublin, Poland
[3]Institute of Metallurgy and Materials Science of Polish Academy of Sciences, W. Reymonta 25, 30-059 Kraków, Poland
[4]Świerk Computing Centre, National Centre for Nuclear Research, A. Soltana 7, 05-400 Otwock-Świerk, Poland
[5]High Energy Physics Division, National Centre for Nuclear Research, A. Soltana 7, 05-400 Otwock-Świerk, Poland
email: marcin.zielinski@cern.ch

Purpose: The purpose of the presented research is the development of the new type of device being a mobile (portable) and flexible (adaptable) PET scanner, which will play a role of an insert to the existing MR scanners, providing a unique worldwide solution for simultaneous (at the place and time) functional and anatomical PET-MRI imaging.
Material and methods: Presented solution of a mobile-PET scanner will enable simultaneous registration of PET and MRI images utilizing existing MRI scanners, without need of any modifications. The developed device is based on the strip-PET concept [1-4], consisting of individual detection modules, each build from a plastic scintillator strip connected optically at both ends with the photoelectric converter. In the proposed solution we utilize the array of the silicon photomultipliers which plays a role of light to electric signal converter. The signal readout and processing system together with the fast front end electronic modules will allow to reconstruct time and place of the annihilation [5,6]. In the proposed solution determination of the point of annihilation along the direction of the gamma quanta flight path, is based on the time difference registered in various detection modules.
It is important to stress that the utilized silicon photomultipliers are insensitive to the MR scanner magnetic field therefore its work will not be disturbed with the presence of high magnetic field. Also small electronic elements will not cause the inhomogeneity of the magnetic field in the diagnosed volumes. Important from the point of view of the simultaneous PET/MRI diagnosis is a matter of positioning of two tomographic images with respect to each other. Therefore we will implement the method of positioning by usage of watermarks, seen by MRI system. For the proposed mobile PET scanner this method appears to be effective and at the same time simplest solution of this problem. Since this method explicitly specify the position of the MRI with respect to PET scanner therefore it enables to synchronize both tomographic images.
The advantage of this solution is the elimination of artifacts in tomographic images hindering the identification of potentially cancerous lesions. At the same time, the proposed solution allows using the existing MRI scanners currently held by hospitals, without interfering in their structure and parameters, which should significantly improve the availability of this combined diagnostic method, taking into account the lower cost of such adaptation in relation to the market price of a new PET-MRI device.
Conclusion: In the talk we will present developed solution of a mobile-PET insert to MR scanners. The presentation will include the characteristics of a proposed device together with the advantages over present solutions [7].

Keywords: PET, MR, mobile PET, hybrid PET-MR, strip-PET,

References:
[1] P. Moskal, Patent granted in 2014, N. EP2454612B1, WO2011008119, EP2454611, WO2011008118
[2] P. Moskal et al., Nucl. Inst. and Meth. A 764 (2014) 317.
[3] P. Moskal el al. Radiotheraphy and Oncology 110, S69 (2014)
[4] P. Moskal el al. Nuclear Medicine Review 15, C68 (2012)

[5] M. Pałka el al. Bio-Alg. and Med-Systems Vol. 10, 1,(2014) 41-45
[6] G. Korcyl et al., Bio-Algorithms and Med-Systems 10 (2014) 37.
[7] B. Głowacz, P. Moskal, M. Zieliński, "Tomographic TOF-PET insert", Patent application no. P.413150.

243

Urethra-sparing SBRT for prostate cancer: dosimetric optimization with VMAT *vs.* IMRT and the learning curve effect

T. Zilli[1], Z. Symon[2], S. Bral[3], A. Bruynzeel[4], H. Minn[5], S. Jorcano[6], A. Oliveira[7], U. Abacioglu[8], C. Rubio[9], R. Miralbell[1,6]
[1] Geneva University Hospital, Geneva, Switzerland.
[2] Sheba Medical Center, Ramat Gan, Israel
[3] Onze-Lieve-Vrouwziekenhuis, Aalst, Belgium
[4] VU University Medical Center, Amsterdam, the Netherlands
[5] University Hospital Turku, Turku, Finland
[6] Teknon Oncologic Institute, Barcelona, Spain
[7] Portuguese Institut of Oncology, Porto, Portugal
[8] Neolife Medical Center, Istanbul, Turkey
[9] Hospital Universitario Sanchinarro, Madrid, Spain

Purpose/Objective: To compare the dosimetric results of intensity-modulated radiotherapy (IMRT) and volumetric modulated arc therapy (VMAT) and to assess the learning curve effect on dosimetric optimization in patients randomized in a prospective multicenter phase II trial of urethra-sparing stereotactic body radiotherapy (SBRT) for localized prostate cancer.
Materials/Methods: Dosimetric data of the first 40 patients randomized between 07/2012 and 03/2014 in 9 different centers were analyzed. The SBRT protocol consisted of 36.25 Gy in 5 fractions of 7.25 Gy to the planning target volume (PTV=prostate with (*n*=20) or without (*n*=20) seminal vesicles (SV) with a 5-mm anisotropic expansion, except 3-mm posteriorly). The prostatic urethra with an additional margin of 3 mm (urethral planning risk volume, uPRV) received simultaneously 5 x 6.5 Gy = 32.5 Gy. Plans were generated using either VMAT (*n*=20) or IMRT (*n*=20) technique, with each modality including (n=10) or not (n=10) SV in the PTV. All plans were optimized until the dose prescription parameters and organs at risk (OAR) dose-volume constraints were obtained. Mean doses (± SD) to the PTV, uPRV, and remaining OAR were analyzed. The PTV homogeneity index (HI) and the dice similarity coefficient (DSC) were also assessed. To evaluate the learning curve effect in VMAT optimization, VMAT plans of the first 20 patients were compared with VMAT plans generated in the last 20 randomized patients (05/2014-08/2015).
Results: Compared to IMRT plans, VMAT required a lower number of MU (2245 *vs.* 3685, *p*=.0001) and resulted in a better HI (0.90 *vs.* 0.11, *p*=.002) and uPRV coverage ($D_{98\%}$ 31.2 *vs.* 30.1 Gy, *p*=.001). Regardless of the RT technique, dose constraints were respected for all OAR. The V_{100}, V_{90} and V_{80} for the rectal wall were 1.6±1.4% *vs*. 2.5±1.9% (ref. <5%), 10.3±3.0% *vs*. 11.0±3.3% (ref. <10-15%) and 16.2±3.7% *vs*. 14.8±4.2 (ref. <20-25%) for IMRT and VMAT patients, respectively, with no significant differences between the two techniques. For the bladder wall, the V_{100} and V_{90} were similar for IMRT and VMAT (7.8±3.7% *vs*. 7.0±3.8%, ref. <10-15% and 15.3±4.0% *vs*. 13.1±4.8%, ref. <20%), while VMAT performed better than IMRT for the V_{50} (28.4±11.6% *vs.* 37.2±9.2% (ref. <50%), *p*=.011). Compared to the first VMAT optimizations, plans generated in the last part of the study showed a better PTV DSC value (0.88 vs 0.78, p=.009), a reduced V_{100} (1.3 *vs.* 2.5%, *p*=.023) for the rectal wall, and an overall better bladder sparing (V_{100}, V_{90} and V_{80}, *p*<.05).
Conclusions: For all participating centers, urethra-sparing SBRT plans met all the dosimetric endpoints in terms of PTV coverage as well as OAR sparing, irrespectively of the technique used. Compared with IMRT, VMAT plans resulted in more homogeneous dose distribution, reduced number of MU, and better uPRV coverage. Conformality and OAR sparing with VMAT may be improved after gaining experience in SBRT plan optimization.

Keywords: prostate cancer; SBRT; learning curve